Investigating the role of dopamine in cognitive impairments in a rat model of Parkinson's Disease

Charlotte Bridge

This thesis is submitted for the degree of Doctor of Philosophy at Cardiff University

September 2023

Supervisors:

Dr Mariah J. Lelos

Dr Emma Lane

CARDIFF UNIVERSITY

PRIFYSGOL CAERDYDD

Thesis Summary

Non-motor symptoms are a major component of Parkinson's Disease and have a significant impact on quality of life. Outcome measures of pre-clinical studies primarily focus on alleviating motor dysfunction with dopamine-replacement strategies. Therefore, the overall aim of this thesis was to understand more about the role of dopamine in cognitive impairments through dopamine depletion and restoration manipulations in the unilateral 6-OHDA rat model using the Lateralised Choice Reaction Time task (LCRT).

Experiment 1 investigated cell replacement therapy on cognitive impairments in the LCRT task using human fetal (hfVM) and two different human embryonic stem cell- (hESC) derived dopaminergic progenitor intrastriatal transplants. Whilst hfVM and hESC-derived grafts could effectively alleviate motor impairments, hESC-derived grafts were unable to restore visuospatial function compared to controls, and on certain LCRT parameters, were significantly impaired compared to hfVM grafted rats.

Experiment 2 used a TH and GCH1 AAV viral vector at two titres, alongside the dopamine precursor, L-DOPA, to evaluate the impact of dose on cognitive function. The highest AAV titre improved simple motor behaviour whilst significantly impairing visuospatial function. L-DOPA at increasing doses improved visuospatial function in high titre AAV rats, whilst in a dose response manner, impairing LCRT performance in lesioned sham rats. Histological analysis revealed off-target cortical expression and limited biodistribution throughout the striatum. Experiment 3 found greater striatal biodistribution of the viral vector to improve visuospatial function.

Experiment 4 used unilateral 6-OHDA infusions in the medial and lateral striatum to understand the contribution of the two major dopaminergic midbrain-striatal circuits on LCRT performance. Medial striatal lesions impaired both visuospatial function and incentive motivation, whereas lateral striatal lesions did not, but did induce forelimb akinesia. Experiment 5 subsequently aimed to restore dopamine restricted to those same striatal subregions and found only lateral AAV infusions improved visuospatial function.

This thesis outlines the complex role of dopamine in cognitive impairments, highlighting that a fine-tuned balance and optimisation of its delivery for therapeutic intervention for PD is required.

Acknowledgments

" *Ah, it'll be reet* ". **Bob Bridge**

First and foremost, I'd like to give my upmost thanks to Dr. Mariah J. Lelos and Dr. Emma Lane for being incredible supervisors. You have been so supportive over the past 4 years and I'm incredibly grateful to have been your PhD student. Your guidance, encouragement and reassurance is unmatched. You've gone above and beyond to help me along this process. A million thanks and flowers coming your way.

Special thank you to Prof. Anne Rosser for your encouragement to start a PhD and your support in my different roles over the years. My upmost thanks also goes to Dr. Claire Kelly, without you offering lab experience many moons ago I quite truly wouldn't be here today.

Thank you to the BRG past and present, especially Prof. Steve Dunnett, Radha, Ngoc-Nga, Oly, Kyle, Harri, Heba, Mengru, Feras, Rachel S and Sophie T. You've made my time in the lab a great experience. Special thanks to Emily and Gareth for being the best master's students.

To Dr. Sophie Rowlands and Anne-Marie, thank you for being a source of reassurance and laughs. To Rachel Hills, you've been the best mentor since my PTY days, all the way through till now and I 100% couldn't have done this without you. Thanks to Dr Ana Garcia for being an amazing friend and encouraging me throughout this journey. To my office buddy Patricia, thank you for going on this crazy journey with me and for your daily chats, coffee walks, and all-around support. You've got this! Thank you to Olivia for the best chats, jokes, and amazing support. You've got this too!

A special shoutout to my ancient laptop for only dying on me once. You can rest now, I promise.

To my second family, Crusaders DBC, I've felt your support all the way from Liverpool for the past 4 years and I'm so thankful to have you in my life. Thank you to JP for taking care of me whilst writing this thesis and being my favourite person. To Mum, Dad and Jo, thank you for always believing in me. Hope I've done you proud.

Table of Contents

Chapter 4 : Evaluating viral-mediated DA biosynthesis on cognitive impairments in the LCRT task..97

Abbreviations

5HT	5-hydroxytryptamine
6-OHDA	6-hydroxydopamine
AADC	Amino acid decarboxylase
AAV	Adeno-associated virus
AD	Alzheimer's Disease
BH4	Tetrahydrobiopterin
COMT	Catechol-O-methyltransferase inhibitors
CTIP-2	Coup TF1-interacting protein 2
DA	Dopamine
DARPP-32	cAMP regulated phosphoprotein 32
DAT	DA active transporter
DBS	Deep brain stimulation
DRN	Dorsal raphe nucleus
E/YOPD	Early or young onset Parkinson's Disease
EN1	Engrailed 1
FOXP1	Forkhead box protein 1
FOXA2	Forkhead box A2
GIRK2	G protein-activated inward rectifier potassium channel 2
GABA	Gamma-aminobutyric acid
GAD	Glutamine acid decarboxylase

GCH1   GTP cyclohydrolase 1

GPe   Globus pallidus external

GPi   Globus pallidus internal

GTP   Guanosine triphosphate

GWAS   Genome-wide association studies

hESCs   Human embryonic stem cells

hiPCS   Human induced pluripotent stem cells

HIV-1   Human immunodeficiency virus-1

HLA   Human leukocyte antigens

hPSCs   human pluripotent stem cells

LC   Locus coeruleus

LCRT   Lateralised choice reaction time task

L-DOPA   Levodopa (L-3,4-dihydroxyphenylalanine)

LIDs   L-DOPA induced dyskinesias

LMX1A   LIM homeobox transcription factor 1a

LV   Lentivirus

MFB   Medial forebrain bundle

MMSE   Mini-mental state exam

MPTP   1-methly-4-phenyl-1,2,3,6-tetrahydropyridine

MS   Multiple sclerosis

NMSS   Non-motor symptoms scale

PD   Parkinson's Disease

PDD   PD dementia

PDQ-39   PD Questionnaire 39

PFC   Prefrontal cortex

PIGD   Postural instability gait difficulty

REM   Rapid eye movement

SNc   Substantia Nigra pars compacta

SNr   Substantia Nigra pars reticulata

STN   Subthalamic nucleus

UPDRS   Unified Parkinson's Disease Rating Scale

VM   Ventral mesencephalon

VTA   Ventral Tegmental Area

Chapter 1 Introduction

1.1 Parkinson's Disease

1.1.1 What is Parkinson's Disease?

Parkinson's disease (PD) is a neurodegenerative disorder, first clinically documented by James Parkinson in his essay on patients presenting with a 'shaking palsy' (Parkinson 1817). The refinement of specific clinical features relating to the disorder, and naming, was later document by Jean Martin Charcot (Charcot 1886). Over 200 years on, the prevalence of PD within the UK, as of 2021, is over 145,000 cases. The projected rate of newly diagnosed cases is around 18,000 a year (parkinsons.org.uk). Worldwide, PD is the 2nd most common neurodegenerative disorder behind Alzheimer's Disease (AD), highlighting how prevalent the condition is and the importance of research required for the ever-growing affected population. As a disease of ageing, PD has an age of onset typically around 65 years with early (or young) onset PD (E/YOPD) being any diagnosis before the age of 50, whilst juvenile PD occurs in rare cases before the age of 21. This early onset is prevalent in around 3-7% of all PD cases (Quinn et al. 1987; Golbe 1991; Niemann and Jankovic 2019).

The most common diagnosis of PD is idiopathic, with no known specific cause of onset. However, there are certain factors that can change the risk of onset of PD. These range from increased likelihood of developing PD due to pesticide exposure in farmlands to decreased likelihood due to smoking and other lifestyle choices (Dick et al. 2007; Ascherio and Schwarzschild 2016). Onset of PD due to genetic risk factors occurs in approximately 10% of total PD cases. Genome-wide association studies (GWAS) and meta-analysis of longitudinal cohort studies have found associations with risk of onset in *loci* such as *LRRK2*, *GBA* and *SNCA* amongst many others (Simón-Sánchez et al. 2009; Pihlstrøm et al. 2018; Iwaki et al. 2019).

1

1.1.2 Pathology of PD

PD is characterised in its pathology by loss of dopaminergic (DAergic) neurons within the ventral midbrain. This loss in patients is up to 90-95% of DAergic neurons residing in the substantia nigra pars compacta (SNc) with other structures such as the ventral tegminal area (VTA) also showing neuronal loss. Approximately 50-60% of DAergic neurons are lost before the onset of motor symptoms with clear structural brain changes prior to diagnosis (Booij and Knol 2007; Kim et al. 2009; Stacy et al. 2010). Damage also occurs in areas external to the midbrain such as the hippocampus, thalamus, septum, and other cortical areas due to specific loss of DA and also disruption to cholinergic, serotonergic, and noradrenergic neurons and their circuitry (Jellinger 1999; Giguère et al. 2018). The loss of DAergic neurons within the SNc leads to a degradation of synaptic input to the striatum leading to the hallmark motor and non-motor symptoms of PD. Many biomarkers have been used to allow confirmation of PD prior to post-mortem analysis. DAergic SNc loss correlates with striatal DA transporter binding (Kraemmer et al. 2014), but this was challenged by Honkanen et al. (2019) who found no correlation between DA neuronal fibers and DAT transporter uptake. Studies tracking the loss of DA neurons as disease progression occurs suggest that loss within the SNc begins in the ventro-lateral tier, then ventromedial tier and finally dorsal tier (Fearnley and Lees 1991).

Lewy bodies

The second key pathological characteristic of PD is the presence of aggregated alpha-synuclein-containing inclusions within the neuron, referred to as Lewy bodies, and Lewy neurites within the neuronal cell processes (Spillantini et al. 1997; Trojanowski and Lee 1998; Kosaka 2014; Engelhardt and Gomes 2017). Some researchers have suggested that it is the Lewy body formation, rather than the fibril formation, is the major driver for degeneration (Mahul-Mellier et al. 2020). Lewy body aggregates also comprise amyloid filaments and are commonly found in the nuclei of the midbrain during post-mortem analysis, but as the disease progresses, these inclusions can be found throughout the central and autonomic nervous system (Bethlem and Den Hartog Jager 1960). The progression of the disease has also been modelled using Braak staging. This model proposes the spread of alpha-synuclein to different areas of the brain, which is believed to begin within the olfactory tubercle in some patients and to progress on to the main central nervous system (Rietdijk et al. 2017). In terms of the involvement of Lewy body pathology to motor symptoms, the

proportion of Lewy bodies were found to be stable in SNc neurons over time, but DA neurons will continue degenerate at a rapid rate (Greffard et al. 2006). Other researchers have argued that alpha-synuclein inclusions may be neuroprotective (Stefanis 2012). Together this suggests the field has not quite reached a consensus on the role of Lewy bodies in PD, and the presence of Lewy bodies can also occur in patients independent of a PD diagnosis.

Gut first or brain first?

Within the field, there is also a dichotomy of thought of where PD originates. Researchers have proposed that in some patients PD originates outside of the brain and may begin within the gut (Eisenhofer et al. 1997; Hawkes et al. 2007; Yang et al. 2019; Borghammer 2023).The 'gut-brain axis', which is the bidirectional communication between the gut and the brain, has become of interest due to the finding that alpha-synuclein inclusions was found within the enteric nervous system (Grathwohl et al. 2013; Klann et al. 2021). Patients, and also animal models of PD, can have poor gut mobility and gastrointestinal problems such as bloating, constipation, and dysphasia (Toti and Travagli 2014; Pfeiffer 2018; Warnecke et al. 2022; Cui et al. 2023). Interestingly, gut microbiota composition has been found to lead to variability in the uptake of levodopa (L-DOPA) and its availability (Maini Rekdal et al. 2019). Treatments such as probiotics have been used with the hopes of improving PD symptoms through altering gut microbiota and reducing inflammation (Magistrelli et al. 2019; Castelli et al. 2020; Martini et al. 2023). Due to the considerable amount of heterogeneity present under the umbrella of PD, it is likely that some people may present with 'brain first' and others with 'gut first' PD (Nuzum et al. 2022).

1.1.3 Clinical motor symptoms

The hallmark clinical features associated with PD are bradykinesia, tremor at rest, rigidity, and postural instability (Jankovic 2008). Other symptoms may include a shuffling gait, hypomimia, flexed posture and freezing motor blocks, yet patients receiving a diagnosis may present with some or all of the cardinal symptoms at that time. Over 90% of patients present with unilateral motor symptoms at the time of diagnosis which becomes more symmetrical as the disease progresses (Yagi et al. 2010; Pagano et al. 2016). Symptoms such as postural instability are the main cause of falls, contributing to the disability increase in PD

(Giladi et al. 2001; Pelicioni et al. 2019) and the psychological impact of the disease on motor confidence.

Diagnosis occurs through scores on specific rating scales such as the Unified Parkinson's Disease Rating Scale (UPDRS) and patients must have at least two of the cardinal symptoms for a diagnosis. Patients must also have a positive response to L-DOPA in order to receive a classical PD diagnosis or may instead have disorders such as multiple system atrophy, corticobasal syndrome, supranuclear palsy or dementia with Lewy bodies that come under the diagnostic umbrella of atypical Parkinson's disorders. These disorders share a common feature of the presence of aggregated protein of either alpha-synuclein or tau, and most have some form of atrophy except dementia with Lewy bodies (Levin et al. 2016).

Motor symptoms in PD get progressively worse as the disease advances with some advancing quicker than others, such as rigidity progressing faster than tremor (Schüpbach et al. 2010). The extent of DA neuronal loss in the lateral part of the SNc has been well correlated to the onset of bradykinesia and akinesia (Rinne et al. 1989; Greffard et al. 2006) but their role in tremor for example is less clear.

Subtypes of PD

The onset of different motor symptoms and the progression of these are affected by multiple factors including age at onset and are heterogeneous amongst PD patients. Broadly, patients can be organised into tremor dominant and non-tremor dominant (also known as PIGD – postural instability gait disorder) and will respond to treatment differently, and symptoms may progress at different rates depending on the sub-diagnosis (Caroline et al. 2013). PIGD patients have more rapid motor progression but respond better to DAergic treatment than tremor dominant patients (Barbagallo et al. 2017; Zach et al. 2020). Differences in these two subtypes are also evident in relation to changes in brain structure seen by fMRI. Patients with PIGD were found to have greater atrophy of grey matter in primary motor areas and reduced activation in the globus pallidus (Prodoehl et al. 2013; Rosenberg-Katz et al. 2013; Zhang et al. 2016)

1.1.4 Clinical non-motor symptoms

Alongside motor impairments, non-motor symptoms are a major part of the clinical picture of PD and a critical aspect of disease progression. The most common rating scale for non-motor symptoms in PD is the PD Questionnaire 39 (PDQ-39) which is disease-specific, separating non-motor symptoms into eight domains, giving a mean value score according to a summary index (Peto et al. 1995). Some of the domains include: activities of daily living, emotional well-being, cognition and bodily discomfort. Rating scales such as the Non-Motor Symptoms Scale (NMSS) is also used to assess a range of non-motor symptoms and their severity and frequency in patients and can be used as a clinical outcome measure (van Wamelen et al. 2021). Like many other neurodegenerative disorders, it is now apparent that PD has a distinctive prodromal stage of impairments evident prior to diagnosis in which a large majority of the pathological disease progression occurs (Figure 1.1). Some of the most common non-motor symptoms that occur in the early stages of PD are those such as REM sleep disorder, anxiety, depression, olfactory dysfunction and constipation (Chaudhuri et al. 2006). REM sleep disorder has been considered a biomarker for the onset of PD due to associations with many other prodromal risk factors and the extremely high conversion of early REM sleep disorder to PD, which has been evaluated at over 70% within 12 years (Postuma et al. 2015; Sixel-Döring et al. 2016). When examining the prodromal phase, Weintraub et al. (2017) identified that lower cognition at the start of the prodromal phase did not predict PD onset, but those who did go on to receive a PD diagnosis performed significantly worse on 5 out of 6 of the cognitive assessments. Imaging studies using [^{18}F]dopa have been used to try and identify the length of the prodromal phase and found that signal in the putamen was the greatest tool to show degeneration over time, with mean length of the prodromal phase in this study of 32 patients, to be 7 years (Morrish et al. 1998). Due to the extensive length of this window, there is countless efforts for biomarkers and other factors to diagnose as early as possible, and therefore provide therapeutic intervention at this stage.

Visual disturbances also occur in PD, as is shown in the mild to moderate stages of PD. Patients were found to struggle the greatest with spatial tasks and visual memory (Uc et al. 2005). As the disease progresses, more taxing cognitive impairments can be present such as visual hallucinations, autonomic dysfunction, cardiovascular, gastrointestinal and urogenital issues and dementia (Weil and Reeves 2020). Similar to motor symptoms,

patients presenting with non-motor symptoms have a high comorbidity with other non-motor symptoms and only a very small percentage present without any non-motor symptoms. Poor sleep quality has a high comorbidity for anxiety, depression, and severity of symptoms, and the better the sleep quality, the better the cognitive performance on scales such as the mini-mental state exam (MMSE) (Shulman et al. 2001; Visser et al. 2009).

Cognitive impairment in PD

Cognitive impairment is a notable aspect of disease progression in PD, with the risk of onset being 6-fold higher than in age-matched healthy individuals (Aarsland et al. 2001). Types of cognitive impairments that patients might present with are attention deficits, difficulties with executive function, memory impairments and visuospatial deficits (Watson and Leverenz 2010). In a cohort of 115 newly diagnosed PD patients, 24% could be classified as cognitively impaired due to their performance primarily in tasks relying on executive function and memory (Muslimovic et al. 2005). Age of onset also correlated to severity of the cognitive impairment. Memory impairments were found to be the most prevalent 3 years after follow-up of newly diagnosed patients in the ICICLE-PD study (Yarnall et al. 2014). Newly diagnosed and untreated patients who made complaints about having memory problems during their initial observations were more likely to develop cognitive impairments (Erro et al. 2014).

Executive dysfunction deficits, as well as memory impairment, have been found to be a predictor of dementia as measured by performance in tests measuring immediate and delayed recall (Levy et al. 2002). Attention deficits in patients have been observed with slower reaction times to tasks such as the network attention test that was independent of accuracy to perform the task (Yang et al. 2021). In terms of visuospatial function, approximately 60% of patients (out of a cohort of 35) performed poorly on the judgement of line orientation and clock drawing (Royall et al. 1998; Pena et al. 2008). Testing mild cognitive impairments such as visuospatial function and attention in animal models is employed throughout this thesis and is discussed in detail in Chapter 3.

Cognitive impairment increases as the disease progresses and is often placed into subcategories throughout that progression, such as mild cognitive impairment and then later on, PD dementia (PDD). PDD was found to occur in up to 80% of patients and greater cognitive impairment and incidence of dementia correlated with DA neuronal loss (Rinne et

al. (1989), specifically within the medial part of the SNc. PIGD patients also display a greater risk of cognitive decline (Burn et al. 2006). A review of patients 15 years after the end of the Sydney Multicentre Study of PD found that there was a >66% mortality rate and cognitive decline in 84% of 149 recruited patients, with almost half able to be clinically diagnosed with dementia. This re-evaluation shows how prevalent cognitive decline is over time and the importance in circumventing with therapeutic treatment at an early stage (Hely et al. 2005).

The importance of non-motor symptoms

Non-motor symptoms are often underdiagnosed by treating neurologists and are poorly understood. A study evaluating 101 patients on scores of standardised non-motor testing in PD compared to neurologists, found neurologists failed to identify common non-motor symptoms such as anxiety, depression, and fatigue more than 50% of the time during routine visits (Shulman et al. 2002). A review of clinical trials, specifically those treating cognitive impairments in PD, found a bias towards reporting positive outcomes, despite the statistical evidence to support this including a large majority of trials not being completed, having only a very short follow-up post-intervention and a small and non-diverse target population (Bayram et al. 2023). Studies such as those detailed by Shulman *et al* (2002) are important, as non-motor symptoms appear to disproportionately impact on quality of life for patients (Barone et al. 2009; Leroi et al. 2012).

Network analysis of over 689 patients found fatigue, depression, hyperhidrosis, impaired concentration as well as daytime sleepiness were the most influential symptoms that impact health-related quality of life (Heimrich et al. 2023). Goldman et al. (2018) details in a report from a multidisciplinary symposium how one of the greatest concerns for caregivers and patients in PD is cognitive decline. Some clinicians and researchers feel the summary index readouts for patients can be ambiguous and may lead to false readings and thus impact treatment options, yet daily diaries alone were not effective to use for assessing non-motor impairments in patients. This highlights the need for extensive and constant critical examination of the assessment criteria for non-motor symptoms (Hagell and Nilsson 2009; Schrag et al. 2009; Buck et al. 2010; Soh et al. 2011).
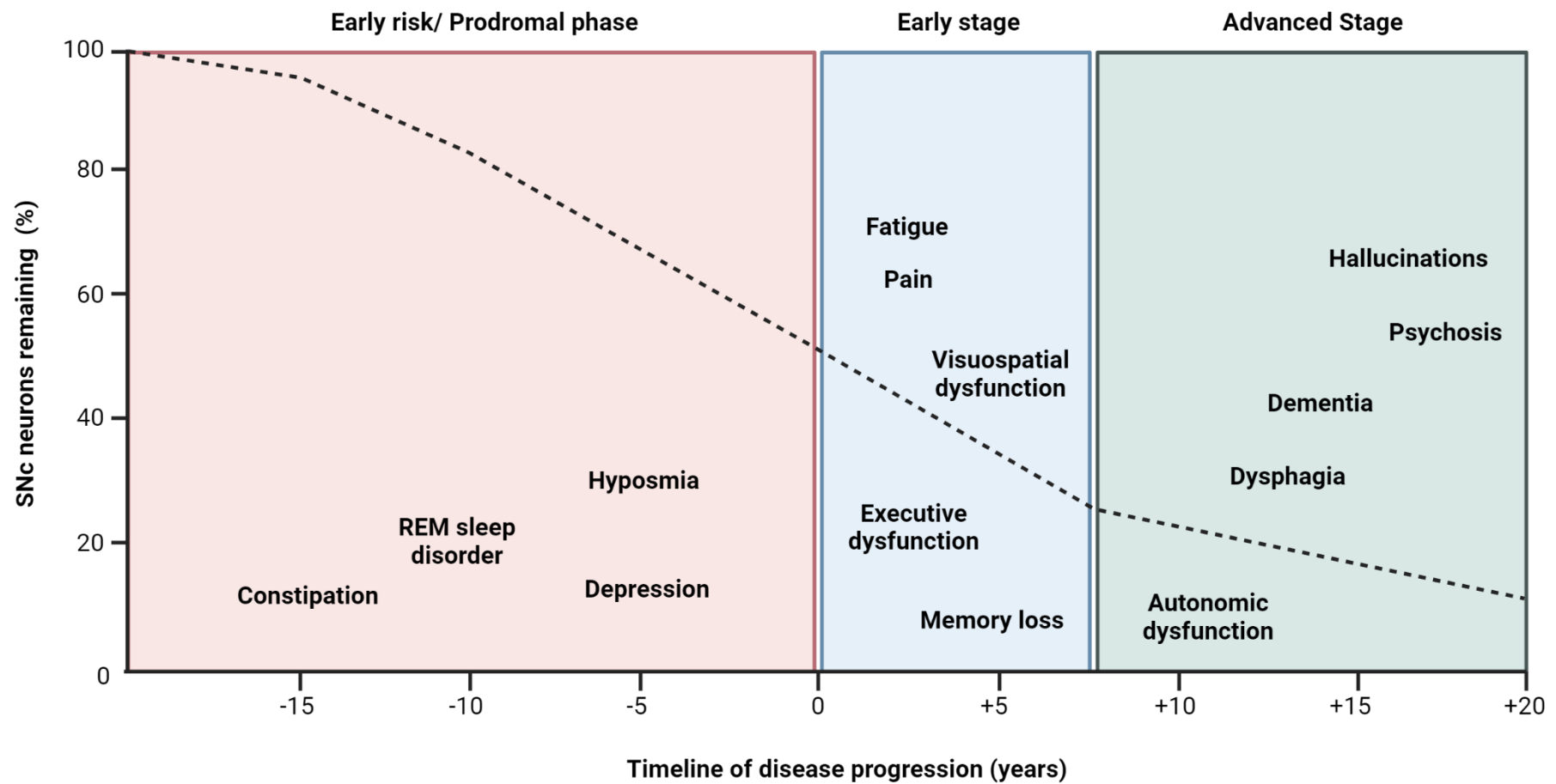
Figure 1.1. Progression of Non-motor symptoms in PD. Y axis indicates the percentage of SNc neurons remaining, that declines over time (dashed line). X axis indicates the timeline of disease, 20 years before and after diagnosis. Modified from Kalia and Lang (2015) and Vermeiren et al. (2020).

1.2 Basal ganglia

In order to understand the neurobiology of PD, it is important to consider what is known of the key circuitry affected by the nigrostriatal loss, in particular the basal ganglia.

The basal ganglia are a group of interconnected nuclei that are fundamental for executive function, voluntary motor coordination and action selection (Alexander et al. 1986). The main nuclei of the basal ganglia are the putamen and caudate nucleus (collectively called the striatum in rodents), the external and internal segments of the globus pallidus (known as the GPe and GPi, respectively), and three adjacent structures known as the subthalamic nucleus (STN), ventral tegmental area (VTA) and the substantia nigra (pars compacta (SNc) and pars reticulata (SNr)). These structures form connections with external basal ganglia nuclei such as the thalamus, cortex, and brainstem to form vital neural circuits.

The striatum is the main output nucleus of the basal ganglia, and its heterogeneous structure has been evolutionarily conserved in mammals (Stephenson-Jones et al. 2011). The main neuronal population residing within the striatum is the gamma-aminobutyric acid (GABA)ergic medium spiny neurons (MSNs), which make up 95% of the striatal architecture. They express DA and cAMP regulated phosphoprotein 32 (DARPP-32), as well as coup TF1-interacting protein 2 (CTIP-2) and forkhead box protein 1 (FoxP1), during development and through into maturity (Walaas and Greengard 1984; Arlotta et al. 2008; Precious et al. 2016). The remaining 5% is believed to be a combination of astrocytes, with GABAergic and cholinergic interneurons, which are critical regulators for striatal functioning (Gittis et al. 2010; Tanimura et al. 2018). The striatal architecture is organised broadly into these dense structures throughout the striatum known as the striosomes (also referred to as patches) and the surrounding labyrinth known as the matrix (Desban et al. 1993). This topological organisation serves a purpose with striosomes receiving almost exclusive innervation of DA projections from the SNc and the matrix containing a mix of both D1 and D2 receptors.

The SNc is a pigmented structure, located in the midbrain. This collection of nuclei is made up of 2 sub-regions: the SNc and SNr (Moore and Bloom 1978; Nuzum et al. 2022). The SNc is densely populated with DAergic neurons known as the 'A9' phenotype, which express tyrosine hydroxylase (TH) and the inward rectifying potassium channel GIRK2 as key biomarkers.

This area is important due to its afferents connecting to striatum along the nigrostriatal pathway. The nigrostriatal pathway is a fundamental network of dopamine supply from the midbrain to areas of the basal ganglia. The nigrostriatal pathway begins in the SNc, with neurons projecting to the dorsal striatum. The nigrostriatal pathway is primarily affected in PD due to the loss of SNc DAergic neurons, with can be seen in post-mortem analysis (Kordower et al. 2013). Located adjacent to this area is the ventral tegmental area (VTA). The mesolimbic pathways begin in the VTA and project up to the nucleus accumbens, amygdala, hippocampus, and prefrontal cortex (Aransay et al. 2015; Caminiti et al. 2017). The VTA is responsible for motivation and prediction error and also contains DAergic neurons, but with an A10 phenotype (expressing TH and the vitamin-d dependant calcium binding protein, calbindin (Cohen et al. 2012)). The topology of the striatum and the circuitry between the striatum and the ventral midbrain and thus, its role in behavioural output is discussed in more detail in Chapter 5.

1.2.1 The classical model

The main consensus for how the basal ganglia operates is through the classical direct and indirect pathway model (Alexander and Crutcher 1990). The direct and indirect pathway are synergistic in nature, with the direct pathway's main function is to promote behaviour, whereas the indirect pathway is to suppress behaviour (Smith et al. 1998).

Direct pathway

The direct pathway begins with excitatory glutamatergic input from the cortex to the striatum, which in turn projects inhibitory GABAergic projections to the GPi and SNr. The GPi and SNr then project to the thalamus, leading to disinhibition of the glutamatergic neurons residing within the nuclei. The thalamus then sends the relayed information to the motor cortex to promote behaviour, completing the circuit. As part of the direct pathway, the striatum receives direct information regarding movement coordination from the SNc through D1 receptors present on the MSNs, releasing DA to mediate striatal functioning and coordinate movement (Gerfen et al. 1990).

Indirect pathway

The indirect pathway begins again with input from the cortex and projections synapsing onto the GABAergic projections within the striatum. Instead, striatal MSNs project initially to the GABAergic neurons of the GPe which project to the glutamatergic neurons of the STN to inhibit firing (Shink et al. 1996). The STN sends out inhibitory projections to the SNr, and on to the thalamus, which relays information to the cortex to begin suppressing behaviour and completing the circuit. Again, the SNc and VTA send projections directly to the striatum releasing DA to D2 receptors (Moore and Bloom 1978; Gerfen et al. 1990). As well as DAergic neuronal projections on the GPe and SNr, these two nuclei also receive information from the amygdala during the process of emotional regulation (Amita et al. 2019).

The dysfunction of the indirect pathway in PD

The regulation of behaviour through the direct and indirect pathway are in constant coordination in order to properly promote or supress action initiation, and disruption in these two pathways has been explored for the basis of symptoms in neurodegenerative disorders such as PD. As previously stated, and also described in greater detail below, DA neuronal projections synapse onto the GABAergic MSNs, specifically targeting D1 (Gs, stimulatory) and D2 (Gi, inhibitory) receptors. In PD, SNc neurons degenerate, leading to a depletion in DA signalling to both D1 and D2 receptors in the striatum. Loss of innervation through D1 receptors leads to reduced activation of the direct pathway, and disinhibition of the D2 receptors causes dysregulation and an over-activation of the indirect pathway. This overactivation of the indirect pathway leads to hyperactivity in the GPi and SNr nuclei, resulting in increased levels of inhibition onto the thalamus, which in turn largely diminishes signalling to the cortex, leading to a decrease in motor function and the onset of motor symptoms such as bradykinesia and others mentioned previously above (Albin et al. 1989).

1.2.2 Brain stem involvement in basal ganglia functioning and PD

Although the DAergic system is the main subtype to be dysregulated within PD, other neurotransmitter systems are impacted by disease onset, and may contribute to disease pathology.

Serotonergic system

The main source of serotonin (5HT) supply for the brain is from the dorsal raphe nucleus (DRN), a structure that makes dense projections to the basal ganglia, specifically the SNc and striatum (Huang et al. 2019). As well as the loss of 5HT neurons in the DRN that has been reported from post-mortem studies, the DRN also contains DAergic neurons that are impacted by the onset of PD (Halliday et al. 1990; Boi et al. 2023). It has been suggested that the caudate preferentially loses 5HT innervation compared to the putamen in PD patients, but this finding was not consistent amongst all PD patients examined (Kish et al. 2008). 5HT dysfunction has been linked to the development of non-motor impairments such as REM sleep disturbances and fatigue (Pavese et al. 2010; Politis and Loane 2011; Wilson et al. 2018).

Noradrenergic system

The main site of noradrenergic innervation, the locus coeruleus (LC), sends out wide-spread projections, mainly to the cortex to support adaptive behaviour, but also sends afferents to the VTA (Mejías-Aponte et al. 2009). In PD, the LC is one of the first regions in which Lewy body accumulation has been identified, likely to occur within the prodromal phase. One theory is that there is overcompensation of the noradrenergic system in PD, contributing to an exacerbation in non-motor symptoms such as autonomic dysfunction, sleep disorder and depression (Paredes-Rodriguez et al. 2020). Later on in disease manifestation, LC neurons are lost, resulting in decreased noradrenaline to the hypothalamus and cortex (Sun et al. 2023).

Cholinergic system

Cholinergic interneurons in the striatum mostly reside within the border regions of the striosomes to regulate incoming DAergic signal from the SNc. Dysfunction of cholinergic interneurons has been implicated in PD (Tanimura et al. 2018; Ztaou and Amalric 2019). Activation of cholinergic interneurons within the striatum reduced anxiety-like-behaviour in 6-OHDA lesioned mice, leading to the suggestion that dysfunction in the cholinergic system could play a role in the onset of non-motor symptoms in PD (Ztaou et al. 2018).

Glutamatergic system

The cortex is the largest input source to the basal ganglia and most regions project directly to the striatum, forming distinct pathways known collectively as the cortico-striatal pathway. The putamen receives afferent connections from the somatosensory cortex, auditory cortex (A1) and motor cortex (Reiner et al. 2010). The caudate receives afferent connections from the prefrontal cortex (PFC) and visual cortex. Afferents from the SNc and VTA to the PFC are disrupted in PD and altered dopamine signalling in the PFC can have substantial effects on working memory processing. Non-human primate and rodent studies have displayed how important the level of dopamine signalling is, showing that greater extracellular dopamine activity can impair PFC-mediated cognitive functions (Murphy et al. 1996). Studies using a D1 receptor agonist reported a dose-related impairment in spatial working memory that could be recovered using a D1R antagonist (Zahrt et al. 1997). Too little dopamine signalling has also been shown to impact spatial working memory which can be recovered using a low dose D1R agonist (Cai and Arnsten 1997). These collective studies support the consensus that cortical DA works on an inverted 'U' function, meaning dopamine levels need to be within a very narrow range to avoid impairing PFC-mediated cognitive function (Vijayraghavan et al. 2007). The concept of the inverted 'U' function of cortical DA circuitry is covered in greater detail in Chapter 4.

Figure 1.2 Classical circuitry of basal ganglia and the impact of PD. Modified from McGregor and Nelson (2019). Dashed lines represent a loss of innervation. Thick lines represent overactivation of that specific pathway. .

1.3 Animal models of PD

The use of animal models for pre-clinical PD research is critical to understand underlying mechanisms of disease, to model motor and non-motor symptoms alongside the extent of degeneration throughout the brain, and thus evaluate the efficacy of treatments in alleviating those deficits. The literature on animal models of PD within this chapter has been separated into three categories: toxin, viral vector-based and transgenic models, and has been summarised in Table 1 and Table 2. Due to the complexity of idiopathic PD, one model is not capable of encompassing all aspects of the disease and often researchers select which model is best for their chosen question (Lama et al. 2021). A breakdown of the most common PD animal models is presented in (Table 1) and further context in relation to the neurobiology is detailed below.

1.3.1 Toxin models

6-OHDA

The 6-hydroxydopamine (6-OHDA) lesion model is one of the most commonly used models for PD research. 6-OHDA is a neurotoxin, which targets the catecholamine neurons (those releasing DA, norepinephrine, or epinephrine) via the DA active transporter (DAT). Transport through the DAT causes selective degeneration of DA terminals and retrograde transport to the cell body, leading to cell death. One mechanism for cell death due to 6-OHDA is through the inhibition of mitochondrial complex I and IV leading to an increase in free radicals (Glinka and Youdim 1995). 6-OHDA is preferred as a method of creating PD animal models due to its relatively stable lesions depending on the target site, causing irreversible loss of DA neurons. 6-OHDA cannot cross the blood brain barrier so must be infused through direct administration to the brain. However, 6-OHDA can impact 5HT and noradrenergic circuits (Descarries et al. 1992; Cunningham et al. 2005) and in order to mitigate any impact on non-DA neurons, desipramine may be administered during surgery to prevent the uptake of 6-OHDA into noradrenergic and 5HT neurons (Türker and Khairallah 1967).

Application of 6-OHDA

6-OHDA can be targeted to cell body regions such as the SNc, along the medial forebrain bundle (MFB) which carries the nigrostriatal projections, and into the striatal terminals, each carrying slightly different profiles of neuronal loss and the time course for that loss. The earliest work using 6-OHDA as a model of PD was an injection into the SNc, which led to anterograde loss of DA in the striatal terminals and ablation of DA neurons (Ungerstedt 1968). Studies of direct injection into the SNc in both rat and mice has found DA cell loss to be progressive with cell degeneration still occurring after loss of DA from the striatal terminals (Cole et al. 1994; Jeon et al. 1995; Grealish et al. 2010).

Striatal lesions induced rapid depletion of DA in the striatal terminals and retrograde loss along axonal projections, causes degeneration of the DAergic neurons of the ventral midbrain. Striatal lesions, when used effectively, can induce comparable motor deficits to both nigral and MFB lesions (Zigmond et al. 1990; Przedborski et al. 1995; Kirik et al. 1998; Heuer et al. 2012). Striatal lesions offer the ability to target specific striatal subregions that receive DA innervation or even regions external to the striatum that receive DA to evaluate behaviour in both operant and motor tasks (Mendes-Pinheiro et al. 2021). Striatal lesions and their application will be discussed in greater detail in Chapter 5.

6-OHDA in the MFB

Bilateral 6-OHDA lesions have severe side effects causing impairments (severe akinesia in both paws and orolingual area) that lead to an inability to eat and drink effectively (Ungerstedt 1971a; Zigmond and Stricker 1972), thus unilateral lesions are the preferred application of 6-OHDA MFB lesions, leaving the animals functionally able to look after themselves. Unilateral 6-OHDA MFB lesions also offer a within-subjects control, as the contralateral hemisphere and nigrostriatal pathway is largely spared. Hallmark motor symptoms of unilateral 6-OHDA MFB lesions are a rotational motor bias that can be exacerbated in response to DAergic drugs such as amphetamine and apomorphine, and can be recorded in an unbiased fashion in automated rotometers (Björklund and Dunnett 2019). In MFB lesions, cell bodies are lost first before the degeneration of projections and denervation of the striatum (Zuch et al. 2000). The unilateral lesion causes a DA imbalance that can be probed with a DA releasing agents such as amphetamine, which drives D1 receptors in the intact striatum, forcing ipsilateral biased locomotion. Apomorphine however,

acts upon the super-sensitised DAergic receptors in the lesioned hemisphere, driving locomotion in a contralateral direction away from the side of the lesion (Ungerstedt and Arbuthnott 1970; Grealish et al. 2008). 6-OHDA MFB lesions also induce impairments contralateral to the lesion, such as forelimb akinesia and sensorimotor deficits (Grealish et al. 2008). As well as motor impairments, the 6-OHDA MFB lesion induces substantial non-motor deficits in visuospatial function, motivation and attentional deficits that can be evaluated in lateralised operant tasks (Carli et al. 1985; Döbrössy and Dunnett 1997; Heuer and Dunnett 2012). The application of operant tasks such as the lateralised choice reaction time task, will be discussed in detail in the Methods (see 2.5) and Chapter 3. 6-OHDA is the toxin employed throughout all chapters within this thesis, due to its rapid onset of nigral degeneration and robust, stable DA depletion within the striatum. The resulting contralateral motor and cognitive deficits can be investigated for improvement when using therapies such as cell, viral-vector based and L-DOPA replacement therapy.

MPTP

Another commonly used neurotoxin model of PD is 1-methly-4-phenyl-1,2,3,6-tetrahydropyridine (MPTP) which was found, accidentally, in humans to produce parkinsonian symptoms as a result of severe toxin-induced DA neuronal loss in the SNc (Langston et al. 1984a; Langston et al. 1984b). MPTP crosses the blood-brain-barrier, is metabolised into MPP^+ and, similar to 6-OHDA, is selectively transported by DAT to DA neurons leading to degeneration due to mitochondrial dysfunction (Javitch et al. 1985). MPTP is the most common method of creating a PD model in non-human primates (NHPs). This means they are often used in pre-clinical efficacy trials as it was found to show the most progressive motor symptoms and selective nigrostriatal DA loss (Jenner and Marsden 1986; Schmidt and Ferger 2001; Fox and Brotchie 2010). The motor and non-motor deficits have also been classified in rating scales adapted from clinical tools with PD patients, increasing the translational relevance and reliability of this model for pre-clinical screening (Choudhury and Daadi 2018). In rodents, rats are much less susceptible to MPTP toxicity. MPTP mouse models are widely employed in pre-clinical research, but display a slower degeneration pattern compared to 6-OHDA, with varied striatal DA loss and accompanying motor deficits, depending on the dose used and administration protocol (Pileblad et al. 1985; Alvarez-Fischer et al. 2008; Meredith and Rademacher 2011; Santoro et al. 2023).

Rotenone

Rotenone is a pesticide and mitochondrial 1 complex inhibitor. Its administration as a model for PD causes loss of DA in striatal terminals and some loss of neurons within the tail end of the SNc, but has had varying degrees of success as a reliable model with high variability within cohorts (Betarbet et al. 2000; Lapointe et al. 2004; Radad et al. 2019). One success of the rotenone model was helping to further support the link between mitochondrial dysfunction and DA neuron degeneration (Greenamyre et al. 2010). Interestingly, it has been shown that subclinical doses of rotenone, combined with subclinical expression of alpha-synuclein, together can result in a significant loss of DA neurons and associated motor impairments (Naughton et al. 2017). This suggests that exposure to pesticides in susceptible individuals may be sufficient to induce PD. Other pesticides have been linked to development of PD such as paraquat and maneb (Table 1). The study of pesticides and their correlation with PD onset is vital to prevent the use of harmful substances in agriculture and limit exposure to the general population.

1.3.2 Viral vector-based models

One of the downsides to neurotoxin models of PD is the severity of the pathology and they lack a comparable level of progression and alpha-synuclein to that seen in humans. Toxin models are also challenging tools for neuroprotection studies due to the rapid and permanent cell death that occurs. Alternatives have been employed, such as viral vector-based models to overexpress wild-type alpha-synuclein, express mutant forms of the alpha-synuclein or express other PD-associated genes (Fischer et al. 2016). One benefit of a viral vector-based model of PD is the ability to modulate the dose and thus the exposure to alpha-synuclein pathology. Most viral vector-based models employ lentivirus or adeno-associated virus to transfer the human PD risk transgene to a rodent for modelling, with the most common being SNCA, (Kirik et al. 2002b; Kirik et al. 2003; Volpicelli-Daley et al. 2016).

1.3.3 Transgenic models

Case studies of familial PD and the discovery of common mutations in specific disease related genes have been the basis for many transgenic mouse models used throughout pre-clinical research in PD (Harvey et al. 2008). Drosophila models of PD are useful to investigate gene interactions and manipulate insertion/deletion of a gene of interest (Xiong et al. 2017). The benefit of using transgenic mouse models of PD is the ability to build up large cohorts of experimental animals for studies without the need for surgical intervention and the ability to study the effect of a particular gene mutation in the whole body. The problem however with transgenic PD models is that they are often limited in terms of motor deficits and midbrain DA loss. Also, the vast majority of PD cases are idiopathic and may have genetic risk for a number of risk genes rather than one gene driving monogenetic disease onset (Reed et al. 2019). Transgenic models were not used within this thesis due to the focus on evaluating cognitive and motor function in a DA depleted striatum, hence the unilateral 6-OHDA MFB model was employed. Nonetheless, a detailed list of the most common transgenic models of PD is presented in Table 2.

Model	Motor deficits	Non-motor deficits	Advantages	Disadvantages
6-OHDA	• Forelimb akinesia (Olsson et al. 1995; Dowd et al. 2005) • Drug-induced rotations (Ungerstedt 1971b; Iancu et al. 2005) • Sensorimotor deficits (Ogura et al. 2005; Chao et al. 2012) • LIDs in response to L-DOPA treatment • Fine motor control impairment (Whishaw et al. 1997)	• Depression-like symptoms (Kamińska et al. 2017) • Visuospatial dysfunction (Heuer and Dunnett 2012; Lindgren et al. 2014b) • Attention (Fan et al. 2020) • Sleep disturbances (Vo et al. 2014) • Poor gut mobility (Blandini et al. 2009; Colucci et al. 2012) • Olfactory issues (Zhang et al. 2019)	• Ability to be used in multiple rodent species. • Can selectively target different parts of the nigrostriatal pathway and targets the catecholamine neurons • Rapid degeneration with model, ~95% degeneration of SNc and Striatal DA content • Unilateral model allows for in-subject control	• Not a useful model in NHP • Has no alpha-synuclein pathology • Rapid and irreversible degeneration of DA neurons minimises use outside of a chronic model. • Increased mortality and seizures in the rat, and further increased mortality in mice • Unilateral model limits behavioural tests to lateralised manipulations
MPTP	• Dystonia (Norris et al. 2023) • LIDs in response to L-DOPA treatment (Blanchet et al. 2004) • Tremor (Tetrud et al. 1986) • Forelimb akinesia (Blume et al. 2009)	• Impaired delayed alternation (Schneider et al. 2013) • Impaired object recognition (Elsworth et al. 1999) • Impaired memory acquisition and attention (Da Cunha et al. 2001) • Slowed gut motility (Ellett et al. 2016)	• Has been used effectively as a model in non-human primates (Fox and Brotchie 2010) • Selective depletion of DA neurons in the SNc (Burns et al. 1983) • Loss of DA terminals in putamen and caudate (Moratalla et al. 1992)	• NHP's are an expensive model and exclusive to certain institutions • Limited Lewy body pathology • Rat model is resistant to MPTP
Viral vector-based	• Limited mobility in balance beam test (Caudal et al. 2015)	• Spatial and working memory (Hall et al. 2013) • Depressive-like symptoms in forced swim test (Caudal et al. 2015)	• Alpha-synuclein pathology • Similar non motor deficits to 6OHDA lesion (Gubinelli et al. 2022) • Progressive degeneration (Dusonchet et al. 2011) • Striatal DA and SNc neuronal loss (Decressac et al. 2012)	• Majority of cases has mild loss of DA neurons and mild • Mild motor impairment • Mouse viral vector-based models have limited alpha-synuclein inclusions

Pesticides	• Locomotion, abnormal gait and reduced grip strength (Morais et al. 2012)	• Impaired in novel object recognition and passive avoidance (Zhang et al. 2021a) • Poor gut mobility (Bhattarai et al. 2021) • Hyposmia (Aurich et al. 2017) • Depression (Morais et al. 2012)	• Early exposure highlights developmental changes and DA neuronal toxicity (Cory-Slechta et al. 2005) • Dose-dependant nigrostriatal depletion (Brooks et al. 1999) • Can pass through the blood brain barrier	• High mortality in models • Criticized as a relevant model due to paraquat not being transported by DAT (Miller 2007)

Table 1. Overview of the most common toxin and lesion models of PD.

Gene	Types of Mutation(s)	Pathology	Motor deficits	Cognitive deficits
SNCA	• A53T • A30P • WT SNCA overexpression • SNCA triplication • SNCA depletion	• Mild reduction in DA in striatum (Abeliovich et al. 2000) • Alpha-synuclein inclusions in midbrain (Masliah et al. 2000) • Synaptic impairments in transmission (Paumier et al. 2013)	• Motor coordination deficits on rotarod and abnormal gait movement (Paumier et al. 2013) • Late onset ataxia and dystonia (Lee et al. 2002)	• Sex-specific decline in learning and memory • Reduced object recognition • Impaired fear conditioning (Freichel et al. 2007)
PARK2	• Knockout	• Reduction in DAT (Itier et al. 2003) • No loss of DA neurons (Goldberg et al. 2003) • No alpha-synuclein inclusions	• Impaired motor coordination on balance beam (Goldberg et al. 2003)	• Impaired exploratory behaviour and orientation in Morris water maze (Zhu et al. 2007)
LRRK2	• Knock in (G2019S, R1441G K) • Human insertion (BAC promotor) (Beccano-Kelly et al. 2015)	• Mitochondria dysfunction and DA neuronal degeneration in drosophila model (Lee et al. 2007) • No substantial nigral degeneration (Andres-Mateos et al. 2009) • No alpha-synuclein inclusions	• Response to L-DOPA (Li et al. 2009) • Reduced locomotor activity (Tong et al. 2009)	• Visuospatial and attentional deficits (Hussein et al. 2022) • Impairments in novel arm discrimination (Adeosun et al. 2017)

Table 2. Overview of some common transgenic models of PD.

1.4 Treatment of PD

1.4.1 L-DOPA

Levodopa (L-DOPA) is a DA precursor that is converted into DA by the rate limiting enzyme AADC (Best et al. 2009). L-DOPA has been used as a treatment for PD for more than 50 years and is a well-tolerated, gold standard for alleviating motor fluctuations in patients. L-DOPA is currently the most effective drug in reducing UPDRS scores and patients have reported significant improvements in their quality of life (Poewe et al. 2010). However, L-DOPA treatment in patients has varying effects on non-motor symptoms depending on the stage of the disease (Rahman et al. 2014). In one study, an acute L-DOPA challenge in late-stage PD patients was compared to the same L-DOPA challenge in those who underwent deep brain stimulation (DBS) (referred to as advanced staged). Researchers measured responsiveness of L-DOPA to pain, anxiety, and fatigue. Advanced stage PD patients had greater pain and anxiety alleviation with L-DOPA, whereas no effect was seen for late-stage patients, with an accompanying adverse effect of drowsiness (Fabbri et al. 2017). L-DOPA has also been found to impact non-motor symptoms after chronic administration, but it is important to recognise that these are often patient specific such as the development of hypomania can be present in one patient, with another experiencing the onset of depression, indicating that the relationship between L-DOPA administration and non-motor impairment progression is not uniform among the PD population (Goodwin 1971; Poletti and Bonuccelli 2013). Further detail on L-DOPA and cognitive function will be provided in Chapter 4.

Dyskinesias

Responsiveness of motor symptoms to L-DOPA has been found to diminish over time and also begins to fluctuate throughout the course of the day (Barbeau 1971). Patients are continuously monitored on the dose of L-DOPA in order to circumvent this loss of efficacy and limit OFF time. ON refers to medication working and patients experiencing benefit, and OFF refers to the onset of motor fluctuations when the medication is wearing off (Cotzias et al. 1969; Lees 1989). With continued administration, L-DOPA induced dyskinesias (LIDs) appear and present as abnormal involuntary movements, including chorea and dystonia which can add to the stigma of the disease and, if severe, can be very debilitating for patients (Prashanth et al. 2011). Some factors can predict the onset of dyskinesias such as age at

disease onset and the dose of L-DOPA administered (Olanow et al. 2013). There is evidence to suggest that the pulsatile nature of L-DOPA administration is a major contributing factor to the onset of LIDs. In the normal rodent striatum, under normal conditions, basal levels of extracellular DA are maintained at a continuous level, but introduction of L-DOPA to the 6-OHDA rat leads to an increase in extracellular DA, creating an environment that is primed for dyskinesias (Abercrombie et al. 1990).

There have been efforts in recent years to optimise delivery of L-DOPA and mitigate side effects such as LIDs. Trials using a mini pump to supply sub-cutaneous release of L-DOPA have shown improvement in both ON and OFF time measures, showing good support for continual release of dopamine as an optimised treatment for PD (Olanow et al. 2021). One side effect of L-DOPA is poor gastric emptying due to its oral administration. In advanced disease, the use of a levodopa-carbidopa intestinal gel (DuoDopa) has been found to be well tolerated. It can improve QoL PDQ-8 scores, as well as improving NMSS scores for domains such as fatigue, attention and memory and gastrointestinal function that began at 12 weeks and was sustained at 60 weeks after commencing treatment (Antonini et al. 2015; Standaert et al. 2017).

Drug treatments for PD

Alongside L-DOPA, in the early stages of disease, patients may be offered other DAergic medication such as dopamine agonists. Bromocriptine which is a D2 receptor agonist has been used in combination with L-DOPA successfully to help alleviate LIDs (Przuntek et al. 1996; Naz et al. 2022). Medications such as anti-depressants have been administered alongside current DAergic medication and were found to improve depression in PD patients without worsening their motor symptoms (Richard et al. 2012). Other alternatives or in combination with L-DOPA has been evaluated such as catechol-O-methyltransferase inhibitors (COMT) like entacapone, which is used to help prevent the side effects caused by DA medication wearing off but may exacerbate nausea (Kaakkola 2000). However, DA agonists bring their own risks with significant impulse control disorders such as gambling (Driver-Dunckley et al. 2003; Weintraub et al. 2006) and non-motor symptoms such as sleep disturbances can also be worsened (Verbaan et al. 2008; Park and Stacy 2011).

1.4.2 Deep brain stimulation

One current treatment for PD is Deep brain stimulation (DBS). Traditionally patients with more severe motor fluctuations and for whom DAergic medication has become less efficacious have been offered DBS. However, this intervention is being offered increasingly to earlier stage patients (Hartmann et al. 2019). In PD, the process of DBS is to surgically implant electrodes, more commonly into the subthalamic nucleus (STN), but this procedure also has been carried out in the globus pallidus (GP). DBS has also been used for other movement disorders such as multiple sclerosis (MS). The benefits of DBS are that it has been shown to be generally safe and well tolerated in patients and was also found to significantly improve motor fluctuations as well as non-motor symptoms such as the sleep disturbances, perception impairments and to reduce severity and frequency of non-motor fluctuations in the OFF state (Kurtis et al. 2017). A small study looking at 10 patients with adaptive DBS and its interaction with L-DOPA administration found improvement in UPDRS scores, suggesting DBS was effective in subduing LIDs (Rosa et al. 2017). An often-reported side effect of DBS is psychiatric problems. The onset of depression due to DBS has been reported, as well as delusions and disinhibition within PD patients (Pinsker et al. 2013).

1.5 Cell replacement therapy

Cell replacement therapy is a promising therapeutic intervention for PD, based on the principle of replacing DA back into the DA depleted system in a physiological manner with the use of DAergic cells, in order to restore function through circuit reconstruction.

The developing ventral mesencephalon (VM) contains all the progenitors that will give rise to DAergic neurons. Early in the development of cell replacement strategies, scientists sought to transplant the developing progenitors into the host brain to allow them to mature and restore DA loss (Hynes and Rosenthal 1999; Jørgensen et al. 2006). The first applications of fetal cell replacement in pre-clinical animal studies were the transplantation of rat VM initially into the parietal cortex and then subsequently in the striatum of the 6-OHDA lesioned rat model (Björklund and Stenevi 1979; Perlow et al. 1979; Freed et al. 1980; Dunnett et al. 1981). These studies were able to show that the transplanted cells would send axonal projections into the striatum, provide DA back into the depleted area and

improve motor deficits (Schmidt et al. 1983). Both mouse and rat VM grafts have also been shown to improve cognitive impairments induced by the 6-OHDA MFB lesion in an operant task (Dowd and Dunnett 2004; Heuer et al. 2013).

The first clinical application of cell replacement therapy in PD patients was adrenal medullary transplants, due to their ability to release DA. However, recovery only typically lasted a few months and the trials reported poor graft survival (Backlund et al. 1985; Lindvall et al. 1987; Drucker-Colín et al. 1999). Therefore, the consensus was to move towards a more biologically relevant source of DA with human fetal derived tissue (hfVM).

1.5.1 Human fetal transplants into PD patients

Case studies have shown long-term survival of grafted tissue in the human brain transplanted into the putamen, with increased [^{18}F] Fluorodopa signal during PET scanning indicating extensive fibre outgrowth supplying DA to the host brain and caudate nucleus (Lindvall et al. 1990; Kordower et al. 1995; Wenning et al. 1997; Kordower et al. 1998; Hauser et al. 1999). Reports from other case studies outlined the potential long-term benefit of hfVM transplants in which patients experienced gradual motor improvement that was sustained for 14, 18 and 24 years post-transplantation, in some cases, remaining free of any DAergic pharmacological intervention (Hallett et al. 2014; Kefalopoulou et al. 2014; Li et al. 2016).

There has been clear therapeutic potential to using hfVM transplants in PD and plenty of work has been undertaken to optimise the delivery of the cells, the switch to cell suspension instead of tissue pieces and optimisation of the age of donor tissue (Mendez et al. 2005; Björklund and Lindvall 2017). However, the practicalities of using hfVM in clinical trials is impacted by poor accessibility to tissue, variable viability during tissue procurement and the onset of graft-induced dyskinesias (Olanow et al. 2003). Another potential cell source is human pluripotent stem cells (hPSCs).

1.5.2 Human pluripotent stem cells

hPSCs, human embryonic stem cells (hESCs) in particular, are derived from the developing blastocyst, specifically the inner cell mass, from IVF donations, and have fewer ethical implications for PD patients than hfVM (Drevin et al. 2022). Unlike fetal primary tissue, hESCs have the ability of continuous self-renewal and can tolerate long-term freezing, which has allowed the generation of immortalised cells lines through clonal expansion such as H7 and H9 and others to date (Thomson et al. 1998; Amit et al. 2000). hESCs are in a state of pluripotency and have the ability to follow lineages of all three germ layers: endoderm, mesoderm and ectoderm.

In human embryonic development, progenitors respond to intrinsic cues that regulate gene expression and guide those progenitors towards a specified fate. Stem cell differentiation to neural precursor, and ultimately DA progenitors, is based on timed cues through transcription factor modulation (Chambers et al. 2009b; Studer 2012; Panman et al. 2014) and there are now many established protocols designed to create a high yield of A9 DA neurons for transplantation (Andersson et al. 2006; Kirkeby et al. 2012; Nolbrant et al. 2017). The confirmation of these progenitors to have adopted a DAergic fate is by the expression of floor plate markers such as LIM homeobox transcription factor 1a (LMX1A), forkhead box A2 (FOXA2) in their infancy, and TH and engrailed engrailed 1 (EN1) in maturity (Kirkeby et al. 2017).

1.5.3 Induced pluripotent stem cells

Another form of hPSCs is induced pluripotent stem cells (iPSCs). hiPSCs can be isolated from human adult cells and re-programmed back into a pluripotent state in order to direct them towards a desired phenotype, such as DAergic progenitors (Takahashi et al. 2007; Yu et al. 2007; Morizane 2023). Transplantation of iPSC-derived DA progenitors can be as allografts, autologous to the patient receiving the transplant, or as human leukocyte antigen (HLA)-matched allografts, reducing the effects of immunogenicity and increasing the possibility of personalised medicine in PD. NHP and rodent grafting studies have shown promising results with good survival, neurite outgrowth and functional recovery (Tetsuhiro et al. 2017; Doi et al. 2020). The use of iPSC-derived DA grafts are currently in a clinical trial in Kyoto, Japan (Takahashi 2020).

1.5.4 Functional efficacy of hESCs

Pre-clinical rodent studies have established that transplanted hESC-derived DA progenitors can survive long-term and improve drug-induced rotational bias as well as improve adjusting steps and forelimb placement in the cylinder task (Bjorklund et al. 2002; Ben-Hur et al. 2004; Kriks et al. 2011; Adler et al. 2019; Tiklová et al. 2020; Piao et al. 2021). Due the promising results from hESC-derived DA grafts, the STEM-PD trial has entered phase 1 of a clinical trial. Despite the extensive pre-clinical research and efficacy studies for hESC-derived grafts, there has been a lack of published data evaluating the impact of these treatments on cognitive impairments with this cell replacement product, which will be discussed in detail in Chapter 3.

1.6 Gene therapy

A novel alternative that has emerged as a potential therapeutic intervention for PD is gene therapy. The main principle of gene therapy is to transfect target cells/tissues with the desired gene(s) of interest for purposes such as enzyme replacement, neurotrophic support, and potentially disease modification (Axelsen and Woldbye 2018). The mechanism by which gene therapy is conducted is through the use of viral vectors. There are two types of viral vectors that have been used in clinical application: lentiviruses (LVs) and adeno-associated viruses (AAVs).

1.6.1 LV

Lentiviruses (LVs) are a type of retroviruses commonly derived from human immunodeficiency virus-1 (HIV-1) that contain a large single-stranded RNA 9kb genome flanked by long-terminal repeats encoding for 9 viral proteins (Sakuma et al. 2012). The three main structural proteins encoded for in LVs include *gag* (structural proteins), *pol* (enzymes required for reverse transcription of RNA to DNA and then integration into the host genome) and *env* (viral surface glycoproteins). LVs are commonly used in gene therapy due to their stable insertion into the host genome and have been modified to render them non-replicable. LVs have been utilised in pre-clinical studies to demonstrate that expression of glial derived neurotrophic factor (GDNF) can prevent SNc neurons from degenerating, improve innervation to the striatum and support motor recovery in both rat and NHPs (Björklund et al. 2000; Quintino et al. 2019). Although LVs have shown pre-clinical benefit and have been employed in a clinical trial (Palfi et al. 2018), safety concerns due to their risk of oncogenesis and limited biodistribution has meant the current focus within the field of gene therapy for PD is AAVs (Buttery and Barker 2020).

1.6.2 AAV

Adeno-associated viral vectors (AAVs) contain a small ~4.7kb single-stranded DNA genome encoding for three genes: *Rep*, *cap* and *aap*. *Rep* encode proteins required for genome replication and packaging. *Cap* encodes for proteins that construct the outer protective shell

and participate in cell binding, and *aap* encodes for the assembly activating protein which performs a scaffolding function during capsid formation (Naso et al. 2017). *Rep*, Cap and *app* coding sequences are flanked by inverted terminal repeats (ITRs) that are necessary for genome replication and packaging (Grieger and Samulski 2005). AAVs can enter the cell through interactions with 3 carbohydrate molecules (sialic acid, galactose and heparin sulfate) on the cell surface by which the AAV is then internalized through clathrin-mediated uptake into endosomes and are subsequently emptied from endosomes to be transported to the nucleus where the transgene is uncoated from the capsid (Naso et al. 2017; Li and Samulski 2020). In order to create an AAV for gene therapy, a recombinant (rAAV) is used which lacks the *rep* gene preventing replication. The genes of interest are inserted between the remaining ITRs, and during the conversion and transcription into DNA, they subsequently form episomes on the nucleus of the transduced cells (Choi et al. 2006) Recombinant episomes do not integrate into the host genome so will be diminished gradually as the cell undergoes repeated rounds of replication (Drouin and Agbandje-McKenna 2013). When targeting non-replicating cells within CNS, AAVs have shown long, stable transmission and are ideal to be applied to gene therapy for PD.

1.6.3 Application of viral vectors for PD

The focus of this thesis in relation to gene therapy is in the application of viral vectors that synthesise and replace DA. However, there are other gene therapy approaches that have been employed in clinical trials for PD such as those for neurotrophic support with an AAV2-neurturin viral vector Bartus et al. (2013) and AAV2-GDNF viral vector (Gill et al. 2003; Lang et al. 2006). Others to modulate the production of GABA in the STN have been utilised in clinical trials for PD by delivering AAV2-Glutamin acid decarboxylase (GAD) (Kaplitt et al. 2007; LeWitt et al. 2011).

1.6.4 Dopamine synthesis

The DA biosynthesis pathway, as first described by Blaschko (1939) states that DA is produced in the cytosol of DAergic neurons. Through the hydroxylation of L-tyrosine by the rate limiting enzyme TH, L-DOPA is produced. This process is highly regulated by the cofactor tetrahydrobiopterin (BH4), which is synthesised product of guanosine triphosphate (GTP) which acts as a cofactor for TH (Best et al. 2009). The conversion of GTP to BH4 is

facilitated by another rate limiting enzyme, GTP cyclohydrolase 1 (GCH1). Once L-tyrosine has been converted into L-DOPA, it is then decarboxylated by amino acid decarboxylase (AADC) into DA, where it can be packaged into vesicles and released into the synaptic cleft and act upon striatal MSNs, relaying information to the basal ganglia circuitry (Figure 1.2). The enzymes involved in the production of DA are highly important to the homeostatic environment and are depleted due to the loss of DAergic neurons in PD (Goldstein and Lieberman 1992).

1.6.5 Application of viral vectors in gene therapy

The application of gene therapy in PD is to use viral vectors to replace one, two or all of the enzymes involved in DA production. One of the approaches, referred to as the 'pro drug' approach, involves the infusion of an AADC viral vector into the striatum alongside L-DOPA administration, in order to promote the conversion of the peripherally supplied L-DOPA into DA (Bankiewicz et al. 2000). One of the proposed benefits for this method is the ability to regulate the production of DA through mediating L-DOPA administrations. Studies have used this method and shown improvement in rotational bias however, microdialysis showed enhanced L-DOPA conversion, but DA was not stored and instead was continuously released into the extracellular space inducing circular behaviour (Sánchez-Pernaute et al. 2001; Ciesielska et al. 2015). A long term follow up study by Bankiewicz et al. (2006) in NHPs found stable [^{18}F]Fallypride uptake in the striatum 6 years after the initial infusion, and subsequently rAAV-AADC viral vectors have been employed in early phase clinical trials with limited to no improvement in UPDRS scores (Eberling et al. 2008; Christine et al. 2009; Pearson et al. 2021).

An alternative to the pro-drug approach is the multi-cistronic approach to gene therapy which aims to replace all enzymes involved in the production of DA. Infusion of an LV-TH-GC1-AADC viral vector into the striatum of the 6-OHDA MFB lesion rat model resulted in gene transfer for all genes up to 5 months post-LV, and caused a reduction in apomorphine induced rotational bias (Azzouz et al. 2002). TH, AADC and GCH1 expressing AAVs have also been through early phase clinical trials and currently show good efficacy and safety up to 5 years post-infusion (Palfi et al. 2018).

The biscistronic gene therapy approach is used throughout this thesis to manipulate DA biosynthesis and is covered in detail in Chapter 4 (see 4.2.1). In brief, striatal MSNs are

transfected with TH and GCH1 to allow the conversion of L-tyrosine into L-DOPA, and rely on the endogenous AADC present in spared 5HT and DA terminal ends to allow the conversion of L-DOPA to DA. All of the above reports have used motor improvement as a measure of efficacy; however, it is unknown what impact viral vector mediated DA biosynthesis would have on cognitive impairments in PD.

1.7 Aims of the thesis

The experiments carried out and presented within this thesis aimed to develop our understanding about the role of DA in the cognitive impairments of PD, using different dopamine depleting and dopamine replacement manipulations. This thesis utilised three forms of DA replacement consisting of cell, gene, and pharmacological DA release, and evaluated their impact in the 6-OHDA lesioned rat model. Cognitive performance was determined by using the LCRT task.

The chapter aims were as follows:

Chapter 3, Experiment 1 aimed to determine whether hESC-derived DAergic progenitor transplants are capable of alleviating cognitive impairments in the 6-OHDA MFB lesion rat model, by comparing hESC cell products with human fetal-derived grafts .

Chapter 4, Experiment 2 aimed to use an AAV-hTH-2A-hGCH1 expressing viral vector for DA synthesis in the 6-OHDA MFB lesion rat model, to determine the impact on cognitive function.

Chapter 4, Experiment 3 aimed to evaluate whether altering the biodistribution of the AAV-hTH-hGCH1 vector would alleviate cognitive impairments in the 6-OHDA MFB lesion rat model.

Chapter 5, Experiment 4 aimed to understand the contribution of medial vs lateral striatal subregions to LCRT performance, by using unilateral 6-OHDA intra-striatal lesions targeted to the medial and lateral striatum.

Chapter 5, Experiment 5 aimed to differentially target the medial and lateral striatum with the with AAV-hTH-hGCH1 vector to probe cognitive recovery in the 6-OHDA MFB lesion rat model.

Chapter 2 Methods

2.1 Experimental Acknowledgements

2.1.1 Chapter 3

All experimental procedures prior to histology were carried out by Dr Mariah Lelos and Dr Harri Harrison. Culture maintenance and differentiation of hESCs was done in their prospective labs by Dr Agnete Kirkeby (hESC-DA1) and Dr Marija Fjodorova (hESC-DA2) prior to transplantation. Histological analysis of TH and HuNu, and STEM121 volume was carried out by Sophie Turner. GIRK2 and Calbindin histological analysis was carried out by Emily Stonelake under the direct supervision of myself during her master's project. Dark field images were taken by Gareth Williams. GIRK2 and Calbindin immunofluorescence (IFC) and dark field analysis, as well as all histological images, graphical representations, correlations, data handling and statistical analysis was carried out by myself.

2.1.2 Chapter 4

[18F]Fallypride administration, PET and CT scan operation and supervision was carried out in collaboration with Dr Stephen Paisey and Dr Mariah Lelos. 6-OHDA surgical procedure was carried out by myself with assistance from Rachel Hills. Viral surgeries for Experiment 3 were carried out by myself with assistance from Dr Mariah Lelos. LCRT training, all behavioural testing and perfusions were carried out by myself. IFC of tTH/FOXP1 and tTH/GFAP was carried out by Gareth Williams under the direct supervision of myself during his master's placement. AADC section was provided by Joanne Lachica. Confocal imagery carried out in the Bio-Imaging Hub with assistance from Dr Anthony Hayes. All other histological analysis, image capturing, data handling, graphical representations, statistical analysis was carried out personally.

2.1.3 Chapter 5

6-OHDA striatal lesions were carried out by myself, as were 6-OHDA MFB lesions with assistance from Rachel Hills. Viral surgeries were carried out with assistance from Dr Mariah Lelos. All LCRT training, behavioural testing, perfusion, histological analysis, image capturing, data handling, graphical representations, statistical analysis was carried out personally.

2.2 Animal husbandry

All experiments conducted within this thesis used female Lister-hooded rats which were acquired from Charles River, UK. All rats were placed in level 1 large rat cages (4 rats per cage) with ad libitum access to lab chow and water as well as all receiving standard cage enrichment of nestlet bedding, wooden tunnels, and chew sticks. Rats were stored in holding rooms in between testing under a 06:00 – 20:00 light-dark cycle in an ambient room temperature of 21°C. Rats were maintained with frequent monitoring, with health and weight checks once per week unless on food restriction (see 2.5.2). All experiments were conducted in compliance with the UK Animals (Scientific Procedures) Act 1986 under Home Office Licence No. 30⁄3036 for with the approval of the local Cardiff University Ethics Review Committee.

2.3 6OHDA lesion

2.3.1 Making 6-OHDA

6-OHDA solution was made by using 12 µg of freebase 6-OHDA (Sigma) with ascorbic acid in sterile saline. Aliquots were stored in the -20 until needed. Prior to surgery, aliquots were thawed and placed on ice for a maximum of 3 hours or until turned brown before being discarded.

2.3.2 Surgery

All surgical equipment (surgical instruments, surgery packs and cotton buds) were sterilised with a tabletop autoclave prior to surgery. Rats were weighed before surgery and placed into an induction chamber with 0.8-1 L/min oxygen for 2 minutes prior to introducing 5% isoflurane (Teva, UK). Once the rats were anaesthetised, the top of the head was shaved with clippers to clear the surgical area and prevent hair entering the incision. Rats were then moved to the surgical area and placed on a heat mat. The animal was secured into a stereotaxic frame (Kopf) with blunt ear bars to create a flat skull as well as upper teeth secured into a tooth bar (set at -3.4) to ensure the head would remain still during surgery. During securing into the stereotaxic frame, animals were placed on 4% isoflurane in 0.8-1 L/min oxygen and were maintained throughout surgery at between 2-2.5%. Once the animal was secured within the frame, the rat received a subcutaneous injection of analgesia (Metacam, Boheringer Ingelheim, 5 mg/ml at 1 mg/kg) to limit pain during recovery. Viscotears solution was applied to the eyes to prevent them from drying out and to avoid irritation. The animal was placed within a sterilised surgical drape, and aseptic techniques were adhered to throughout the entire surgical procedure, until the animal was ready to be taken from the frame at the end of surgery. Using a cotton bud, diluted iodine solution (Videne) was applied to the shaved area to prevent bacterial infection and wiped thereafter with 70% ethanol to dry the area. With a sterile scalpel blade, an incision down the midline of the head was made to expose the skull. In order to visualise bregma, the blunt end of the scalpel and pressure was applied with a cotton bud to break down the tissue under the scalp.

2.3.3 Infusing 6-OHDA

Using the drill arm of the stereotaxic frame, the location of bregma was recorded and calculations were made in order to locate the target site for MFB lesions. The coordinates from bregma were as follows: Anterior-Posterior axis (AP): -4.0 and Medial-Lateral axis (ML): -1.3 and a hole was drilled through the skull at the injection location. Dura location was determined, and 6-OHDA was delivered, with a stainless-steel 30-gauge cannula fixed to fine polyethylene tubing. The end of the tubing was secured to a 5ml SGE syringe using

sterile saline to create a closed system, and the syringe was attached to a Harvard micro-drive infusion pump. Once dura was located, the cannula was lowered to a depth along the Dorsal-Ventral (DV) axis of -7.0. 6-OHDA (4 µg/µl) was administered in 1 x 3 µl deposit at an infusion rate of 1 µl/min. The 6-OHDA solution was infused for 3 minutes before slowly withdrawing the cannula. The incision was sutured with Vicryl Rapide (Ethicon) and the area wiped with sterile saline, followed by a dry cotton bud. Each animal received a subcutaneous injection of 5 ml glucose-saline, and isoflurane was removed, leaving 1 L/min oxygen to flow through the nose piece whilst the animal was removed from the frame. The animal was placed within a 30°C recovery box and left to recover until fully mobile and conscious. Post-surgery, rats were supplemented with food to aid recovery and sawdust bedding was removed for one day after surgery to prevent sawdust contaminating the sutured incision during healing. Animals were weighed and health-checked for 3 days post-surgery to monitor for any adverse effects.

2.4 Behavioural testing

2.4.1 Drug-induced rotations

A bank of 16 bowls had small amounts of sawdust placed in each and inserted into large transparent cylinders. Elastic bands were attached to an automatic rotometer arm (Rotorat, Med Associates), suspended into each bowl. Animals received an intraperitoneal (i.p) injection of 2.5 mg/kg (volume of 1 ml/kg) of methamphetamine hydrochloride (Sigma-Aldrich, UK) in 0.9% sterile saline (sodium chloride). Animals were then secured into the elastic band behind their forepaws on their abdomen and remained undisturbed in an ambiently lit room for 90 minutes. Both clockwise and counterclockwise rotations were recorded every minute for the full 90 minutes. Net rotations per minute were calculated by: (the number of partial clockwise turns / 4) – (the number of partial anti-clockwise turns / 4). Data is presented and analysed by an average of all net rotations per minute, across the 90 minutes. For apomorphine-induced rotations, animals received a subcutaneous injection of 0.05mg/kg apomorphine in cold sterile saline. Animals were placed in the rotometers and tested for 60 minutes as described above and net rotations were recorded by (the number of quarter counter-clockwise turns / 4) – (the number of quarter clockwise turns / 4).

2.4.2 Adjusting steps task

Rats were assessed for the development of forelimb akinesia with the simple motor test referred to as adjusting steps task. A bench top was marked for a distance of 80cm, of which the number of steps would be evaluated across. Rats were restrained loosely, and one free forelimb was placed on top of the bench allowing them to weight-bear. Rats moved horizontally across the surface of the bench from 0 to 80 cm at a similar speed for all animals, and the number of adjusting steps made within that distance was recorded. If the animal turned away from the horizontal positioning or struggled during restraining, they were held in place until calm and continued with the test. If the animal needed to be restrained, they were returned to the start of the line and new scores were recorded. Adjusting steps was recorded in both a forward and backward direction for each ipsilateral and contralateral forelimb. All four measures were recorded during one trial, and the animal was returned to their home cage, during testing the next animal. A total of 3 individual trials were recorded per animal. Due to the 6-OHDA unilateral MFB lesion, rats are robustly impaired in their contralateral forward adjusting steps, and the mean average of their three trials are presented throughout this thesis.

2.4.3 Vibrissae-evoked paw touching task

The sensorimotor test, vibrissae-evoked paw touching task, was used to evaluate whether the sensorimotor reflex was still intact post-DA depletion. The animal was restrained with one forearm able to freely move. The rat was held parallel to the side of a bench top, and lifted up vertically so that their whiskers could brush against the bench top edge. Control animals will respond to the brushing of whiskers by extending their freely moving paw out to touch the bench top surface. Animals received a score of 1 if they are able to place their paw on the table or attempt to reach out to the surface. No attempt or placement of the paw on the surface was recorded as 0. A total of 10 trials per side was recorded, before repeating with the opposite paw. An average of the score across 10 trials is presented throughout.

2.5 Lateralised Choice Reaction Time task (LCRT)

2.5.1 Apparatus

A bank of 12, nine-hole operant boxes, were manufactured by Campden instruments (860600A-CP, USA). The apparatus was set up with a 9-hole array on a curved wall furthest from the door (Figure 2.1) (Box dimensions: 26 cm L x 25 cm W x 22 cm H). Each hole contained a photocell detector that records a non-perseverant beam break when the animal pokes their nose inside the hole (Hole dimensions: 2 cm diameter, 4 cm depth, 0.5 cm apart). The wall closest to the door was fitted with a panel that gives access to sucrose pellets (AIN-76A Rodent Tablet, TestDiet, UK) delivered from a pellet dispenser located on the outside of the operant box (pellet hopper dimensions: 4 cm L x 4 cm W x 3 cm D). The side walls were fitted with house lights that are programmed to turn on at the start of a new trial and when an error is performed to signal the initiation of a new trial. All data collected within the test was recorded by Campden instruments in real time and extracted from the computer after training for data analysis. One operant box had a green stimulus light instead of bright white in the rest of the boxes. Once an animal was trained or tested within that box, they received testing or training within that box only, for the duration of their testing period.

2.5.2 Food restriction

Prior to testing, animals were placed on food restriction. Animals' daily lab chow was removed in the evening and a baseline weight recorded. Animals were initially given 12 g of food per rat at the same time every 24 hours with weight recorded every other day. Food allocation was reduced gradually between the range of 12 g - 5g minimum per rat until 85% of their baseline weight was achieved. Once an 85% reduction was achieved uniformly as possible amongst all groups (approximately 1 week duration), operant training could commence. Animals were maintained at their 85% baseline weight throughout operant training. In the interim between training weeks, food was returned *ad libitum*. When testing was due to return, animals were placed back on food restriction one week prior.

2.5.3 LCRT procedure

Each animal was placed into the operant chamber with the glass door and external door shut to prevent noise and distraction during the session. The house lights remained on until a trial has commenced. The first 3 testing lessons are designed to habituate the animal to the operant environment by reinforcing the association between the panel and a reward and subsequently nose poking into the illuminated holes is an action that will result in a reward (Table 3). Once animals were capable of performing a high number of lateralised pokes within a 30-minute testing session, the scheduled training program could begin (Table 4,5,6).

Once a trial started, the rat was presented with an illuminated centre hole (Figure 2.2). The rat must manoeuvre to the hole and nose poke for a specified duration to initiate a useable trial. If the animal failed to nose poke in the centre hole, this would initiate a 5sec time out and the house lights would turn on initiating a new trial. Once the animal had poked within the centre hole, the centre hole light was extinguished and a light in either the left or right hole was shown for a specified duration. The animal then withdrew its nose from the centre hole (recording a reaction time) and manoeuvred to the correct hole (recording movement time) and nose poked into the hole causing the pellet hopper to be illuminated for 2 seconds to signal that the response was correct, and a reward was delivered.

Subsequently, a schedule of programs was carried out that got progressively more difficult for the animal to perform to receive the reward. The duration the animal was required to hold their nose in the centre hole to initiate a trial was gradually extended. This was carried out to ensure the animals were engaging in the task. The lateralised stimulus light duration was also gradually made shorter. Receiving the lateralised stimulus (for a very short duration) whilst the animal was nose-poking in the centre hole, allowed for the separation of the visual processing to each hemisphere, without influence from the other visual field.

The program detailed in Table 4 is the same as described in Lelos et al. (2016) and carried out in Experiment 1. In Experiment 2, more than 50% of animals stopped responding once an 800 msec centre hold duration was introduced, so the task was modified to only require a 400 msec maximum hold (Table 5). Experiment 3-5 experienced the same drop in responding at 600 msecs, but animals were dropped down to an earlier program and were re-tested at 600 msecs, then continued along the program (Table 6). A baseline was recorded on 3-5 consecutive days in which the centre hole was randomised in order to

encourage attention. Any animals that failed to initiate responses during training were dropped down to previous programs to reinforce the behaviour, and once responding had returned, they were incrementally taken along the remaining programs. This led to some staggering of groups within the cohort who had their baseline performance recorded at a later time-point than the main group. If an animal could not feasibly perform the task by the time the staggered group was ready to record a baseline performance, they were considered a non-responder and were removed from the experiment.

Measures calculated for the LCRT task are described below. Response accuracy, overall accuracy, movement time and reaction time are recorded on the ipsilateral and contralateral side, so calculations for each side is based off of responses on that side only.

- **Response accuracy** (%) : (no. correct responses / (correct + incorrect)) * 100
- **Overall accuracy** (%) : (no. correct responses / usable trials) * 100
- **Movement time** (msecs) : (sum of latency to poke in the correct hole / no. of correct responses)
- **Reaction time** (msecs) : (sum of latency to remove nose from centre hole / no. of correct responses)
- **Total useable trials (TTU)** : ipsilateral + contralateral useable trials
- **Efficiency** (%) : (total useable trials / total trials started) * 100
- **Omission errors**: Failure to perform a lateralised response after initiating a useable trial
- **Panel Press errors**: Panel press response after initiating a useable trial
- **Early centre hole withdrawal**: Failure to hold nose poke for specified duration and prevent initiation of a useable trial
- **Omissions/ TTU** (%): (no. of omission errors / total useable trials) * 100
- **Panel press/TTU** (%) : no. of panel press errors / total useable trials) * 100

A

B
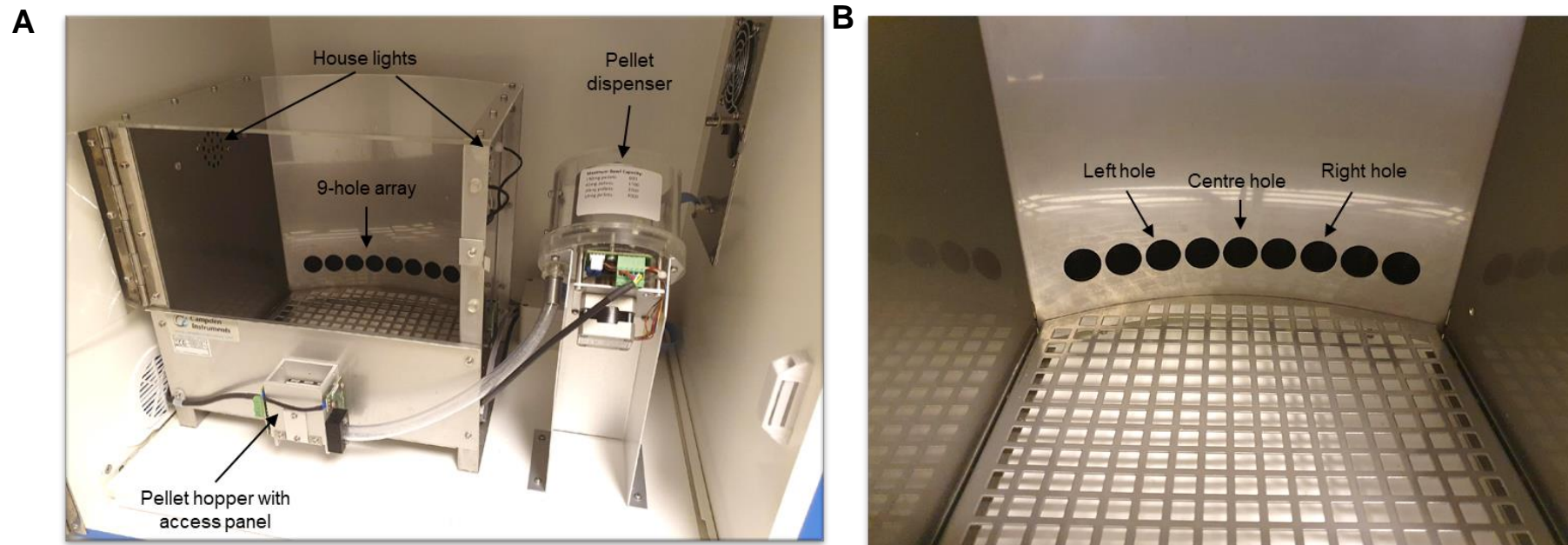
Figure 2.1. A) Photograph of nine-hole operant box. Pellet dispenser holds small sucrose pellets that are released along the tubing to the pellet hopper if a correct trial has initiated. Animal can access sucrose pellet by nose poking through the panel. The start of a new trial is indicated by a flash of the house lights. Animals must nose poke in the 9-hole array to participate in the task. B) Close up image of the 9-hole array, highlighting with arrows the centre, left and right hole in which the animal is required to poke their nose for a reward.

A

Operant box layout

Stimulus Lights

Photocell detectors

House Lights

Pellet hopper

B

Useable Trial

Centre hole shown for 5sec

Must hold for set time to
initiate trial

Contra   Ipsi

Lateral holes shown at random,
for a set duration

Reaction Time

Withdraw nose from centre hole

Movement time

Must move and nose poke in
correct hole

Accuracy

Reward given on response to
correct holes

C

Possible Errors

Early centre hole
withdrawal

Incorrect hole

Omission

Panel press too early

Figure 2.2. Lateralised choice reaction time task (LCRT). A) schematic of the operant box layout with arrows indicating the 9-hole array with stimulus light and photocell detectors to register a beam break. House lights indicate the start of a new trial or an incorrect trial prompting the new trial to start. If the animal nose pokes in the correct hole, a sucrose pellet will be dispensed to the pellet hopper. B) Schematic of the LCRT from initiation of the trial to reward. Animal is placed inside the operant chamber and is presented with a centre light. The animal must hold their nose in the centre hole for a pre-determined amount of time to initiate a useable trial. If the animal withdraws its nose too early, an early centre withdrawal error (C) is performed, and the house lights will turn on to start a new trial. If the animal does hold for the correct amount of time, a lateralised stimulus light on either the ipsilateral (ipsi) or contralateral (contra) side to the lesion is presented for a short duration. The animal must remove their nose from the centre hole (which registers a reaction time) and position themselves to nose poke in the correct stimulus hole (which registers a movement time). If the animal fails to nose poke in the correct hole or doesn't poke at all (c) they will receive an error and the house lights will be turned on and a new trial begins. If the animal correctly nose pokes in one of the lateralised holes, they will receive a sucrose pellet in the pellet hopper for which they can poke through the panel to receive the reward. If the animal presses the panel before they have correctly performed the task, an error has been made, the house lights will be switched on and a new trial started. Trials on the ipsilateral and contralateral side are present at random during a 30-minute testing period.

Starting Program	
Lesson	Details
Panel press (15 min)	10 pellets delivered on session start, then panel light illuminated until panel press. 1 sucrose pellet per panel press
Centre hole poke + panel press (30 min)	Centre hole light presented until nose poke into centre hole. Light switched off and panel illuminated until panel press. 1 sucrose pellet per panel press
Centre hole + either Left or right hole (30 mins)	Centre hole light presented until nose poke into centre hole. Light switched off, left **OR** right hole illuminated until nose poke. Light switched off and panel illuminated until panel press. 1 sucrose pellet per panel press

Table 3. LCRT task preliminary training

Carli Program no.1 (Experiment 1)			
Lesson (30 mins)	Centre hold nose poke duration	Stimulus light duration	Limited hold (Trial Length)
Carli-Train-1	100 msec	10 sec	10 sec
Carli-Train-2	100 msec	5 sec	10 sec
Carli-Train-3	100 msec	2 sec	10 sec
Carli-Train-3b	200 msec	1 sec	10 sec
Carli-Train 3c	250 msec	1 sec	5 sec
Carli-Train 3d	250 msec	500 msec	5 sec
Carli-Train 4	400 msec	500 msec	5 sec
Carli-Train 5	600 msec	500 msec	5 sec
Carli-Train 6	800 msec	500 msec	5 sec
Carli-Train 7	600 msec	350 msec	5 sec
Carli-Train 8	800 msec	200 msec	5 sec
Carli-Test (Baseline)	200,400,600,800 msec	200 msec	5 sec
Carli-Test (Post-Lesion)	50,100,150,200 msec	200 msec	10 sec

Table 4. LCRT program details for experiment 1

Carli Program no.2 (Experiment 2)			
Lesson	Centre hold nose poke duration	Stimulus light duration	Limited hold (Trial Length)
Carli-Train-1	100 msec	10 sec	10 sec
Carli-Train-2	100 msec	5 sec	10 sec
Carli-Train-3	100 msec	2 sec	10 sec
Carli-Train-3b	200 msec	1 sec	10 sec
Carli-Train 3c	250 msec	1 sec	5 sec
Carli-Train 3d	250 msec	500 msec	5 sec
Carli-Train 4	400 msec	500 msec	5 sec
Carli-Train 5	600 msec	500 msec	5 sec
Carli-Train 7	400 msec	350 msec	5 sec
Carli-Train 8	400 msec	200 msec	5 sec
Carli-Test (Baseline)	100,200,300,400 msec	200 msec	5 sec
Carli-Test (Post-Lesion)	50,100,150,200 msec	200 msec	5 sec
Carli-Test (Week 7 and 10 -Modified)	50 msec	500 msec	10 sec

Table 5. LCRT program details for Experiment 2

Carli Program no.3 (Experiment 3,4,5)			
Lesson	Centre hold nose poke duration	Stimulus light duration	Limited hold (Trial Length)
Carli-Train-1	100 msec	10 sec	10 sec
Carli-Train-2	100 msec	5 sec	10 sec
Carli-Train-3	100 msec	2 sec	10 sec
Carli-Train-3b	200 msec	1 sec	10 sec
Carli-Train 3c	250 msec	1 sec	5 sec
Carli-Train 3d	250 msec	500 msec	5 sec
Carli-Train 4	400 msec	500 msec	5 sec
Carli-Train 5	600 msec	500 msec	5 sec
Carli-Train 7	400 msec	350msec	5 sec
Carli-Train 8	400 msec	200 msec	5 sec
Carli-Test (Baseline)	100,200,300,400 msec	200 msec	5 sec
Carli-Test (Post-Lesion)	100,200,300,400 msec	200 msec	5 sec

Table 6. LCRT program details for Experiments 3,4 and 5

2.6 Histological techniques

2.6.1 Perfusion

All animals received a terminal intraperitoneal injection of 0.9 ml of sodium pentobarbital (Dolethal) and subsequently transcardially perfused using a peristaltic pump with pre-wash solution (di-sodium hydrogen phosphate (dihydrate) and sodium chloride in distilled water, pH 7.3) for 2 minutes and 4% paraformaldehyde (PFA in pre-wash solution, pH 7.3) for 6 minutes. Whole brain tissue was removed and post-fixed for 4 hours before being transferred to sucrose solution (25% sucrose in pre-wash) for a minimum of 24 hours. Brains were coronally sectioned on a freezing sledge microtome (Leitz, Wetzlar). Brains were cut in a 1:12 series at 30 μm into a 48 well plate with an antifreeze solution (di-sodium hydrogen orthophosphate anhydrous, sodium dihydrogen phosphate, ethylene glycol and glycerol in distilled water) and stored at -20°C indefinitely.

2.6.2 Immunohistochemistry (IHC)

One series per rat, of the 12 series cut per rat, was placed into individual pots and washed with tris-buffered solution (TBS) to remove antifreeze and placed on an orbital shaker (Tris-base and sodium chloride in distilled water, pH 7.4). Sections were treated with citrate buffer (pH 6.0) in a water bath at 70°C for 30 minutes to permeabilise the tissue. Sections were allowed to cool and then washed in TBS. Sections were then transferred to a quenching solution (10% methanol, 3% hydrogen peroxide (10% w/v) in distilled water) to reduce endogenous peroxidase activity for 5 minutes prior to washing in TBS, 3 times for 10 minutes each. The sections were blocked in 3% normal serum (NS) in TXTBS solution (0.2% Tritron-X-100 in TBS) for 1 hour prior to a primary antibody solution (Table 7) with 1% NS in TXTBS placed on the tissue overnight at room temperature or stored at 4°C over the weekend. The next day, the sections were washed with TBS before being placed in a secondary antibody solution (1% NS in TBS) and returned to the orbital shaker for 3 hours. For 30 minutes before use, an avidin-biotin complex (Vectastain ABC HRP kit, PK-4000) kit (1:200 concentration) was premixed in the required volume of TBS and 1% NS to allow binding of the complex. The ABC solution was placed on the sections for 2 hours. Sections were washed in TBS

and TNS and placed at 4°C in TNS overnight (Tris-base in distilled water without NAOH, pH 7.40). In order to stain, a 3,3'-diaminobenzidine (DAB, sigma) solution (2 ml DAB in 40 ml of TNS, with 12 µl of 30% hydrogen peroxide) was added onto the sections for 10-30 minutes depending on the intensity of the staining and then washed thoroughly in TNS to stop the reaction. Sections were washed in TBS and kept in TBZ until mounted (TBS with 0.02% sodium azide). All tissue sections were mounted on double-subbed gelatinised slides and air-dried overnight. The next day, mounted slides were dehydrated in 70%, 95% and 100% ethanol for 10 minutes each before being cleared in xylene to remove fat cells in the tissue. Slides were cover-slipped using DPX and dried in a fume hood.

2.6.3 Immunofluorescence modifications to the IHC protocol

To visualise the co-labelling of markers, immunofluorescence (IFC) was employed. One-well of the 1:12 well series per rat was taken for IFC, and the exact same protocol was followed as described in IHC above until it was time to apply the secondary antibody. Alexa-fluor secondary antibodies (Invitrogen) were utilised at three different wavelengths to visualise co-labelling of markers within the tissue (Table 8). Alexa-fluor 488, 594, and Hoescht (350 nm) was applied to the sections in TBS solution with 1% NS for 3 hours. From this point, all tissue sections remained in the dark and covered at all times. After 3 hours, the sections were washed with TBS and mounted, dehydrated and cover-slipped as described in 2.6.2.

Primary antibody	Concentration	Species	Supplier	Cat no.
TH	1:2000	Rabbit, polyclonal	Millipore	AB1542
TH	1:2000	Mouse, monoclonal	Millipore	MAB318
tTH	1:400	Mouse, monoclonal	ThermoFisher	MA1-24654
STEM-121	1:3000	Mouse, monoclonal	Takara	Y40410
HUNU	1:1000	Mouse, monoclonal	Millipore	MAB1281
GIRK2	1:400	Rabbit, polyclonal	Alomone	APC-006
Calbindin	1:10,000	Rabbit, polyclonal	Swant	CB-38
FoxP1	1:500	Rabbit, polyclonal	Abcam	AB16645
GFAP	1:1000	Rabbit, monoclonal	Dako	Z0334
GCH1	1:1000	Rabbit, polyclonal	Sigma	HPA028612

Table 7. Primary Antibody details

Secondary antibody	Concentration	Species	Supplier	Cat no.
Horse: Anti-mouse	1:200	Rat adsorbed – Biotin IgC	Vector	BA2001
Goat: Anti-rabbit	1:200	Biotin IgC	Vector	BA1000
Goat: Alexa Fluor 488	1:200	Anti-Mouse, Igc (H+L) Highly cross-adsorbed	Invitrogen	A11029
Goat: Alexa Fluor 594	1:200	Anti-Rabbit, IgC (H+L) cross-adsorbed	Invitrogen	A11037
Hoechst	1:10,000	Nucleic acid stain	Invitrogen	H3570

Table 8 Secondary antibody details

Chapter 3 : Can hESC-derived DAergic grafts alleviate cognitive impairments in the PD rat model?

3.1 Summary

Previous pre-clinical animal studies using mouse, rat, and human-derived fetal grafts have shown improvement in cognitive deficits in the LCRT task. The current focus within the field of cell replacement therapy is the use of hPSCs for clinical application, yet it is unknown whether hESC-derived DAergic transplants could also be capable of alleviating cognitive impairments.

Experiment 1 described in this chapter aimed to compare two hESC-derived cell therapy products to the current gold-standard, hfVM, on their ability to alleviate motor and cognitive impairments. Transplanted into the 6-OHDA lesioned rat model, all graft types were able to alleviate motor deficits after 21 weeks post-transplantation, whereas only hfVM grafts were capable of restoring visuospatial function to the level of controls, whereas hESC-derived DA grafts were significantly worse at the task. hfVM grafts differed in graft volume and A10 DA-ergic neurons within the graft core to hESC-derived grafts. Correlational analysis suggests greater outgrowth proximal to the graft core may support greater motor recovery, as well as greater outgrowth into the medial striatum may support greater accuracy in the LCRT task.

Chapter 3 highlights that two forms of DAergic cell replacement therapy can have differential impacts on cognitive recovery in the PD rat model, leading to further questions about the role of DA in cognitive function and what factors of DA replacement is important for recovery.

3.2 Introduction

3.2.1 The importance of treating non-motor symptoms in PD

As discussed in Chapter 1, non-motor impairments in PD are a critical aspect of disease progression which begin during the prodromal phase and worsen as the disease progresses (Figure 1.1). Non-motor symptoms in PD have a significant quality of life impact for patients (Schrag et al. 2000). Chaudhuri and Schapira (2009) reviewed how management of non-motor symptoms is currently sup-optimal due to often cases of misdiagnosis, symptoms being under-observed, and incorrect medication administration all resulting in treatment not being applied effectively (Freeman et al. 2007; O'Sullivan et al. 2008; Kallik et al. 2021). Therefore, it is important to develop treatments with a conscious focus on non-motor symptoms for people with PD.

As described in 1.1.2, DA depletion is the major cause of motor symptom onset due to the loss of DA neurons in the SNc, so it seems plausible that replacement of DA would support cognitive recovery. There is evidence of non-motor symptoms being DA dependant in cases such as cognitive decline (Wang et al. 2022b), visual disturbances (Bodis-Wollner et al. 1982) and reward processing amongst others (Sharp et al. 2020). In further support of this, Mattay et al. (2002) observed patients under fMRI in a hypo-DAergic and hyper-DAergic state whilst performing a working memory and cued sensorimotor task. In a hypo-DAergic state, cortical regions supporting working memory were more active and correlated with greater errors performed during the task. This study highlights the DA modulation supports cognitive function; therefore, it is also important to evaluate current and novel DA treatments for their effectiveness in alleviating cognitive impairments in PD.

3.2.2 hPSC-derived DA progenitors

As discussed in Chapter 1, current cell replacement strategies use novel stem cell-derived DA progenitor cell products as a therapeutic intervention for PD and are currently either

entering or are in the early phase of clinical trials. However, it is unknown what impact hPSC-derived DA grafts would have on cognitive function.

In this chapter, two hESC-derived cell therapy products differentiated according to two different protocols were used; one cell therapy product, referred to as hESC-DA1, used H9 neural stem cells and was differentiated according to Kirkeby *et al.* (2012) and a second cell therapy product, hereafter referred to as hESC-DA2, used the H7 cell line and was differentiated according to a modified version of (Chambers et al. 2009), published in Jaeger *et al.* (2011). Both are established protocols that are designed to yield a population of A9 midbrain DAergic neurons and are informed by developmental patterning of human DA neurons, aiming to create an 'authentic' population of A9 neuronal progenitors for transplantation (see 1.6.2). Detail of the differentiation protocols are shown in Figure 3.3. The primary difference between protocols were Kirkeby *et al* differentiated progenitors as embryoid bodies until day 11, yet both protocols followed a conserved protocol of dual SMAD inhibition to enhance neural induction (Chambers et al. 2009) and the regulation of sonic hedgehog (SHH) to ventralise the patterning of the progenitors (Brady and Vaccarino 2021).

Although hESC-DA1 & 2 have variation within their differentiation protocols which may influence the neuronal composition within the graft, the primary focus of this chapter was to determine if any hPSC-derived DA grafts could improve cognitive function, rather than directly comparing hESC-derived DA cell therapy products.

3.2.3 Assessment of functional recovery

As discussed briefly in Chapter 1, the unilateral 6-OHDA MFB lesion model of PD is used throughout this chapter to model DA denervation of the striatum and robust cell loss in the ventral midbrain. As shown in (Table 1), this model leads to the onset of motor and cognitive impairments that are analogous to some aspects of clinical PD and is used throughout the field to evaluate therapeutic interventions. This chapter will evaluate cell therapy products on three distinct motor tasks to evaluate the functional efficacy of the graft: drug-induced rotations, adjusting stepping task and vibrissae-evoked paw touching task (Jerussi and Glick 1975; Schallert et al. 2000; Glajch et al. 2012; Björklund and Dunnett 2019). As discussed

in 1.5, both hfVM and hESC-derived DA grafts have supported robust recovery of motor deficits on all of these tasks, making them reliable indicators of a functional graft.

3.2.4 Lateralised choice reaction time task

In order to effectively evaluate cognitive impairments in PD, it is important to use a test that can encapsulate different types of cognitive processing and can be used in conjunction with unilateral lesion rodent models of PD. This chapter, and all subsequent chapters, employ the LCRT task. The ability to test animals in a lateralised task was first described by Carli et al. (1985). In brief, the LCRT task is based on stimulus-response associations in which rats respond firstly to a centre light in a 9-hole array with a nose poke which they must hold for a specified duration to initiate a useable trial. Once a usable trial has commenced, the rodent is presented with a contralateral or ipsilateral stimulus light in a lateralised hole for a very brief duration. Once the stimulus light has flashed, the animal must poke in the corresponding (correct) hole to receive a sugar pellet reward and to initiate a new trial (Figure 2.2). This task allows for the isolation of each hemisphere's visuospatial processing by presenting the stimulus light whilst the rat is actively maintaining their nose in the centre hole operandum. This makes it ideal for the unilateral PD model to be used to evaluate lesion-induced deficits and thus recovery of lateralised performance on the task with DAergic grafts. The LCRT task is able to measure DA-dependant visuospatial processing, incentive motivation, attention, and movement execution deficits within this one operant task (Brown and Robbins 1989; Döbrössy and Dunnett 1997). Lindgren et al. (2014) demonstrated that these behaviours are DA-dependent by testing rats on the LCRT with DA loss alone, or in conjunction with 5-HT or noradrenaline depletion. Other than a subtle change in attentional function in the noradrenaline depleted rats, all groups performed similarly in the LCRT, confirming that the deficits are predominately DA-dependent.

Pre-clinical application of the LCRT task

The efficacy of fetal grafts (rat, mouse, and human) in alleviating cognitive impairments have been shown in pre-clinical studies using the LCRT task. As described in Dowd and Dunnett (2004) E14 rat VM tissue transplanted into 6-OHDA MFB lesioned rats led to improvement in contralateral visuospatial function, efficiency and movement time 8 weeks post-transplantation, when observed over a 3 week period. Heuer et al. (2013b) used E14 mouse

VM transplants in the same PD rat model, with unilateral near/far hole modifications to increase task difficulty which will be discussed in Chapter 4. At 12 weeks post-transplant, grafted rats improved their total trials, far hole visuospatial function and movement time. Alleviation of visuospatial dysfunction and incentive motivational deficits on the LCRT task was also reported with hfVM transplants 18 weeks post-graft (Lelos et al. 2016). This is currently the only published evidence to show hfVM-derived cell replacement therapy can alleviate cognitive impairments. This novel finding highlighted the importance of assessing cognitive functioning alongside motor behaviour in pre-clinical studies and has importance for future clinical application. These results are promising, and if hPSCs were capable of alleviating cognitive deficits also, this would provide greater efficacy to cell replacement therapy for clinical trials and also further establish the relationship between physiological DA release supporting cognitive function.

3.2.5 Chapter aims

As hESC-derived DAergic grafts have shown similar motor recovery to hfVM grafts and the literature above has outlined the effectiveness of hfVM grafts in alleviating cognitive impairments in the LCRT task, it is therefore reasonable to hypothesise that hESC-derived DA grafts would also alleviate cognitive impairments in the unilateral 6-OHDA lesion rat model.

The aims of this chapter were as follows:

1. ***To determine whether stem cell-derived transplants were capable of alleviating cognitive impairments in the LCRT task***. Transplants of two different hESC-derived cell therapy products and hfVM tissue were performed in the unilateral 6-OHDA PD rat, followed by an evaluation of both motor and cognitive function up to 21-weeks post-graft. It was hypothesised that both hfVM and hESC-derived DA grafts would alleviate motor and cognitive function.

2. ***To conduct histological analysis on post-mortem brain tissues and correlate graft characteristics with functional data to investigate attributes that may facilitate cognitive and motor recovery***. Histological analysis was carried out to (1) identify human positive cells present within the graft, (2) measure the fibre outgrowth from the graft core to A9 and A10 brain target regions and (3) evaluate the composition of DA neurons in the graft. It was hypothesised that hfVM and hESC-derived DA grafts would differ characteristically on measures such as graft volume and DA neuronal population but would be similar in projection profile to different regions.

3.3 Methods

3.3.1 Experimental design

Female Lister-hooded rats ($n = 59$) were acclimatised to the animal unit for 1 week prior to being placed on food restriction (see 2.5.2). Animals were food restricted to 85% of their baseline weight for one week prior to commencing training on the LCRT task to establish stable baseline performance (see 2.5.3). Rats were trained for 7 weeks on the LCRT task and rats who failed to learn the task were excluded from further experimentation ($n = 4$). Rats ($n = 45$) received a unilateral 6-OHDA infusion into the MFB with the intact hemisphere acting as a within-subject control (see 2.3). One group of rats remained a naive control ($n = 10$). At 3- and 4-weeks post-lesion, all rats were assessed on the amphetamine-induced rotations task (see 2.4.1). The net rotation data was averaged across both weeks to determine the extent of rotational bias and to confirm the nigral lesion. Any rats below 6 net rotations per minute were excluded from further experimentation ($n = 2$). To assess post-lesion cognitive deficits, all rats were tested daily on the LCRT task for one week and, for each behavioural measure, their week average was calculated. Rats were counterbalanced into experimental groups based on amphetamine rotation scores and LCRT contralateral response accuracy. Rats were divided into 4 groups: One group received a unilateral intra-striatal transplantation of hfVM cell suspension ($n = 12$). Another group ($n = 10$) received a cell suspension of hESC-DA1, and the final group ($n = 12$) received a cell suspension of hESC-DA2. The final group remained as a lesion control ($n = 11$). Amphetamine-induced rotations were tested at 3-week intervals up to 21 weeks post-graft. Testing on the LCRT task was undertaken between weeks 20 and 21 post-graft. Apomorphine-induced rotations and performance on the vibrissae-touch test were undertaken at 21 weeks and all rats were subsequently transcardially perfused with 4% PFA and whole brain tissue was removed for histological analysis (see 2.6). Two rats from hfVM and 1 rat from hESC-DA1 were excluded due to poor graft survival. The final n's of each group analysed throughout this chapter is as follows: Control $n = 10$, Lesion $n = 9$, hfVM $n = 10$, hESC-DA1 $n = 9$, hESC-DA1 $n = 12$. Experimental design is depicted below (Figure 3.1).

Group	n = 59		n = 45		n = 34								Control n = 10
													Lesion n = 9
													hfVM n = 10
													hESC-DA1 n = 9
													hESC-DA2 n = 12
Weeks	-12	-9	-6	-3	0	+3	+6	+9	+12	+15	+18		+21
Task	LCRT training		6-OHDA MFB lesion	Drug rotations	Intra-striatal transplantation	Drug rotations							Drug rotations
				LCRT									LCRT
				Hand-testing		Hand-testing							Perfuse

Figure 3.1. Schematic of the experimental design for experiment 1. Hand-testing refers to the adjusting steps task and the vibrissae-evoked paw touch task. Drug rotations refer to amphetamine and apomorphine-induced rotations task. Apomorphine rotations were only evaluated at 21 weeks post intra-striatal transplantation.

3.3.2 Transplantation

Starting 1 day prior to transplantation, rats were immunosuppressed with intraperitoneal injections of 10 mg/kg cyclosporine (Sandoz Pharmaceutical, U.K.) and were immunosuppressed daily until the end of experimentation. All cell therapy products were deposited into the striatum using a 5 µl Hamilton syringe over two sites (Figure 3.2). At each site, 2 µl of cell suspension was deposited at an infusion rate of 0.5 µl l/min. hfVM and hESC-DA2 were deposited in a suspension of approximately 190,000 cells/µl (760,000 cells in total per rat) and hESC-DA1 was deposited in a suspension of 93,750 cells/µl (375,000 cells in total per rat) due to having fewer available cells in each vial.

	AP	ML	DV1	DV2
Site 1	+0.5	-3.0	-5.0	-4.0
Site 2	+1.2	-2.7	-5.0	-5.0
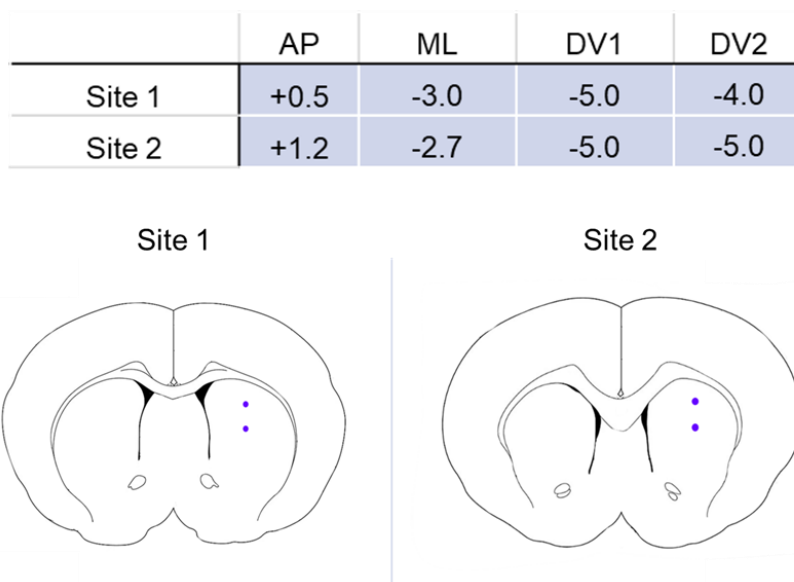
Figure 3.2. Coordinates for transplantation surgery during Experiment 1. Representative images of the locations of each injection site and the depth. AP = Anterior-Posterior axis, ML = Medial-Lateral axis, DV = Dorsal-Ventral axis.

3.3.3 Cell preparation

hESC-DA1 was differentiated to day 16 according to the protocol previously described (Kirkeby et al. 2012) and transplanted as fresh cells. hESC-DA2 was differentiated to day 16 according to the protocol previously described (Jaeger et al. 2011) and transplanted as fresh cells. Differentiation protocol is detailed in Figure 3.3. Cells were transplanted in transplantation media (HBSS + 1:6 Dornase alfa (20 U/ml, Pulmozyme, Roche)).
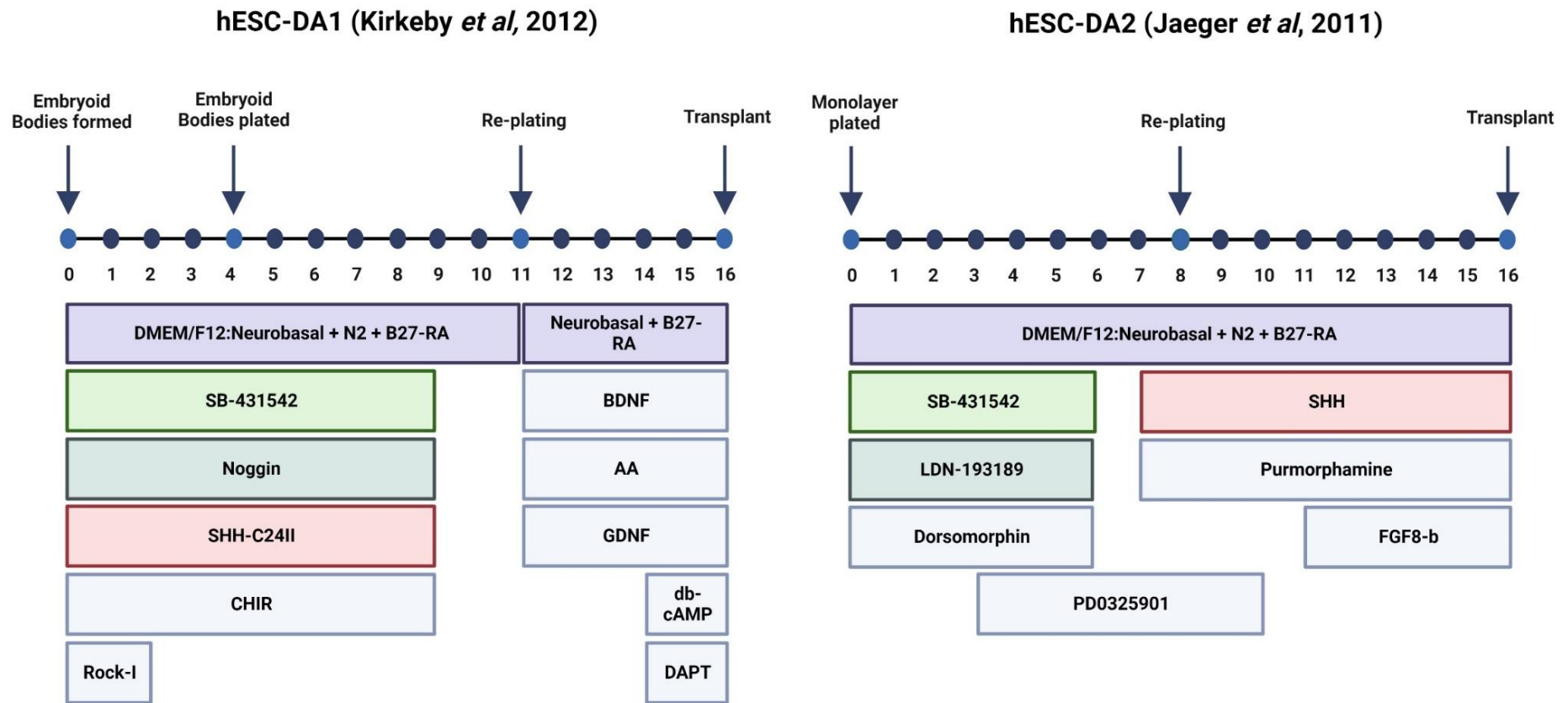
Figure 3.3. Differentiation protocol for hESC-DA1 and hESC-DA2 from Day 0 to Day 16. RA = Retinoic acid, AA = Ascorbic acid, SHH = Sonic hedgehog, BDNF = brain-derived neurotrophic factor, GDNF = Glial cell line-derived neurotrophic factor, FGF = fibroblast growth factor

3.3.4 Fetal tissue preparation

Human fetal tissue was obtained with full donor consent from medical terminations of pregnancy (mTOP) through the South Wales Initiative for Fetal Tissue bank (SWIFT) (http://www.biobankswales.org.uk/swift-research-tissue-bank), under UK Human Tissue Authority research licence (no. 12457) held by Cardiff University, and used for research with ethical approval of the project from the Bro Taf local research ethics committee. Gestational age was estimated through ultrasound scan. The hfVM tissue was harvested from four foetuses of ~ 9 weeks gestation, with a mean crown-rump length of 23.25 mm (Table 9). Tissue was used as individual suspensions and not pooled. Tissue was incubated at 37 °C for 20 min in TryplE Express (Life Technologies Inc) containing 20U/ml Dornase alfa. Tissue was dissociated by trituration in DMEM/DA to obtain a quasi-single cell suspension. The viability for each sample is presented in Table 9.

	CRL (mm)	Viability (%)
SWIFT 2120	21	89
SWIFT 2101	16	84
SWIFT 2100	22	90
SWIFT 2119	34	89

Table 9. SWFT number associated with harvested fetal tissue. SWIFT number allocated at the time of procurement. CRL = crown rump length as a measure for gestation. Viability of cell suspensions prior to transplantation was above 80% for all tissue preparations.

3.3.5 Histological analysis

Tissue sectioning and histological analysis is described in general methods (see 3.3.5). The primary antibodies used were as follows: TH (1:2000), Human nuclei (HuNu, 1:1000); GIRK2 (1:400), Calbindin (1:10,000), STEM121 (1:3000). Bright field images, stereological analysis and visualisation was undertaken using the Lecia upright microscope with Leica CTR6 LED camera, using the Visuopharm image acquisition software (v2017.2). IFC images were taken using the Carl Zeiss upright microscope with the Axiovision Rel 4.8 software.

Multidimension acquisition was used to overlay fluorescence signal at 488 nm (Green) and 594 nm (red) with a x20 objective (200x magnification).

3.3.6 Stereological analysis

Graft volume

STEM121 was used to evaluate graft volume throughout the striatum. A region of interest (ROI) drawn around the graft core to determine the area covered of the graft per section, for all sections containing positive (+ve) STEM121 expression. Graft volume was calculated by the following formula: Graft volume (mm^3) = ($\sum$ of all areas (µm^2) * section thickness (µm) * series frequency) / 1000000000 (to normalise the data). Mean volume was calculated for each group.

TH and HuNu cell count

Due to the large population of HuNu and TH +ve cells per graft, stereological analysis using random sampling was undertaken with Abercrombie correction. Using visiopharm software, ROIs were drawn around the graft core to establish the area for counting. Meander sampling was set up to sample cell number in approximately 20 areas per section within a counting frame of 99.04 µm x 79.23 µm. Cells were counted within the counting frame at 400x magnification.

Estimated total cell number was calculated as follows:

1. Estimated cell number = $\sum$ cells counted * ($\sum$ ROI area / counting frame size * $\sum$ samples) * 12

2. Abercrombie correction = (1)Estimated cell number * (section thickness/(mean cell diameter + section thickness))

Data is presented as an average of each animal per group and expressed as total cells. In order to account for differences in the volume of grafts between animals, estimated total cell number was normalised by dividing by the total TH population and expressing the data as

cells per mm^3. To calculate the percentage of TH +ve cells within the graft, the total TH +ve cells was divided by the total HuNu +ve cell count and multiplied by 100.

GIRK2 and calbindin cell count

Identification of A9 and A10 populations within the graft was carried out using GIRK2 and calbindin positive +ve staining, respectively. Total counts of GIRK2 and Calbindin +ve cells within every graft-present section was carried out using the 200x magnification for each rat. The sections used were co-labelled with HuNu in order to confirm GIRK2 and calbindin +ve cells were of human origin rather than, in the case of calbindin, were the endogenous interneurons within the host striatum. The estimated manually counted total cell counts for GIRK2 and calbindin was calculated as follows: $\sum$ cells counted * series frequency. The total cell count was then calculated as a percentage of the total TH+ cells within the graft per animal.

3.3.7 Projection profiling

TH

Analysis was undertaken of the TH fibre outgrowth both in a medial and lateral direction from the graft core. One section per rat with the largest graft present was selected and observed at 125x magnification. A ROI line was drawn horizontally across the graft core. A counting frame of 100 μm^2 was set up and placed on either the outer medial or lateral edge of the graft, with the ROI line running directly through the centre of the counting frame. The number of fibres that crossed the border of the counting frame closest to the graft was counted. Fibres were counted every 100 μm^2 increments until the edge of the striatum was reached. Data is presented as the average of total projections per group, the maximum projection length averaged per group and the total number of projections within the 1st 200 μm. Each of these quantifications is presented for the results in both the medial and lateral direction from the graft.

GIRK2

In order to analyse the GIRK2 outgrowth from the graft core, one section with the largest graft area for each animal was chosen and observed at 200x magnification. A counting frame of 1000 μm^2 was set up and positioned at 5 points, 300 μm apart, along both medial and lateral edge of the graft border in order to sample from enough of the graft to be representative of the length of the graft. At those 5 points, visible projections were counted within the counting frame at 100 μm increments away from the graft core in both the medial and lateral direction respectively. A distance of 900 μm in each direction was analysed. The data presented within this thesis is (1) the total medial and lateral projections as an average per group, (2) the maximum projection distance reached of GIRK 2 outgrowth as an average per group, and (3) the total projections within the first 200 μm as a group average.

3.3.8 Darkfield analysis

Darkfield imaging was used to visualise the innervation of human fibres (using STEM121 immunostaining for human cytoplasm) into extra-striatal cortical and subcortical regions. Preliminary analysis prior to darkfield consisted of comparing the intact and lesioned hemisphere within the lesion group for specific areas of interest with strong denervation of TH. Areas of interest with strong TH denervation in the lesioned hemisphere were as follows; infralimbic cortex, cingulate gyrus, claustrum, nucleus accumbens, olfactory tubercule, septum. The claustrum was not an area of strong TH denervation but was included due to being an A10 target area. To compare axonal fibre density in those selected areas, images of STEM121 staining were taken at x200 magnification using a darkfield lens on a Carl Zeiss upright microscope, utilising Axiovision Rel 4.8 software. To account for variability in axon fibre density, one image was taken per region based on the Paxinos and Watson rat brain atlas (Paxinos and Watson 2006). The infralimbic cortex, cingulate cortex and claustrum images were taken on +2.7 AP from bregma. The nucleus accumbens, olfactory tubercule and septum on +1 AP from bregma. All images were analysed using ImageJ and presented as a percentage of area covered with positive immunostaining.

3.3.9 Statistics

Statistical analyses were conducted using SPSS (v27, IBM). Any missing values were calculated in SPSS using linear interpolation. The data was analysed using one-way analysis of variance (ANOVA), with Tukey's *post hoc* test to perform multiple comparisons with Group (Control, Lesion, hfVM, hESC-DA1 and hES-DA2) as a between-subjects factor. Changes in amphetamine-induced rotations over time were conducted using a one-way ANOVA with repeated measures with week (0,3,6,9,12,15,18,21) as a within-subjects factor. Graphical data is presented as group mean and error bars determined by standard error of the mean (SEM). Bivariate correlation analyses were carried out using Pearson's correlational coefficient. Results were considered statistically significant with a threshold of *p* <0.05.

3.4 Results
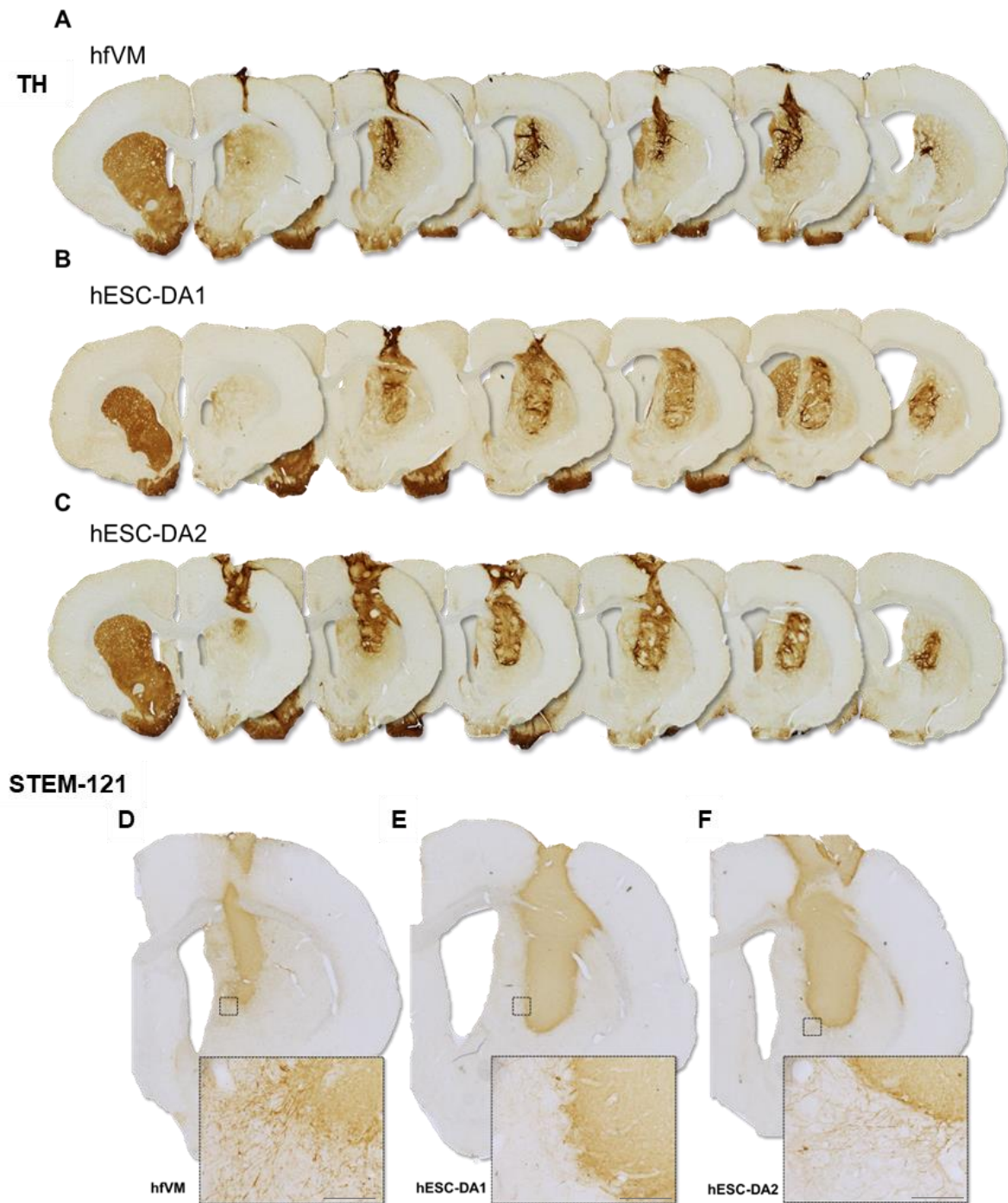
*Figure 3.4. **A-C** Histological representation hfVM and hESC derived DA grafts transplanted within the 6-OHDA lesion rat model, 21-weeks post-graft. A) hfVM B) hESC-DA1 C) hESC-DA2 transplants show clear graft survival after 21-weeks and strong TH staining throughout the grafted area and the cortex superior to the transplant site. D) hfVM **E)** hESC-DA1 and **F)** hESC-DA2 display +ve human neuronal (STEM121) projection staining innervating into the host striatum. Images taken at 1205x magnification, with close-up image accompanying D-F taken at 100x magnification. Scale bar represents 100μm.*

3.4.1 Histological analysis of DAergic grafts

All grafts had similar levels of survival and similar gross morphology

Graft survival for each group was very high with hfVM and hESC-DA1 having 90% of rats having surviving grafts and hESC-DA2 having 100% graft survival. Histological analysis of TH staining within the striatum was undertaken in order to understand greater detail about the morphology and characteristics of the grafts (Figure 3.4.A-C). All grafts were located centrally within the striatum, with evidence in the majority of each grafted group, of the graft present in the motor cortex, likely due to reflux up the needle track. All groups showed evidence of patchy TH expression, with dense fibrous areas within the graft core, but also some areas within that core being absent of TH staining. TH expression was also present along the rostro-caudal axis of the striatum in all grafted groups.

All transplants had axonal projections from the graft core integrating into the host brain

In Figure 3.4, the presence of human positive cells within the graft is shown by STEM-121 immunostaining (Figure 3.4.D-F), which also confirmed the presence of human-derived neuronal outgrowth into the host striatum. All grafts across all groups showed some extent of fiber outgrowth from the graft core. Histological analysis of innervation of STEM-121 fibers was measured by darkfield analysis into A9 and A10 target areas and is described in detail below.
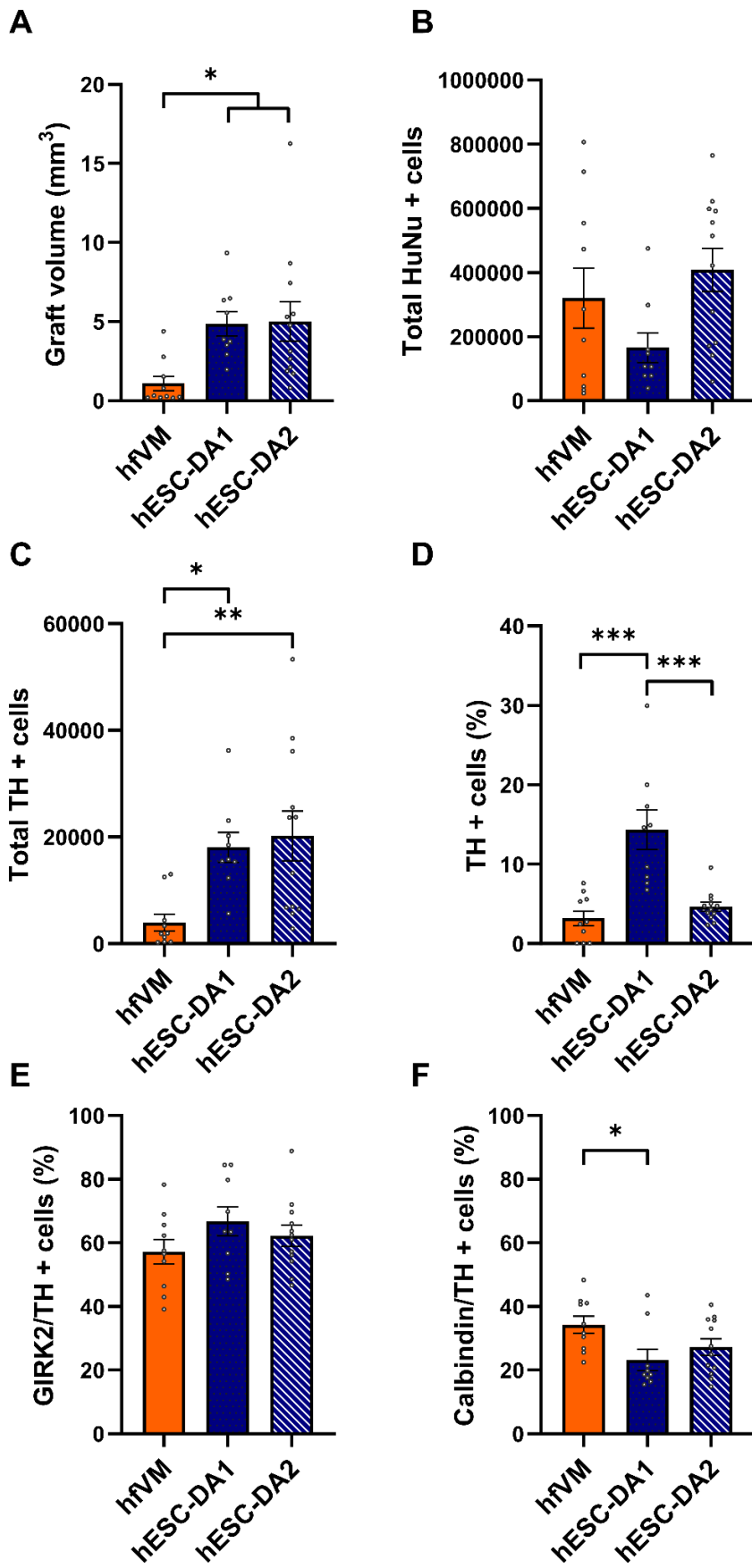
Figure 3.5. Histological analysis of cell populations within the graft. ***A)*** *Graft volume determined by TH expression revealed that hfVM grafts were smaller than both hESC-derived grafts.* ***B)*** *Total number of HuNu +ve cells comprising the graft core did not differ among groups.* ***C)*** *Total number of TH +ve cells indicate hfVM grafts had a smaller population of TH +ve neurons.* ***D)*** *When comparing TH +ve cells as a percentage of the total HuNu +ve cells, hESC-DA1 grafts had the highest percentage compared to hfVM and hESC-DA2 grafts.* ***E)*** *The percentage of A9 (GIRK2) +ve cells as a percentage of the total TH+ve cells was found to be similar among grafted groups.* ***F)*** *The percentage of A10 (Calbindin) +ve neurons was greater in hfVM grafts than hESC-DA1 grafts. Error bars represent standard error of mean. Significant differences between groups are presented as * p < .05, ** p <.01, *** p <.001.*
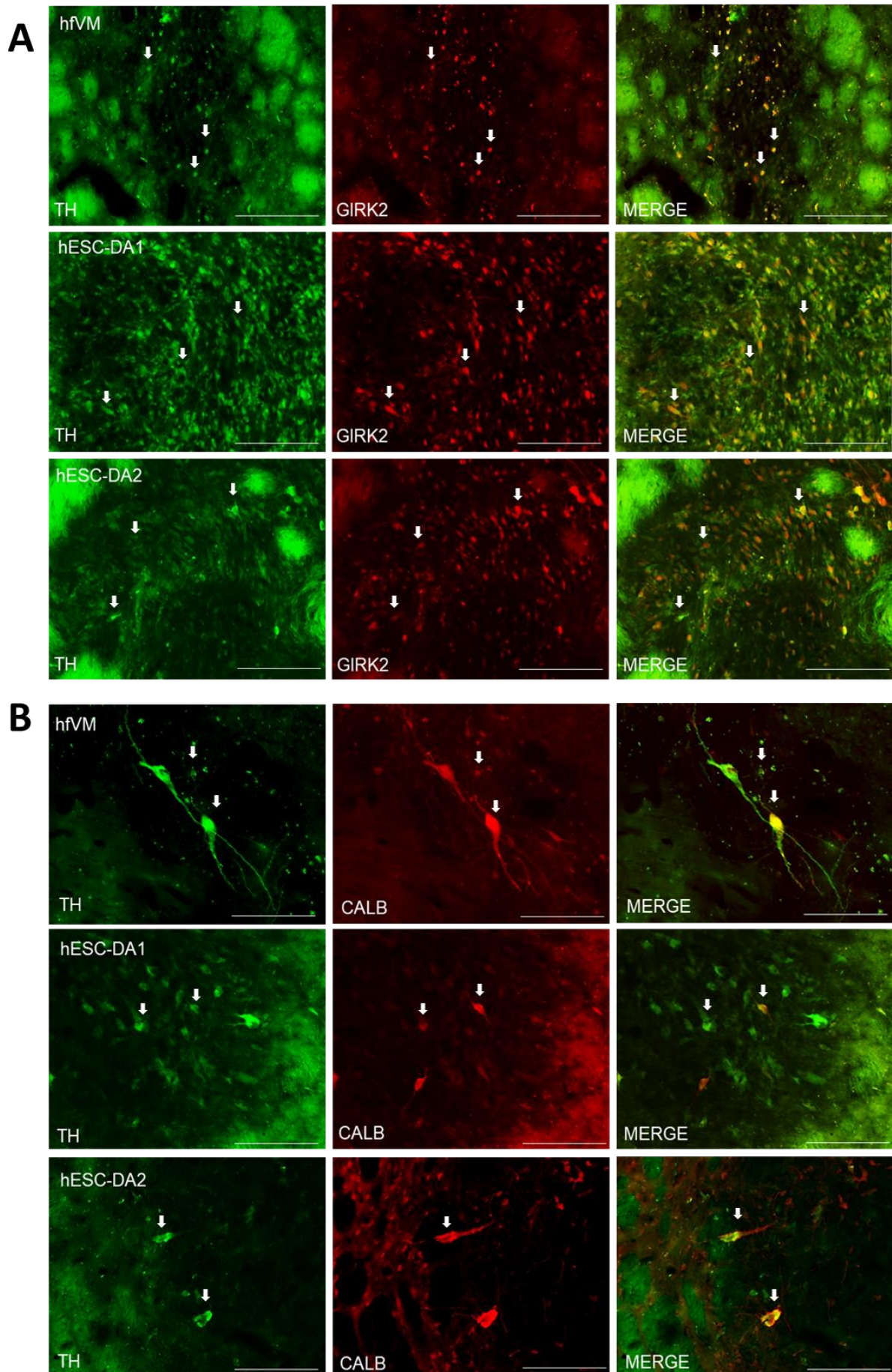
Figure 3.6. Immunofluorescence of A9 and A10 DAergic neurons in the graft at 21-weeks post-transplantation. **A)** *A9 +ve cells (red) expressing GIRK2 and* **B)** *A10 +ve cells (Red) expressing calbindin (CALB), were co-labelled with TH (green) to evaluate A9 and A10 DAergic composition within the graft. Images taken on 200x magnification within the graft core in all groups. Scale bars = 100µm. White arrows represent co-labelling.*

hfVM tissue produced smaller grafts than hPSCs-derived DA progenitors

The difference in graft volume depicted within Figure 3.4 was also supported by stereological analysis of the STEM-121 staining. Graft volume of hfVM grafts were significantly smaller than both hESC-derived grafts Figure 3.5 A. Group: $F(2,28) = 5.399$, $p = .010$, hfVM vs hESC-DA1 $p = .032$ & hESC-DA2 $p = .015$). There were no significant differences in total HuNu +ve cells between the grafted groups (Figure 3.5.B. Group: $F(2,28) = 2.774$, $p = $ n.s).

hfVM had fewer TH+ve neurons than hPSC-derived DA grafts

hfVM grafts harboured fewer TH +ve cells within the graft compared to hESC-DA1 and hESC-DA2 grafts (Figure 3.5.C. Group: $F(2,28) = 6.297$, $p = .006$). When analysing TH as a percentage of Total HuNu +ve cells, hESC-DA1 grafts had the highest percentage of TH +ve cells (Figure 3.5.D. Group: $F(2,28) = 19.982$, $p = <.001$), and no difference was found between hfVM and hESC-DA2 grafts ($p = $ n.s).

Composition of cell populations in DA grafts are almost equivalent, despite low TH+ content

The two most common subtypes of DAergic neurons were also analysed within the graft. All grafts had a similar percentage of GIRK2/TH +ve cells (Figure 3.5.E Group: $F(2,28) = 1.416$, $p = $ n.s). There was a difference in the percentage of TH positive cells staining for calbindin (Figure 3.5.F. Group: $F(2,28) = 3.649$, $p = .039$), with hfVM grafts having a higher percentage of calbindin +ve cells than hESC-DA1 grafts ($p = .039$). Figure 3.6.A, depicts that all grafts had substantial levels of GIRK2 (A9) +ve neurons, making up the largest population of DAergic neuronal subtypes within the graft. Figure 3.6.B illustrates the presence of A10 neurons in the graft, as indicated by calbindin staining, but to a lesser extent than GIRK2 +ve neurons. There was also a surrounding population of calbindin +ve neurons that are not positive for TH, suggesting an intermix of host striatal interneurons into the graft core.
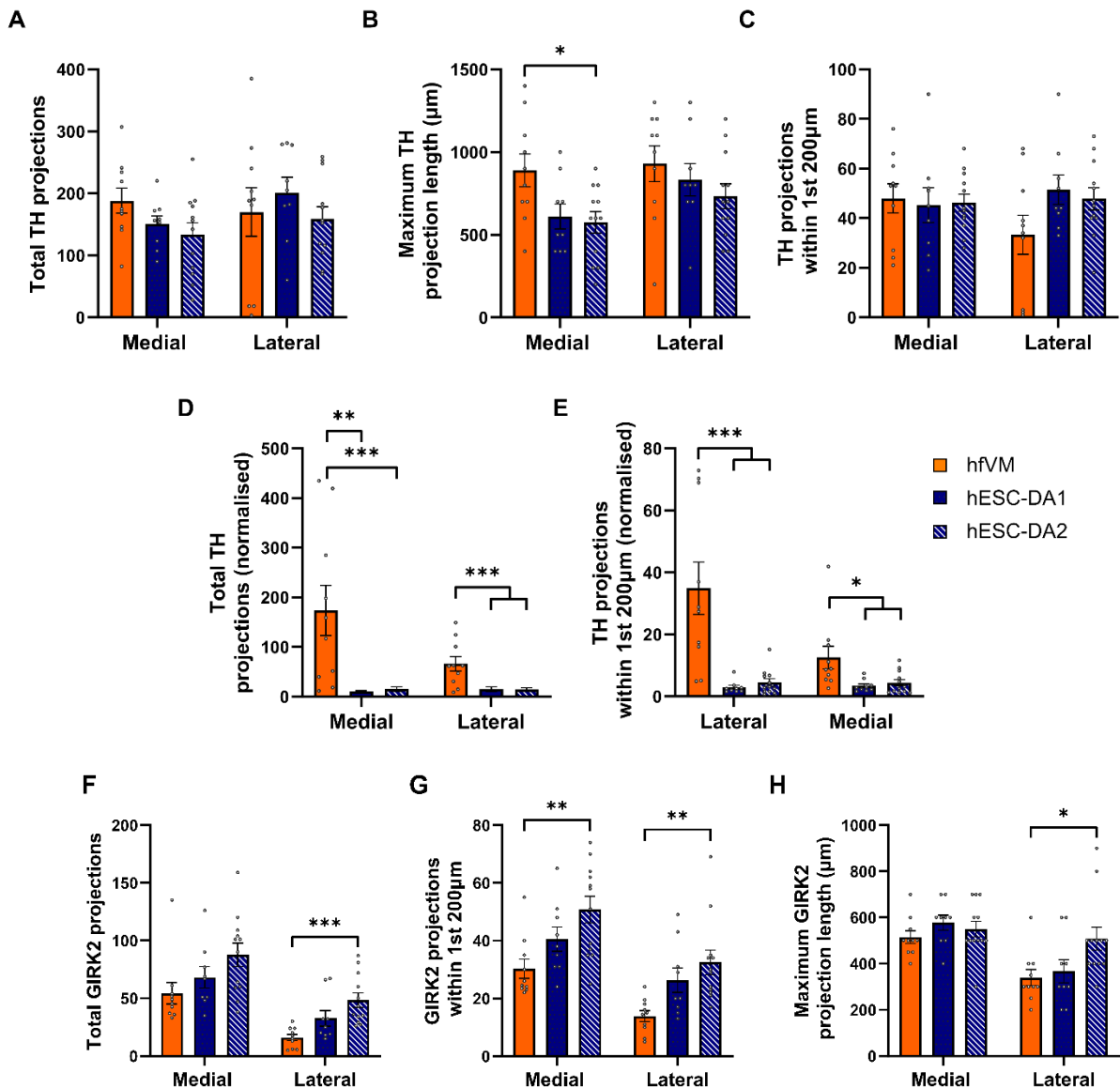
*Figure 3.7. Innervation of DAergic neurons throughout the striatum. Innervation was measure from the graft core outward into the host striatum in either a medial or lateral direction. **A)** Total number of TH projections extending from the graft did not differ among groups. **B)** Mean maximum length of TH neuronal projections from the graft was significantly greater from hfVM grafts in the medial direction compared to hESC-DA grafts. **C)** TH projections within the 1st 200μm did not differ in any direction among groups. When the data was normalised to the TH population within each group, hfVM projection outgrowth was significantly greater **(D)** and more substantial within the 1st 200μm **(E)** both medially and laterally compared to hESC-DA grafts. **F)** The total number of A9 (GIRK2) projections was greater in a lateral direction in hESC-DA1 grafts compared to hfVM. **G)** Immediate GIRK2 projections within the 1st 200μm in both medial and lateral direction was greater in hESC-DA2 grafts compared to hfVM. **H)** The maximum projection length of GIRK2 +ve fibres was greater laterally in hESC-DA2 grafts compared to hfVM. Error bars represent standard error of mean. Significant differences are presented as * p < .05, ** p <.01, *** p <.001.*

3.4.2 Innervation into the host striatum

hfVM grafts have more TH fiber outgrowth that hESC-derived DA

Total number of TH projections extending from the graft did not differ among groups (Figure 3.7. A: Medial: $F(2,28) = 2.424$, p = n.s, Lateral: ($F(2,28) = .558$, p = n.s), however, projections normalised to the number of TH neurons within each graft indicate hfVM grafts had a significantly greater number of projections per neuron, extending in both a medial (Figure 3.7. D. Group: $F(2,28) = 10.548$, p <.001. hfVM vs hESC-DA1 p = .002, hfVM vs hESC-DA2 p = .001) and lateral direction ($F(2,28) = 11.305$, p <.001. hfVM vs hESC-DA1 p = .001, hfVM vs hESC-DA2 p <.001). The maximum distance projected by hfVM grafts was greater medially than hESC-DA2 grafts (Figure 3.7.B: $F(2,28) = 4.624$, p = .018, hfVM vs hESC-DA2 p = .021), but all groups were similar in their maximum projection length laterally ($F(2,28) = 1.201$, p = n.s). The number of proximal projections from the graft, within the first 200um in either a medial or lateral direction did not differ among groups (Figure 3.7.C. Medial: $F(2,28) = 0.64$, p = n.s, Lateral: $F(2,28) = 2.382$, p = n.s). When normalised to TH neurons, hfVM grafts have a greater proportion of TH projections within the 1st 200µm compared to hESC-derived grafts (Figure 3.7. E. Medial: $F(2,28) = 13.836$, p <.001, hfVM vs hESC-DA1 & hESC-DA2 p < .001, Lateral: 1st 200 ($F(2,28) = 5.216$, p = .012, hfVM vs hESC-DA1 p = .021 & hESC-DA2 p = .027).

DA populations within the graft

There was more innervation from GIRK2 positive neurons in hESC-DA2 grafts extending laterally compared to hfVM grafts (Figure 3.7.F. $F(2,28) = 7.747$, p = .002, hESC-DA2 vs hfVM, p = .002). The maximum projection length differed among groups. In relation to immediate outgrowth from the graft (within 1st 200um), hESC-DA2 grafts had a greater number of GIRK2 projections in the 1st 200um in both medially and laterally compared to hfVM grafts (Figure 3.7.G. Medial: $F(2,28) = 6.319$, p = .005, hESC-DA2 vs hfVM, p = .004. Lateral: $F(2,28) = 6.718$, p = .004, hESC-DA2 vs hfVM, p = .003). The maximum GIRK2 projection length was no different in the medial direction (Figure 3.7.H. $F(2,28) = .909$, p = n.s), but hESC-DA2 grafts extended significantly longer laterally compared to hfVM grafts ($F(2,28) = 4.114$, p = .027), hESC-DA2 vs hfVM p = .034).
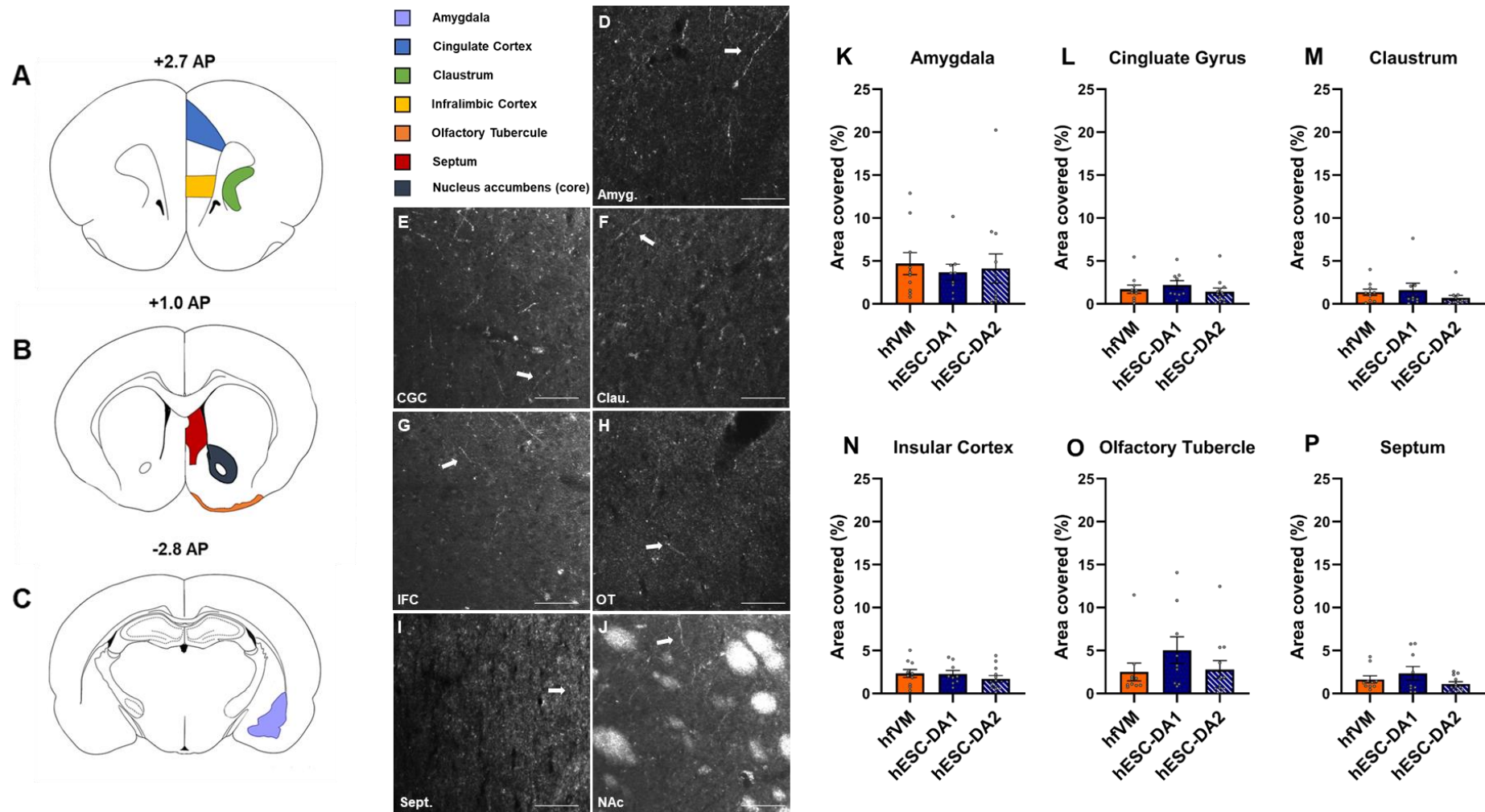
Figure 3.8. Neuronal outgrowth into A10 target areas amongst grafted groups. A-C. Schematic of brain regions at three distinct points along the rostral-caudal axis in which A10 DA neuron target areas were evaluated using STEM-121 staining. D-J Representative areas from one rat in the hfVM group. K-P Area fraction covered of the image taken in each A10 target area. No differences were found amongst grafted groups. Error bars represent standard error of the mean. Scale bar = 50μm

3.4.3 Neuronal outgrowth into A10 target regions

No difference in innervation to A10 target regions between graft groups

In order to investigate the density of fibres that have extended into A10 target areas, STEM121 staining using dark field analysis was conducted (Figure 3.8). All groups had evidence of fibre outgrowth in the regions examined demonstrating extensive outgrowth by each graft to both A9 and A10 areas. When comparing differences in innervation, no differences was found in the level of fibre density amongst groups (Figure 3.8. Group: (K) Amygdala: $F(2,28)$ = .115, p = n.s, (L) Cingulate gyrus: $F(2,28)$ = .669, p = n.s, (M) Claustrum: $F(2,28)$ = .986, p = n.s, (N) Insular cortex: $F(2,28)$ = .684, p = n.s, (O) Olfactory tubercle: $F(2,28)$ = 1.250, p = n.s, (P) Septum: $F(2,28)$ = 1.599, p = n.s). Darkfield analysis was carried out to systematically quantify projections in A10 regions, but due to high level of autofluorescence from the fibre bundles when examining the NAc, this area was not included in the analysis. Alongside darkfield, each image for all groups was observed for the visible presence/absence of projections (white arrows indicating a visible projection, Figure 3.8 D-J). The NAc had the greatest presence of fibres across groups (23/31 animals) with the lowest being the claustrum (3/31).
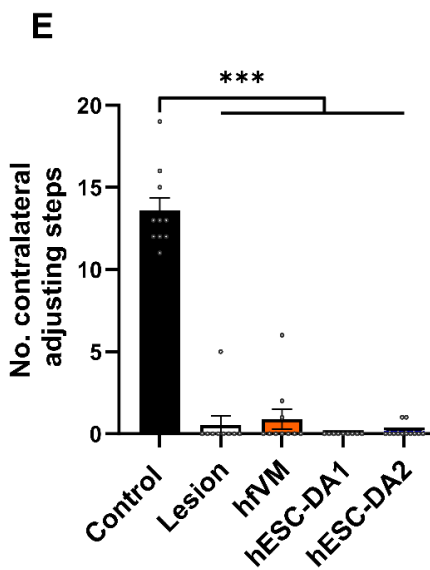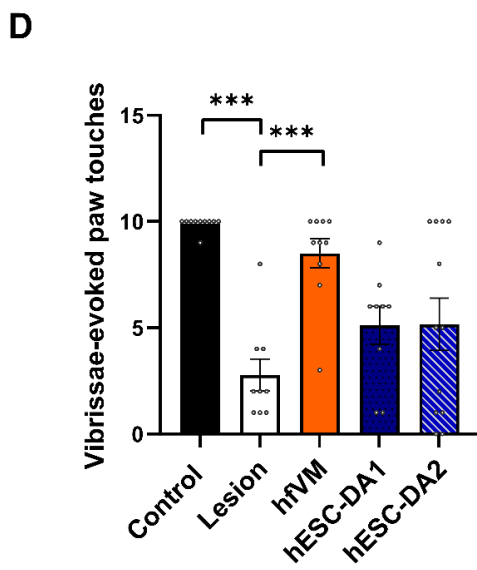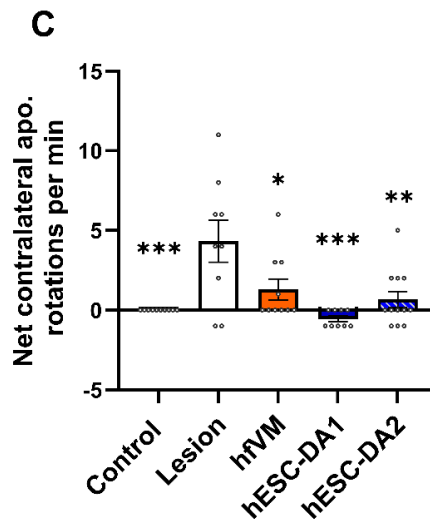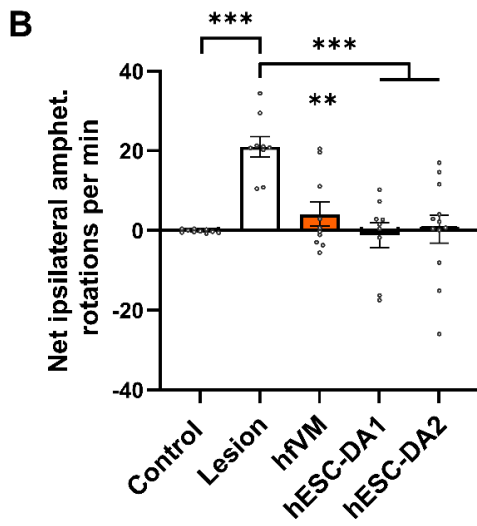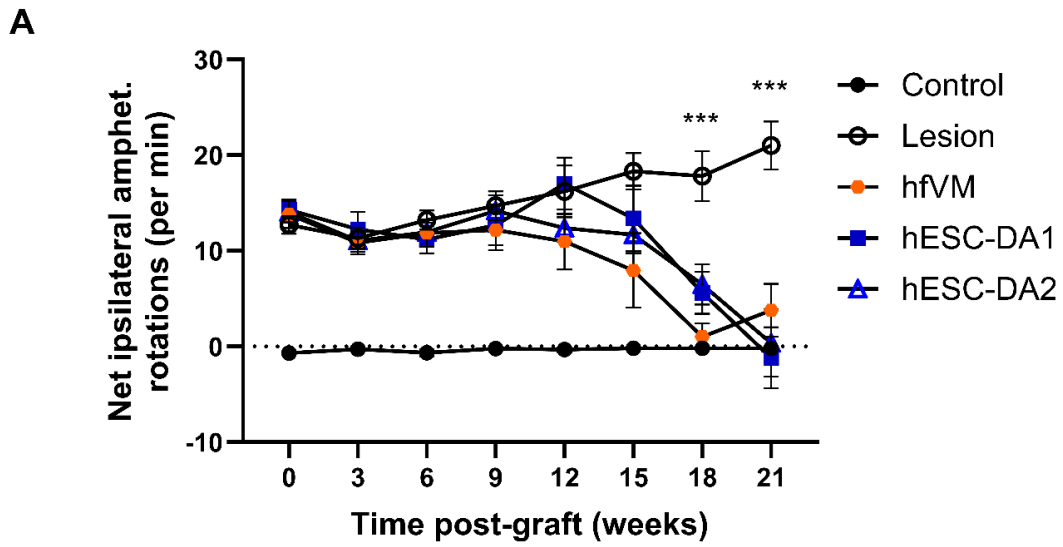
*Figure 3.9. Impact of grafts at 21-weeks post-transplantation on motor behaviours. **A)** Net amphetamine-induced ipsilateral rotations per minute 0-21 weeks post-transplantation shows a gradual reduction of rotational performance in graft groups across the 21 weeks. **B)** Net amphetamine-induced ipsilateral rotations per minute 21-weeks post-transplantation shows rotations in the lesion group, but few/no rotations in control and graft groups All grafted groups reduced rotational bias after 18 weeks. **C)** Net apomorphine-induced contralateral rotations per minute 21-weeks post-transplantation. All grafts improved rotational bias induced by apomorphine. **D)** Vibrissae-evoked contralateral paw touches 21-weeks post-transplantation. Sensorimotor improvement was seen at 21-weeks in with hfVM and hESC-DA2 grafts compared to lesion, but not hESC-DA1. **E)** Contralateral adjusting steps after 21-weeks post-transplantation. No grafted groups improved on the adjusting steps test. Error bars represent standard error of mean. Significant differences are indicated as * p < .05, ** p <.01, *** p <.001.*

3.4.4 Assessment of motor recovery 21 weeks post-graft

All grafts reduce amphet-induced rotational bias over 21 weeks

The DA agonist amphetamine (amphet.) was used to evaluate the functionality of the grafts and their ability to alleviate rotational bias. Analysis of the data across time demonstrates that, prior to grafting, all treated groups demonstrated strong rotational bias compared to controls Figure 3.9.A. Group*time: $F(28, 315) = 6.907$, $p < .001$, Control vs all groups at 0 weeks $p < .001$). All grafted groups significantly reduced their rotational bias after 18 weeks and consistently at 21 weeks, returning to the absence of rotational bias shown in the control group. When analysing at 21 weeks post-graft, amphet-induced rotational bias was reduced in all transplant groups Figure 3.9.B. Group: $F(4,45) = 14.135$, $p < .001$). Lesion rats demonstrated significantly greater rotational bias compared to controls rats ($p < .001$), whereas rotational bias was not present in all grafted groups after 21 weeks ($p < .001$).

DA grafts alleviated apo-induced rotational bias

Grafted groups were evaluated on changes to their DA receptor sensitivity in response to the DA receptor agonist apomorphine (apo.), 21 weeks post-transplantation. Control animals displayed no contralateral rotational bias, whereas lesion animals were significantly impaired Figure 3.9.C. Group: $F(4,45) = 7.473$, $p < .001$, Lesion vs Control $p < .001$). Post-transplantation apo-induced contralateral rotational bias was alleviated in all transplant groups (Lesion vs hfVM $p = .025$, & hESC-DA1 $p < .001$, & hESC-DA2 $p = .003$).

Grafts induce sensorimotor improvements 21-weeks post-transplantation

In the sensorimotor vibrissae-evoked paw touch test, control animals have intact sensorimotor processing after their whiskers were sensitised, whereas lesioned rats remained significantly impaired in this response Figure 3.9.D. Group: $F(4,45) = 10.466$, $p < .001$, Control vs lesion $p < .001$). After 21-weeks post-graft, only hfVM showed some restoration of sensorimotor processing compared to lesion (Lesion vs hfVM $p = <.001$, & hESC-DA1&2 $p = $ n.s). Despite some improvement in the vibrissae-evoked paw touch test, no improvement was observed in forelimb akinesia at 21 weeks post-transplant Figure 3.9.E. Group: $F(4,45) = 144.115$, $p < .001$. Control vs all groups $p < .001$).
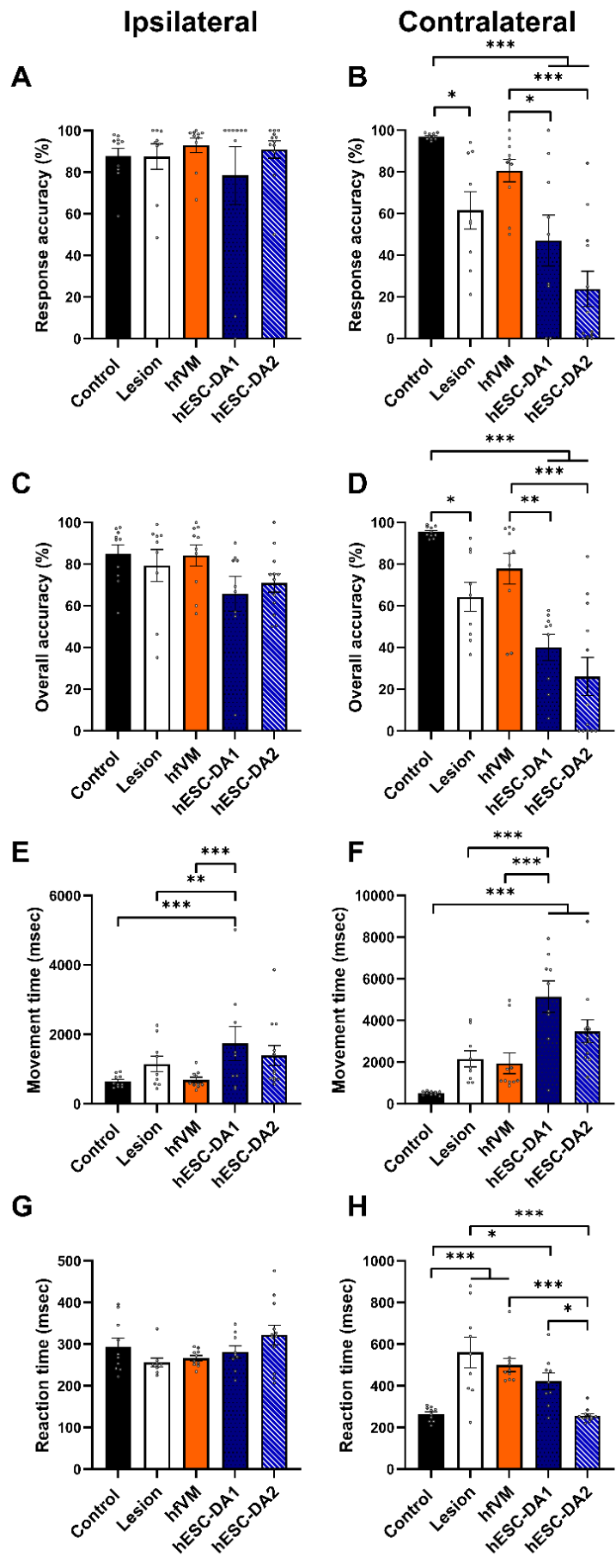
Figure 3.10. Ipsilateral and contralateral responses on the LCRT task after 20-weeks post-grafting.
A&C) *Response and overall accuracy did not differ across groups on the ipsilateral side* ***B&D)***
Response accuracy and overall accuracy showed similar findings on the contralateral side, as
accuracy was significantly impaired in lesion rats compared to controls. hfVM grafts did not differ
compared to controls and was significantly more accurate than hESC-derived DA grafts. ***E)***
Movement time on the ipsilateral side was made slower by hESC DA1 grafts compared to control,
lesion and hfVM grafted rats. ***F)*** *Movement time on the contralateral side was significantly slower*
due to hESC-derived DA grafts compared to controls. hESC-DA1 grafted rats were significantly
slower than hfVM and lesioned rats. ***G)*** *Reaction time on the ipsilateral side did not differ between*
groups. ***H)*** *hESC-derived DA grafts were significantly quicker to complete the task on the*
contralateral side compared to lesion Reaction time. Error bars represent standard error of mean.
Significant differences are presented as * p < .05, ** p <.01, *** p <.001.

3.4.5 Impact of DAergic grafts on performance during the LCRT task

hESC-derived DA grafts could not alleviate visuospatial deficits

Response accuracy

Performance on the LCRT task was averaged across 20- and 21-weeks post-graft in order to evaluate any improvement in visuospatial function due to transplantation of either hfVM or hESC-derived DAergic progenitors. Control rats were over 90% accurate in their response accuracy on the contralateral side, whilst lesion rats were significantly less accurate at around 60% (p = .029). Contralateral response accuracy was impacted by transplantation after 21 weeks (Figure 3.10.B. Group: $F(4,45)$ = 13.839, p <.001). Rats who received hfVM transplants were not significantly more accurate compared to lesion (p = n.s), however, hfVM were also not significantly different in response accuracy compared to controls, having a response accuracy of just below 80%, indicating a trend of hfVM grafts alleviating visuospatial function (p = n.s). Despite the hypothesis that all grafts would alleviate contralateral visuospatial processing deficits, neither hESC-derived DA grafted groups showed improvement on the task (Control vs hESC-DA1&2 p <.001), in fact, hESC-DA2 was significantly impaired on the task compared to lesion (p = .012) and compared to hfVM grafts (hESC-DA1 p = .044, & hESC-DA2 p <.001).

Overall Accuracy

Overall accuracy on the task was similar to response accuracy (Figure 3.10.D. Group $F(4,45)$ = 16.766, p <.001). Control animals were highly accurate responders, whereas lesioned rats were significantly worse (Control vs Lesion p = .030). hfVM grafted rats were above 75% accurate in their overall contralateral performance but were not significantly improved compared to lesion (p = n.s), however they were not significantly different to controls (p = n.s). As shown in their response accuracy, hESC-derived DA grafted animals were also significantly worse in their overall accuracy compared to controls (p <.001) and hfVM grafted animals (hESC-DA1 p = .005 & hESC-DA2 p <.001). hESC-DA1 grafted rats were significantly worse in overall accuracy compared to lesion (p = .003).

Ipsilateral responding

Due to the unilateral lesion, impairment in performance is restricted to the contralateral side, resulting in ipsilateral performance to act as a within-subject control. Response accuracy (Figure 3.10.A. Group: $F(4,45) = .620$, $p = $ n.s) and overall accuracy (Figure 3.10.C Group: $F(4,45) = 1.941$, $p = $ n.s) on the ipsilateral side was not significantly different among groups.

hESC-DA1 grafts led to substantially impaired movement time

Movement time was recorded to evaluate how long animals took to complete a correct trial. Control, lesion and hfVM grafted rats showed no difference in their movement time, however hESC-DA1&2 grafts led to slower responding (Figure 3.10.F. Group: $F(4,45) = 11.500$, p <.001). hESC-DA1 grafted rats were significantly slower than control (p <.001), lesion ($p = $ .003) and hfVM grafted rats (p <.001). hESC-DA2 grafted animals were slower compared to control (p <.001). Movement time on the ipsilateral side was also impaired due to hESC-DA1 grafts, indicating these animals were struggling overall to initiate a response (Figure 3.10.E. Group: $F(4,45) = 6.354$, p <.001. hESC-DA1 vs Control p <.001 & Lesion $p = $ .040 & hfVM p <.001).

Reaction time deficits alleviated by hESC-DA2 grafts

The time taken for an animal to withdraw their nose from the centre hole was analysed as a surrogate measure of attention during the task. Control animals were very quick in their reaction time, at approximately 200msecs, and the Lesion group was significantly slower (Figure 3.10.H. Group: $F(4,45) = 13.957$, p <.001. Control vs Lesion, p <.001). hfVM grafts did not alleviate reaction time deficits, nor did hESC-DA1 (Control vs hfVM, p <.001 & hESC-DA1 $p = $ .039). Interestingly, hESC-DA2 grafts improved reaction time compared to Lesion (p <.001), hfVM grafts (p <.001) and hESC-DA1 grafts ($p = $ .020). Reaction time on the ipsilateral side did not differ amongst groups (Figure 3.10.H. Group: $F(4,45) = 2.333$, $p = $ n.s).

DAergic grafts did not alleviate incentive motivation deficits or improve efficiency

The number of total trials useable (TTU) were recorded and is indicative of the rats' incentive motivation to perform the task. Control animals performed many useable trials within the 30-minute testing period, and those within the Lesion group performed significantly fewer, which was not improved by the addition of hfVM grafts or hESC-derived DA grafts (Figure 3.11.A.

Group: $F(4,45) = 14.053$, $p < .001$. Control vs all groups, $p < .001$.). Efficiency (the number of TTU as a percentage of total trials started) was approximately 50% in Control animals after 20 weeks of testing. Lesioned rats were approximately 20% efficient at the task, which was not improved in hfVM grafted rats and was impaired in hESC-derived DA grafted rats (Figure 3.11.B. Group: $F(4,45) = 16.438$, $p < .001$. Control vs Lesion and hfVM, $p = .002$, Control vs hESC-DA1&2, $p < .001$. hfVM vs hESC-DA1, $p = .034$).
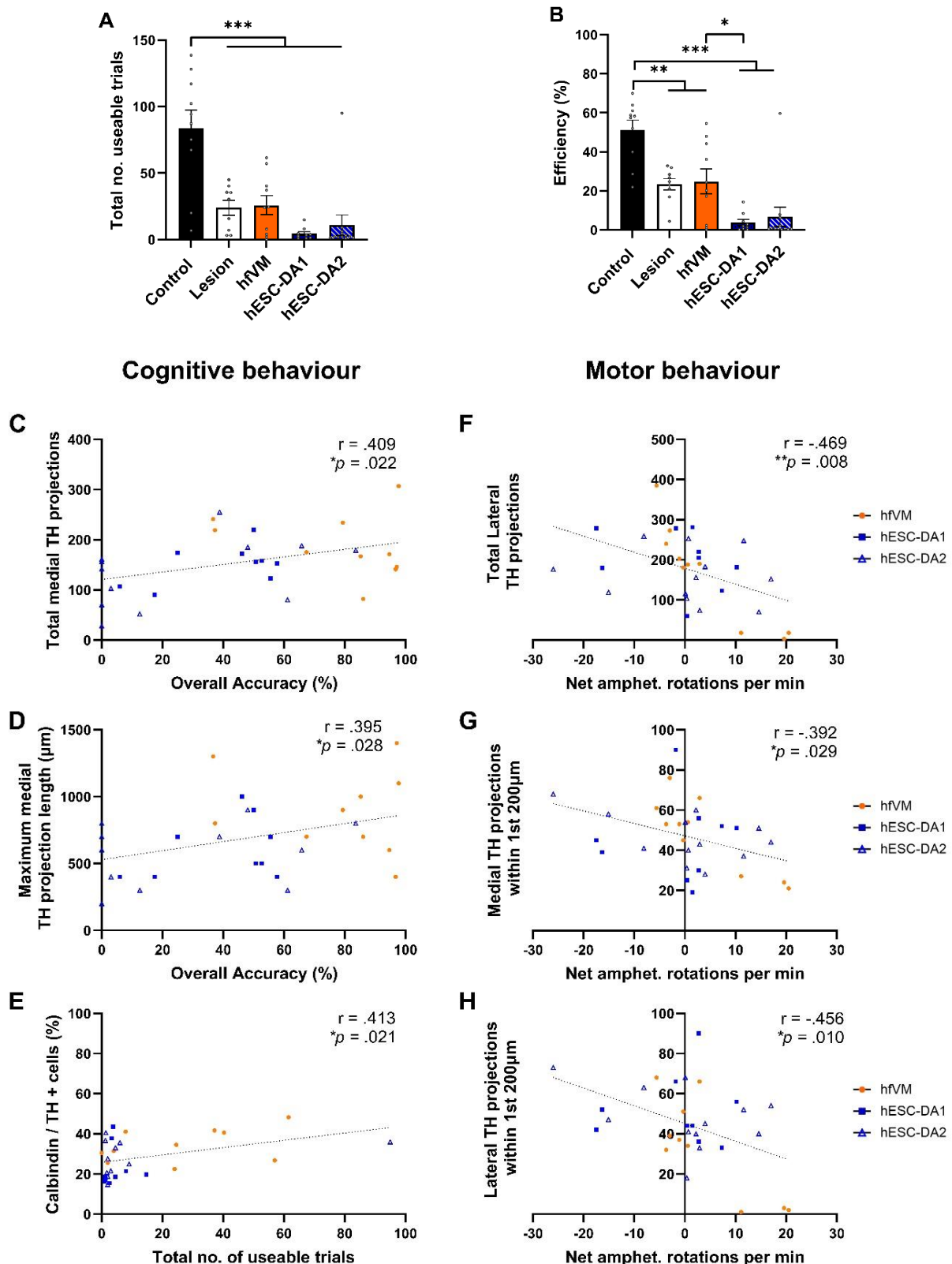
*Figure 3.11. Non-lateralised aspects of LCRT task and correlational analysis between graft characteristics with motor and cognitive behaviour. **A)** Total useable trials were significantly reduced in all treated groups compared to control **B)** Lesion and hfVM grafted animals were less efficient on*

the task compared to Controls, as were both hESC-derived DA groups. hESC-DA1 rats were significantly less efficient than hfVM grafted rats. Error bars represent standard error of the mean. Statistical differences are represented as * p = < .05, ** p = <.01, *** p <.001. **C)** *A greater number of TH+ve projections and* **D)** *maximum length of both medial projections from the graft correlated with better overall accuracy on the LCRT task.* **E)** *A higher percentage of calbindin +ve cells within the graft correlated with a greater number of useable trials.* **F)** *A greater number of lateral TH projections correlated with lower to amphet-induced rotations bias as well as projections within the 1ˢᵗ 200µm in both a* **G)** *medial and* **H)** *lateral direction. Line indicates a linear relationship.*

3.4.6 Correlation analysis

Graft outgrowth correlates with cognitive and motor recovery

Correlational analysis was conducted in order to understand the extent to which there was a relationship between different graft characteristics observed through histological analysis and behavioural recovery. The analysis in Figure 3.11 focuses on the relationship to overall accuracy and Total useable trials in the LCRT task as a way to understand important factors for cognitive improvement (Figure 3.11.C-E). Secondly, correlations presented also focus on amphetamine-rotations to identify which factors correlate with motor recovery (Figure 3.11.F-H). TH outgrowth into the medial striatum correlated with better overall accuracy. Specifically, the total number of medial TH projections (Figure 3.11.C. $r = .409$, $p = .022$) and a greater outgrowth distance into the medial striatum (Figure 3.11.D. $r = .395$, $p = .028$) both correlated with greater accuracy. A greater percentage of calbindin +ve cells making up the TH+ve neurons present within the graft correlated with a greater number of useable trials (Figure 3.11.E. $r = .413$, $p = .021$). In relation to motor recovery, a greater number of TH projections into the lateral striatum was negatively associated with higher number of rotations per minute, suggesting more lateral projections correlate with better motor recovery (Figure 3.11.F. $r = -.469$, $p = .008$), as well as a greater immediate neurite outgrowth from the graft core in a medial (Figure 3.11.G. $r = -.392$, $p = .029$), and lateral direction (Figure 3.11.H. $r = -.456$, $p = .010$).

3.5 Discussion

The aim of this chapter was to determine whether hESC-derived DAergic cell therapy products were capable of alleviating cognitive impairments in the LCRT task. The results reveal that, while hESC-derived DA grafts can effectively alleviate motor impairments, they were unable to restore visuospatial function compared to controls and, at times, rats grafted with hESC-derived cells were significantly impaired compared to hfVM grafted rats. Interestingly, the number of HuNu +ve cells did not differ between grafted groups, but hfVM grafts had greater overall TH projections into the host striatum, despite having the lowest number of TH+ve cells. The finding that two different forms of DA cell replacement therapy can lead to different outcomes in relation to cognitive recovery highlights that (1) hESC-derived grafts may not be equivalent to hfVM grafts and (2) more work is needed to understand what factors are important for DA-mediated recovery.

3.5.1 Only hfVM grafts alleviate visuospatial function on the LCRT task

The data presented here are the first to indicate discrepancies between hfVM and hESC-derived DA grafts in alleviating cognitive deficits in the PD rat model. When DA is depleted in the striatum, either due to MFB or nigral lesions, we see deficits in processing visuospatial information (Lindgren et al. 2014b). It was hypothesised that replacing the lost DA, either by hfVM or hESC-derived DA grafts would facilitate recovery that was previously observed using human fetal grafts (Lelos et al. 2016). As shown in Figure 3.10.B&D, hfVM grafts did not improve contralateral response or overall accuracy as compared to lesioned animals, however, they also were not significantly impaired compared to controls, whereas lesioned rats were significantly less accurate than controls. As for hESC-derived DA grafted rats, performance was significantly worse compared to controls and hfVM grafted rats (Figure 3.10.D).

Although Lelos et al. (2016) found hfVM grafts to alleviate visuospatial processing deficits compared to lesion, it is important to note that lesion animals within this study were still able to perform the task with approximately 60% accuracy and showed greater variability within the group to what was observed in Lelos et al. (2016) within the lesion-only group. In the present study, lesioned rats showed a robust ipsilateral rotational bias, indicative of SNc cell loss, that was consistent over 21 weeks of testing (Figure 3.9.A), so it is reasonable to suggest these animals are DA depleted. Lesioned rats were also still impaired in contralateral accuracy compared to controls rats. Full stereological analysis of the midbrain will be required to confirm that the extent of lesion was similar between experiments.

Improvement in TTU was reported in Lelos et al. (2016) for hfVM grafted rats, but there was no improvement in TTU for any of the grafted rats in this experiment (Figure 3.11.A). As discussed in Lelos et al. (2012), pre-feeding intact control rats reduced their incentive motivational state, affecting the TTU performance, but not accuracy on the LCRT task. This suggests that TTU performance is driven by the incentive motivational state of the rats.

3.5.2 Factors contributing to cognitive recovery

As presented in this chapter and supported by Lelos et al (2016), two DAergic cell therapy products can have different impacts on cognitive function. It is therefore important to consider factors that may contribute to cognitive recovery. Factors that will be discussed in relation to LCRT performance are (1) graft volume, (2) DAergic populations within the graft and their authenticity (3) differences in physiological release of DA and (4) differences in graft-to-host innervation patterns.

Size of the grafts

One of the main differences between the two graft types was the volume size. hfVM grafts were noticeably smaller in terms of graft volume, determined by STEM121 expression (Figure 3.5. A), and also had the smallest population of TH +ve neurons compared to hESC-derived DA grafts (Figure 3.5.C). Dowd and Dunnett (2004) report that improved accuracy on the LCRT task by rat VM grafts correlated with a greater number of TH +ve neurons within the graft core. It is plausible to hypothesise that the greater number of TH neurons, the greater the supply of DA to the DA-depleted striatum, the better chance of improving

DA-dependant visuospatial deficits. However, this was not observed within this experiment. It could be hypothesised instead in the case of this experiment, that the larger graft size was detrimental to cognitive function. As mentioned in Chapter 1, there is a well-established fine balance of DA that is required for normal cortical function, which has been proposed to be the same for DA transmission in the striatum (Cools and D'Esposito 2011; Vaillancourt et al. 2013; Cools et al. 2019).

Potential involvement of graft size in reaction time?

In contrast to response accuracy and movement time, hESC-DA2 grafts were able to alleviate contralateral reaction time deficits (Figure 3.10.H). One potential hypothesis for this improvement may relate to the size of the graft inducing impulsivity. hESC-DA2 grafts had the largest number of TH +ve neurons compared to hfVM grafts (Figure 3.5.C). As stated in Chapter 1 (see 1.4.1), DA agonists have been associated with the onset of impulsive behaviour. In Yates et al. (2016), greater DA uptake in the orbitofrontal cortex in a cued go/no-go created a hyperdopaminergic state and increased impulsive action. In addition to this, hESC-DA2 grafts had the greatest TH innervation into the lateral striatum. Moreno et al. (2021), using microdialysis, found greater DA release into the dorsolateral striatum to lead to high impulsivity. Therefore, it could be hypothesised that the hESC-DA2 grafts due to their large TH content are causing a dysregulation of dopamine signalling into the lateral striatum leading to impulsivity, and as a consequence, poor goal-directed decision making (Pine et al. 2010; Tedford et al. 2015). It is important to note however that surrogate measures for impulsivity such as premature withdrawal from the centre hole or panel press errors were not analysed. Furthermore, there was no parameters during cognitive testing to explicitly probe for impulsivity, so further tests such as the 5-choice serial reaction time task and the cued go, no-go would need to be carried out in order to confirm this. There was also no direct measurement of TH content by methods such as HPLC in this study.

DAergic populations within the graft

One factor that could potentially affect cognitive recovery is the differences in the DAergic populations within the the different grafts. hfVM grafts had a greater population of calbindin +ve neurons which suggests more of the A10 DA subtype (Figure 3.6.B & Figure 3.5.F). As discussed in Chapter 1 (see 1.2) A10 DA neurons reside largely in the VTA and are important in cognitive and motivational processing (Simon et al. 1980; Fu et al. 2016;

Farassat et al. 2019). VTA neurons are lost in PD (McRitchie et al. 1997), and circuit reconstruction to A10 target areas could be the important factor for cognitive recovery, hence, darkfield analysis of DA-depleted A10 target areas was evaluated (Fullard et al. 2017; Wong et al. 2021; Kamalkhani and Zarei 2022; Wang et al. 2022b; Wang et al. 2023).

Despite the increase in calbindin +ve neurons within hfVM grafts, there were no differences between graft groups in the extent of innervation to A10 target regions (Figure 3.8.K-P). However, there was no normalisation to account for smaller grafts that may be influential on these results. Grealish et al. (2014) transplanted hfVM and hESC-DA progenitors into the SNc in unilateral 6-OHDA MFB lesioned rats to examine the innervation of those grafts to A9 and A10 areas. Differences in TH+ fibers in A10 target regions were found between graft types when comparing hfVM to hESC-derived DA grafts in the septum and infralimbic cortex, but all other areas were similar. Informative studies such as those by Adler et al. (2019) looked at the synaptic connectivity of graft-to-host circuitry of hESC-derived DA grafts and found they could appropriately integrate into the basal ganglia circuitry with communication from the host neurons to the graft, and vice versa. Monosynaptic tracing of the functional synaptic connections was not assessed in the present study. A more systematic approach to analyse fibre density in A10 target areas similar to Grealish et al. (2014) and Adler et al. (2019) might pull out discrepancies that are not able to be caught with area fraction analysis.

Non-DAergic cell types within the graft

Figure 3.5.D highlighted that the percentage of TH +ve cells within the graft was between 5-15% across the grafted group, indicating there are large proportions of non-TH +ve cells. Kirkeby et al. (2012) and Jaeger et al. (2011) protocols are designed to create a pure population of A9 DA neurons, and have reported a high yield of DA progenitors *in vitro* with floor plate markers such as LMX1A and FOXA2. Other possibilities are human derived astrocytes which have been reported in both hfVM grafts and hPSCs (Bye et al. 2019; de Luzy et al. 2022). However, human specific GFAP (STEM123 antibody) was not directly analysed in this study so cannot report on the quantity of astrocytes present within the graft. it is important to note that the differentiation protocol by Kirkeby et al. (2012) has been optimised in recent years (Nolbrant et al. 2017), so graft composition here may not directly apply to the current standard heading to clinical trial, which may caveat any conclusions on graft cell composition in this experiment.

3.5.3 Physiological release of DA

A factor that could be impacting the cognitive recovery is authenticity of the hESC-derived grafts and thus, the physiological release of DA to the striatum and external target regions. Firstly, relating to the authenticity of hESC-DA grafted neurons, hfVM grafts are derived from the developing embryo and are already specified in their fate to become DAergic neurons (Wictorin et al. 1992; Jiang et al. 1995). This therefore suggests that DA release is biologically authentic and can infer that they can project to the correct target regions and support recovery. There has been extensive work within the field to try and ensure 'authenticity' of hPSCs for clinical application (Sonja et al. 2011; Grealish et al. 2014; Barker et al. 2015; de Luzy et al. 2021; Piao et al. 2021; de Luzy et al. 2022; Wang et al. 2022a).

This study did not employ analysis of DA release, so cannot confirm, or refute whether DA release from hESC-derived DA grafts is physiologically relevant, but there are predictive marks of graft efficacy that has been measured such as motor recovery. All grafts were able to alleviate apomorphine-induced rotational bias (Figure 3.9.C) which indicates a normalisation of striatal DA receptors (Rath et al. 2013). No discrepancies between hfVM grafts and hESC-derived DA grafts in alleviating amphetamine-induced rotational bias were present Figure 3.9. A-B). This functional recovery is supported by the innervation of DA fibres from the graft which was present. Neurite outgrowth is critical to graft efficacy, as shown recently by Hills et al. (2023) examining IPSCs from PD patient lines. It would be important to understand what kind of DA release (tonal or phasic) each graft type supports and whether there are discrepancies between hfVM grafts and hPSC-derived grafts. One potential technique to employ here could be electrophysiology.

Differences in movement time

Movement time was not significantly improved by hfVM grafts and hESC-DA derived grafts resulted in significantly slower movement time than lesion (Figure 3.10.E-F). Interestingly, hESC-DA grafts also impaired ipsilateral movement time, indicating these rats are strongly impaired in their ability to execute a response. As detailed in Lelos et al. (2012), unilateral lesions are capable of inducing bilateral impairments. It is interesting to note that the movement impairment appears to be independent of visuospatial processing as accuracy on the ipsilateral side was not impaired (Figure 3.10.A&C). Impairments in movement time

during lateralised responding has been suggested to be a marker for motor readiness to perform the task (Brown and Robbins 1991). PD patients have also been reported to experience delays in cognitive processing, leading to greater amount of time taken to complete a task (Cooper et al. 1994).

3.5.4 Differences in graft-to-host innervation patterns

TH and GIRK2 projections were analysed to understand the extent of neurite outgrowth from the grafts by TH neuronal fibers overall and also specifically A9 neurons with GIRK2 expression, into the surrounding host striatum. hfVM grafts were found to project more TH fibres into the medial striatum compared to hESC-DA2 grafts (Figure 3.7.B). These results were associated with better overall accuracy (Figure 3.11.C&D). The opposite was seen for GIRK2 projections in which hESC-DA2 had a greater number of projections found to innervate into the lateral striatum and extended a greater distance into this striatal subregion Figure 3.7.F and H). Greater total TH fibres into the lateral striatum was associated with smaller rotational bias (Figure 3.11). It is unknown currently what the role of the medial and lateral striatum, and subsequently the SNC and VTA projections to those striatal regions, have in the LCRT task. There is evidence within the literature to suggest that the medial and lateral striatum govern different behaviours, in particular, the medial striatum is responsible for associative behaviours such as goal-directed behaviour, cognitive flexibility, set shifting and spatial learning (Reading et al. 1991; Yin et al. 2005; Balleine and O'Doherty 2010; Nakamura et al. 2012; Lee et al. 2014), whereas the lateral striatum is responsible for motor coordination and habit formation (Bhatia and Marsden 1994; Cousins and Salamone 1996; Voorn et al. 2004; de Wit et al. 2011; Durieux et al. 2012). The role of the striatal subregions in cognitive and motor processing will be discussed in greater detail in Chapter 5.

3.5.5 Conclusion

Chapter 3 found that rats receiving hfVM grafts had better contralateral visual processing compared to hESC-derived DA grafts, which had a significant impairment on the LCRT. The issues surrounding large-scale clinical application of hfVM has led the way for hESCs to emerge as a new option for cell replacement therapy in PD, which highlights how important

these results are for the field. The data presented here may suggest that we are not creating an 'authentic' DAergic neuronal population with current hESC protocols that support cognitive recovery comparable to primary tissue. Differences in graft size and composition may not be optimised to support normal neural processing in the striatum. The data presented in this chapter highlights that innervation into striatal subregions could be an important factor, not only for motor recovery but also cognitive recovery.

Chapter 4 : Evaluating viral-mediated DA biosynthesis on cognitive impairments in the LCRT task

4.1 Summary

Experiment 1 highlighted how fetal and stem cell-derived DA replacement therapies could have differential impacts on cognitive function. This discovery raised questions concerning what factors may be important for cognitive recovery when using DA replacement therapy. One potential factor important to cognitive function is the dose of DA to the striatum. To address this, Experiment 2 used two forms of DA replacement to evaluate cognitive impairments in the LCRT task: (1) viral-mediated DA biosynthesis in the form of gene therapy, infused at two different titres, and (2) the gold-standard treatment for PD, L-DOPA, administered across a range of doses. A biscistronic AAV expressing hTH and hGCH1 improved motor function at a high titre but did not alleviate cognitive impairments in the PD rat model. Furthermore, L-DOPA, in a dose response manner, impaired performance on the LCRT task in lesion only rats and induced onset of abnormal dyskinetic-like behaviours. Restricted biodistribution of AAV-htTH-2A-hGCH1 was found at both titres within the striatum, and off-target expression within the piriform cortex.

These results led to questions about the impact better biodistribution of viral-mediated DA biosynthesis could have on cognitive function. To address this, Experiment 3 employed another biscistronic tTH and GCH1 expressing AAV, and modified coordinates were used to reduce off-target cortical expression and improve biodistribution within the striatum. It was found that AAV-htTH-hGCH1 infusions improved visuospatial function LCRT whilst subtly improving forelimb akinesia.

Chapter 4 highlights the complexity of achieving DA-mediated cognitive improvement with dopamine-replacement, in the PD rat model, compared to improving motor deficits. This chapter also indicates a more fine-tuned supply and distribution of DA throughout the striatum to be beneficial for cognitive recovery.

4.2 Introduction: Experiment 2

Chapter 3 highlighted that hfVM and hESC-derived grafts can differentially impact cognitive impairments on the LCRT task. This brought about questions surrounding what specific aspects of DA replacement supports cognitive recovery. Some benefits of cell replacement therapy are that it offers DAergic synapse formation to relevant basal ganglia structures and also has the potential for physiological release of DA within the host brain. Two factors that could impact cognitive function are (1) the amount of DA being released at the synapse and also (2) the biodistribution of DA supply within the depleted PD rat model striatum, due to innervation projection patterns. It is also unknown if DA replacement alone, without circuit reconstruction, would be sufficient to support cognitive recovery in the LCRT task.

4.2.1 Biscistronic gene therapy approach to DA replacement

In order to address the question surrounding the dose of DA and its role in alleviating cognitive impairments in the LCRT task, in Experiment 2, a viral vector is used to probe passive DA release directly within the DA depleted striatum at two different titres. A biscistronic viral vector, specifically, the delivery of two rate-limiting enzymes involved in the synthesis of DA, truncated TH and GCH1 was used.

Chapter 1 (see 1.6) provided some brief detail about the structure and function of AAV-based viral vector constructs and how they can be modified for clinical application with factors such as the serotype (Li and Samulski 2020). Different serotypes result in different binding receptors, which will affect their preference for transfecting a certain cell type (Srivastava 2016). The viral vectors used throughout this chapter are a combination of an AAV2/1 pseudotype, in which the ITR is AAV2, but with the capsid of an AAV1 serotype. The benefit of using the AAV2/1 pseudotype is the high specificity at which it transfects neurons due to the AAV2 ITR, with limited expression in astrocytes, as well as better biodistribution due to AAV1 capsid (Burger et al. 2004).

As shown in Figure 4.1, DA biosynthesis in the intact DA neuron has the correct building blocks for DA synthesis, and DA neurons can form synaptic connections onto striatal MSNs to release DA (Blaschko 1939). As described in Chapter 1, in the 6-OHDA MFB lesion model there is an almost complete loss of DA innervation to the striatum. In the biscistronic gene therapy approach to DA replacement, the viral vector is infused into the striatum, transfecting striatal neurons with human copies of TH and GCH1 gene. The reason for supplying TH and GCH1 specifically, is that GCH1 directly initiates the conversion of GTP into BH4, which then allows BH4 to work as a co-factor with TH to catalyse the hydroxylation of L-Tyrosine to L-DOPA (Porenta and Riederer 1982). In this approach, AADC, involved in the conversion of L-DOPA to DA is not supplied to the striatal neuron. Instead, this model relies on the spared terminal ends of DA and 5HT neurons supplying AADC to the striatum to then allow the conversion of L-DOPA to DA, and thus supply MSNs with a continuous DA release (Björklund and Kirik 2009).

4.2.2 Rationale of manipulating dose of viral vector

Based on the approach above, biscistronic viral vectors have been used in pre-clinical animal studies and researchers report substantial improvement in sensorimotor tasks, such as adjusting steps and drug-induced rotations (Kirik et al. 2002a; Björklund et al. 2010). One benefit to using viral vectors is the ability to manipulate the titre of virus particles and thus the level of gene expression. Below details two studies that highlight the value of optimising dose of viral vector based DA synthesis to evaluate the impact on behavioural outcome.

A dosing study was undertaken by Cederfjäll et al. (2013) using a previously designed biscistronic AAV2/5 viral vector construct with human TH and GCH1 expressed under the human synapsin 1 (syn1) promotor in Cederfjäll et al. (2012). When infused into the striatum of the unilateral 6-OHDA MFB rat model, the viral vector had induced complete recovery of simple motor function on the adjusting steps, cylinder, staircase task and a 50% reduction in apomorphine induced rotational bias was observed. Cederfjäll et al. (2013) tested five doses between 9×10^8 and 2×10^{11}, with the lowest dose offering no minimal TH expression within the striatum and both 1×10^{11} and 2×10^{11} displaying complete coverage of the striatal nuclei with off-target expression in the piriform cortex and the motor cortex. Full recovery was observed with titres 1×10^{11} and 2×10^{11} from as early as three weeks post-infusion in the

corridor test and 5 weeks post-infusion in the adjusting steps and cylinder test. Interestingly, the magnitude of improvement was no greater with $2x10^{11}$ than with $1x10^{11}$ indicating a potential ceiling effect. Titres below $5x10^9$ offered partial to no recovery, indicating that viral vector mediated DA biosynthesis may act in a dose response manner to a certain point.

A further dosing study detailed in Rosenblad et al. (2019b) utilised a biscistronic AAV5 TH and GCH1 construct at a titre of $9x10^9$ and $9x10^{10}$. An initial pilot experiment in 6-OHDA MFB lesioned rats observed the same full recovery in motor tasks from 8 weeks with $1x10^{12}$ as previously described in Cederfjäll et al. (2013). The viral vectors were intra-striatally infused into MPTP treated NHPs and evaluated on motor impairments and observed for the onset of LIDs. They report a dose-dependent improvement in motor scores OFF L-DOPA with $9x10^{10}$ and did not observe any adverse effects on LIDs nor viral-induced dyskinesias.

All of the literature mentioned above have manipulated the viral vector titre and found a dose-dependent response in alleviating motor impairments. It is unknown what impact viral-mediated DA biosynthesis at two different titres will have on cognitive function observed in the LCRT task.
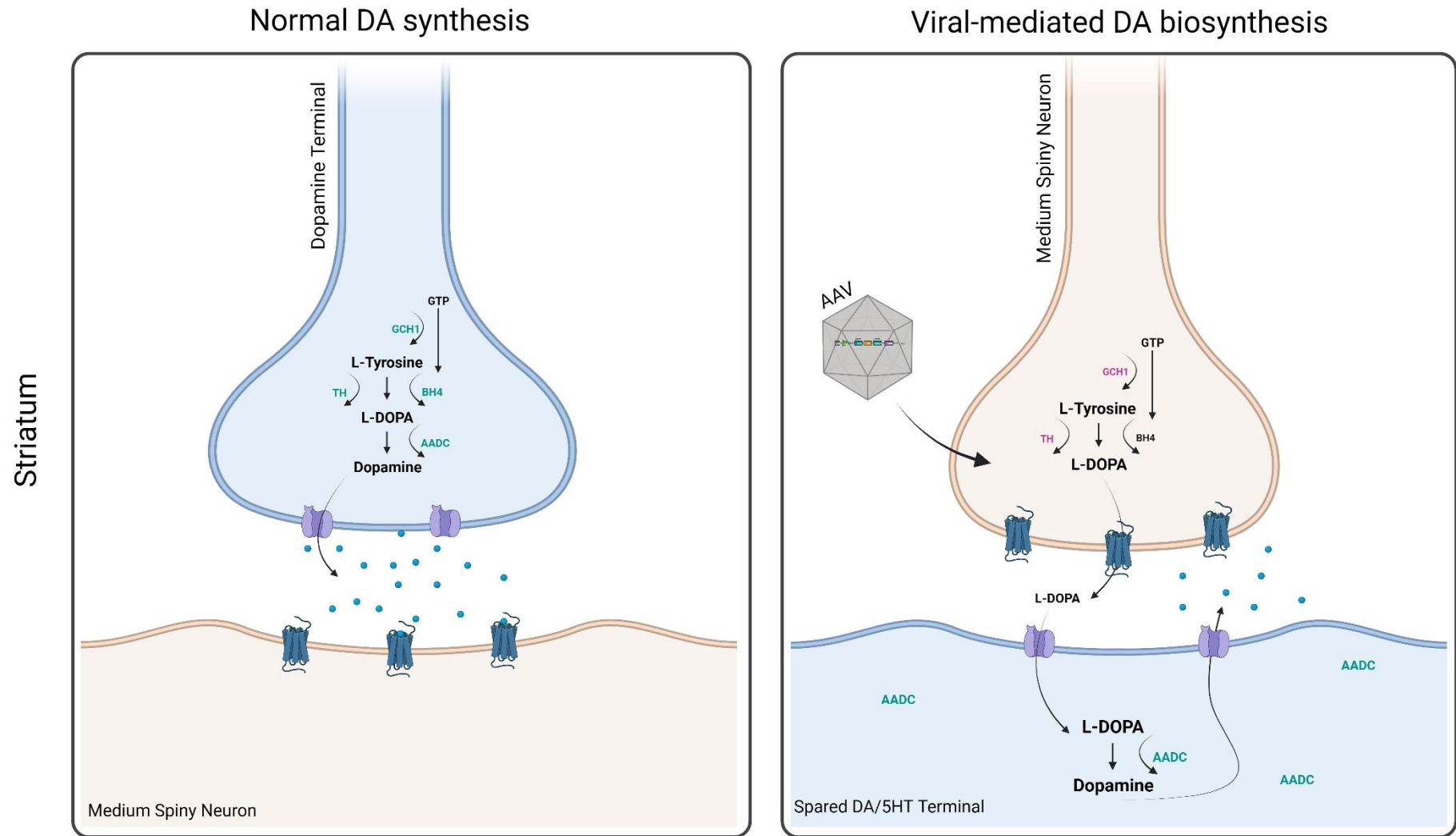
Figure 4.1. Schematic of the biscistronic approach to viral-mediated dopamine (DA) biosynthesis. Adapted from Bjorklund and Kirik 2009.

4.2.3 Gene therapy and cognitive function

Viral vectors as a method of DA biosynthesis are being trialled as a gene therapy in PD (Eberling et al. 2008; Christine et al. 2009; LeWitt et al. 2011; Cederfjäll et al. 2015; Chen et al. 2020; Christine et al. 2022). Motor improvements relating to gene therapy are described in Chapter 1 (see 1.6). The data on cognitive improvements using viral vectors, however, is limited both pre-clinically and clinically. In Palfi et al. (2018), no difference in UPDRS scores were observed in the ProSavin clinical trial relating to part 1 (mental state and behaviour), 2 (daily life activities) and 4 (complications) scores up to 2 years post-baseline, with some improvement but mostly sustained scores from individual baselines up to 4 years post-LV. No improvement was observed up to 2 years on the PDQ-39 questionnaire scores, detailing patients' difficulties on 8 subsections of daily living. Some patients experienced a gradual decline in their PDQ-39 scores. Christine et al. (2022) reported on the Voyager clinical trial, which used a putamenal infusion of a vector to synthesise AADC and highlighted some minor quality of life improvements in their PDQ-39 scores, however this improvement was only observed in 2/3 cohorts, with marked improvement from 12 months but continued to decline over time. The literature above details the complexity of non-motor and cognitive recovery, thus highlighting further work is needed pre-clinically with a direct focus on current therapeutic strategies and their interaction with cognitive function.

One benefit of using a gene therapy for PD would be to reduce or completely remove oral DA therapies such as daily L-DOPA or other DA agonists, which provide pulsatile infusions of DA, with a vector that allows a continual, constant level of DA to be synthesised. However, published clinical trial data has not successfully achieved this goal. Potential reasons for this are due to the substantial effect of L-DOPA withdrawal worsening motor and cognitive symptoms (Koschel et al. 2022). Therefore, patients have received gene therapy alongside their current DAergic medication. Thus, it is important to investigate any interaction between the two forms of DA replacement in relation to cognitive function as this could have wider implications for the clinic.

4.3.4 L-DOPA in cognition

Oral administration of L-DOPA is the gold standard symptomatic treatment for PD (see 1.4.1). In this chapter, L-DOPA was used as a second tool providing pharmacological replacement of DA to determine whether this is sufficient to improve cognitive function in a model of DA depletion. There is substantial evidence for the short-term efficacy of L-DOPA treatment improving motor symptoms in the early stages of disease progression (Uitti et al. 1993; Growdon et al. 1998). Yet, the evidence on L-DOPA's impact in relation to cognitive function is quite varied.

There have been reports of cognitive improvement in early-stage PD with L-DOPA in stop-signal tasks which requires them to inhibit their responses, as well as non-complex spatial working memory tasks and incidental sequence tasks, as well as other studies highlighting the benefit of DA in cognitive tasks (Beato et al. 2008; Beigi et al. 2016; Ikeda et al. 2017; Cai et al. 2022). L-DOPA has also been reported to have no adverse effect on visuospatial tasks such as the Stroop test, yet it was reported to be detrimental to reaction time on a Wisconsin card sorting task without impairing accuracy (Kulisevsky et al. 1996; Morrison et al. 2004; Pascual-Sedano et al. 2008). Cools et al. (2001) and Cools (2006) highlighted that the effects of L-DOPA can be associated with L-DOPA plasma levels, and also the demands of the task.

Asymmetry in early PD

One factor that has been found to impact response of L-DOPA in cognitive function is asymmetry of DA depletion. Right hemisphere deficits in PD patients were found to be improved with L-DOPA in verbal memory tasks, but left hemisphere dominant deficits responded to L-DOPA by exacerbating memory recall deficits (Hanna-Pladdy et al. 2015). The onset of cognitive deficits in response to L-DOPA due to asymmetry in DA depletion is thought to be due to over-saturation in less denervated areas of the brain (Gotham et al. 1988; Tomer et al. 2007; Fiorenzato et al. 2021; Zhang et al. 2021b). This effect of hypo and hyper-DAergic states highlight that DA is required at an optimal level to support cognitive function. Cools and D'Esposito (2011) detail evidence within the literature for the 'inverted U' paradox to DA transmission and cognitive function, that too little can lead to the onset of cognitive impairments, and over saturation can disrupt other cognitive processes. Thus, it is

important to evaluate the role of L-DOPA in cognitive tasks such as the LCRT and compare a state of DA depletion and restoration with L-DOPA in sham animals in the same task.

4.3.5 Chapter aims

Chapter 4 overall aimed to evaluate whether using different tools to replace DA can help probe the impact of DA replacement therapies on cognitive function. It is reasonable to theorise that as motor impairments will improve in a dose response manner, as will recovery in the LCRT task.

The aims of this chapter were as follows:

1. ***To determine whether viral-mediated DA replacement at two doses can improve cognitive impairments on the LCRT task.*** Unilateral 6-OHDA MFB lesioned lister-hooded rats received an intra-striatal infusion of AAV-htTH-2A-hGCH1 in either a mid or a high titre and were observed on cognitive and motor tasks periodically for up to 12 weeks. It was hypothesised that gene therapy would improve both motor and cognitive deficits from at least 6 weeks post-AAV.

2. ***To examine the impact of L-DOPA on cognitive impairments in the LCRT task.*** Performance on the LCRT test was observed on 4 doses of L-DOPA. It was hypothesised that deficits in visuospatial function and motivation shown by lesioned, sham rats in the LCRT task would be alleviated in a dose response manner due to L-DOPA administration.

3. ***To use [18^F]Fallypride PET/CT imaging to determine whether D2 receptor expression was normalised in AAV-htTH-2A-hGCH1 treated rats.*** A subgroup of 12 rats (Sham n = 6 and AAV-High n = 6) were analysed after [18^F]Fallypride administration for any receptor binding changes. It was hypothesised that AAV-htTH-2A-hGCH1 treated rats would have evidence of normalised D2 receptor binding compared to Shams.

4.3 Methods: Experiment 2

4.3.1 Experimental design

Female lister-hooded rats (n = 56) were acclimatised to the animal unit for one week prior to being placed on food restriction (see 2.5.2). Rats were trained on the LCRT task for 8 weeks to establish baseline performance (see 2.5.3). A total of 5 rats were excluded from further experimentation due to not successfully learning the task. All remaining animals underwent a unilateral 6-OHDA medial forebrain bundle lesion (see 2.3). Three rats did not recover from surgery. At 4-weeks post-lesion, rats were tested on the LCRT task, hand-tests (vibrissae-evoked touch test and adjusting steps) and amphetamine-rotations task to identify lesion-induced deficits. 9 animals were excluded for not meeting a threshold of > 6 rotations per minute. Rats were then allocated into groups based on their contralateral response accuracy. Animals either received a sham infusion (n = 13), a mid (8.46×10^{12}gc/ml) (n = 12) or high titre (1.69×10^{13}gc/ml) (n = 10) of htTH-2A-hGCH1 AAV viral vector. A total of 3 animals were excluded from the AAV-High and 2 animals from the AAV-Mid group due to lack of adequate viral expression post-mortem. A total of 3 rats were culled during the experiment due to health concerns. The remaining animals (n = 30): Sham (n = 10), AAV-Mid (n = 10) and AAV-High (n = 10) were included in the final analysis (Figure 4.2).
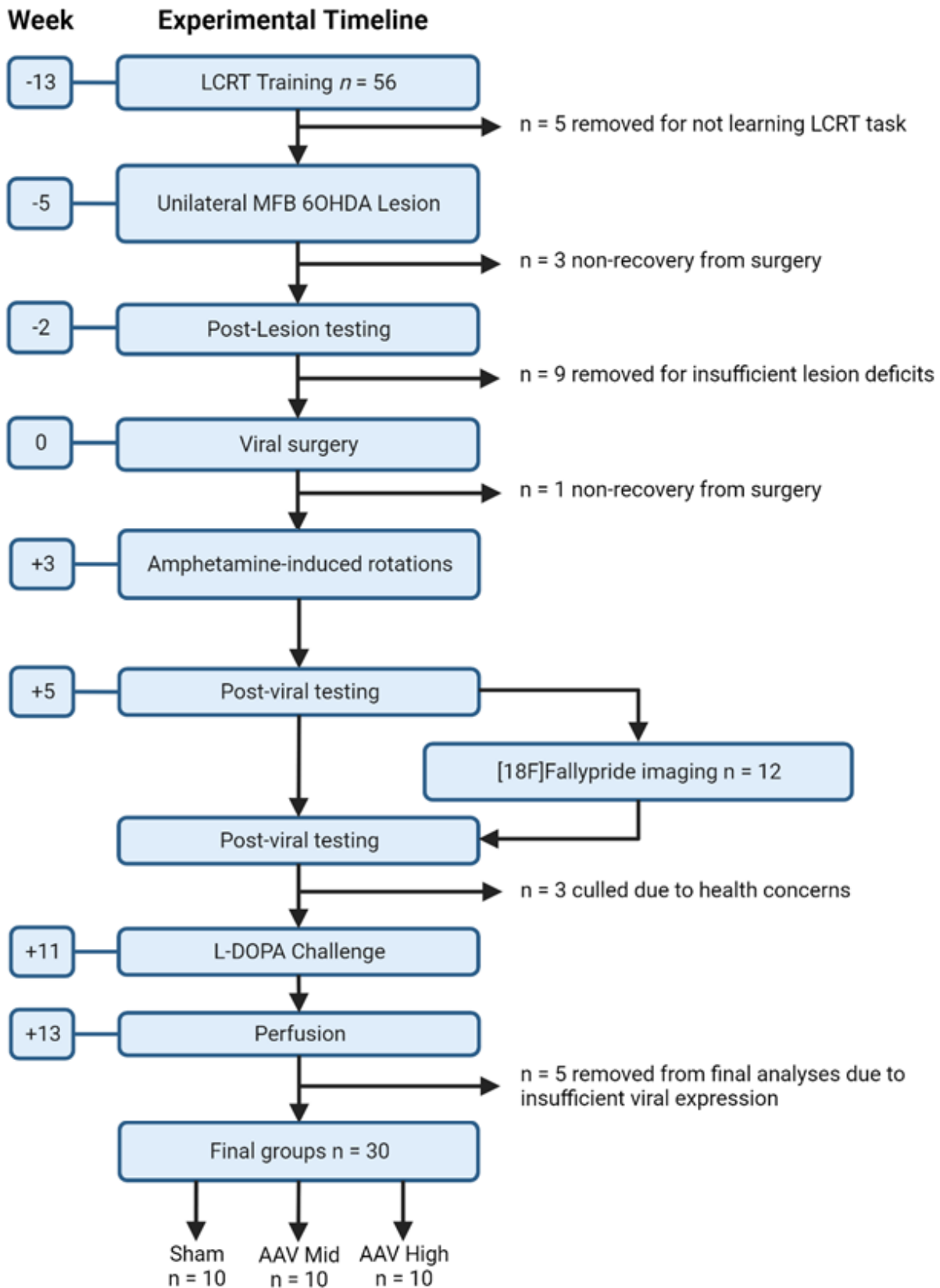
Figure 4.2. Timeline for Experiment 2.

4.3.2 Viral construct

Figure 4.3. Diagram of biscistronic viral vector used in Experiment 2.

The htTH-2A-hGCH1 AAV (depicted in Figure 4.3) was designed by Dr Mike McDonald and produced and titrated by Vigene Biosciences. The htTH-2A-hGCH1 viral vector was produced by triple transfection of HEK293 cells and purified by gradient ultracentrifugation to produce the viral particles. The titre was calculated as viral genome copy number per ml (gc/ml) by quantitative real-time PCR against the AAV2 ITR sequence. htTH-2A-hGCH1 Mid titre (named AAV-Mid throughout) was a concentration of 8.46×10^{12}gc/ml, and AAV-High (named AAV-High throughout is 1.69×10^{13}gc/ml). The viral construct is on a promoterless backbone SnapFast™ (pSF) cloning vector core, containing human truncated TH and human GCH1 connected with a 2A-linker. Expression of the two transgenes is driven under the CMV promoter with a woodchuck hepatitis virus post-transcriptional regulatory element (WPRE). Transfection of human TH can lead to large negative feedback due to free cytosolic DA release and thus a down-regulation of mRNA transcription (Kumer and Vrana 1996). The viral vector utilised in this experiment contains a truncated form of the human TH gene (called tTH throughout), that lacks the regulatory N-terminal fragment leading to transcription being constitutively active, irrespective of cytosolic DA (Moffat et al. 1997).

4.3.3 Surgical procedure

All animals receiving AAV-htTH-2A-hGHC1 had 5.5 µl of viral vector product deposited unilaterally across three sites within the striatum, infused at a rate of 0.4 µl per minute with 1-minute diffusion between depths, and 3-minute diffusion per site. 1.5 µl was infused at DV1 for site 1 &2, 1 µl was infused at DV2 and 0.5 µl was infused at site 3. Infusions were performed with a 10 µl Hamilton syringe. The syringe was cleaned between each animal

with 3% hydrogen peroxide and ethanol, prior to Dulbecco PBS (DPBS). The surgical coordinate for each viral surgery is indicated in the table below (Figure 4.4). Animals within the Sham group received an infusion of DPBS in one of the 3 sites.

	AP	ML	DV1	DV2
Site 1	+0.0	-4.0	-5.0	-4.0
Site 2	+1.0	-2.8	-4.5	-3.5
Site 3	+1.0	-2.2	-4.0	
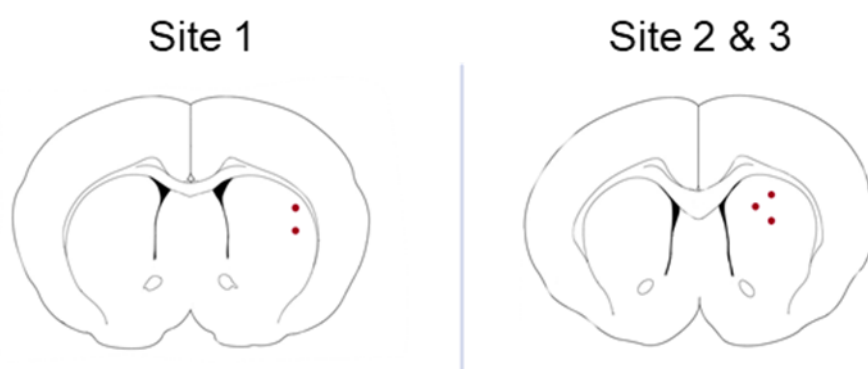
Figure 4.4. Surgical coordinates for AAV-htTH-2A-hGCH1 infusions into the striatum for Experiment 2. Representative images of the locations of each injection site and the depth. AP = Anterior-Posterior axis, ML = Medial-Lateral axis, DV = Dorsal-Ventral axis.

4.3.4 LCRT Behavioural testing

After 5 weeks post-AAV infusion, rats were tested on the LCRT task in order to assess any behavioural improvement associated with AAV-tTH-2A-hGHC1. After 3 days of operant testing in the LCRT test, behavioural performance was found to be suboptimal due to all lesioned rats executing an extremely low number of total trials (an average of 13 total trials across all groups, data not presented). It was anticipated that the MFB lesion would significantly reduce accuracy and the total trials completed, but in this instance, performance was lower than usual. Continuing with the current task parameters risked both quantity and quality of data that could be collected. To prevent this, some modifications were made to the LCRT task parameters. The amount of time the centre stimulus was presented was

increased to 500msec (from the previous 200msec). The amount of time required to hold their nose within the lateralised holes was modified to only 50msec, (Table 5). Therefore, given that the task parameters differed between days 1-3 and days 4-5, the Week 5 LCRT data was not analysed alongside any other data points.

4.3.4.1 Unilateral probe test

One trial of the LCRT task was conducted as a unilateral probe test, with a modification in which the ipsilateral hole was removed and replaced with a second contralateral hole (now called Far) at a greater distance away from the remaining contralateral hole (now called Near). This probe test was undertaken to further challenge the rats by restricting all responses to contralateral space and including a response option (Far) known to be challenging to 6-OHDA lesioned rats. In this context, it was possible to explore whether viral mediated DA replacement could alleviate the deficits seen in the Far hole in rats with a 6-OHDA MFB lesion (Lelos et al. 2016).
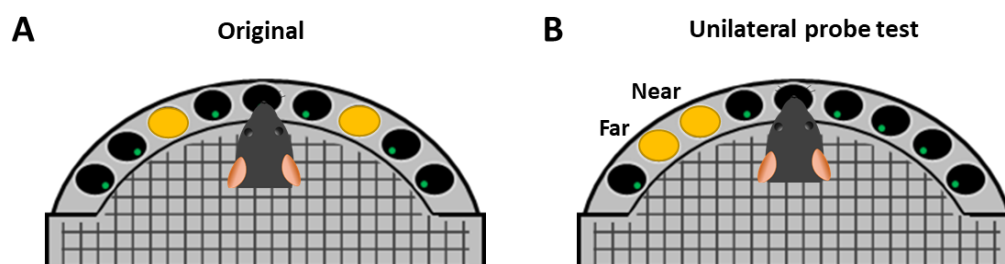
Figure 4.5. Schematic image depicting the original and unilateral probe test during the LCRT task. Unilateral probe test. A) Original parameters of the LCRT task in which, after a useable trial is initiated, hole 3 (left) OR hole 5 (right) is illuminated for 200msecs. B) In the unilateral probe test, Hole 3 remains (Near) but hole 5 shifts to hole 2 (Far).

4.3.5 [^{18}F] Fallypride

Rats

At 8 weeks post-AAV infusion, 12 rats (n = 6 AAV-High, n = 6 sham) were transferred to the Positron Emission Tomography Imaging Centre at Cardiff University (PETIC) for one week, for [^{18}F]Fallypride imaging. Rats were selected for inclusion based on their performance on

the adjusting step and vibrissae. Rats in the Sham group were chosen due to having the consistently lowest number of contralateral adjusting steps and vibrissae-evoked paw touches, whereas those showing the greatest improvement on the same motor function tasks were chosen for the AAV-High group. Animals were returned to their normal lab housing environment subsequently and allowed to re-acclimatise for one week prior to experimentation starting again at 10 weeks post-AAV infusion.

Procedure

[^{18}F]Fallypride was produced in-house via nucleophilic substitution reactions carried out on a Trasis AllinOne universal synthesiser. [^{18}F]Fallypride was produced from ^{18}O enriched water via the ^{18}O (p,n) ^{18}F reaction using an IBA Cyclone 18/9 cyclotron. Rats were anaesthetised with 2-4% isoflurane in 0.8-1L/min oxygen in a warmed induction chamber (37°C) and temporarily transferred to a nose cone to be injected with 20 MBq [^{18}F]Fallypride (~300 µL injection volume) via tail vein. Rats were returned to the induction chamber where isoflurane was maintained at 1.5-2% in 0.8-1 L/min oxygen for 50 minutes. Rats were placed in the Mediso multicell rat bed within the scanner and secured in earbars where isoflurane was maintained through a nose cone at 1.5-2% isoflurane in 0.8-1 L/min oxygen. Body temperature was continually maintained at 37°C by heated air circulating through the bed. Breathing rate was monitored via an integrated pneumatic pressure sensor.

Analysis

A scout CT scan was acquired and then a 60-minute PET scan centred on the head was started at 60 minutes post injection time. PET data was reconstructed with Mediso's proprietary Tera-tomo-3D-algorithm (with attenuation, random and scatter corrections applied). A 12 frame dynamic time series with frame times of 3x20 minutes was prepared along with an averaged static image (100-120 min post injection) for VOI, preparation, and display purposes. Using the vivoquant software, PET and CT scan were loaded and were processed to measure in SUVmm^3. A normalisation of the intensity of all PET scans was carried out to fall within the range of 0-10 SUV mm^3. Using an ROI tool with a connecting threshold, the whole left and right striatal nuclei and an area of absent signal in the cerebellum was selected for each animal. Mean SUV measurements were calculated for the 3 x 20 mins separately. In order to understand the D2/D3 receptor binding discrepancies

between the two hemispheres, data is presented as the binding ratio between the lesioned/treated and intact hemisphere and was calculated as follows: (lesion / intact) * 100. Once immunohistological analysis of tTH expression was carried out for each brain, the vivoquant software was used to measure the D2/D3 receptor changes within the specific tTH expressing region. Images were taken at 125x magnification and used as a guide to draw an ROI, 4 pixels in size, at 3 separate points: Inside the tTH expressing core (referred to as AAV), outside the tTH expressing core in the surrounding striatum (referred to as Host) and the intact hemisphere within the same animal (referred to as Intact). The average SUV value was calculated for each area across the 3x20 minute scans and is presented as the binding ratio between (1) AAV vs Host, (2) AAV vs Intact and (3) Host vs Intact.

4.3.6 L-DOPA dose response

At 11 weeks post-AAV infusion, rats underwent an L-DOPA challenge to investigate the impact of L-DOPA treatment in 6-OHDA lesion-only rats on their performance in the LCRT task, and also to investigate any interaction with gene therapy and L-DOPA. On day 1, all rats were placed into 2 groups and received either 3mg/kg of L-DOPA or saline via subcutaneous injection and were returned to the home cage. At 30-minutes post-drug administration, the adjusting step task was carried out. At 40-minutes post-L-DOPA, rats were tested on the LCRT task (Breger et al. 2013). On day 2, all rats received the alternate drug, and the same experimental design was carried out. Observations were noted of L-DOPA induced dyskinesia-like behaviours. After a washout period of two days over the weekend, rats received two further L-DOPA administrations on two consecutive days, instead with 1.5 or 4.5mg/kg L-DOPA and observations of abnormal behaviours were made for each animal. Behaviours observed and noted for severity were as follows; spontaneous rotations, spontaneous hyperkinetic forelimb movement, axial twisting, orolingual & tongue protrusions.

4.3.7 Histological analysis

Animals were transcardially perfused with 4% PFA 13 weeks post-AAV infusion (see 2.6.1) Brains were sectioned on the freezing microtome at 30 μm thickness for

immunohistochemical analysis. IHC and IFC were carried out as described in (2.6.2 & 2.6.3). Antibodies used were as follows: truncated TH (tTH. 1:400), FOXP1 (1:1000), GFAP (1:1000), GCH1 (1:1000) and more detail for primary and secondary antibodies are listed in Table 7 and Table 8.

Optical density

Images of a 1:12 tTH staining were taken at x1.25 objection and processed in image J to calibrate for optical density. The striatum was divided into 3 different regions: Dorsolateral, dorsomedial and ventral based on architectural lines indicated within the literature (Voorn et al. 2004). An area of the motor cortex without positive staining was used to normalise the data. Data is presented as the mean optical density units. Biodistribution of tTH expression at a mid and high titre was analysed at 4 positions throughout the entire striatal architecture (AP +2.3, +1.37, +0.74, -0.51 from bregma). To determine the expression of tTH in off-target areas of the cortex, biodistribution was measured in ROIs from the edge of the motor cortex to the most medial edge of the ventral pallidum, across a majority of 4 sections. Data is presented as a mean percentage area covered.

Ventral midbrain counts

ROIs were drawn around the entire structure of the SNc and VTA in the intact and lesion hemisphere for all visible ventral midbrain sections per animal. Tissue orientation for the intact and lesioned hemisphere was aided by a needle stick injury during microtome tissue processing in a non-relevant section of the anterior midbrain. Manual counts of all TH +ve cells were counted per rat and estimated total cells was calculated by: (sum of all cells counted * series frequency). Data is presented as average percentage loss and was calculated for the SNc and VTA respectively as follows: 100 – ((Lesion / Intact) * 100)).

4.3.8 Statistics

To analyse the performance on the LCRT task, a one-way repeated measures ANOVA was used with Group (Sham, AAV-Mid and AAV-High) and Time (7 weeks and 10 weeks as a factor. Tukey's *post hoc* test was used throughout to perform multiple comparisons between Sham, AAV-Mid and AAV-High. For motor tasks such as drug-induced rotations task,

adjusting step task and vibrissae-evoked task, one-way repeated measures ANOVA was also used with the same Groups as a factor, however, the factor of Time was altered accordingly depending on when the data was recorded. When analysing the L-DOPA challenge, a one-way ANOVA with repeated measures was used with Group and Drug (Saline, 1.5 mg/kg, 3mg/kg, 4.5mg/kg) as a factor. Area covered within the cortex of the viral vector between AAV-Mid and AAV-High was calculated by independent samples t-test. Any missing values were calculated in SPSS using linear interpolation. All measurements for [^{18}F]Fallypride are analysed as a paired t-test comparing the mean to 100. Graphical data is presented as group mean and error bars represent the standard error of the mean (SEM). Results were considered statistically significant with a threshold of p <0.05.

4.4 Results: Experiment 2
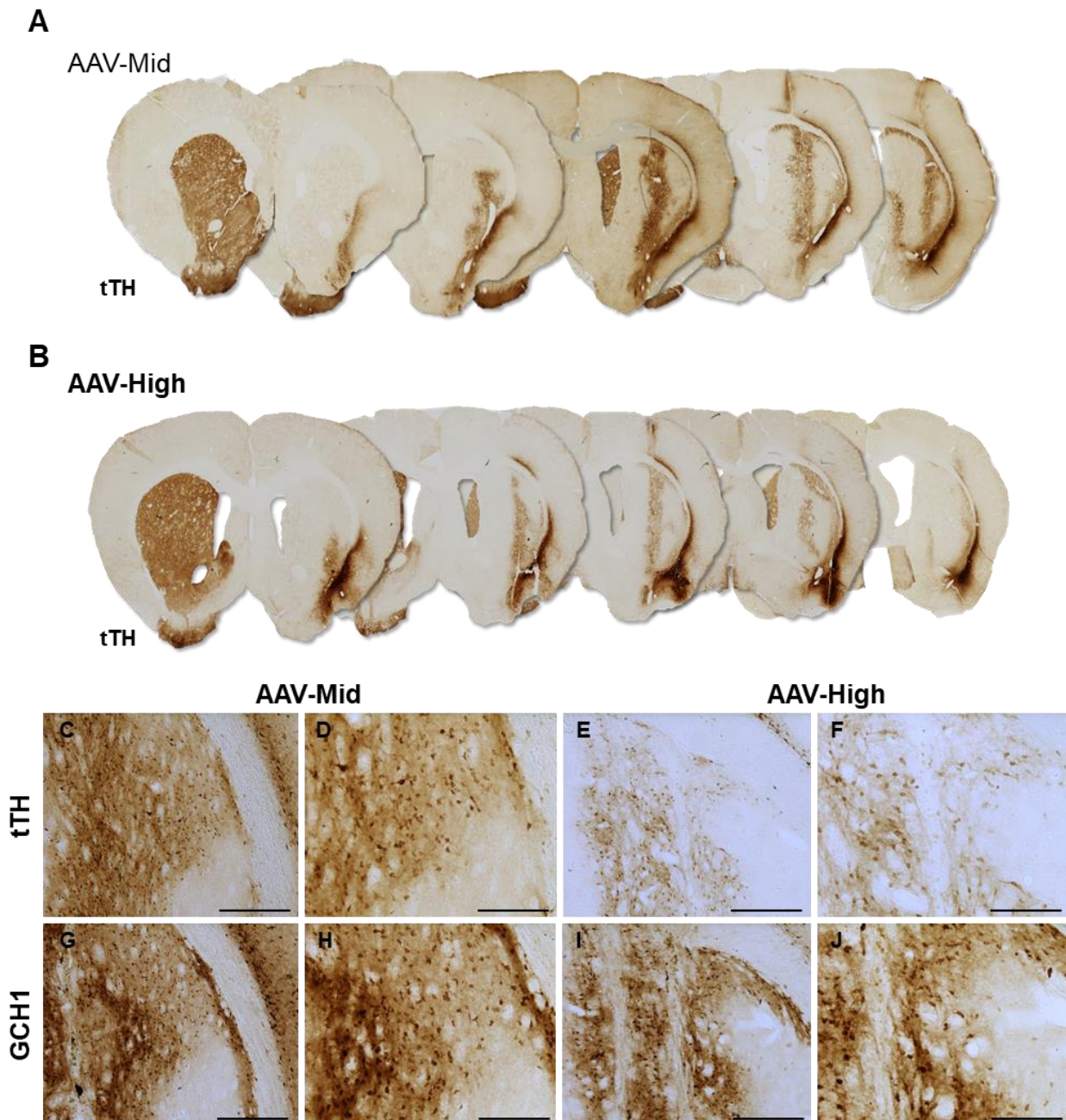
*Figure 4.6. Representative images of tTH and GCH1 expression in AAV-hTH-hGCH1 treated rats . **A-B**) truncated-TH (tTH) in AAV-Mid and AAV-High. Images taken at 50x magnification **(C,E,G,I)** and at 100x magnification **(D,F,H,J).** Scale bar at 50x magnification represents 350 µm, and at 100x magnification represents 200µm.*
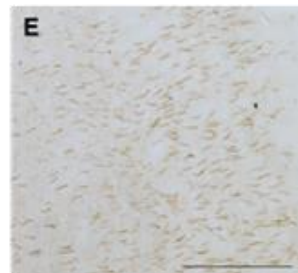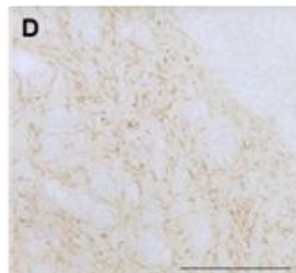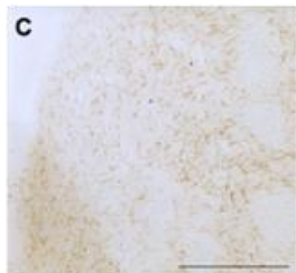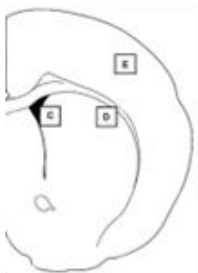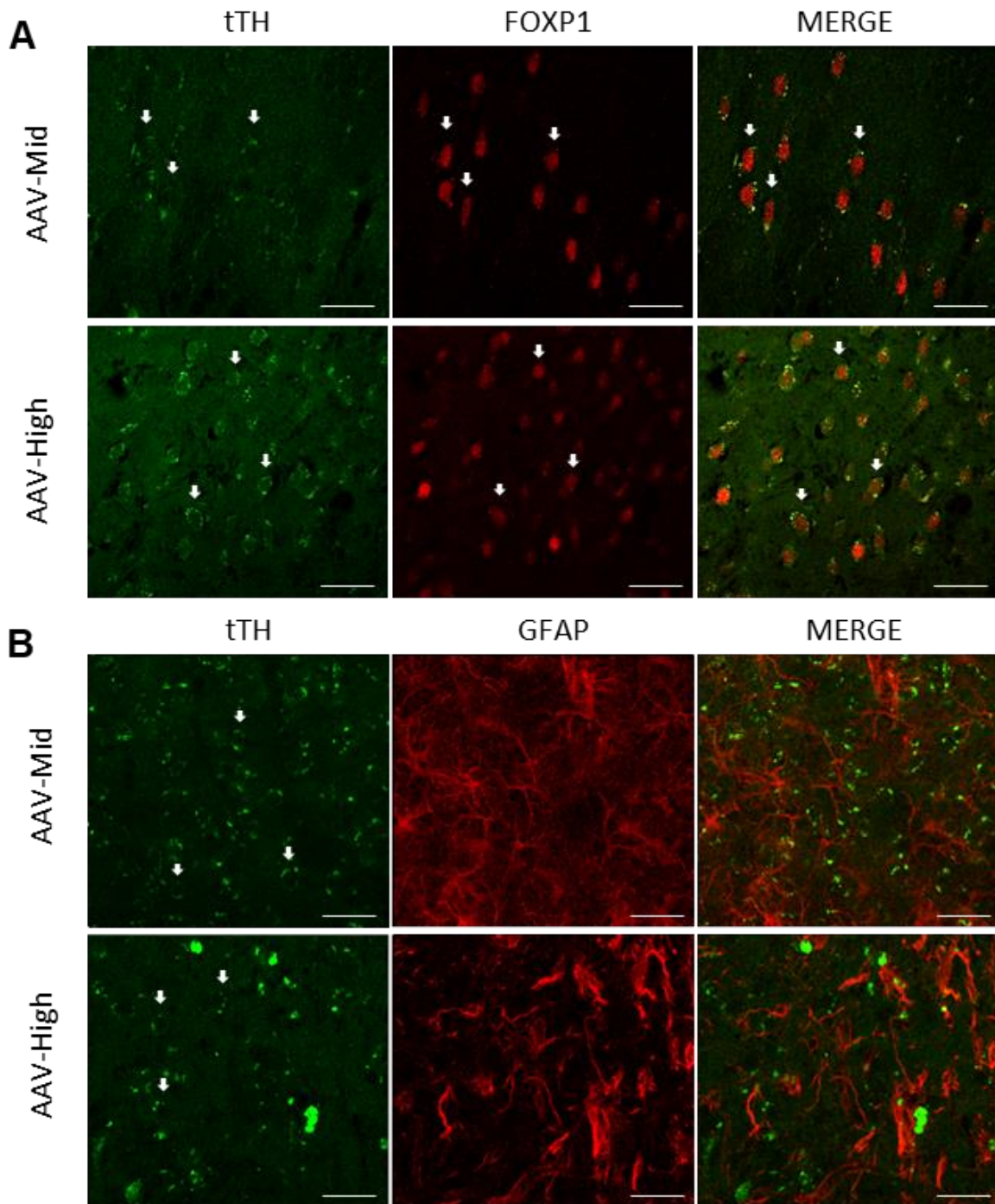
Figure 4.7. Immunofluorescence of truncated TH and a striatal MSN (FOXP1) or astrocyte (GFAP) marker. **A-B***) Evidence of co-labelling between tTH and FOXP1 indicates htTH-2A-hGCH1 virus is being expressed by MSNs with no observable uptake in GFAP +ve cells. White arrow indicates neuron Scale bar at 630x magnification equal 15µm. Representative image of AADC immunostaining in the dorsomedial* **(C)** *dorsolateral* **(D)** *and cortical region* **(E)***. Scale bars at 200x magnification represent 100µm.*

4.4.1 Histological characterisation of AAV-tTH-2A-hGCH1 expression

htTH-2A-hGCH1 expression was mostly localised, but not conserved to the striatum

Histological analysis was undertaken after 13 weeks post-AAV infusion to determine the extent of htTH-2A-hGCH1 viral expression, utilising tTH and GCH1 immunostaining (Figure 4.6), expression of htTH-2A-hGCH1 in both AAV-High and AAV-Mid can be observed by tTH staining of cell bodies within the striatum (Figure 4.6.C-G). There was evidence of off-target expression of tTH with dissipation into the piriform cortex. The average earliest expression is approximately +1.2 AP from bregma, and the most caudal expression is -2.3. Every animal in each group has some extent of tTH expression in the piriform cortex. Most have expression in the claustrum and tTH expression extending along the rostral caudal extent of the cortex. Expression that is most caudal also falls within the amygdala nuclei. The majority of tTH expression is collected along the corpus callosum. AADC +ve immunostaining was confirmed in a 6-OHDA lesioned rat in the dorsolateral and dorsomedial striatum as well as the cortex (Figure 4.7.C).

htTH-2A-hGCH1 mostly transfecting neurons

IFC was used to evaluate whether striatal neurons or astrocytes were preferentially transfected by AAV-htTH-2A-hGCH1. Co-labelling for tTH and the medium spiny neuron (MSN) marker, FOXP1 (Figure 4.7.A) indicated that the htTH-2A-hGCH1 viral vector was effective in gene transfer to striatal MSNs. In contrast, there was no clear evidence of co-labelling with the astrocytic marker, GFAP, with no observable cell body expressing GFAP and co-labelling with tTH Figure 4.7.B).
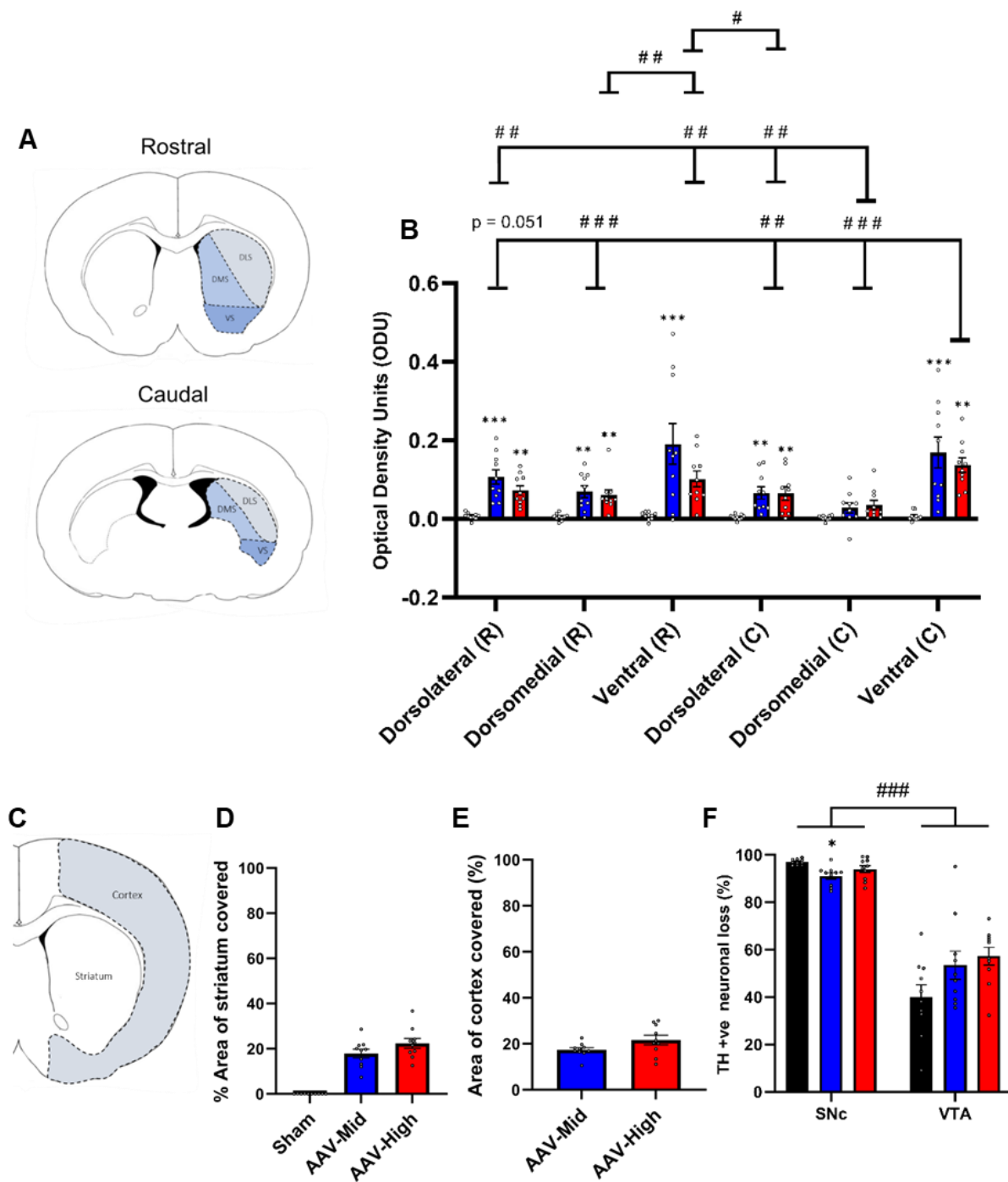
*Figure 4.8. Optical density, biodistribution and midbrain counts of AAV-htTH-2A-hGCH1 treated rats. **A)** Schematic of locations of optical density. **B)** Optical density measures taken in different regions of the striatum along the Rostral (R) - Caudal (C) axis. Overall greater tTH expression in the ventral region than both the dorsolateral and dorsomedial striatum, and more caudally than rostrally expressed tTH. **(C-E)** Percentage area covered of tTH was approximately 20% for both groups, as was the tTH expression in the cortex. **F)** Ventral midbrain counts of the percentage loss of TH +ve neurons within the SNc and VTA. Error bars represent standard error of mean. Biodistribution did not differ between AAV-Mid and AAV-High. Significant differences to sham are indicated as ** p < .01, *** p <.001. Significant differences between region are indicated as #p < .05, ##p <.01, ###p <.001.*

4.4.2 Histological analysis of tTH expression in AAV treated groups

AAV-htTH-2A-hGCH1 expression in all areas except caudal part of dorsomedial striatum

Optical density was used to measure the intensity level of tTH expression in Sham, AAV-Mid and AAV-High animals along the rostro-caudal plane in three striatal subregions (Dorsomedial, Dorsolateral, and Ventral Figure 4.8.A). The intensity of tTH expression in both AAV-Mid and AAV-High was greater than Sham in all regions other than the caudal dorsomedial striatum and variable levels of tTH expression in the rostro-ventral striatum in AAV-High that was not significantly greater than Sham. (Figure 4.8.B: Group*Region $F(10,135) = 5.002$, $p < .001$. **Dorsolateral-R**: Sham vs AAV-Mid $p < .001$ and High $p = .004$, **Dorsomedial-R**: Sham vs AAV-Mid $p = .002$ and AAV-High $p = .009$, **Ventral-R**: Sham vs AAV-Mid $p = .001$ and AAV-High $p = $ n.s, **Dorsolateral-C**: Sham vs AAV-Mid $p = .008$ and AAV-High $p = .009$, **Dorsomedial-C:** Sham vs AAV-Mid and AAV-High $p = $ n.s, **Ventral-C**: Sham vs AAV-Mid $p < .001$ and AAV-High $p = .003$).

tTH expression more localised to ventral striatum

The greatest collection of tTH expression was found to be in the ventral striatum (Figure 4.8.B. Region $F(5,135) = 15.554$, $p = <.001$, Ventral-C vs Dorsolateral-R $p = .051$ & Dorsomedial-R $p = <.001$ & Dorsolateral-C $p = .001$ & Dorsomedial-C $p <.001$) and the lowest in the caudal parts of the dorsomedial striatum (Dorsomedial-C vs Dorsolateral-R $p <.001$ & Ventral-R $p = .003$ & Dorsolateral-C $p = .004$). In the rostral parts of the striatum, there were no differences in tTH expression in the dorsolateral or dorsomedial region. In the caudal parts of the striatum however, there was greater expression in the dorsolateral region than the dorsomedial region.

Same level of tTH expression in striatum as in cortex

The expression of tTH was analysed at 4 locations along the rostro-caudal axis in order to understand the biodistribution of the viral vector throughout the striatum. The percentage area of the striatum covered by tTH was around 20% in treated groups (Figure 4.8.D. Group:

$F(2,27) = 50.932$, $p = <.001$. Sham vs AAV-Mid and AAV-High, $p = <.001$, AAV-Mid vs AAV-High, p = n.s). As shown in Figure 4.6, there was cortical expression of AAV-htTH-2A-hGCH1 in both AAV-Mid and AAV-High. Using area fractioning, the amount of tTH expression in the treated hemisphere was carried out. There was no statistical difference between the AAV-Mid and AAV-High (Figure 4.8.E. $t(18) = -1.880$, p = n.s).

6-OHDA lesion causes severe loss of SNc and VTA neurons

Histological analysis of the ventral midbrain was carried out to quantify the loss of DA neurons due to the unilateral 6-OHDA MFB lesion prior to receiving AAV infusions. Groups were analysed separately rather than one lesion group in order to determine is the scale of loss in the VTA differed amongst groups and could be driving behavioural changes. All groups lost approximately over 95% of TH +ve neurons within the SNc and approximately 50% of TH +ve neurons present in the VTA. The magnitude of loss in the SNc was significantly greater in Sham than in AAV-Mid, but loss in AAV-Mid was still over 90% (Figure 4.8.F. Region*Group: $F(2,27) = 5.870$, $p = .008$. SNc loss: Lesion vs mid $p = .004$. All groups SNc vs VTA loss $p <.001$).
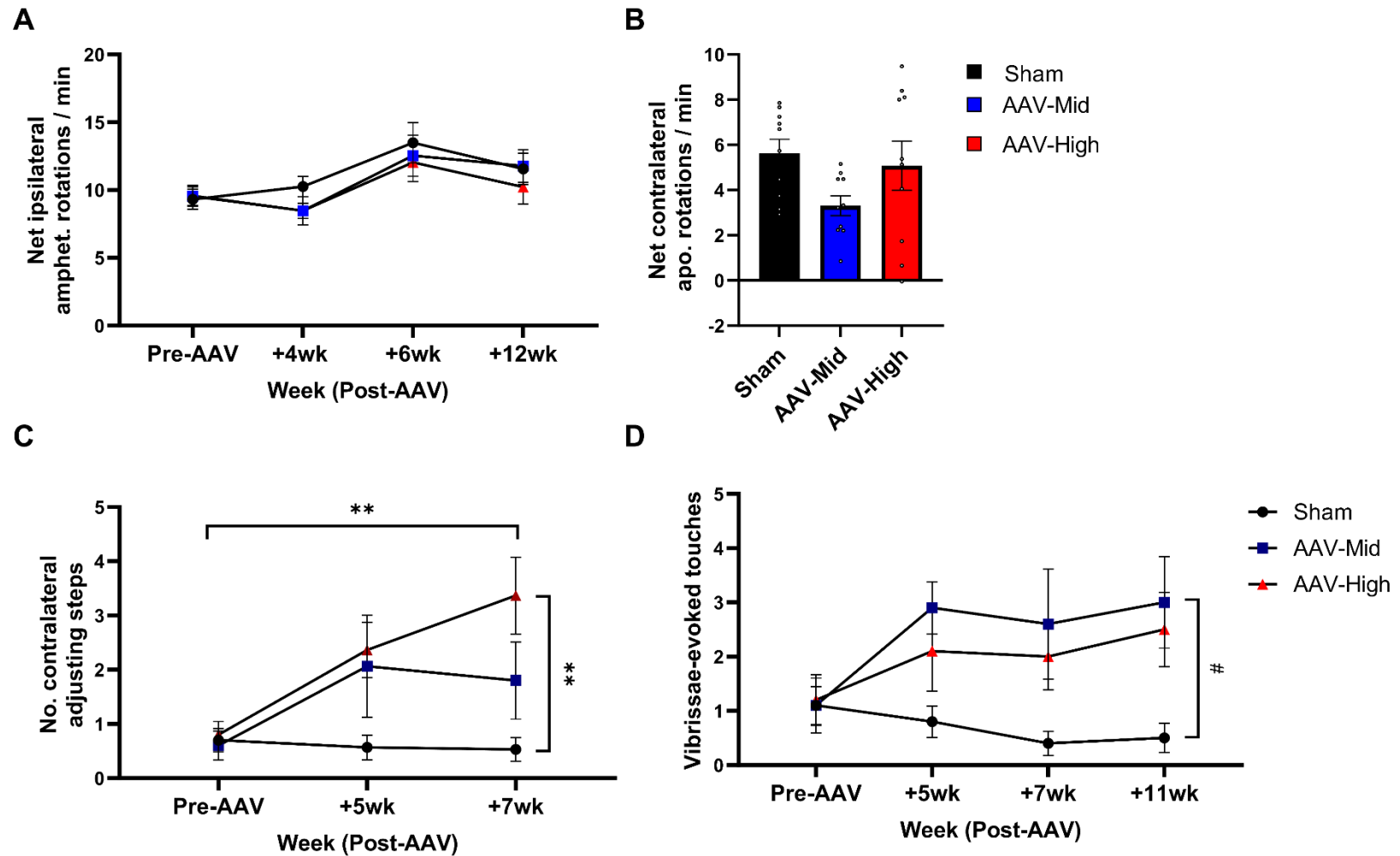
*Figure 4.9.Impact of viral mediated DA synthesis on motor behaviour. **A)** No reduction in contralateral rotational bias was observed 4-12 weeks post-AAV infusion. **B)** No reduction in apomorphine induced ipsilateral rotational bias was observed at 13 weeks post-AAV infusion. **C)** AAV-High group displayed improved adjusting steps from its own baseline at 7 weeks post-AAV and were significantly improved from Sham. **D)** Only mid animals improved vibrissae evoked touches at 11 weeks post-Sham. Error bars represent standard error of mean. Significant differences are indicated as * p < .05, ** p <.01.*

4.4.3 AAV-htTH-2A-hGCH1 treated rats improved motor deficits

Prior to AAV-htTH-2A-hGCH1 infusion, all rats displayed pronounced drug-induced rotations and deficits on sensorimotor and forelimb akinesia measures (Figure 4.9). Contralateral motor side bias induced by administration of amphet. or apo. remained high after 13 weeks (Figure 4.9.A-B). However, AAV-High rats had a 3-fold improvement in forelimb adjusting steps (Figure 4.9.C. Group*Time: $F(4,54) = 3.107$, $p = .013$). Sham animals continued to show strong deficits up to 7 weeks post-AAV, whereas animals in the AAV-High titre group performed more steps compared to their own baseline ($p <.001$) and more steps compared to Sham ($p = .007$). No improvement was seen in steps in the AAV-Mid group ($p =$ n.s). In the vibrissae-induced touch test, improvement in paw touches was seen in AAV-Mid animals only, but the AAV-High group did appear to have a trend towards recovery (Figure 4.9.D. Group*Time: ($F(6,81) = 2.154$, $p = .056$. Group: $F(2,27) = 3.478$, $p = .045$, Sham vs AAV-Mid $p = .043$).
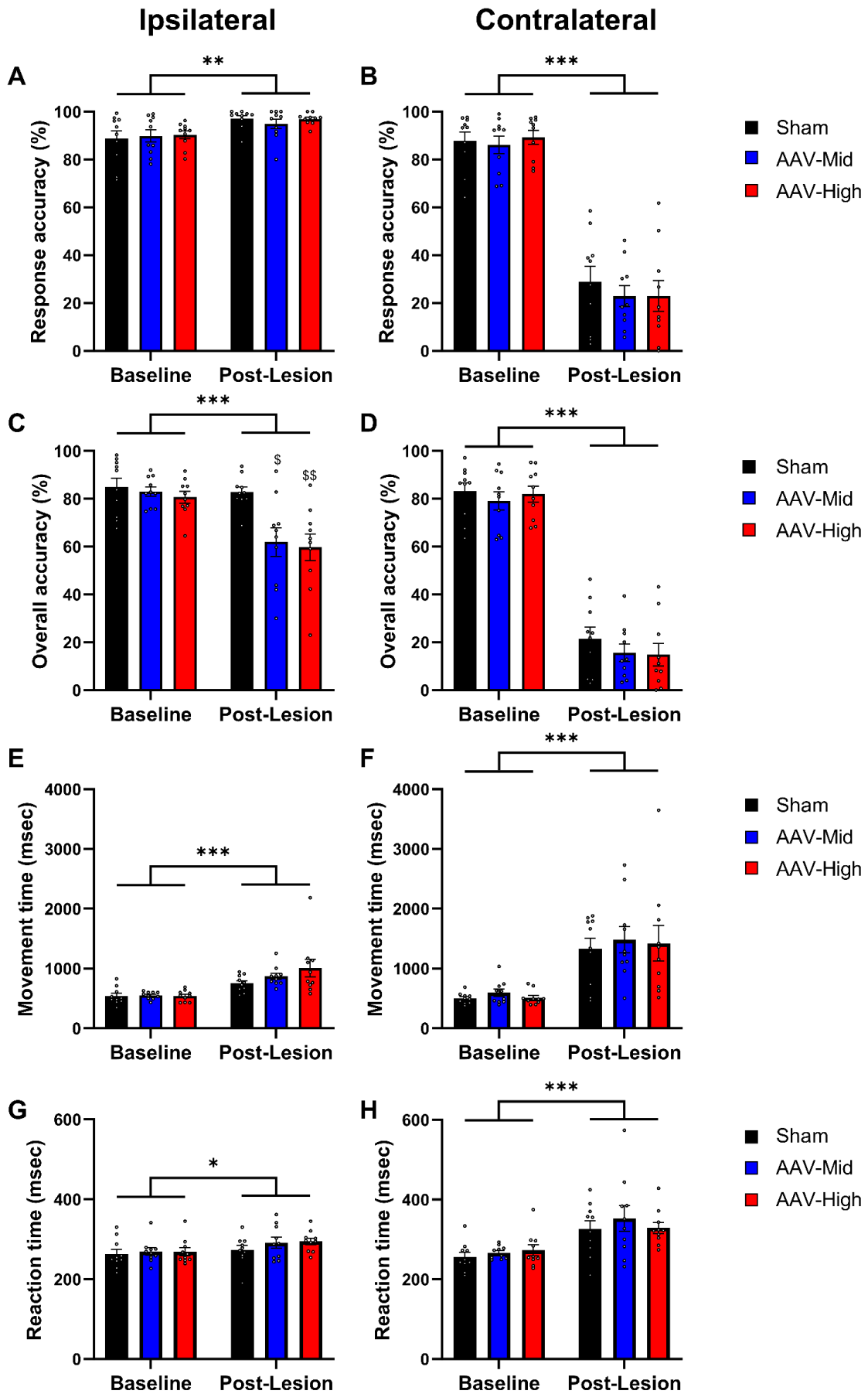
*Figure 4.10. Baseline and Post-lesion LCRT performance. **A)** Response accuracy on the ipsilateral side improved post-lesion **(B)** whereas response accuracy on the contralateral side significantly worsened post-lesion. **C)** Overall accuracy on the ipsilateral side had become worse post-lesion, and AAV-Mid & High was significantly worse on the ipsilateral side compared to Sham. **D)** Overall accuracy on contralateral side was significantly impaired post-lesion. **E-F)** Overall animals had a slower movement time post-lesion on the ipsilateral and contralateral side. **G-H)** Reaction time was significantly impaired post-lesion also on the ipsilateral and contralateral side. Error bars represent standard error of the mean. Significant differences between groups compared to Sham is indicated by $p <.05, $$p<.01. Differences between baseline and post-lesion is indicated by *p <.05, **p <.01, ***p <.001.*

4.4.4 6-OHDA MFB Lesion induces deficits in LCRT task

All animals underwent a unilateral 6-OHDA MFB lesion and was analysed on their LCRT performance at baseline and post-lesion to identify lesion-induced cognitive impairments (Figure 4.10 & Figure 4.11). Rats were analysed within their designated groups (Sham, AAV-Mid, AAV-High) prior to receiving AAV-htTH-2A-hGCH1 to identify any between-group differences that may impact post-AAV results.

Response and overall contralateral accuracy are impaired in the rat PD model

At baseline, all animals were approximately 80-90% accurate at performing the LCRT task. Post-lesion, all animals suffered performance deficits on the contralateral side. All animals were less accurate in responding to the correct contralateral hole (Figure 4.10.B. Lesion: $F(1,27) = 367.157$, $p <.001$. Group: $F(2,27) = .270$, p = n.s) and were less accurate overall compared to baseline (Figure 4.10.D. Lesion: $F(1,27) = 557.068$ $p <.001$. Group $F(2,27) = .678$ p = n.s).

6-OHDA PD rats are slower at responding during and completing the LCRT task

The time taken to complete a correct contralateral trial was approximately 500 msecs at baseline. Post-Lesion, all animals were approximately a full second slower (Figure 4.10.F. Lesion: $F(1,27) = 37.401$ $p <.001$. Group $F(2,27) = .293$, p = n.s). Post-lesion, there was also a slight increase in the speed of response removing their nose from the centre hole. (Figure 4.10.H. Lesion: $F(1,27) = 25.564$ $p <.001$. Group $F(2,27) = .465$, p = n.s). In relation to the ipsilateral side, all animals showed a slight increase in their time taken to complete a correct trial (Figure 4.10.E Lesion: $F(1,27) = 34.004$ $p <.001$. Group: $F(2,27) = 1.655$, p = n.s) and also in their reaction time (Figure 4.10.G. Lesion: $F(1,27) = 5.362$, $p = .028$. Group $2,27 = .883$, p = n.s).

6-OHDA MFB lesion can impact ipsilateral accuracy on LCRT task

At baseline, all animals were approximately 90% accurate at responding to the correct ipsilateral hole, almost identical to their contralateral baseline performance. Post-lesion, all groups performed with slightly greater accuracy on the ipsilateral side (Figure 4.10.A Lesion: $F(1,27) = 11.955$, $p = .002$. Group: $F(2,27) = .291$, p = n.s). Overall accuracy on the task however was reduced post-lesion on the ipsilateral side and both AAV groups were less

accurate overall compared to sham. (Figure 4.10.C. Lesion: $F(1,27)$ = 25.418, p <.001, Time*Group: $F(2,27)$ = 4.694, p = .018, Post-Lesion; AAV-High vs Sham p = .007, Sham vs AAV-Mid p = .016).
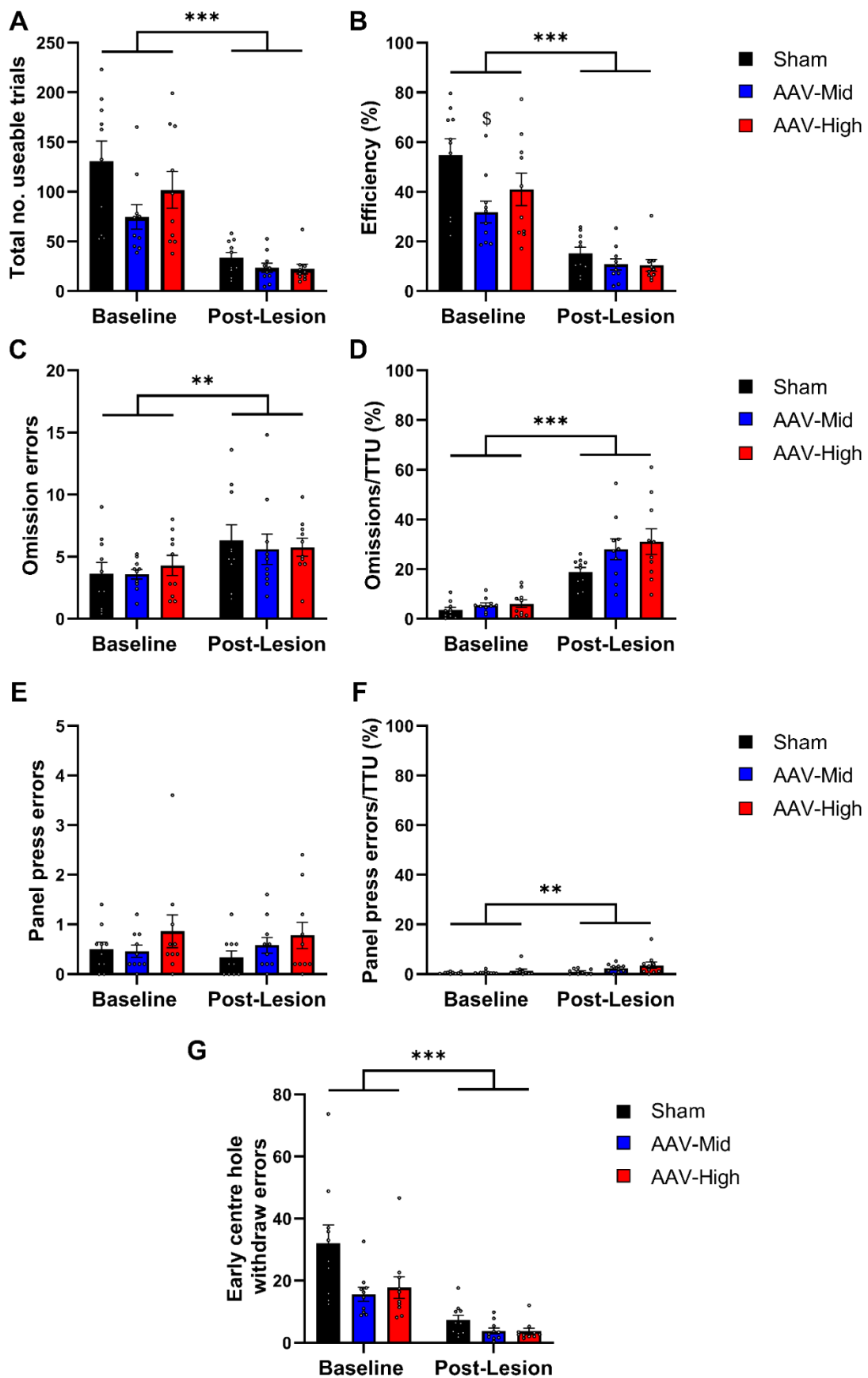
Figure 4.11. Non-side bias LCRT measures at baseline and post-Lesion. **A)** *Total no. of useable*

trials was significantly reduced post-lesion (B) as was efficiency, with AAV-Mid being less efficient at baseline compared to Sham. C) Omissions D) omissions as a percentage of total useable trials F) Panel press errors as a percentage of total useable trials were performed more frequently post-lesion. E) No effect of panel press errors was seen due to lesion. Early centre hole withdrawals were reduced post-lesion. Error bars represent standard error of the mean. Significant differences between groups compared to Sham is indicated by $p <.05. Differences between baseline and post-lesion is indicated by **p <.01, ***p <.001.

4.4.5 6-OHDA MFB lesion impairs non-lateralised aspects of LCRT task

6-OHDA MFB lesion reduces incentive motivation

At baseline, animals were well motivated to complete many trials during a 30-minute testing period. Post-lesion, all animals had a significant reduction in the number of useable trials during the same testing period (Figure 4.11.A. Lesion: $F_{(1,27)}$ = 78.811 p <.001. Group: $F_{(2,27)}$ = 2.542 p = n.s). Animals overall were less efficient on the task post-lesion (Figure 4.11.B Lesion: $F_{(1,27)}$ = 102.031, p <.001). However, there was also a main effect of group, with Sham being more efficient than AAV-Mid (Group: $F_{(2,27}$ = 3.640 p = .040. Sham vs AAV-Mid p = .035).

Variable differences in common LCRT errors induced by 6-OHDA MFB lesion

Errors performed during the LCRT task can lead to rats not receiving a reward. Omission errors, indicating that a rat hasn't responded once a useable trial has been initiated, are relatively low at baseline (Figure 4.11.C). Post-lesion all rats have a slight increase in omission errors (Figure 4.11.C Lesion: $F_{(1,27)}$ = 8.565 p = .007. Group: $F_{(2,27)}$ = .115, p = n.s). When omissions were calculated as a percentage of the total useable trials, omission errors were also increased post-lesion (Figure 4.11.D Lesion: $F_{(1,27)}$ = 87.803 p <.001. Group: $F_{(2,27)}$ = 3.040, p = n.s). Post-lesion, rats did not differ in the number of pre-emptive panel presses compared to baseline (Figure 4.11.E. Lesion: $F_{(1,27)}$ = .072, p = n.s. Group: $F_{(2,27)}$ = 1.699 p = n.s), however, when analysed as a percentage of total trials, panel press errors were significantly increased post-lesion (Figure 4.11.F. Group: $F_{(1,27)}$ = 8.684, p = .007. Group $F_{(2,27)}$ = 3.091, p = n.s. Early withdrawal from the centre hole (preventing a useable trial) was reduced in all groups post-lesion, likely due to the reduced number of useable trials (Figure 4.11.G. Lesion: $F_{(1,27)}$ = 54.610 p <.001. Group: $F_{(2,27)}$ = 5.391 p = .011. Sham vs AAV-Mid p = .016 and AAV-High p = .032).
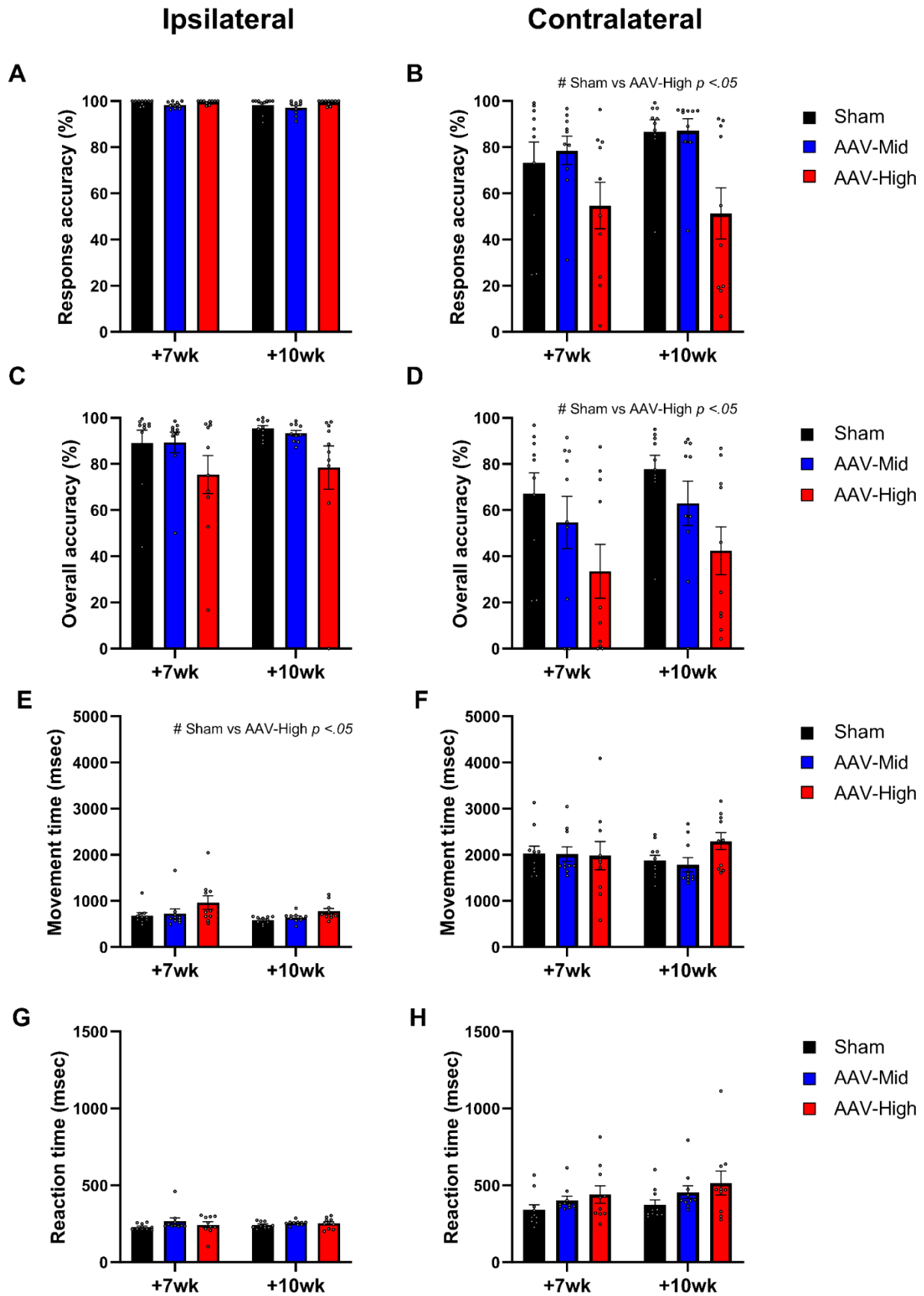
*Figure 4.12. Impact of viral mediated DA synthesis on the LCRT task. Response accuracy **(A)**, overall accuracy **(C)** and reaction time **(G)** on the ipsilateral side did not differ among groups at 7 and 10 weeks post-AAV infusion. Movement time on the ipsilateral side **(E)** was significantly longer in the AAV-High titre group at 7 and 10 weeks. On the contralateral side **(B-H)**, Response accuracy and overall accuracy was significantly worse due to AAV-High across testing weeks, but no differences were observed in movement or reaction time. Error bars represent standard error of mean. Significant main effect of group is indicated as # p < .05.*

4.4.6 Impact of AAV-htTH-2A-hGCH1 on performance in the LCRT task

AAV-High were impaired movement time on ipsilateral side

All groups were tested on the LCRT at weeks 7 and 10 post-AAV infusion (Figure 4.12). Both response (Figure 4.12.A) and overall accuracy (Figure 4.12.C) as well as reaction time (Figure 4.12.G) on the task did not differ across weeks on the ipsilateral side. However, AAV-High rats were significantly slower at responding to the correct stimulus light on the ipsilateral side compared to Sham (Figure 4.12.E. Group: $F(2,27) = 3.451$, $p = .046$, Sham vs AAV-High $p = .050$).

AAV-High were significantly impaired in contralateral LCRT performance

On the contralateral side, AAV-High rats were less accurate in their response accuracy on the task at both 7 and 10 weeks compared to AAV-Mid and Sham (Figure 4.12.B: Group: $F(2,27) = 4.678$, $p = .018$, Sham vs AAV-High $p = .030$, AAV-Mid vs AAV-High $p = .040$). AAV-High rats were also less accurate overall compared to Sham (Figure 4.12.D. Group: $F(1,27) = 7.140$, $p = .013$, Sham vs AAV-High $p = .037$). Movement time was not impaired across groups (Figure 4.12.F: ($F(2,27) = 2.458$, $p = $ n.s). Reaction time (Figure 4.12.H) did not differ between groups across testing weeks.
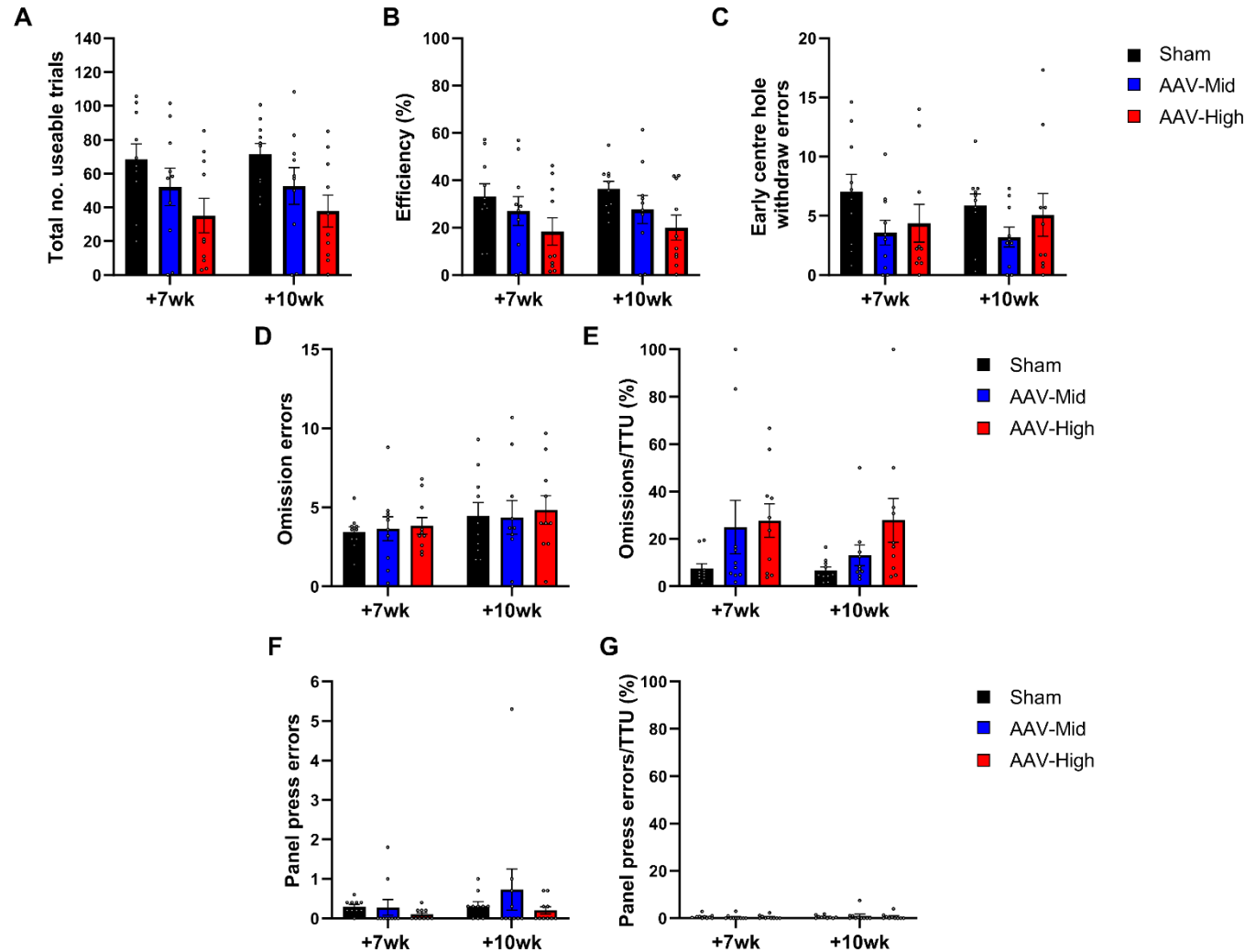
Figure 4.13. Impact of viral-mediated DA synthesis on non-side biased measures and a unilateral probe test on the LCRT task. **(A)** Total useable trials did not differ compared to Sham at 7 and 10 weeks. **(B)** Efficiency performing the task did not differ among the groups. Errors made whilst performing the LCRT such as early withdrawal from the centre hole **(C)**, omissions **(D-E)** and panel press errors **(F-G)** did not differ among the groups. Error bars represent standard error of mean. Significant main effect of group is indicated as * p < .05, *** p <.001.

4.4.7 No statistical differences between non-lateralised measures of LCRT at 7 or 10 weeks post-AAV

Useable trials did not significantly differ across weeks (Figure 4.13.A. Group: ($F(2,27) = 3.291$ $p = .053$.). Across weeks 7 and 10, efficiency performing the LCRT task remained low across all groups but was not significantly impaired (Figure 4.13.B. $F(2,27) = .204$, $p = $ n.s). In relation to specific errors, early withdrawal from the centre hole (Figure 4.13.C. $F(2,27) =.422$, $p = $ n.s), omissions (Figure 4.13.D. $F(2,27) = .099$, $p = $ n.s) and panel press errors (Figure 4.13.F. $F(2,27) = .722$, $p = $ n.s) were not observed in any group to a greater extent across the weeks, nor when omissions and panel press errors were analysed as a percentage of total useable trials (Figure 4.13.E. Omissions/TTU: Group: $F(2,27) = 2.878$, $p = $ n.s. Figure 4.13.G. Group: $F(2,27) = .900$, $p = $ n.s).
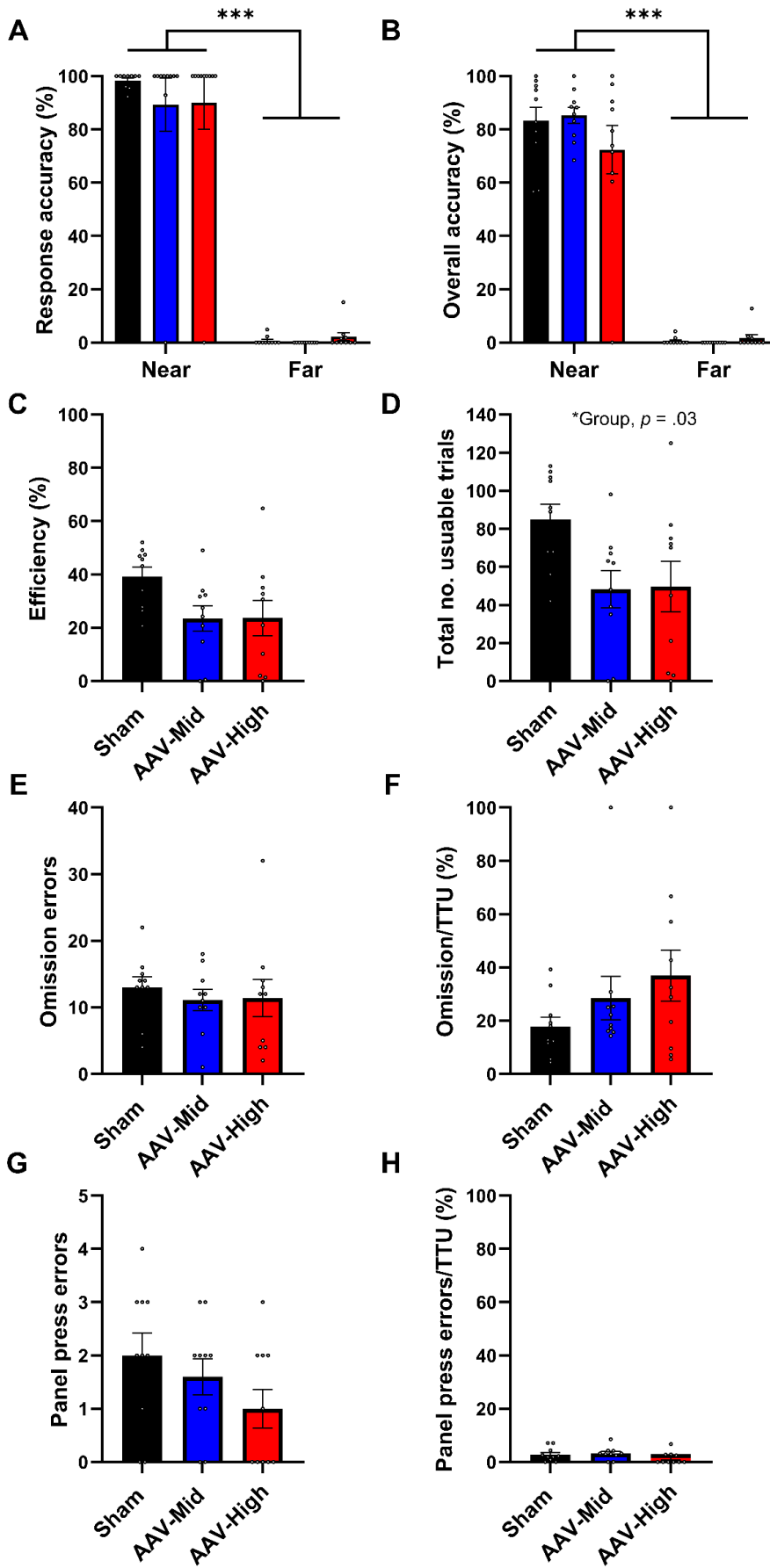
*Figure 4.14. Unilateral probe test placing both nose poke responses on the contralateral side. **A-B)** Response and overall accuracy in the near hole did not differ among groups and all groups had poor accuracy when responding in the far hole. **C)** Efficiency, **(D)** Total useable trials **(E)** Omissions (F) Omissions/TTU, **(G)** Panel press and **(H)** Panel press/TTU did not differ among groups in the unilateral probe test, however there was a group effect in total useable trials. Differences between the near and far hole are indicated as ***p <.001.*

4.4.8 LCRT performance of AAV-htTH-2A-hGCH1 treated rats in a unilateral probe test

One trial of the LCRT task was conducted as a unilateral probe test, with a modification in which the ipsilateral hole was removed and replaced with a second contralateral hole (now called Far) at a greater distance away from the remaining contralateral hole (now called Near) (Figure 4.5). This probe test was undertaken to further challenge contralateral responding and explore whether viral mediated DA replacement could alleviate the deficits seen in the Far hole in rats with a 6-OHDA MFB lesion (Lelos et al. 2016). Another benefit of this probe test was to confirm that the significant deficit seen with an AAV-High titre of htTH-2A-hGCH1 is not due to factors such as motor deficits induced by the 6-OHDA MFB lesion limiting them in responding on the contralateral side.

AAV-High were not impaired during unilateral probe test

Even though previously the AAV-High titre group significantly struggled to perform correct trials on the contralateral side, their overall accuracy became indistinguishable from the other groups in both the Near and Far hole. All animals are significantly worse in both response accuracy in the Far hole compared to the Near (Figure 4.14.A. Side: $F(1,27) = 383.076$, $p <.001$. Group: No effect of group $F(2,27) = .368$, $p = $ n.s) as well as overall accuracy (Figure 4.14.B. Side: $F(1,27) = 519.137$, $p <.001$. Group: $F(2,27) = .849$, $p = $ n.s).

No difference on non-lateralised measures on the unilateral probe test

Efficiency on performing this task in both near and far holes was up to 40%, with no differences between groups (Figure 4.14.C Group: $F(2,27) = 3.139$, $p = 0.59$). There was an overall group effect in total useable trials, but it did not reach significance in multiple comparisons (Figure 4.14.D. Group: $F(2,27) = 3.872$, $p = .033$, AAV-Mid vs Sham, $p = .053$). Common errors made during the LCRT task did not differ between groups in the unilateral probe test in terms of Omissions (Figure 4.14.E. Group: $F(2,27) = .246$, $p = $ n.s), Omissions/TTU (Figure 4.14.F. Group: $F(2,27) = 1.612$, $p = $ n.s), Panel press errors (Figure 4.14.G. Group: $F(2,27) = 1.781$, $p = $ n.s) and Panel press/TTU (Figure 4.14.H. Group: $F(2,27) = 1.414$, $p = $ n.s).
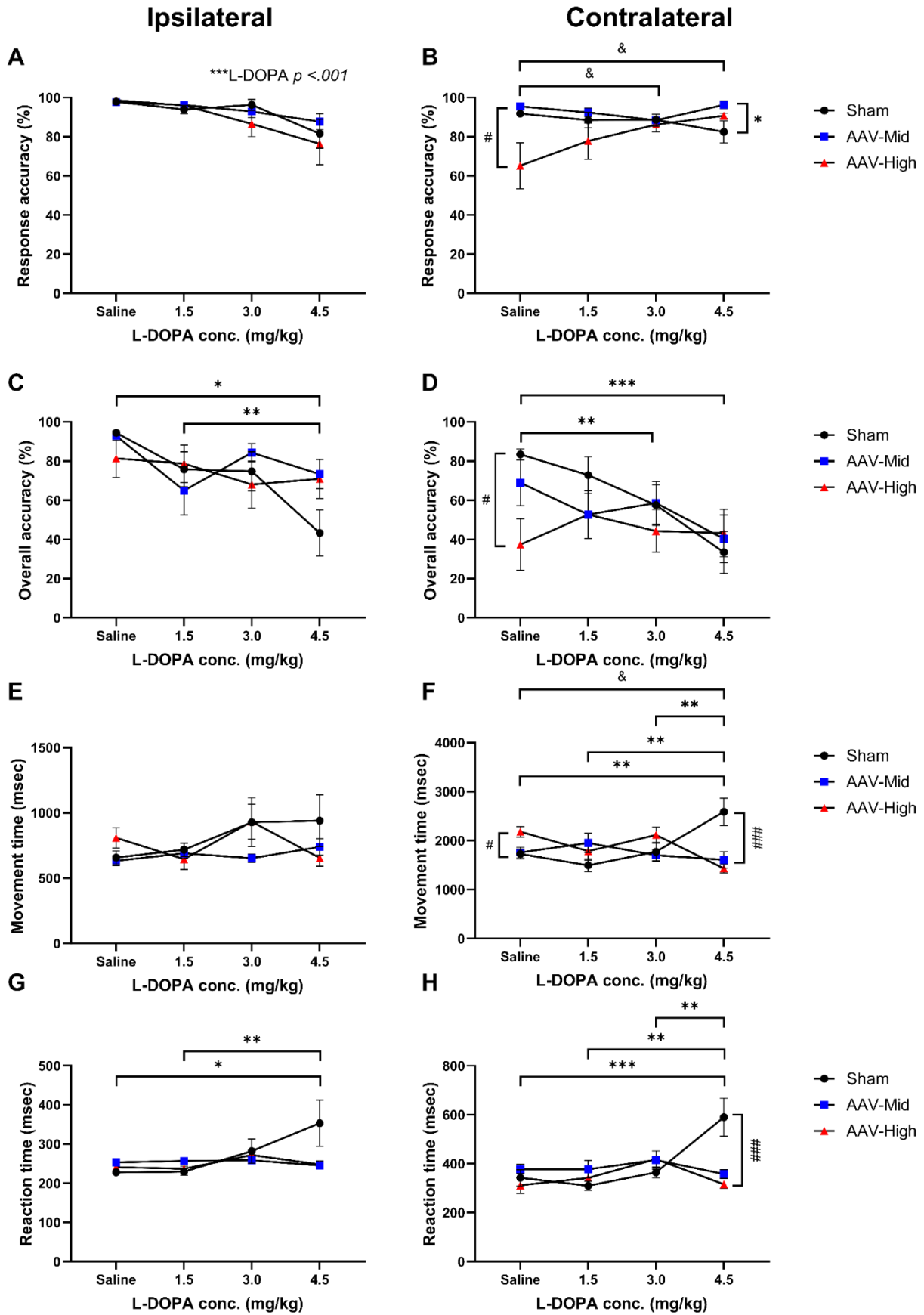
Figure 4.15 Increasing doses of L-DOPA affects performance on the LCRT. **A)** *ipsilateral response*

*accuracy decreased as L-DOPA concentration increased **B)** AAV-High group significantly improve response accuracy on the contralateral side, whereas the Sham group significantly declined in their response accuracy, overall accuracy on both the ipsilateral (**C**) and contralateral side **(D)** with increasing L-DOPA doses. **E)** Movement time on the ipsilateral side was not affected by L-DOPA, however the Sham group was significantly slower in completing the contralateral tasks **(F)** and were also significantly slower on the ipsilateral **(G)** and contralateral side **(H)** in their reaction time. Error bars represent standard error of mean. Significant differences between groups are indicated as # p < .05, ## p <.01, ### p <.001. Significant changes across the drug within a group are specific by Sham (*), AAV-high (&).*

4.4.9 L-DOPA affects performance on the LCRT task

L-DOPA improves response accuracy in AAV-High group, but impairs accuracy in Sham rats

At 11 weeks post-AAV, animals received four increasing doses of L-DOPA and were tested in the LCRT task. All groups were above 90% accurate in their response accuracy ipsilaterally when administered saline and there was an effect of L-DOPA to reduce overall accuracy as L-DOPA concentration increases (Figure 4.15.A. Drug: $F(3,81) = 9.487$, p <.001. 4.5mg vs Saline p =.010 & 1.45mg p = .025 & 3.0mg p = .032). Response accuracy on the contralateral side was also significantly affected by L-DOPA treatment (Figure 4.15.B. Group*Drug: $F(6,81) = 2.495$, p = .029). When given saline-only, Sham and AAV-Mid were significantly more accurate in their responses compared to AAV-High titre group (p = .01). As dosing of L-DOPA increased, AAV-High titre-treated animals' response accuracy significantly improved (AAV-High - Saline vs 3mg p = .047, AAV-High - Saline vs 4.5mg p = .025). No impact of L-DOPA was observed in the AAV-Mid, however Sham's accuracy was worse than AAV-Mid after receiving 4.5mg/kg L-DOPA (p = .030).

L-DOPA impairs overall accuracy in Sham rats

Increasing L-DOPA doses appeared to have the greatest impact on the Sham group, evidenced by their overall accuracy (Figure 4.15.D. Group*Drug: $F(3,81) = 6.794$, p <.001). On the contralateral side, when given saline, the AAV-High-titre group was poorer in their accuracy compared to Sham rats (p = .01), which follows the trend for what was seen at 7 and 10 weeks previously (Figure 4.12). However, as L-DOPA doses increased, overall accuracy of Sham animals declined (Sham - Saline vs 3mg p = .009, Saline vs 4.5 mg p = <.001) whilst no impact on overall accuracy was seen in mid or AAV-High titre groups (p = n.s). On the ipsilateral side, increasing doses of L-DOPA also lead to a decline in overall accuracy (Figure 4.15.D. Group*Drug: $F(6,81) = 3.149$, p = .008. Sham: Saline vs 4.5mg p = .012, Sham 1.5mg vs 4.5mg p = .003), indicating that L-DOPA was having an overall effect on their performance during the task.

L-DOPA increases movement time in Sham rats, whilst decreasing movement time in AAV-High rats

When saline was administered, the AAV-High group was significantly slower in completing the task compared to Sham and AAV-Mid (Figure 4.15.F. Group*Drug: $F_{(6,81)}$ = 7.407, p = <.001. Sham vs AAV-High Saline p = .015 & AAV-Mid vs AAV-High p = .024). When administered 4.5mg/kg L-DOPA, Sham-only rats were significantly slower to complete the task compared to the AAV-High-titre group (p <.001) and were slower to complete the task based on their own performance when administered saline (Sham Saline vs 4.5mg p = .008, Sham 1.5mg vs 4.5mg p = .003, Sham 3mg vs 4.5mg p = .013), and AAV-High were significantly quicker compared to when given saline (p = .026). No effect was seen on the ipsilateral side (Figure 4.15.E).

L-DOPA increases reaction time in Sham rats

Reaction time taken to was also significantly affected by L-DOPA treatment (Figure 4.15.H. Group*Drug: $F_{(6,81)}$ = 6.711, p = <.001). Sham rats were slower in their reaction time when given 4.5mg/kg compared to saline (p = <.001), 1.5mg/kg (p = .005) or 3mg/kg L-DOPA (p = .002). Also, at 4.5mg/kg, Sham-only rats were slower in their reaction time than the mid and AAV-High-titre group (p <.001). On the ipsilateral side, no impact was observed within the AAV-Mid or AAV-High titre group, but Sham rats were slower in their reaction time when given 4.5mg/kg compared to being administered saline or 1.5mg/kg L-DOPA (Figure 4.15.G. Group*Drug: $F_{(6,81)}$ = 3.149 p = .008. Sham: Saline vs 4.5mg p = .012, Sham 1.5mg vs 4.5mg p = .003).
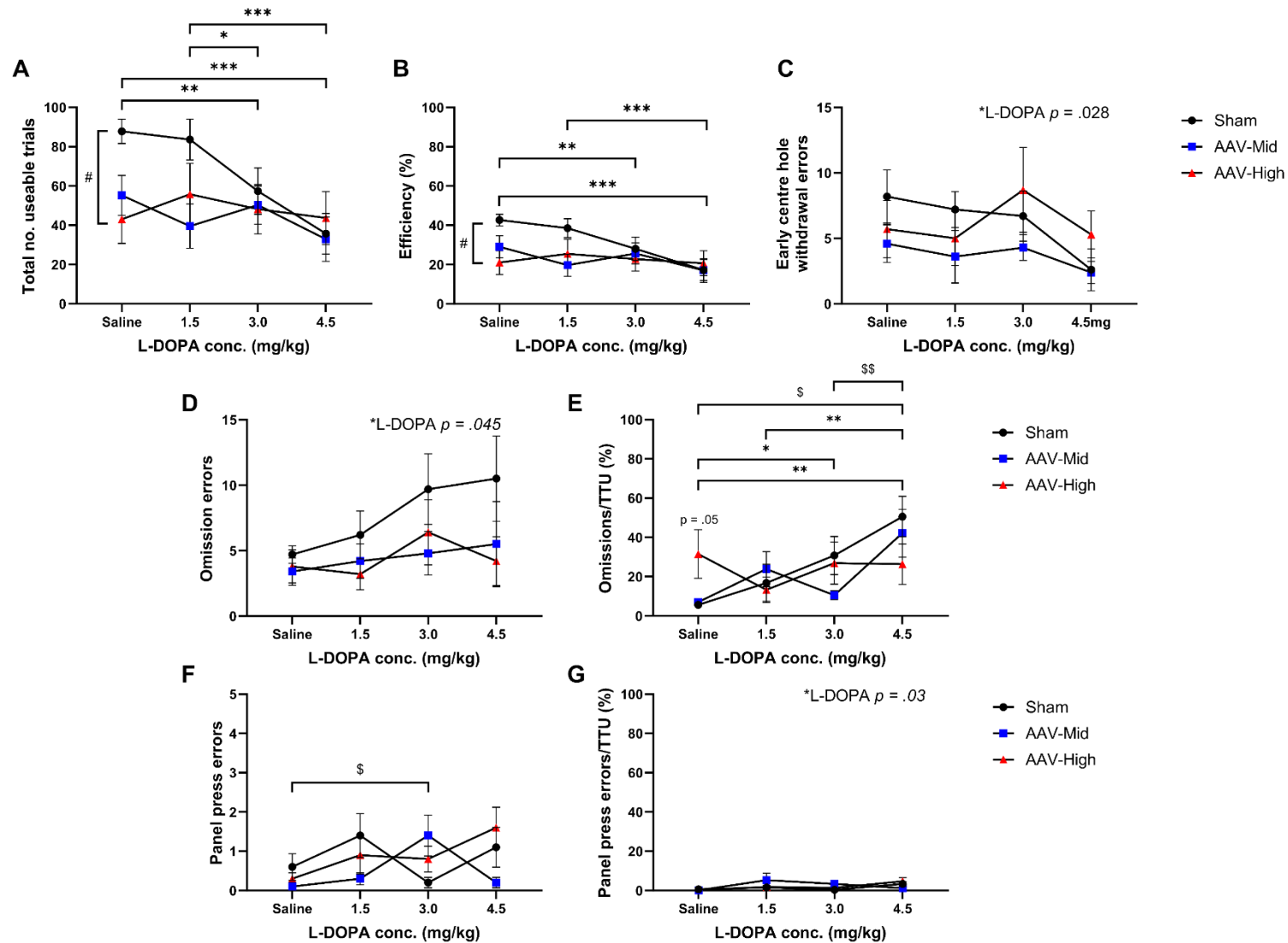
Figure 4.16. Effect of L-DOPA on non-side bias measures during LCRT. **(A)** *Total usable trials (TTU) are significantly impaired in AAV-High titre group compared to Sham when given saline, however, when given increasing doses of L-DOPA, Sham only rats decline in their ability to perform*

useable trials, as does their efficiency on the task (B). Increasing doses of L-DOPA has no impact on early centre hole withdrawal errors (C) or omissions (D). E) Omissions as a percentage of TTU was trending for being more frequent in AAV-High than Sham under Saline administration. When L-DOPA was increased, AAV-Mid and Sham performed more Omissions. F)   AAV-Mid performed significantly more panel press errors on 3mg/kg L-DOPA then when given saline G) L-DOPA had an overall effect on Panel press errors as a percentage of TTU. Error bars represent standard error of mean. Significant differences between groups are indicated as # p < .05, ## p <.01, ### p <.001. Significant changes across the drug within a group are specific by Sham (*), AAV-Mid ($).

4.4.10 Impact of L-DOPA on non-lateralised aspects of LCRT performance in AAV-htTH-2A-hGCH1 treated rats

L-DOPA impairs total usable trials in Sham rats

In relation to non-side bias measures on the LCRT, the total number of useable trials was also affected by L-DOPA treatment (Figure 4.16.A. Group*Drug: $F_{(6,81)}$ = 3.698, p = .003). When given saline, rats with AAV-High-titre AAV performed significantly fewer useable trials compared to Sham-only group (p = .010), similar to the overall effect seen at weeks 7 and 10 previously. Similar to their response and overall accuracy on the task, as the dose of L-DOPA increased, the number of useable trials performed by the Sham-only group declined (Sham Saline vs 3mg p = .007, Saline vs 4.5mg p = <.001, 1.5mg vs 3mg p = .034, 1.5mg vs 4.5mg p = <.001), whilst the number of useable trials performed by the mid and AAV-High titre group were stable across L-DOPA doses.

L-DOPA impaired efficiency in Sham rats

The same effect as observed in total useable trials was seen in efficiency at the task during L-DOPA administration (Figure 4.16.B. Group*Drug: $F_{(6,81)}$ = 3.176, p = .008). The Sham group was significantly more efficient at the task compared to AAV-High rats when given saline (p = .016), with efficiency for Sham rats declining with increasing L-DOPA doses (Saline vs 4.5mg p <.001, Saline vs 3mg p = .007, 1.5 vs 4.5mg p <.001). There was an overall effect of L-DOPA of centre hole withdrawal errors (Figure 4.16.C Drug: $F_{(3,81)}$ = 3.200, p = .028. 3mg vs 4.5mg p = .033).

L-DOPA increased Omissions and Panel press errors

Omissions are worsened with L-DOPA overall, however pairwise comparisons did not meet statistical significance (Figure 4.16.D Drug: $F_{(3,81)}$ = 2.796, p = .045). When omissions were analysed as a percentage of total useable trials, AAV-High was on trend to have a higher percentage of omissions during saline administration, and AAV-Mid and Sham had increasing omissions as L-DOPA dose increased (Figure 4.16.E Drug*Group: $F_{(6,81)}$ =

8.434, p = .003. Saline: AAV-High vs Sham p = .050. Sham: Saline vs 3mg p = .024 & 4.5mg p = .002. 1.5mg vs 4mg p = .005. AAV-Mid: Saline vs 4.5mg p = .019, 3mg vs 4.5mg p = .007). However, AAV-Mid group made more panel press errors when given 3mg/kg L-DOPA compared to saline (Figure 4.16.E Group*Drug: (F(6,81) = 3.008, p = .011. AAV-Mid: Saline vs 3mg, p = .015). When panel press errors were analysed as a percentage of the total useable trials, there was an overall effect of L-DOPA increasing the number performed by all groups as L-DOPA dose increased (Figure 4.16.F. Drug: F(3,81) = 3.097, p = .03. Saline vs 3mg p = .006 & 4.5mg p = .009).
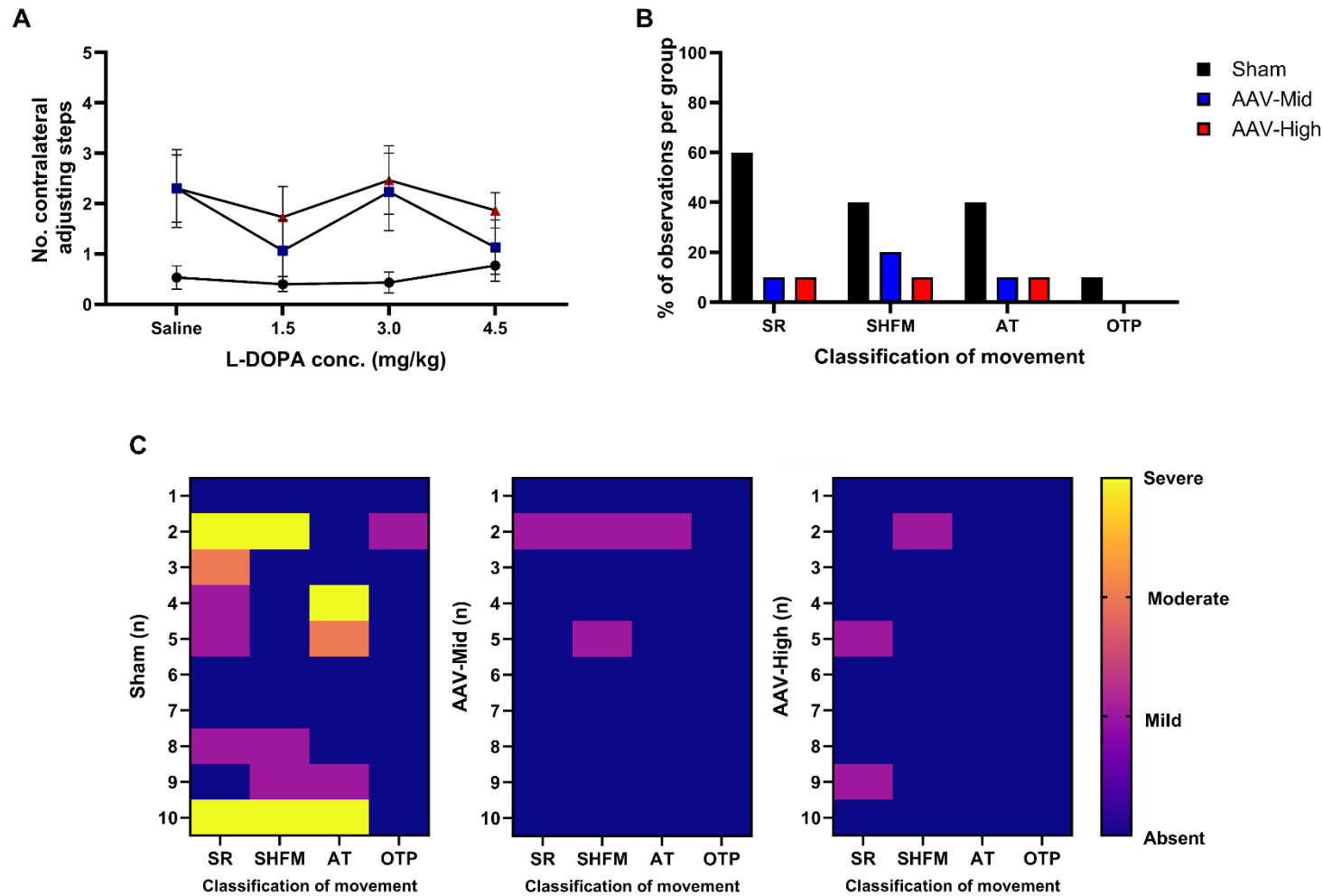
*Figure 4.17. Impact of L-DOPA on motor behaviour. **A)** Contralateral adjusting steps did not significantly differ across L-DOPA doses. Abnormal body movements were observed and recorded for observed event and severity after 1.5 and 4.5mg/kg L-DOPA. **B)** Sham animals experience more abnormal movements than AAV-High or Mid Titre group. The onset of these abnormal movements was also more severe for Sham animals **(C).** SR = Spontaneous Rotations, SHFM = Spontaneous Hyperkinetic Forelimb Movement, AT = Axial Twisting, OTP = Orolingual Tongue Protrusions. Error bars represent standard error of mean.*

146

4.4.11 L-DOPA impacts motor performance

Motor improvement due to AAV-High seen at 7 weeks on adjusting steps was not observed during this L-DOPA challenge. There was a trend towards AAV-High treated rats performing significantly more steps than Shams (Figure 4.17.A. Group: $F(2,27) = 3.226$, $p = .055$, AAV-High vs Sham $p = .052$), however this separation between AAV-tTH-2A-hGCH1 treated groups and Sham animals is diminished at 1.5mg/kg and 4.5mg/kg. In relation to the type of behaviours observed during 1.5mg/kg and 4.5mg/kg L-DOPA (Figure 4.17.B), the greatest observed abnormal behaviour was spontaneous rotations with 60% of Sham-only rats displaying this behaviour post-L-DOPA treatment. The Sham group overall displayed the most observable L-DOPA-induced abnormal movements, whereas only one or two rats per group in the AAV treated groups displayed some dyskinetic-like behaviours. Sham only animals were also more severe in the onset of these behaviours compared to mid or AAV-High rats, in which the severity of these behaviours was mild (Figure 4.17.C).
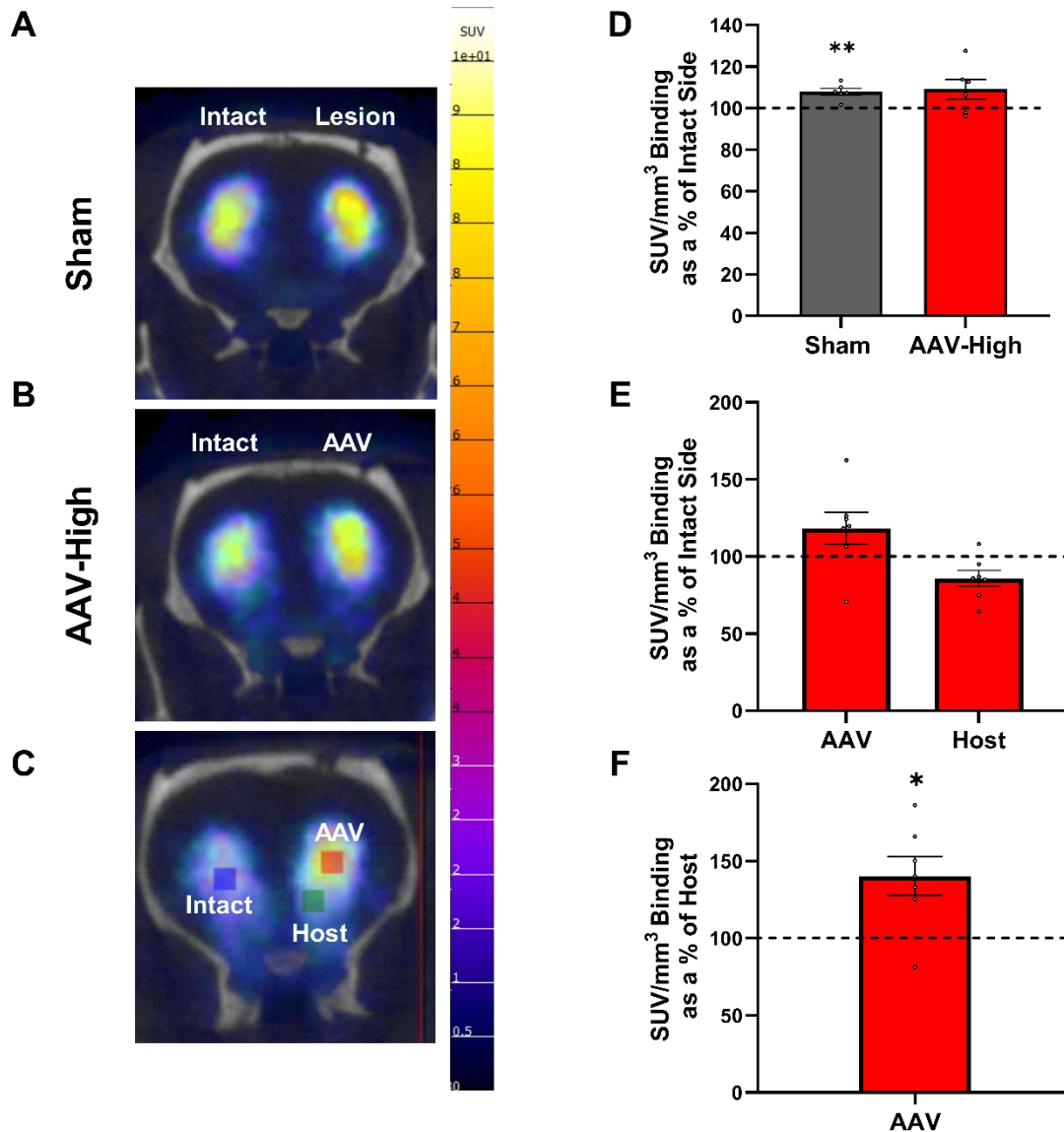
*Figure 4.18. PET-CT analysis of [18F] Fallypride 1hr post-injection. **A-B)** Representative images of PET scan with CT overlay for anatomical reference. Evidence of increased D2 binding in the right striatum in both Sham and high titre group in the right hemisphere. **C)** Representative image of locations for measuring D2 binding difference within striatum. Blue square = Intact side, Red square = inside AAV, green square = outside AAV. **D)** Mean SUV binding ratio of the treated vs intact hemisphere in both Sham and AAV-High titre group. **E)** Mean SUV value binding ratio in three distinct regions of the CT scan.*

4.4.12 Evaluating D2/3 receptor binding with [18F]-Fallypride at 8 weeks post-AAV

Dense AAV-htTH-hGCH1 core had upregulated D2/D3 receptor binding

[18F]Fallypride imaging was carried out in order to investigate receptor changes within the striatum in Sham animals and AAV-High rats (Figure 4.18). Images of PET/CT co-registered scans indicate specific [18F]Fallypride binding to the striatum in both lesioned and intact hemispheres in both groups (Figure 4.18.A-B). The ratio of [18F]Fallypride binding in the lesioned hemisphere was calculated as a percentage of the intact hemisphere. Sham had an imbalance in D2 receptors between the two hemispheres that was normalised with AAV-High largely due to the variation amongst the group (Figure 4.18. D. Sham: $t(5) = 5.051$, $p = .004$. AAV-High: $t(5) = 1.926$, $p = $ n.s). In order to further investigate receptor changes due to viral vector administration, [18F]Fallypride binding was measured inside the core of the virla vector expression (AAV), in the outside striatum (Host) and in the intact hemisphere (Intact) (Figure 4.18.C). The ratio of [18F]Fallypride binding between the AAV core and the Host when compared as a percentage of the intact side showed no different between the two hemispheres (Figure 4.18.E. AAV:Intact – $t(5) = 1.502$, $p = $ n.s. Host:Intact – $t(5) = -2.287$, $p = .071$). Interestingly, when the binding ratio between the AAV core and the surrounding host striatum was analysed, there was an upregulation of [18F]Fallypride within the AAV core (Figure 4.18.F. $t(5) = 2.713$, $p = .042$).

4.5 Discussion: Experiment 2

The aim of Experiment 2 was to assess the impact of DA replacement on cognitive function using viral-mediated DA biosynthesis and pharmacological DA replacement with L-DOPA. Unilateral 6-OHDA-lesioned rats received an intra-striatal infusion of htTH-2A-hGCH1 at either a mid or a high titre and was examined on both motor and cognitive tasks, as well as an L-DOPA challenge up to 12 weeks post-AAV. AAV-High worsened already impaired visuospatial processing whilst improving adjusting steps. Administration of L-DOPA improved response accuracy of AAV-High treated rats, but also lead to a dose-response decline in performance on the LCRT in the Sham group and the onset of abnormal involuntary movements. Histological analysis revealed clear uptake of the viral vector to the striatal MSNs but also off-target expression in the piriform cortex. This section will aim to discuss the impact of dose of continuous and intermittent pharmacological DA replacement on motor and cognitive performance and what factors may have contributed to the results observed within this experiment.

4.5.1 Impact of dose on motor function

Performance on drug-induced rotations as well as simple motor and sensorimotor function was evaluated at 5, 7 and 11 weeks post-AAV to determine if motor recovery was dose-dependent. No improvement of drug-induced rotations was observed (Figure 4.9.A). However, AAV-High partially alleviated forelimb akinesia on the adjusting step task at 7 weeks post-AAV (Figure 4.9.B), whilst sensorimotor deficits were improved by AAV-Mid only (Figure 4.9.C) indicating a varying impact of dose on motor recovery.

As detailed in Chapter 1 (see 1.6), studies utilising other viral vectors encoding TH and GCH1 found motor recovery to be dose dependant (Cederfjäll et al. 2013; Rosenblad et al. 2019a). Leriche et al. (2009) dual-infused TH (1.2×10^{13}) and GCH1 (1.0×10^{13}) rAAV5 vectors into the striatum and found a significant reduction in amphetamine and apomorphine rotational bias when evaluated 39 weeks post-AAV as well as a 50% recovery in the cylinder test from 12 weeks post-AAV. The AAVs used in Leriche et al. (2009) is of a similar titre to

AAV-High (1.69×10^{13}), yet they saw reduced rotational bias. However, it should be noted that length of the study was 6 months longer than what was carried out here, so future use of viral vectors for pre-clinical analysis may require a longer timeframe to observe full recovery. However, Reimsnider et al. (2007) evaluated the time-course dependency of different pseudotypes and found AAV2/1 to reach maximum effect within 4 weeks, indicating the timeframe of 12 weeks in Experiment 2 should have been efficient to effectively evaluate AAV-Mid and AAV-High. Other factors such as placement of the viral vector within the striatum may be playing a role in the scale of motor recovery and will be discussed in conjunction with cognitive function below.

4.5.2 Impact of dose on cognitive function

Rats with an intra-striatal infusion of AAV-htTH-2A-hGCH1 in a mid or a high titre were evaluated on a simplified version of the LCRT task at 7 and 10 weeks post-AAV. AAV-Mid rats showed no improvement on the LCRT task and were comparable to Sham throughout testing weeks, whilst AAV-High rats were significantly impaired in response and overall accuracy on the task compared to Sham (Figure 4.12.B&D). AAV-High rats were marginally slower on the ipsilateral side overall (Figure 4.12.E). It must be noted that Sham animals were more accurate overall on the ipsilateral side at baseline compared to AAV-Mid and AAV-High (Figure 4.10.C) and were more efficient at baseline between Sham and AAV-Mid (Figure 4.11). The difference seen between Sham and AAV-High could be an exacerbation of pre-existing group differences causing AAV-High to appear impaired post-AAV.

Furthermore, a probe test was carried out placing responding solely within the contralateral space. All groups were able to now respond with a high degree of accuracy in the nose poke operandum that was previously challenging , and responding was favoured on the near hole compared to the far (Figure 4.14.A-B). This unilateral probe was reported in Heuer et al. (2013b) and Lelos et al. (2016). Responding within the contralateral space in DA depleted rats is not due to spatial neglect but instead, now responding in a previously difficult hole displays an element of bias towards an easier choice due to disrupted coding of visuospatial responses. As AAV-High showed no impairment in response or overall accuracy in the unilateral probe, there may be other reasons why AAV-high has impaired visuospatial processing in the LCRT task. Importantly though, all groups were impaired relative to each

other post-lesion on the contralateral side, and midbrain counts found all groups to have over 95% loss in the SNc and 40-50% loss in the VTA (Figure 4.8.F). Furthermore, the task parameters were made markedly easier compared to the parameters in Chapter 3 (see 2.5.3), so cannot rule out the effect of viral-mediated DA biosynthesis impairing performance in the LCRT task.

4.5.3 Limited biodistribution of the virus

It is important to understand what factors may be impacting the function of the viral vector beside dose. When evaluating tTH and GCH1 immunostaining (Figure 4.6), both AAV-Mid and AAV-high had positive tTH and GCH1 immunostaining within the striatum but optical density found the majority of tTH expression was located in the ventral striatum and predominantly in the lateral region (Figure 4.8.B). The biodistribution of tTH expression in AAV-Mid and AAV-High in 4 sections throughout the rostral-caudal plane showed an average of 20% coverage of the striatal nuclei (Figure 4.8.D). It is reasonable to assume that the limited biodistribution of AAV-htTH-2A-hGCH1 throughout the striatum and off-target cortical expression revealed by histological analysis is an important factor for the impact of AAV-High on cognitive and motor function within this experiment. Thus, the impact of improving viral-mediated DA biosynthesis distribution throughout the striatum was assessed in Experiment 3 below.

As well as limited biodistribution of tTH throughout the striatum, the same relative level of immunostaining was seen in the surrounding cortex (Figure 4.8.E). Areas that had marked off-target tTH immunostaining were the piriform cortex, claustrum and amygdala. Potts and Bekkers (2022) detail the strong modulatory role DA has in the piriform cortex, which is responsible for receiving and discriminating odours through D1 receptor activation on fast-spiking GABAergic interneurons. Disruption in the piriform cortex can affect olfactory processing (Sancandi et al. 2018; Torres-Pasillas et al. 2023). In order to evaluate the impact of off-target gene transfer in the piriform cortex, tasks such as olfactory testing would be valuable to see if disrupted olfactory processing would impact their sucrose preference (Athanassi et al. 2021). DA is also responsible for mediating amygdala function in fear conditioning, emotional processing, and over activation of amygdala D2 receptor activation was found to decrease sucrose intake in a progressive ratio task (Tessitore et al. 2002;

Anderberg et al. 2014; Frick et al. 2022). The amygdala is also implicated in response-outcome instrumental conditioning, however it is unknown if responses made during the LCRT are based on goal-directed behaviour (Corbit et al. 2013).

One hypothesis for the interaction between extra-striatal AAV-htTH-2A-hGHC1 gene expression and impairment in visuospatial function is that DA influx in cortical regions disrupts cortical processing and thus dysregulates cognitive function. Cortical DA receptors are highly sensitive to environmental changes and different regions require different cytosolic levels of DA (Juárez Olguín et al. 2016). Cognitive function is considered to work on the principle of the 'inverted U hypothesis' which refers to cortical neurons acting on a bell-shaped curve in response to DA concentrations (Seamans and Yang 2004). As mentioned briefly in Chapter 1, too little DA will prevent the regulation of associative functions such as working memory, spatial memory, cognitive flexibility and other behaviours (Brozoski et al. 1979; Kulisevsky 2000) and too much will cause an oversaturation on post-synaptic terminals and disrupt circuitry (Braver and Cohen 2000).

It is important to state that the previous studies detailed in the Chapter 4 introduction such as Cederfjäll et al. (2013) and Leriche et al. (2009) have off-target expression the higher the titre of viral vector was used. Expression followed the same pattern as shown in Figure 4.6, with off-target expression following the corpus callosum and into cortical regions. This off-target expression did not negate recovery in motor deficits such as the adjusting steps task and cylinder, but no cognitive tasks were carried out during their assessment. Therefore, it is important to consider the side effects to extra-striatal TH and GCH1 gene transfer in cortical circuitry dysfunction and what effect that could have on LCRT performance. Experiment 3 aimed to reduce the amount of off-target expression to prevent confounding factors in evaluating viral-mediated DA synthesis in cognitive recovery.

4.5.4 Impact of striatal D2/D3 receptors

At 8 weeks post-AAV, a subset of animals from Sham and AAV-High underwent a PET/CT scan with the radioactive tracer [^{18}F]Fallypride (Figure 4.18). [^{18}F]Fallypride is a common radioligand used for evaluating D2/D3 receptor binding, which has reported upregulation of D2 receptors in the 6-OHDA lesioned rat (Mukherjee et al. 2002; Choi et al. 2012). Sham rats had an imbalance in the binding ratio between the lesioned and intact hemisphere,

which suggests that they present with the anticipated upregulation of D2/3 receptors that would be expected post-lesion. Data from the AAV-High rats suggested no difference to the intact hemisphere, which could indicate a normalisation of receptor expression. However, it is important to note that AAV-High rats had greater variation in [^{18}F]Fallypride binding within the group, which may account for why they did not show an imbalance compared to the intact side (Figure 4.18.D). The binding ratio between the AAV core and surrounding host striatum were normalised to the intact hemisphere (Figure 4.18.D) and the results suggested potential normalisation of D2/3 receptors outside the core region of AAV expression. However, [^{18}F]Fallypride binding in the AAV core was significantly higher than the surrounding host striatum (Figure 4.18.E). Overall, these results suggest a trend for normalisation of D2/D3 receptors due to AAV infusion, but the reason for the imbalance in the AAV core compared to the host striatum is unknown.

Dual-infused TH (1.2x10^{13}) and GCH1 (1.0x10^{13}) rAAV5 vectors have been evaluated for normalisation of D2 receptors with other radioligands such as [^{11}C]Raclopride microPET and accompanying HPLC at post-mortem in the same animals (Leriche et al. 2009). It was reported that the synaptic pool of endogenous DA was restored to normal levels when compared to a lesioned 6-OHDA rat control. In addition to this, they used a partial saturation PET experiment to determine the binding affinity of [^{11}C]Raclopride and the D2 receptor density of the striatum. They found that within the lesioned hemisphere of the 6-OHDA MFB lesioned rat, there is an increase in affinity for [^{11}C]Raclopride to bind without affecting the density of D2 receptors due to reduced competition in binding due to the loss of DA availability in the pre-synaptic terminals, and viral vectors were effective in normalising that binding affinity by supplying DA.

Due to not carrying out partial saturation PET analysis, we cannot determine if the incongruity between [^{18}F]Fallypride binding in the AAV core and is due to an upregulation of D2 receptors in MSNs or if there is a greater binding affinity. However, the impact of gene transfer on striatal MSN function is important to consider.

Striatal MSNs which have been induced with the gene transfer of TH and GCH1 do not possess the appropriate DA regulation mechanisms such as auto-receptors or ability to package and store DA in vesicles for release (Coune et al. 2012; Ford 2014). Therefore, the lack of feedback and storage could cause DA to be continuously released and may saturate D2 receptors, that in turn would be upregulated to effectively manage this influx of DA. In

support of this, long-term administration of D2 antagonists such as antipsychotics have been found to upregulate D2 receptors (Silvestri et al. 2000). Electrophysiology of DA receptors may help to provide an answer as to whether striatal MSNs are dysregulated due to a biscistronic viral vector infusion.

4.5.5 Challenges of L-DOPA administration

One aim of this study was to evaluate pharmacological DA replacement on cognitive function in the LCRT task. L-DOPA administered at 4 doses was found to improve visuospatial function at 4.5mg/kg in AAV-High rats (Figure 4.15.B), whilst subsequently impairing performance on the LCRT in a dose-response manner in Sham rats (Figure 4.15.& Figure 4.16). One suggestion for the improvement seen in AAV-High rats is that the global availability of L-DOPA throughout the striatum after administration is affecting areas of the striatum that support visual processing. Lesions of the dorsomedial striatum have been found to induce impaired spatial processing and may require greater DA replacement to support stimulus response tasks such as the LCRT, however it is unknown what role the medial striatum has in LCRT performance (Lee et al. 2014). Further investigation of the impact of supplying DA to striatal subregions to probe for cognitive function is described in Chapter 5.

One of the complications of L-DOPA administration to the 6-OHDA lesioned rat is the onset of LIDs. This study was designed to use acute administrations of L-DOPA to probe DA-dependant cognitive recovery in the LCRT task, however, the majority of Sham rats developed abnormal movements, and as a result, were impaired in almost all LCRT parameters. The 6-OHDA model is commonly used to create a model of LIDs but these typically develop following chronic adminstration for a few weeks (Westin et al. 2001; Tronci and Francardo 2018). Acute doses have been shown to induce AIMs but generally at higher doses. One hypothesis for the onset of LIDs in this experiment is due to priming. Priming occurs after acute adminstration of DA replacement in a DA depleted environment, in which the first dose 'primes' the environment for subsequent doses and alters behavioural responses accordingly (Di Chiara et al. 1992). The onset of LIDs after acute administration

makes the application of pharmacological L-DOPA on cognitive tasks difficult if the animal can no longer perform the task efficiently.

Due to not expecting the onset of LIDs prior to adminstration, systematic AIMS scoring was not able to be performed, so observations of abnormal movement were based broadly on Breger et al. (2013). In order to confirm the impact of viral-mediated DA biosynthesis on the onset of dyskinesias, further analysis is required. Due to the observation of abnormal involuntary movements during this experiment and the impact this had on LCRT performance in Sham rats, only a single acute dose of 4.5mg/kg was given to mitigate the onset of LIDs in subsequent chapters, which led to systematic video analysis of each animal and individual AIMS scoreing was applied.

One interesting observation was the markedly fewer animals within the AAV-Mid and AAV-High group that presented with L-DOPA induced abnormal movements (Figure 4.17.B-C), and there was reduced severity in these behaviours in the viral vector treated groups. One predicted benefit of gene therapy is the continous supply of DA to prevent its pulsatile release (Calabresi et al. 1993; Nutt et al. 2000; Björklund and Kirik 2009; Jarraya et al. 2009). As indicated by the [18^F]Fallypride data, there was a normalisation of D2/D3 receptors in AAV-High treated rats, to which this normalisation of abberent DA receptor expression after 6-OHDA lesion could be playing a role in the reduced effect of L-DOPA on abnormal movements. Both D2 and D3 receptors have been implicated in the onset of LIDs however the involvement of D2 has been contested within the literature (Visanji et al. 2009; Mela et al. 2010). It is important to note that D1 receptors have also been implicated in the onset of LIDs (Taylor et al. 2005). Future investigations on the interaction between AAV viral vector expression and LID onset using D1 PET ligand for imaging would be beneficial.

4.5.6 Conclusion and future directions

Experiment 2 aimed to use viral mediated DA biosynthesis to probe the impact of a mid and high tire vector on cognitive function using the LCRT task. AAV-Mid did not improve deficits in the 6-OHDA MFB lesioned rat model and AAV-High was found to impair visuospatial function from 7 weeks post-AAV. This chapter suggested a dose response impairment in cognitive function due to DA replacement and also identified factors that could be potentially impacting cognitive function, such as the biodistribution of the vector throughout the striatum

and off-target expression in non-striatal regions. With the knowledge gained from this chapter, modifications were made to appropriately target the whole striatal nuclei with another biscistronic TH and GCH1 AAV to probe for cognitive function on the LCRT task.

4.6 Introduction: Experiment 3

Experiment 3 highlighted important factors that may impact the effectiveness of viral-mediated DA synthesis in alleviating cognitive impairments in the LCRT task. One hypothesis for these findings is that low biodistribution of the AAV-htTH-hGCH1 did not provide sufficient or well-distributed DA biosynthesis within the appropriate striatal nuclei. Another hypothesis is that off-target expression within the piriform cortex led to dysfunctional signalling due to overload of DA in an area that requires a fine-tuned balance of DA release. Thus, in Experiment 3, it was important to address the impact of a more even biodistribution of DA when confined to the striatum, on cognitive function in the LCRT task.

4.6.1 Would greater biodistribution improve LCRT performance?

The rationale for greater biodistribution of the vector having a different outcome than in Experiment 2 is the role of the striatum in cognitive processing. As detailed in Chapter 1 (see 1.2), the striatum is the main relay target of the basal ganglia and has been implicated in a number of cognitive processes that have been implicated in DA loss and varying degrees of success with DA replacement. These cognitive processes include goal-directed behaviour (Farrell et al. 2022), habit formation (Balleine and O'Doherty 2010), attentional set shifting (Lewis et al. 2005; Moustafa et al. 2008) and action selection (Schultz et al. 1989; Matsumoto et al. 1999; Frank 2005; Mark et al. 2006). Depletion of the nigrostriatal pathway in the unilateral 6-OHDA model shown in Experiment 4 and within the literature has shown a significant impairment on visuospatial processing, incentive motivation, attentional deficits and motor readiness in the LCRT task (Döbrössy and Dunnett 1997; Heuer et al. 2013c; Lindgren et al. 2014b). Successful lesions result in complete unilateral loss of DA innervation in the striatal nucleus. Whole striatal nucleus lesions have resulted in non-motor impairments in the forced swim test and anxiety-like phenotype in the open field test (Mendes-Pinheiro et al. 2021).

It is unknown which region(s) of the striatum are directly driving behaviour on the LCRT task, but due to the global loss of DA within the structure, it seems reasonable that more even

biodistribution of the viral vector would improve the likelihood of being sensitive to any beneficial effects of the gene therapy on LCRT performance.

Despite the onset of abnormal involuntary movements present in Experiment 2, it was important to use L-DOPA again to confirm whether L-DOPA has different impacts in the Sham and treated cohorts. We chose to use 4.5mg/kg L-DOPA as this was the dose with the greatest impact in the Sham and AAV-High groups.

4.6.2 Experiment 3 Aim

As detailed above, even DA biodistribution throughout the striatum is likely to be beneficial for both cognitive and motor function. Therefore, it is reasonable to hypothesise that better biodistribution of the viral vector within the striatal nucleus would support recovery on the LCRT task.

The aim of this chapter was as follows:

1. ***To evaluate whether more even biodistribution of the vector within the striatum, and reduced off-target expression would improve cognitive impairments in the LCRT task***. Lister-hooded rats received a unilateral 6-OHDA MFB lesion prior to an intra-striatal infusion of AAV-tTH-hGCH1 (with surgical modifications made from Experiment 2) and periodically assessed on motor and the LCRT task 4,6, and 8 weeks post-AAV infusion. It was hypothesised that greater biodistribution of the viral vector to the striatal nucleus and limited off-target expression would therefore lead to more effective DA biosynthesis. It was further hypothesised that this would in turn lead to an improvement in motor behaviour on adjusting stepping task, vibrissae-evoked task, and improve visuospatial function and incentive motivation on the LCRT task.

4.7 Methods: Experiment 3

4.7.1 Experimental design

Female Lister-hooded rats ($n = 19$) were acclimatised to the animal house for one week prior to being placed on food restriction. Animals were trained on the LCRT task for 7 weeks. 2 rats were removed from the experiment due to not being able to efficiently learn the task. Subsequently, all rats received a unilateral 6-OHDA MFB lesion to create the PD rat model. After 3 weeks post-lesion, rats were placed back on food restriction and underwent testing again on the LCRT task, amphetamine-induced rotations, adjusting stepping task and vibrissae-evoked sensorimotor task to identify lesion-induced deficits. Animals were sorted into two groups based on their response accuracy: Sham ($n=7$) and AAV-htTH-hGCH1 ($n=10$). Animals in the AAV treated group received an intra-striatal infusion of AAV-htTH-hGCH1 with coordinates designed for improved biodistribution relative to Experiment 2 (Figure 4.21). The other group of rats underwent a sham surgery. A total of 3 rats did not recover from surgery in the AAV-htTH-hGCH1 group and 1 Sham was culled due to health concerns 1-week post-surgery.

All rats were tested periodically at 4, 6, and 8 weeks post-AAV on all the previous tasks to identify any motor or cognitive improvement over time. At 5 weeks, rats underwent a two-day L-DOPA challenge (detailed in methods of Experiment 2) in which they received subcut. saline or 4.5mg/kg of L-DOPA and were tested on the adjusting stepping task 30 minutes after administration, and the LCRT task after 40 minutes. Rats were filmed from the point of drug administration to starting the LCRT task to observe any potential abnormal movements induced by L-DOPA. Rats were perfused at 9 weeks post-AAV and brain tissue was processed for histological analysis. A total of 2 rats were excluded from AAV-htTH-hGCH1 analysis; one rat was excluded due to a partial lesion confounding behavioural and histological analysis, and another rat due to insufficient AAV expression in the striatum. The final groups analysed throughout this experiment were as follows: Sham (n = 6) and AAV-htTH-hGCH1 (n = 5).

Group	n = 19													n = 17											Sham n = 6 AAV-htTH-hGCH1 n = 5
Weeks	-13	-12	-11	-10	-9	-8	-7	-6	-5	-4	-3	-2	-1	0	+1	+2	+3	+4	+5	+6	+7	+8	+9
Task		LCRT training						MFB lesion			LCRT Hand-testing	Amphet-induced rotations		AAV infusion				LCRT Hand-testing	L-DOPA Challenge	LCRT Hand-testing		LCRT Hand-testing	Perfuse

Figure 4.19. Experimental design for Experiment 3. Animals were trained on the LCRT task for 7 weeks prior to receiving a unilateral 6-OHDA lesion. Animals were tested at 3- and 4-weeks post-lesion for behavioural deficits. Rats subsequently received a unilateral infusion of AAV-htTH-hGCH1 or a sham infusion. Rats were periodically tested on behavioural tasks up to 8 weeks post-AAV and was perfused at 9 weeks for histological analysis. Hand-testing (adjusting step task and vibrissae-evoked paw task).

4.7.2 Viral vector

The biscistronic vector used in Experiment 3 was constructed in the same manner as in Experiment 2 with two human transgenes: tTH and GCH1, but in this instance is separated by the IRES linker EMCV.
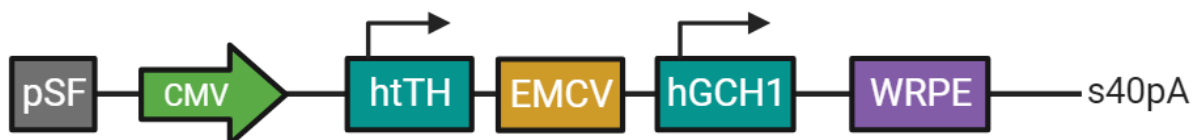
Figure 4.20. Schematic of AAV-htTH-hGCH1.

4.7.3 Surgical procedure

Rats in the treatment group received a unilateral intra-striatal infusion of AAV-htTH-hGCH1 at a titre of 1.45×10^{13}. The viral vector was infused using a cannula system as described for 6-OHDA MFB lesions previously. Each animal received 6.5 µl, infused at a rate of 0.4µl/min of viral product across three sites and two depths for each site. For Site 1 and 2, 1.25 µl was deposited at DV1 and 1 µl at DV2. For Site 3, 1 µl was deposited at each depth. 1 minute of diffusion time was implemented in between each depth and 3 minutes of diffusion time before retracting the cannula.

	AP	ML	DV1	DV2
Site 1	+0.6	-3.6	-5	-4
Site 2	+1.2	-2.8	-4.5	-3.5
Site 3	+1.2	-2.2	-4.5	-3.5

Figure 4.21. Surgical coordinates used for AAV-htTH-hGCH1 infusion. Representative images of the

locations of each injection site and the depth. AP = Anterior-Posterior axis, ML = Medial-Lateral axis, DV = Dorsal-Ventral axis

4.7.4 LCRT program

Animals were trained on the LCRT task for 7 weeks on the protocol detailed in Table 6. Post-lesion, animals were tested on the short version of the task with 200ms stimulus duration and 100-400ms random limited hold and were not tested on the modified version presented in chapter 4 due to a reasonable number of useable trials and accuracy post-lesion. Post-lesion data and week 6 average was calculated over 3 days. Average performance for week 4 and week 8 was calculated over 5 days.

4.7.5 AIMS scoring

From administration of 4.5mg/kg subcut. injection, rats were filmed immediately after and continuously for 40 minutes prior to being placed in the operant box to observe any potential dyskinetic behaviours. During this time, at the peak of L-DOPA onset (30 minutes), rats were AIM scored using the detailed scaling in Breger et al. (2013) for 5 minutes to determine the amplitude and duration of 7 subtypes of behaviours. The behaviours and corresponding amplitude scores were: **neck dystonia** (0.5 = mild head tilt, 1 = mild displacement of head posture but returns to neutral, 1.5 = mix of mild and moderate posture, 2 = displacement more than 45 degrees with no return to normal position, 2.5 = mix of moderate and severe posture, 3 = severe torsion of neck musculature), **trunk distortion** (1 = less than 45 degrees between upper and lower torso, 1.5 mix of mild and moderate dystonia, 2 = dystonia greater than 45 degrees with some loss of balance when ambulating, 2.5 = mix of moderate and severe dystonia, 3 = severe dystonia, animal completely twisted or unable to ambulate), **forelimb dyskinesia** (1 = abnormal posturing of limb with return to neutral position, 2 = mix of mild and severe extension of the hind-limb, 3 = limb severely hyper extended in abnormal position), **hindlimb dystonia** (1 = small amplitude side to side, up and down wiping, 2 = same as 1 plus downward hyperextension greater than 50%, 3 = severe downward hyperextension, pulls opposite of neck), **orolingual** (1 = chewing, 2 = chewing plus tongue protrusions and/or open mouth chewing), **head bobbing** (1 = small amplitude, 2 = large amplitude), **forelimb-facial stereotypy** (1 = if present). The amplitude score for each

subtype of behaviour is multiplied by a duration score (0 = none, 1 = less than 50% of the observation, 2 = more than 50% of the observation, 3 = continuous), resulting in the final AIMS score. The AIMS score for each animal is out of a maximum of 51. Data is presented as the amplitude and duration for each animal displaying dyskinetic behaviour, and the final resulting AIMS score.

4.7.6 Baseline change modification of analysing LCRT performance

Due to groups not being matched at baseline in some measures, a subset of data from the LCRT task, (those that were not matched at baseline and have a significant interaction or effect between groups), was normalised to their own baseline, in order to understand if there was actual improvement (or worsening) of LCRT measures over the course of 8 weeks post-AAV. Data is presented as the percentage change from baseline and was calculated by change from baseline = (post-AAV at **X** week/ baseline) x 100. Statistics was carried out as mentioned below.

4.7.7 Statistics

Statistical analysis was undertaken using a one-way ANOVA with Group (Sham, AAV-htTH-hGCH1) and Week (Pre-AAV, 4,6,8 or 9) as the factor. During the 4.5mg/kg L-DOPA test, a one-way ANOVA with repeated measures was used with Drug (Saline, L-DOPA) and Group as a factor. A number of animals during the L-DOPA challenge did not perform the task, creating too many missing variables to feel confident in the data when using linear interpolation, so only the data that did not require missing values was included. Graphical data is presented as group mean and error bars determined by standard error of the mean (SEM).

4.8 Results: Experiment 3
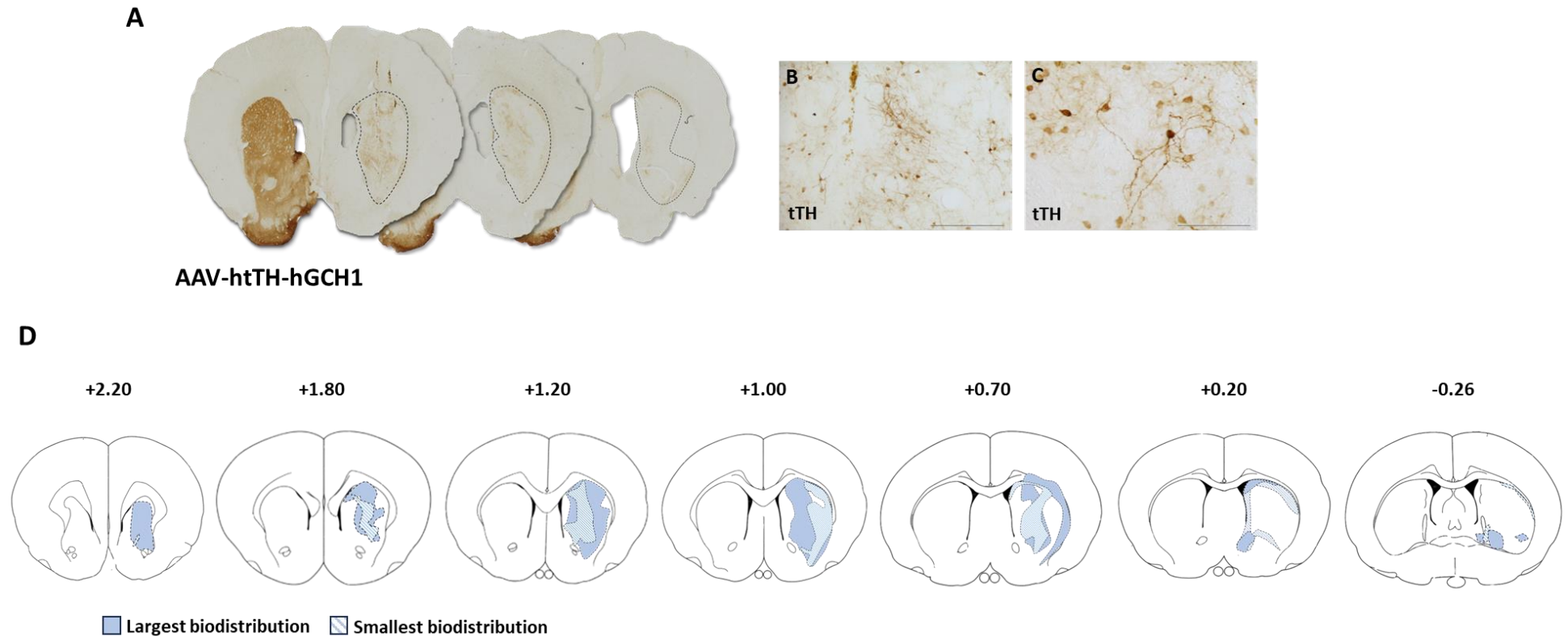
*Figure 4.22. Histological characterisation of tTH expression induced by AAV-tTH-hGCH1.**A-C)** Expression of the viral vector was restricted to the striatum with very minimal evidence of off target tTH expression. **D)** Expression of the viral vector in the largest and smallest biodistribution indicated the majority of the tTH expression was in the rostral striatum.*

4.8.1 Modified surgical coordinates improved biodistribution of viral vector

In Experiment 2, histological analysis of htTH-2A-hGCH1 expression highlighted off-target expression into the surrounding piriform cortex. Here, modifying the surgical coordinates led to better biodistribution of AAV-htTH-hGCH1 across the striatum and minimal off-target expression in the cortex (Figure 4.22.A-C). Expression of AAV-htTH-hGCH1, using tTH as a marker, shows mostly transfection of striatal neurons with high detail of axonal projections. Expression of AAV-htTH-hGCH1 was also greater in the rostral striatum compared to the biodistribution seen in Experiment 2 mostly in the caudal parts of the striatum. Average earliest rostral position across AAV-htTH-hGCH1 is +2.3AP from bregma (Earliest seen is +2.7AP) Average latest caudal position is -0.3AP (latest seen is -0.5). In order to understand the level of biodistribution between the groups, a characterisation of the smallest and largest tTH biodistribution was carried out and indicated an even biodistribution of tTH expression in the rostral striatum that dissipated to only be expressed at the striatal edge in the caudal sections (Figure 4.22 D).
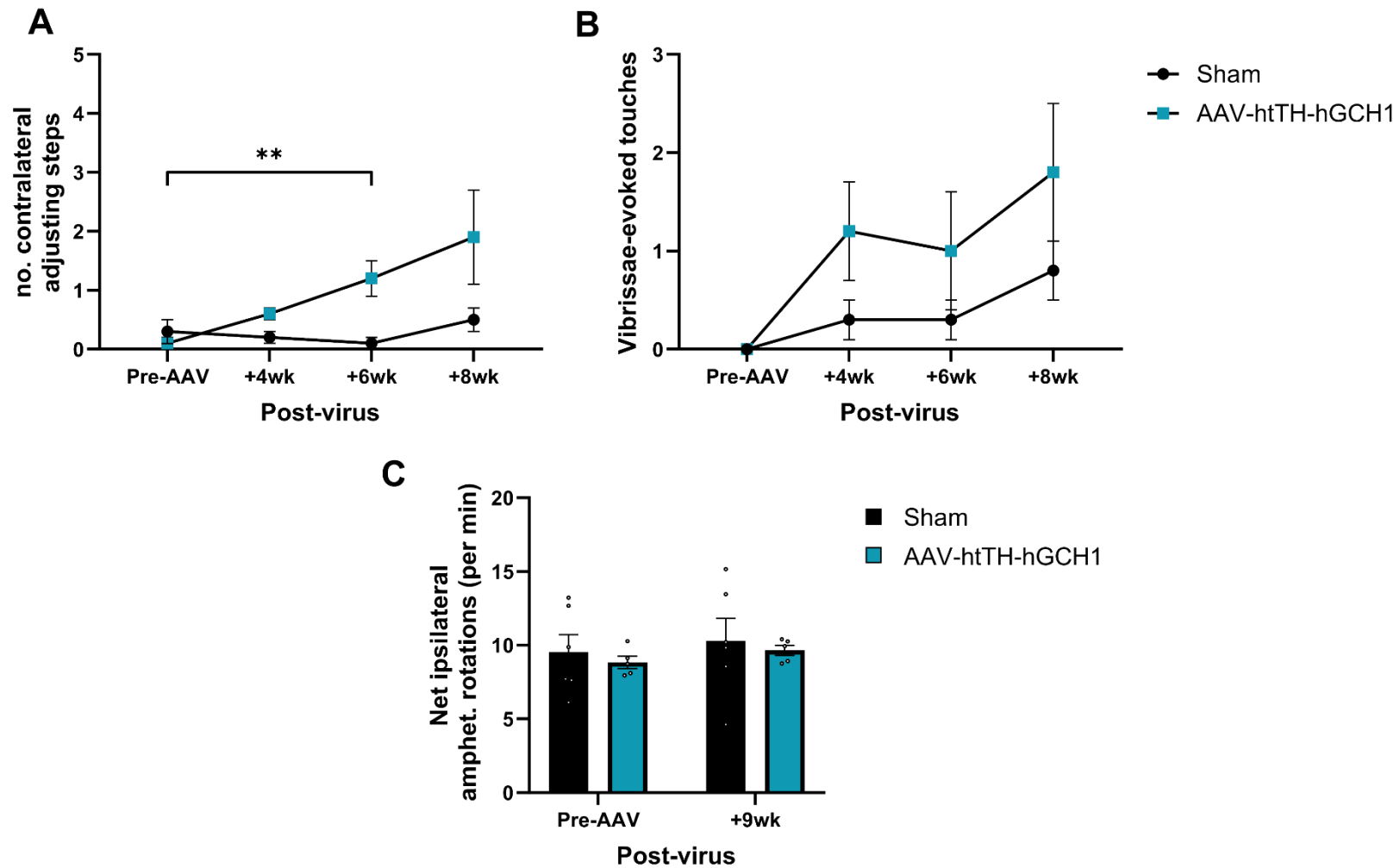
*Figure 4.23. Modifying coordinates using AAV-htTH-hGCH1 displays some motor improvement. **A)** Contralateral adjusting steps was significantly improved from baseline at 6 week's post-AAV infusion. **B)** Vibrissae-evoked paw touches was improved. **C)** Rotational bias was not reduced due to AAV-htTH-hGCH1 viral infusion after 9 weeks post-AAV. Error bars represent standard error of the mean. Significant differences between the two groups are indicated as ** p <.01.*

4.8.2 Full striatal biodistribution of AAV-htTH-hGHC1 improved adjusting steps

Contralateral adjusting steps are significantly improved from baseline after 4 and 6 weeks post-AAV infusion and had a greater number of adjusting steps at 6 weeks compared to sham (Figure 4.23.A. Week*group; $F_{(3,27)} = 3.452$, $p = .03$. Sham vs AAV-htTH-hGCH1 at +6wks, $p = .007$). However, vibrissae-evoked touches did not improve across weeks (Figure 4.23.B. Week*group; ($F_{(3,27)} = .915$, $p =$ n.s, Group; $F_{(1,9)} = 3.230$, $p =$ n.s) and ipsilateral rotational bias remained similar to sham 9 weeks post-AAV infusion (Figure 4.23.C. Group: $F_{(1,9)} = 0.222$, $p =$ n.s)
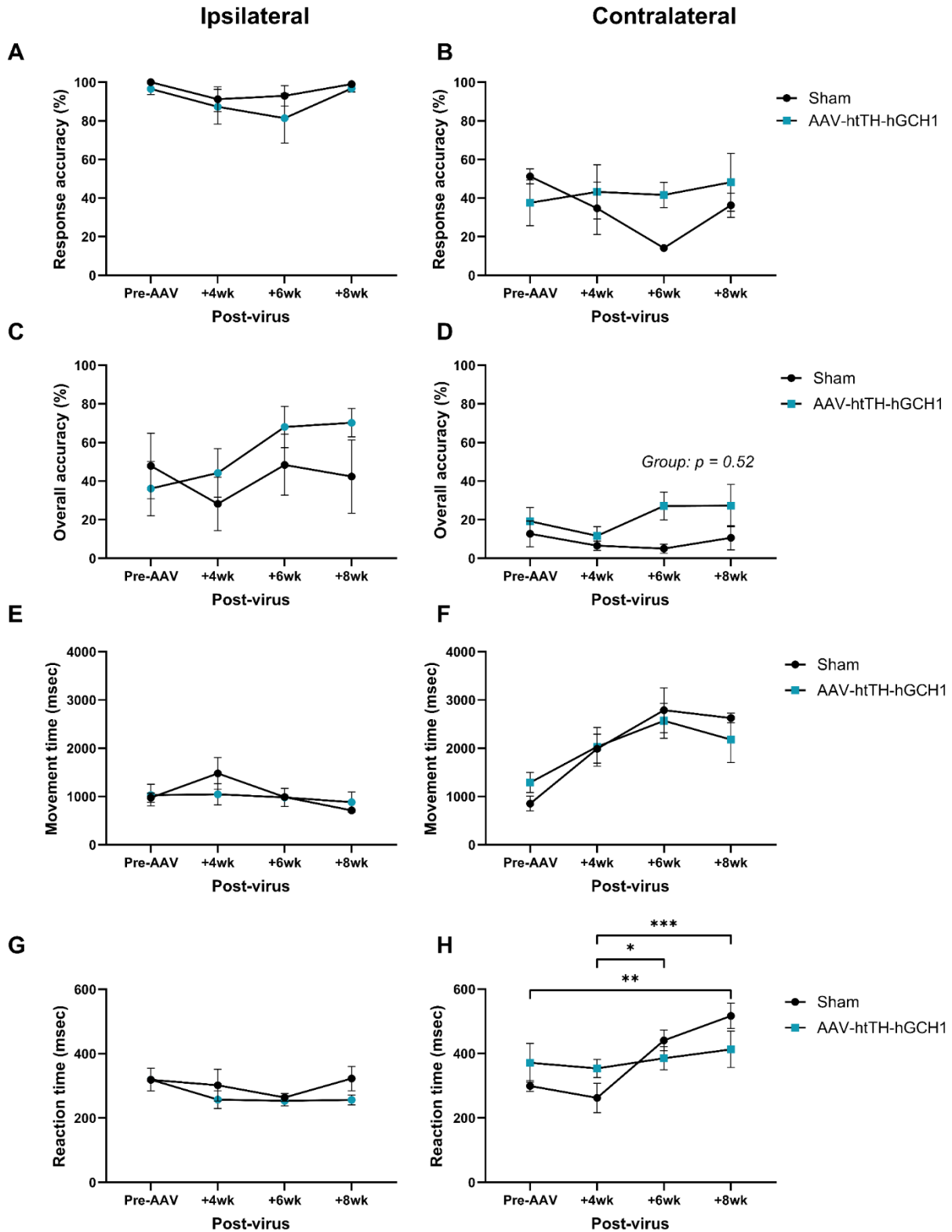
*Figure 4.24. Modifying coordinates utilising AAV-htTH-hGCH1 shows a trend for improvement in LCRT performance. No differences between groups were observed on the ipsilateral side (A,C,E,G). B) AAV-htTH-hGCH1 did not improve response accuracy, D) however AAV-htTH-hGCH1 did lead to a trend in improving overall accuracy. F) No difference in movement time amongst groups. H) Sham animals got significantly slower at completing the task over 8-week post-AAVI infusion. Error bars represent standard error of the mean. Significant differences between groups are indicated as *p = <.05, ** p = <.01, *** p = <.001).*

4.8.3 Improved biodistribution has positive impact on LCRT performance

Improved AAV-hTH-hGCH1 biodistribution lead to improvement in response accuracy on LCRT task

AAV-htTH-hGCH1 infusion with modified surgical coordinates resulted in a different pattern of results to those reported in Experiment 2. LCRT performance on the contralateral side indicated no improvement in response accuracy compared to sham (Figure 4.24.B. Group; $F(1,9) = .624$, p = n.s), however, due to the mis-matched baseline pre-AAV, contralateral response accuracy was calculated as percentage change from baseline to normalise the data. Contralateral response accuracy was overall higher in AAV-htTH-hGCH1 treated rats compared to sham, and significantly better accuracy was achieved at 6 weeks post-AAV (Figure 4.26.A Week*Group: $F(3,27) = 3.416$, $p = .031$. +6wk AAV vs Sham $p = .011$. Group = 1,9 = 7.815, $p = .021$). In relation to overall accuracy, there was a trend towards AAV-htTH-hGCH1 treated rats improving performance (Figure 4.24.D. Group; $F(1,9) = 4.985$, p = .052).

All groups increased their movement time over the 8 weeks of testing (Figure 4.24.F. Week; $F(3,27) = 16.129$, $p = <.001$). Reaction time remained stable for AAV-htTH-hGCH1 treated rats across the 8 weeks, however reaction time for shams significantly slowed across weeks (Figure 4.24.H. Group*week; ($F(3,27) = 3.683$, $p = .024$). When movement time was analysed as change from baseline, the pattern was still present but with no effect of week (Figure 4.26.B. Week*Group; $F(3,27) = 3.742$, $p = .023$. Group 1,9 = 7.078, p = .026. Lesion baseline vs 4wk $p = .014$, baseline vs 6wk $p = .010$ baseline vs 8wk <.001).

LCRT performance on the ipsilateral side did not differ with AAV-htTH-hGCH1 viral infusion compared to sham (Figure 4.24.(A) Response accuracy; $F(1,9) = 2.106$, p = n.s, (C) Overall accuracy; $F(1,9) = .493$, p = n.s. (E) Movement time; $F(1,9) = .107$, p = n.s, (G) Reaction time; $F(1,9) = 2.106$, p = n.s).
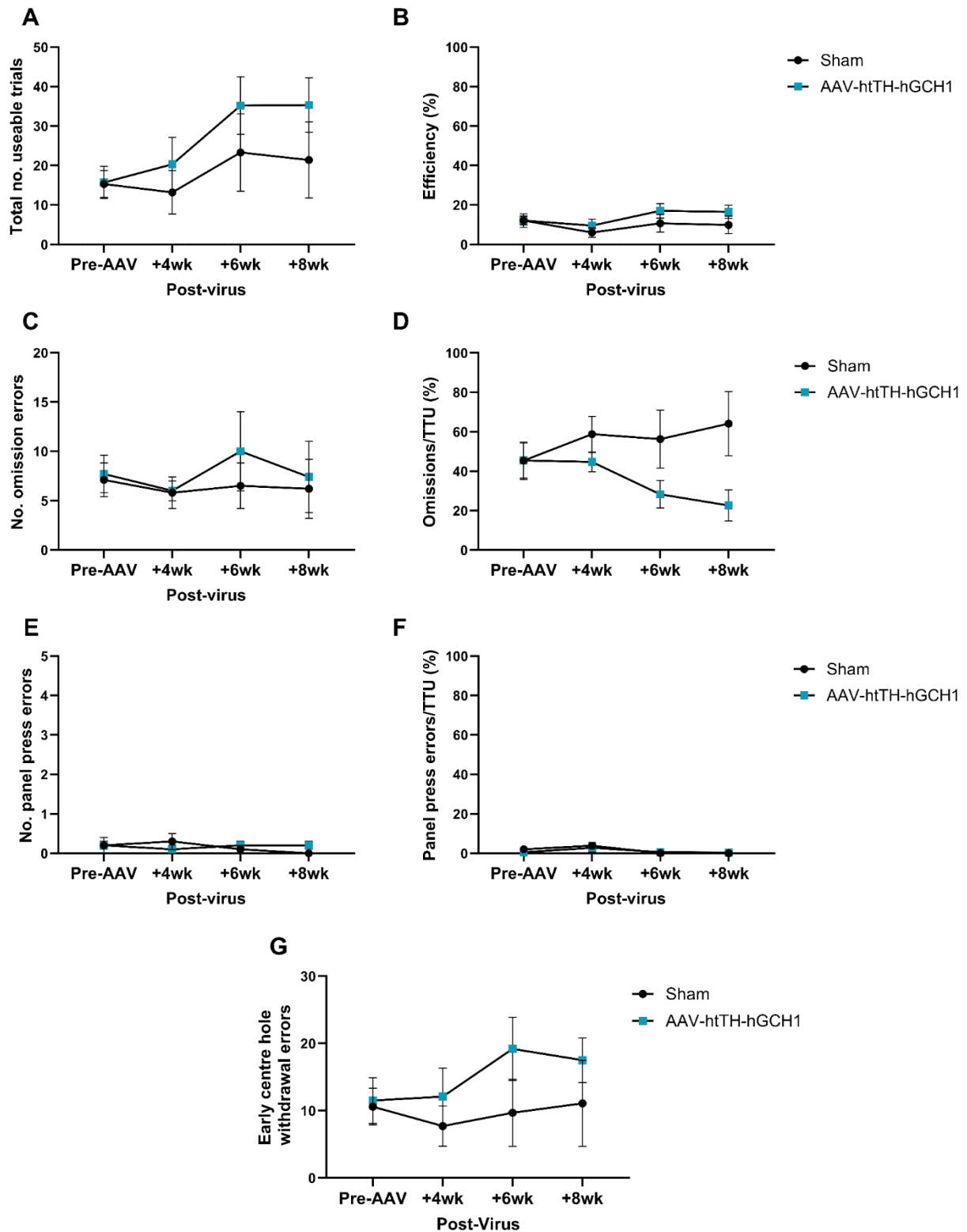
*Figure 4.25. Effect of AAV-htTH-hGCH1 on non-side bias performance on LCRT. **A)** Total usable trials. **B)** efficiency, **C)** omission errors **(D)** omission errors/TTU **(E)** Panel press errors **(F)** panel press errors/TTU and **(G)** early centre hole withdrawal errors were not significantly altered by AAV-htTH-hGCH1 compared to cham across 8 weeks of testing. Error bars represent standard error of the mean.*
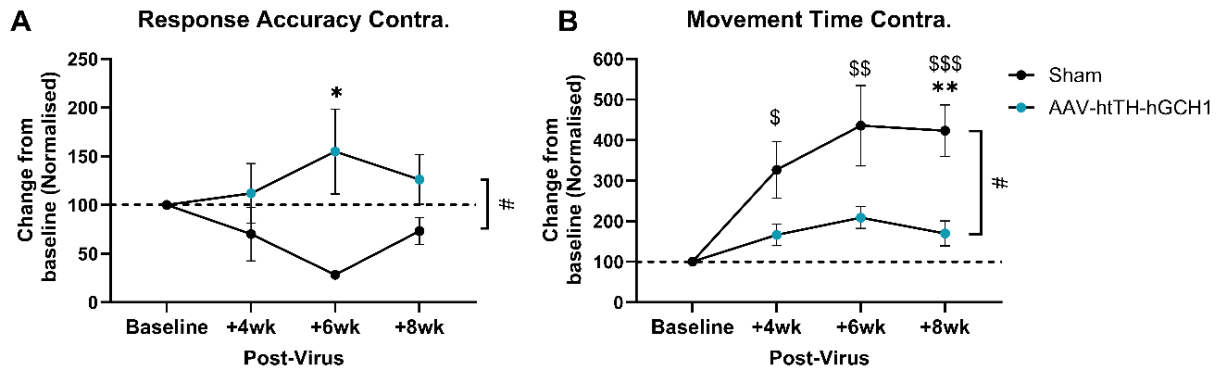
Figure 4.26. Normalisation of mis-matched baseline during LCRT performance. **A)** *Contralateral response accuracy was improved by AAV-htTH-hGCH1 infusion.* **B)** *Contralateral movement time is significantly increased in Sham animals compared to AAV treated rats. Error bars represent standard error of the mean. Vertical line at 100 indicates baseline. Main effect of group is indicated as #p <.05. Significant difference to baseline in sham are indicated as $p <.05, $$p <.01, $$$p <.001. Significant differences between AAV-htTH-hGCH1 and Sham are indicated as *p <.05, **p<.01.*

4.8.4 No impact of biodistribution on non-lateralised aspects of LCRT

Total usable trials increased over the testing weeks (Figure 4.25.A. Week; $F(3,27) = 5.212$, $p = .006$) but AAV-htTH-hGCH1 did not perform significantly more usable trials compared to shams ($F(1,9) = .961$, p = n.s) nor were they more efficient at performing the task (Figure 4.25.B. Group; $F(1,9) = .292$, p = n.s). Any errors were not significantly different amongst groups (Figure 4.25. C) Omission errors; $F(1,9) = .292$, p = n.s, (D) Omissions/TTU; $F(1,9) = 2.797$, $p = .076$ (E) Panel press errors; $F(2,14) = .015$, p = n.s. (F) Pannel press/TTU $F(1,9) = .250$, p = n.s. (G) Centre hole withdrawal errors; $F(1,9) = 1.077$, p = n.s).
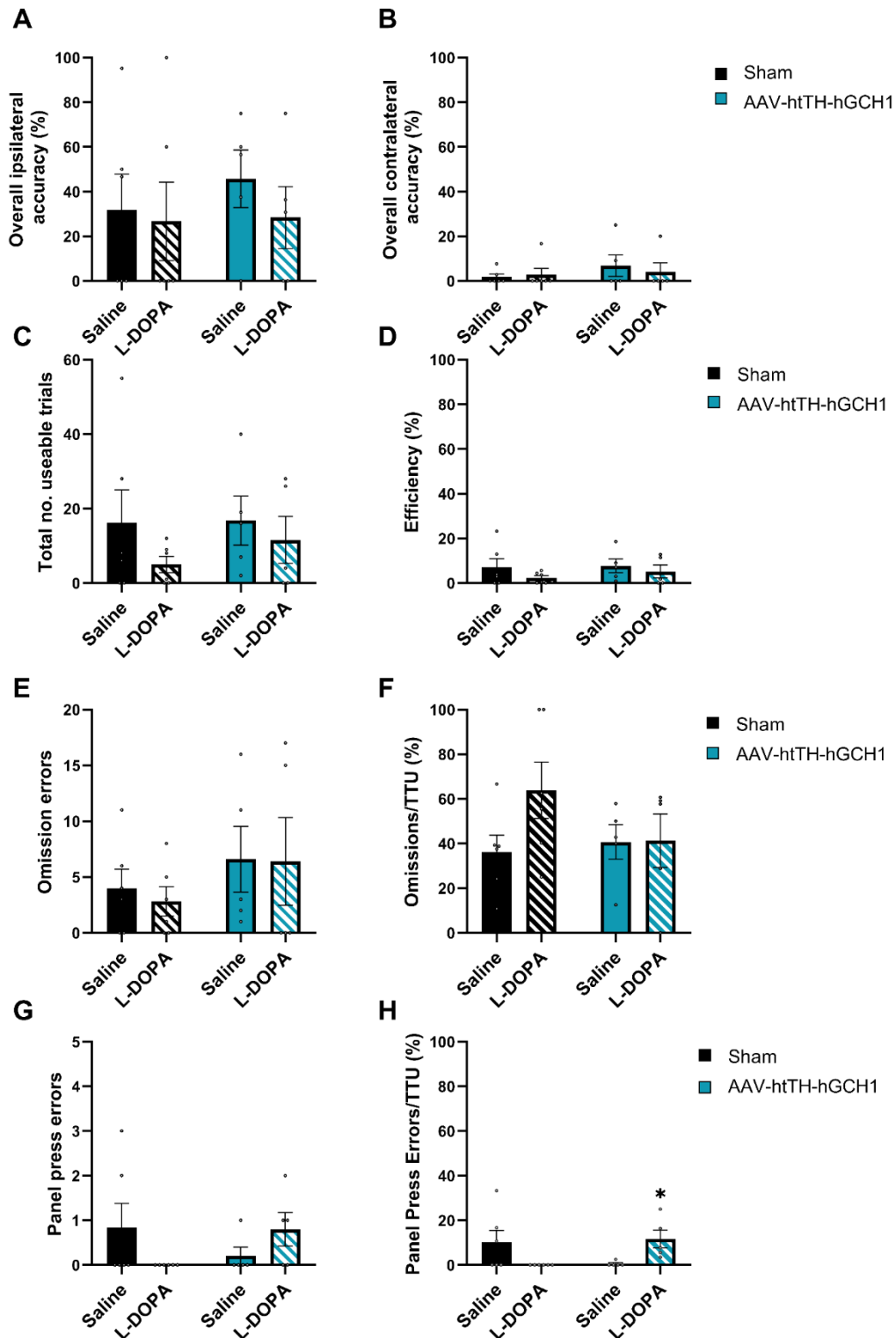
*Figure 4.27. Effect of 4.5mg/kg L-DOPA on Sham and AAV-htTH-hGCH1 treated rats 5 weeks post-AAV infusion. **A)** Ipsilateral overall accuracy, **B)** Contralateral overall accuracy, **C)** Total usable trials, **D)** Efficiency **E)** Omissions **F)** Omissions/TTU and **G)** Panel press errors did not differ between Sham and AAV-htTH-hGHC1 and what not impacted by L-DOPA. **H)** Panel press errors as a percentage of TTU is significantly higher in AAV-htTH-hGHC1 when given L-DOPA. Error bars represent standard error of the mean. Significant difference is indicated as p <.05.*
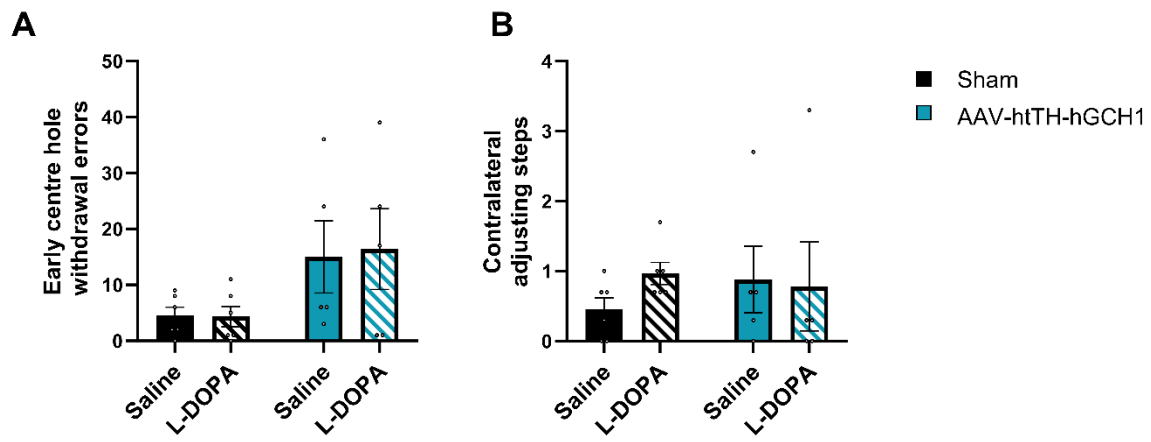
*Figure 4.28. No effect of 4.5mg/kg L-DOPA on Sham and AAV-htTH-hGCH1 treated rats 5 weeks post-AAV infusion on **A)** Centre hole withdrawal and **B)** contralateral adjusting steps. Error bars represent standard error of the mean.*

4.8.5 L-DOPA did not impact LCRT performance or motor behaviour 5 weeks post-AAV

L-DOPA was administered to sham and AAV-htTH-hGCH1-treated rats at 5 weeks post-AAV infusion. Overall accuracy on the ipsilateral side did not differ among groups (Figure 4.27.A. Drug; $F_{(1,9)}$ = .689, p = n.s, Group; $F_{(1,9)}$ = .199, p = n.s), and neither did overall accuracy on the contralateral side (Figure 4.27.B. Drug; ($F_{(1,9)}$ = .057, p = n.s, Group; ($F_{(1,9)}$ = 1.296, p = n.s). Any other non-side bias LCRT parameters were not affected by L-DOPA administration, and AAV-htTH-hGCH1 treated rats were not significantly different to Sham (Figure 4.27.(C) Total useable trials: Drug; $F_{(1,9)}$ = 1.726, p = n.s, Group; $F_{(2,14)}$ = .229, p = n.s. (D) Efficiency: Drug; $F_{(1,9)}$ = 1.771, p = n.s, Group; $F_{(1,9)}$ = .328, p = n.s. (E) Omission errors: Drug; $F_{(1,9)}$ = .116, p = n.s, Group $F_{(1,9)}$ = 1.105, p = n.s. (F) Omissions/TTU: Drug $F_{(1,9)}$ = 4.098, p = n.s. (G) Panel press errors: Drug; $F_{(1,9)}$ = .133, p = n.s, Group; $F_{(1,9)}$ = .046, p = n.s. (H). Panel press/TTU Drug*week: $F_{(1,9)}$ = 9.015, p = .015. Sham vs AAV-htTH-hGCH1 at L-DOPA p = .010). Figure 4.28.A. Drug; $F_{(1,9)}$ = .027, p = n.s, Group; $F_{(1,9)}$ = 4.671, p = .059. (B) Contralateral adjusting steps $F_{(1,9)}$ = 1.947, p = n.s, Group; $F_{(1,9)}$ = .056, p = n.s).

4.8.6 No observed LIDs in AAV-htTH-hGCH1 treated rats

All rats were observed 0-40 minutes after L-DOPA administration to observe and AIMS score the onset of LIDs. One rat with AAV-htTH-hGCH1 infusion displayed some increased contralateral turning 30 minutes after L-DOPA administration but did not present with any behaviours to qualify AIMS scoring. One Sham rat presented with severe LIDs, however due to two experiments having the same Sham group, the AIMS score data will be presented in Chapter 5, Experiment 5.

4.9 Discussion: Experiment 3

The aim of Experiment 3 was to evaluate whether more even biodistribution of viral-mediated biosynthesis would lead to improvements in motor and cognitive impairments in a PD rat model. Histological analysis indicated greater distribution of tTH expression within the striatal nuclei, with predominantly more immunostaining in the rostral part of the striatum. AAV-htTH-hGCH1 treated rats had improved contralateral response accuracy at 6 weeks post-AAV and a subtle improvement in adjusting steps. The data in this experiment indicates that viral-mediated DA biosynthesis within the striatum can support visuospatial processing. This discussion will evaluate the differences between experiment 2 and 3 on factors that could be responsible for visuospatial recovery.

4.9.1 Differences in biodistribution throughout the striatum

Histological analysis of tTH expression in Experiment 2, as shown in Figure 4.8, indicated limited biodistribution throughout the striatum, with a large collection of gene transfer occurring in the piriform cortex. In Experiment 3, biodistribution throughout the entire rostral-caudal plane was still limited, however there appeared to be significant coverage of the striatum within the rostral part of the striatum compared to what was evident in Experiment 2. This difference in rostral vs caudal expression between the two experiments may be an important factor for cognitive recovery, suggesting that placement of the viral vector may have a role here. Vogelsang and D'Esposito (2018) highlighted in detail the difference between the rostral and caudal striatum in terms of striatal-cortical loops and the impact this could have on behaviour. In addition, Valjent and Gangarossa (2021) found the tail end of the striatum to be sensitive to DA transmission. In order to understand the true extent of difference in the rostral-caudal divide between Experiment 2 and Experiment 3 full stereological analysis should be undertaken.

4.9.2 Improved visuospatial function due to AAV-htTH-hGCH1, but not other LCRT parameters

The improvement in visuospatial function in AAV-htTH-hGCH1 treated rats supports the hypothesis that improved biodistribution might support cognitive recovery (Figure 4.24.B). However, it is important to note that overall, there was a group effect, and the improvement was only present at 6 weeks, suggesting the improvement may be transient. In addition, this study is very under-powered with only 5 animals in the AAV-htTH-hGCH1 group. A replication of this experiment with a larger cohort would be important in order to ensure the robustness of these findings.

AAV-htTH-hGCH1 infusion did not lead to an improvement in total useable trials (Figure 4.25.A) which is associated with the rats' incentive motivation to perform the task (Olney et al. 2018). Total useable trials were also not increased by hfVM grafts or hESC-derived DA grafts in experiment 1, but were alleviated by hfVM in (Lelos et al. 2016).

4.9.3 The impact of acute L-DOPA on LCRT performance

As shown in Figure 4.27, the acute L-DOPA challenge was confounded by very low response rate in both AAV-hTH-2A-hGCH1 and Sham rats. Only one rat in each cohort was able to initiate a contralateral response under L-DOPA administration (Figure 4.27.B). Also, overall accuracy in AAV-htTH-hGCH1 dropped to about 10% with the same rate of efficiency (Figure 4.27.C). The number of omissions/TTU is approximately 40% on the task indicating a high number of useable trials did not result in any lateralised nose pokes (Figure 4.27.H). Interestingly, the L-DOPA challenge was carried out at 5 weeks, yet at 6 weeks, AAV-htTH-hGCH1 treated rats were found to have improved visuospatial function, indicating that this diminished performance in the LCRT task during an L-DOPA challenge did not persist or decline over the testing weeks.

4.9.4 Is the level of gene transfer sub-optimal for motor recovery?

At stated in the Chapter 4 introduction (see 4.2), AAV-hTH-2A-hGCH1 works on the premise that AADC is produced in spared 5-HTergic and DA terminals to be available in the host striatum in order to produce DA. Serotonergic neurons are also affected by the 6-OHDA MFB lesion so this may not be the best model to apply this gene therapy (Björklund and Kirik 2009). As found in patients, AADC expression levels are diminished and specific AADC deficiency can result in chronic dystonia and motor impairments (Swoboda et al. 2003). To counter this, AADC was present in the 6-OHDA lesioned animal, indicating that AADC is still present in the host striatum, which should allow viral-mediated DA biosynthesis to occur. However, it must be acknowledged that AADC staining was not conducted in this experiment, nor were midbrain counts to quantity the extent of SNc and VTA loss completed in time for submission. To rectify this, it would be important to analyse the expression levels of AADC on an animal-to-animal basis and evaluate whether AADC availability correlates to improvement of cognitive function. Nevertheless, there was visible expression of tTH in the striatum within transfected neurons, improvement in response accuracy and a mild improvement in adjusting steps, indicated some efficacy of the gene therapy.

4.10 Chapter Discussion

Chapter 4 detailed the use of a biscistronic viral vector to manipulate dose and biodistribution of DA release as factors that could impact cognitive function on the LCRT task. Experiment 2 identified that higher titres of the viral vector may be beneficial for motor recovery but can negatively impact visuospatial function. Experiment 3 found better biodistribution of DA across the striatal nucleus can be supportive of cognitive recovery and sufficient to lead to marginal alleviation of forelimb akinesia.

The importance of this chapter is that it highlights the complexity of using DA to alleviate motor and cognitive function and indicates that variation in application of gene therapy can impact behavioural recovery. Chapter 5 will aim to develop understanding of this further by evaluating the impact of placement of the viral vector in medial versus lateral subregions of the striatum, effectively targeting different basal ganglia circuit loops.

Chapter 5 : Evaluating the contribution of striatal subregions to cognitive function in the LCRT task.

5.1 Summary

Chapter 4 highlighted (1) biodistribution of DA across the striatal architecture could support viral-mediated cognitive recovery, and (2) off-target expression in external cortical regions such as the piriform cortex could contribute to worse performance on the LCRT task. This led to the question of how viral-mediated DA biosynthesis was affecting distinct subregions of the striatum. Thus, Chapter 5: Experiment 4 aimed firstly to evaluate in more detail how the two main circuits supplying DA to the striatum (SNc to lateral striatum and VTA to medial/ventral striatum) support performance in the LCRT task. 6-OHDA was unilaterally infused into the medial or lateral striatum and rats were tested on the LCRT task, adjusting step task and L-DOPA challenge up to 4 weeks post-toxin infusion. Rats with a lateral 6-OHDA infusion developed forelimb akinesia, without impaired performance on the LCRT task. Rats with a medial 6-OHDA displayed no forelimb akinesia, but after 4 weeks had reduced accuracy and impaired incentive motivation on the LCRT task. Subsequently, Chapter 5: Experiment 5 explored how targeting viral-mediated DA biosynthesis in each of those subregions supported recovery of function on the LCRT task. Both medial and lateral AAV infusion improved motor function, whilst only AAV administered laterally improved visuospatial function on the LCRT task. This data was contrary to our hypothesis that medial infusions would support cognitive recovery, and raises questions for targeted dopamine therapy in PD.

5.2 Introduction

In Chapter 4: Experiment 2, AAV-hTH-2A-hGCH1 infused into the striatum improved forelimb akinesia and sensorimotor deficits at 7-weeks post-lesion, whilst also worsening visuospatial function and incentive motivation on the LCRT task at a high titre. Histological analysis showed greater expression in the caudal striatum and off-target expression in the piriform cortex. However, when the biodistribution of the viral vector was improved in Chapter 4: Experiment 3, there was a trend for improving visuospatial function whilst also alleviating motor deficits. This is a promising result and indicates that placement of the viral vector, and thus the availability for DA synthesis within the striatum, is an important factor to consider for gene therapy when used as a therapeutic intervention for PD. This also brings into question, what regions of the striatum require DA to sustain cognitive function on the LCRT task.

5.2.1 The importance of analysing region-specific contribution to the LCRT task

The aim of experiment 4 was then to understand the contribution of the two major striatal circuits, SNC to lateral striatum and VTA to medial striatum, on performance in the LCRT task. Within the 6-OHDA model used throughout Chapter 3 and 4; the nigrostriatal pathway is ablated, resulting in over 95% loss of A9 DA neurons within the SNc, approximately 50% of A10 VTA neurons and total loss of DA terminals in the striatum. The near complete loss of striatal DA innervation in the 6-OHDA MFB rat model makes understanding the contribution of each striatal region to deficits present in the LCRT task, difficult to define. There is ample evidence on the importance of DA in visuospatial function and incentive motivation on this operant task (Döbrössy and Dunnett 1997; Heuer et al. 2013c; Lindgren et al. 2014b). However, there is currently no published evidence on the contribution of medial or lateral striatal innervation on the LCRT task.

5.2.2 Topological organisation of the striatum

As detailed in Chapter 1, the striatum is the main input and output target of the basal ganglia, having a vital role in action selection (Bolam et al. 2000). The striatum receives afferent connections from the ventral midbrain (SNc and VTA), motor and prefrontal cortex, as well as the thalamus. The striatum also sends efferent connections to the globus pallidus which provide a feedback loop to cortical areas supporting behaviours such as motor coordination and goal-directed behaviour through the direct and indirect pathway (Gerfen and Surmeier 2011). Although the striatum forms one large structure in the rodent brain, which differs to the separated caudate and putamen in humans, the segregation of function by region within the striatum is still present in rodents.

5.2.3 Dopaminergic projections from the midbrain

As displayed in Figure 5.1, the projections of DAergic neurons from the ventral midbrain nuclei innervate the striatum in a gradient manner, from medial to lateral. The VTA projects mostly to ventro-medial striatum and NAc, and the SNc innervates mostly the dorsolateral striatum (Ikemoto 2007; Haber 2014). The projection profile of the ventral midbrain nuclei also differs along the rostro-caudal axis, with the rostral striatum receiving innervation from the VTA. The SNc directs most of its projections to the central and caudal regions of the striatum. (Menegas et al. 2015; Miyamoto et al. 2019; Basile et al. 2021). Studies using optogenetics and DA neuronal projection mapping have shown even single DA neurons have dense axonal arborisations which can spread over large areas of the striatum and even across hemispheres (Gauthier et al. 1999; Prensa and Parent 2001; Matsuda et al. 2009; Fox et al. 2016). The supply of DA provided to the striatum through the A9 and A10 DA neurons from the SNc and VTA respectively, supports a range of cognitive processing and behavioural output, which is suggested in the literature to be separated by region (Balleine and O'Doherty 2010).
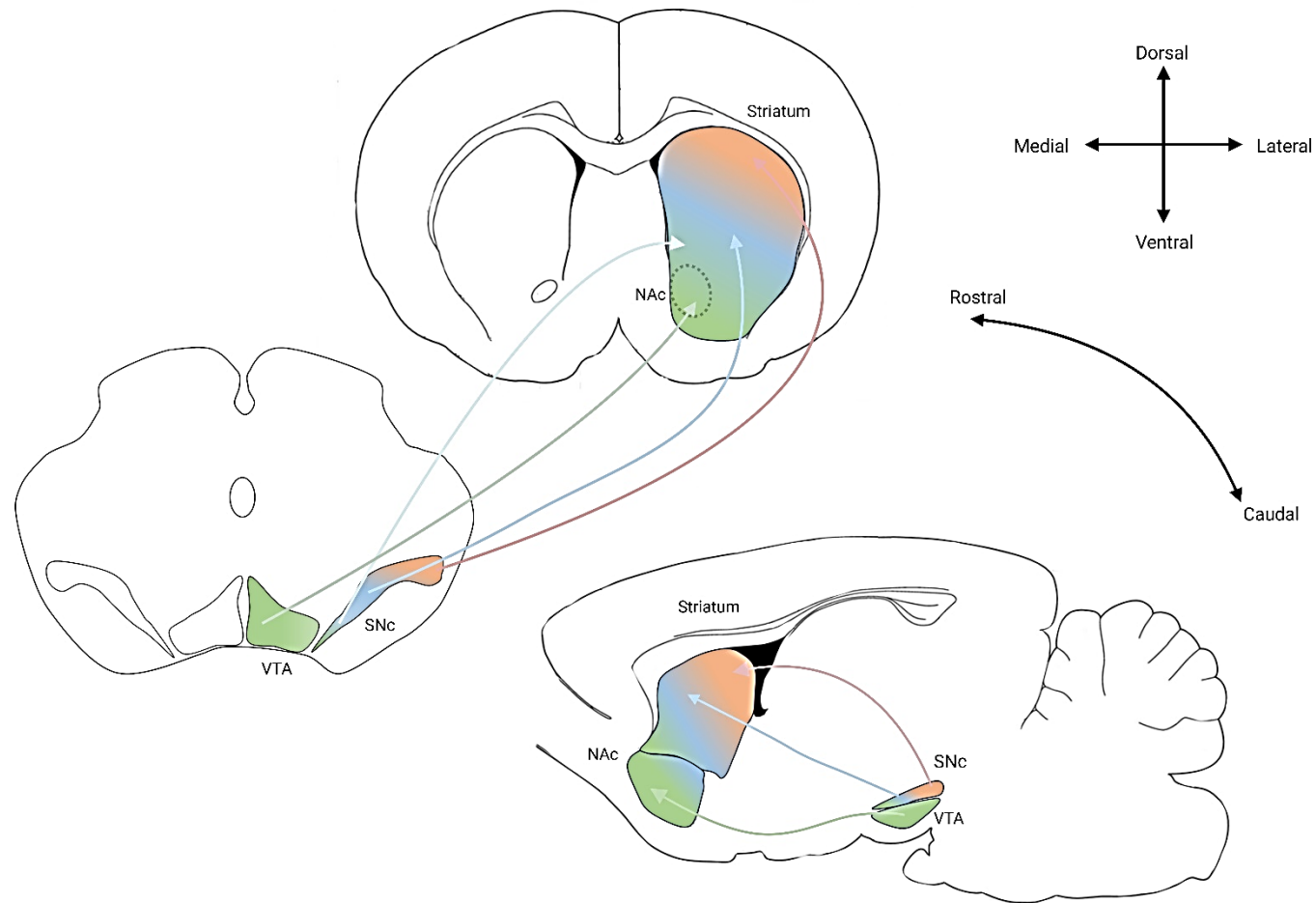
Figure 5.1. Mapping of striatal and midbrain connections, modified from McCutcheon et al. 2019. The Ventral Tegmental area (VTA) projects to the medial striatum mostly and Nucleus Accumbens (NAc), whereas the SNc, mostly the lateral end of this structure, projects to the dorsolateral striatum along the nigrostriatal pathway.

5.2.4 Role of the dorsomedial striatum in cognitive functions

A key aspect of cognitive function supported by the dorsomedial striatum is goal-directed behaviour. In brief, goal-directed behaviour is a part of instrumental learning in which an individual's response to a task is driven by their motivation to seek the reward (Hammond 1980). Shan et al. (2014) investigated the role of the direct and indirect pathway DA receptors in the acquisition of goal-directed behaviour and found an increase in D1-R signalling and a decrease in D2-R signalling within the dorsomedial striatum, indicating the flexibility of this region required to modulate these actions and the important role of midbrain to DA circuits in this type of behaviour. Lesion studies of the striatum have shown the importance of the dorsomedial region in goal-directed behaviour (Yin et al. 2005). Bilateral dorsomedial QA lesions were found to impair behavioural flexibility and altered perception in space (Lindgren et al. 2013). In non-human primates, the GABA agonist muscimol has been used to stimulate inhibitory pathways and disrupt striatal connectivity in different regions within the striatum (Miyachi et al. 1997). Injections into the caudate and anterior putamen were able to prevent the acquisition of a new skill, without disrupting the performance of already well-learned motor skills. The role of the dorsomedial striatum in goal-directed behaviour was indirectly studied by Faure et al. (2005) in which the dorsolateral striatum, and SNc through retrograde loss, was targeted with 6-OHDA. The authors found that dorsolateral 6-OHDA lesions impair habitual aspects of a cued instrumental learning task, but when DA is no longer available in the dorsolateral region, behaviour depends on the dorsomedial striatum for reward seeking.

Another role of the dorsomedial striatum in cognitive processing is to coordinate reversal learning. Studies have employed the NMDA receptor antagonist AP-5 to disrupt glutamate transmission and therefore disrupt striatal circuitry in the dorsomedial striatum, rendering rats unable to effectively alter their behaviour in accordance with the shift in testing parameters (Palencia and Ragozzino 2004; O'Neill and Brown 2007). Bilateral 6-OHDA dorsomedial lesions were also found to impair reversal learning (Grospe et al. 2018; Wang et al. 2020). In contrast to the dorsomedial striatum, impacting NMDA receptors in the dorsolateral striatum prevented habitual learning of a cross maze discrimination task but had no impact on reversal learning in the same task (Palencia and Ragozzino 2005). This further supports the segregation of the medial and lateral striatum in instrumental learning,

and thus makes it important to evaluate the role of DA denervation in those subregions on the LCRT task.

5.2.5 Role of the dorsolateral striatum in cognitive function

The dorsolateral striatum has been implicated in several studies as being responsible for habit formation. Habitual behaviour occurs due to a transition away from goal-directed responses when the anticipated relationship between the outcome and reward changes, and the response will be carried out independent of the value of the outcome. The conversion of goal-directed to habitual processing can be done through over-training and many researchers use devaluation as a probe to measure habitual behaviour (Adams and Dickinson 1981; Dickinson et al. 1995). Lesion studies have been employed to directly link processing in the dorsolateral striatum to habit formation. Yin et al. (2004) lesioned the dorsolateral striatum in rodents with NMDA and found that after training on a lever pressing-reward task, if the reward was devalued, those with dorsolateral lesions would not press the lever. This is indicative of the findings that these animals, due to the lesions, can no longer form a habit. The researchers also induced dorsomedial lesions and found no effect when the reward was devalued (Yin et al. 2005).

5.2.6 Goal-directed vs habitual behaviour in humans

The separation of the striatum into medial and lateral shown in rodents and non-human primates has also been demonstrated in humans with fMRI imaging studies (Balleine and O'Doherty 2010; Morris et al. 2022). As detailed in McNamee et al. (2015), When participants were asked to perform a decision-making task, the dorsolateral striatum encoded information related to the response to the stimulus but not the outcome, whereas the dorsomedial striatum could encode information for both responses and outcomes. The author suggests processing in the two distinct striatal subregions is segregated into goal-directed behaviour and habit formation due to the information these regions are processing at the time of decision-making. Similar findings have been shown in human participants in which over-training on the task prevented a response to reward devaluation (Tricomi et al.

2009) and Tanaka et al. (2008) highlights that the dorsomedial striatum is important for comprehending the value of an outcome and changing behaviour accordingly.

5.2.7 Experiment aims

The studies above have identified that the medial and lateral striatum are responsible for different associative processes. Therefore, it is reasonable to hypothesise that DA denervation of these striatal subregions may differentially impact performance on the LCRT task which relies on stimulus-response associations.

The aims of Experiment 4 are:

1. ***To understand the contribution of DA projections to either the medial or lateral striatum on performance in the LCRT task***. A unilateral intra-striatal infusion of 6-OHDA into the medial or lateral striatum was carried out, followed by assessment on the LCRT task and simple motor behaviour compared to intact controls. It was hypothesised that medial striatal lesions would impair LCRT performance, with minimal motor deficits. Conversely, it was hypothesized that lateral striatal lesions would impact motor function and but induce minimal LCRT impairments.

2. ***To determine whether pharmacological DA replacement would improve deficits on the LCRT task.*** Each group was measured on the LCRT and simple motor tasks 30 minutes after receiving subcutaneous injections of 4.5mg/kg L-DOPA. It was hypothesised that L-DOPA would improve motor and cognitive performance.

5.3 Methods: Experiment 4

5.3.1 Experimental design

22 female lister-hooded rats were trained on the LCRT task for 7 weeks to establish baseline performance (Table 6). Rats were sorted into groups based on response accuracy performance on the contralateral side (Figure 5.2). Rats in each group subsequently received either a unilateral infusion of 6-OHDA across two sites into the lateral striatum (n =8) or medial striatum (n =7). One rat did not recover from surgery. A group of rats did not undergo any surgical procedures and remained as an intact control (n = 7). Animals were tested on the LCRT task at 3 weeks post-lesion to identify any cognitive impairments induced by the toxin. Rats were also tested on the adjusting step task to observe any forelimb akinesia. At 4 weeks post-lesion rats underwent a L-DOPA challenge in order to assess if L-DOPA could improve any motor and cognitive deficits established at three weeks. Rats were assigned to two groups and received a sub-cutaneous injection of either saline or 4.5mg/kg of L-DOPA solution on Day 1. On Day 2, rats received a sub-cutaneous injection of the alternate solution. On each day, rats were filmed for 30 mins after drug administration prior to testing on the adjusting step task to observe and score the onset of any L-DOPA induced abnormal movements. At 40mins post-drug administration, rats were tested on the LCRT task. Finally, all rats received a high dose of L-DOPA (24mg/kg) and filmed for 1 hour in order to identify any L-DOPA induced dyskinesias. Rats were then transcardially perfused with 4% PFA and brain tissue was taken for histological analysis. The final n's for this experiment is as follows: Control n = 7, Lateral n = 7 and Medial n = 7.

Group	n = 22	Intact Control n = 7										
		Lateral 6-OHDA infusion n = 7						n = 15				
		Medial 6-OHDA infusion n = 7										
Weeks	-7	-6	-5	-4	-3	-2	-1	0	+1	+2	+3	+4
Task		LCRT training						Unilateral Striatal lesion			LCRT	L-DOPA
											Hand-testing	Perfuse

Figure 5.2. Experimental design timeline of Experiment 4. 22 lister-hooded rats were trained on the LCRT task for 7 weeks prior to receiving either a medial or lateral striatal lesion or remaining as an intact control (n = 7 per group). At 3 weeks post-lesion, rats were tested on the LCRT task and the adjusting steps task. At 4 weeks post-lesion, rats received 4.5mg/kg L-DOPA and tested again on motor and cognitive tasks. Prior to perfusion, rats were given 24mg/kg L-DOPA and observed for dyskinetic-like behaviours.

5.3.2 Surgical procedure

Animals were maintained under aseptic surgical parameters as previously described (see 2.3). 5 µl of 6-OHDA was infused into either the lateral or medial coordinates below using a 5 µl SGE syringe (Figure 5.3). All depths received 1.25 µl, except Site 2 of the medial infusion, in which DV2 received 1µl and DV3 received 0.25 µl. The toxin was left to diffuse for 2 minutes at each site prior to removing the syringe. The toothbar was set to -2.3. One rat did not recover from surgery.

A

Lateral	AP	ML	DV1	DV2
Site 1	+0.6	-3.6	-5	-4
Site 2	+1.6	-3.0	-4.5	-3.7

B

Medial	AP	ML	DV1	DV2	DV3
Site 1	+0.6	-2.0	-5.5	-4.2	
Site 2	+1.6	-1.6	-6.5	-4.5	-3.7
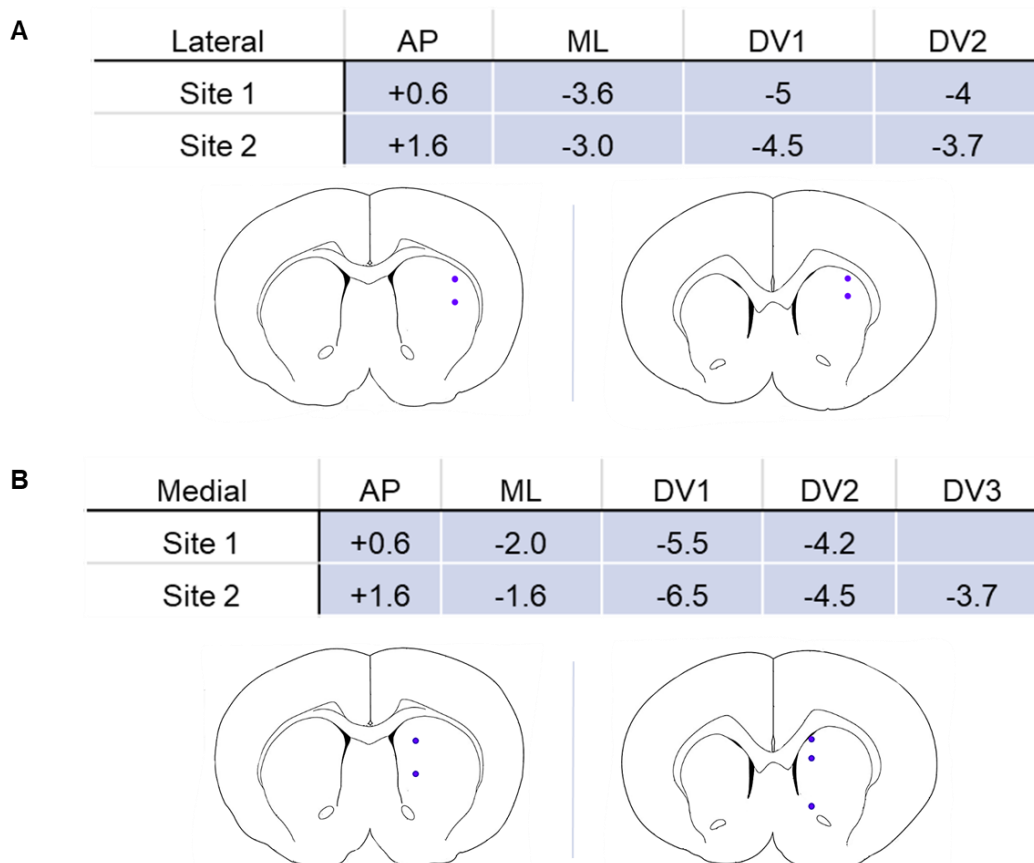
Figure 5.3. Surgical coordinates for striatal lesions. A) Coordinates used in relation to bregma to target the lateral and (B) medial striatum. Representative images of the locations of each injection site and the depth. AP = Anterior-Posterior axis, ML = Medial-Lateral axis, DV = Dorsal-Ventral axis.

5.3.3 Tissue processing

Rats were transcardially perfused with 4% PFA and processed as described above. (see 2.6.1 and 2.6.2). Brains were cut at 30µm in thickness on a freezing microtome. The primary antibodies used were as follows: TH (1:2000, Table 7 and Table 8).

5.3.4 Midbrain counts

Regions of interest were drawn around the structure of the VTA and SNc in both the intact and lesioned hemisphere. Tissue orientation for intact or lesioned hemisphere was aided with needle stick entry into a non-essential midbrain area on the intact hemisphere during tissue processing. Two sections per rat at -5.3 to -5.5 AP from bregma were used for manual counts of TH +ve cells within the regions of interest. Data is represented as an estimated cell count which is the sum of the total cells counted across the two midbrain sections.

5.3.5 Statistics

Statistical analysis was undertaken using a one-way ANOVA with Group (Control, Medial and Lateral) as the factor, with Tukey's post hoc test for multiple comparisons across the groups. One rat from the Lateral group was excluded from all LCRT analysis as no trials were performed across the duration of the testing period. During the 4.5mg/kg L-DOPA test, a one-way ANOVA with repeated measures was used with Drug (Saline, L-DOPA) and Group as a factor. One animal from the Lateral group was removed from the L-DOPA challenge analysis as no trials were performed after saline or L-DOPA administration. Graphical data is presented as group mean and error bars determined by standard error of the mean (SEM).

5.4 Results: Experiment 4
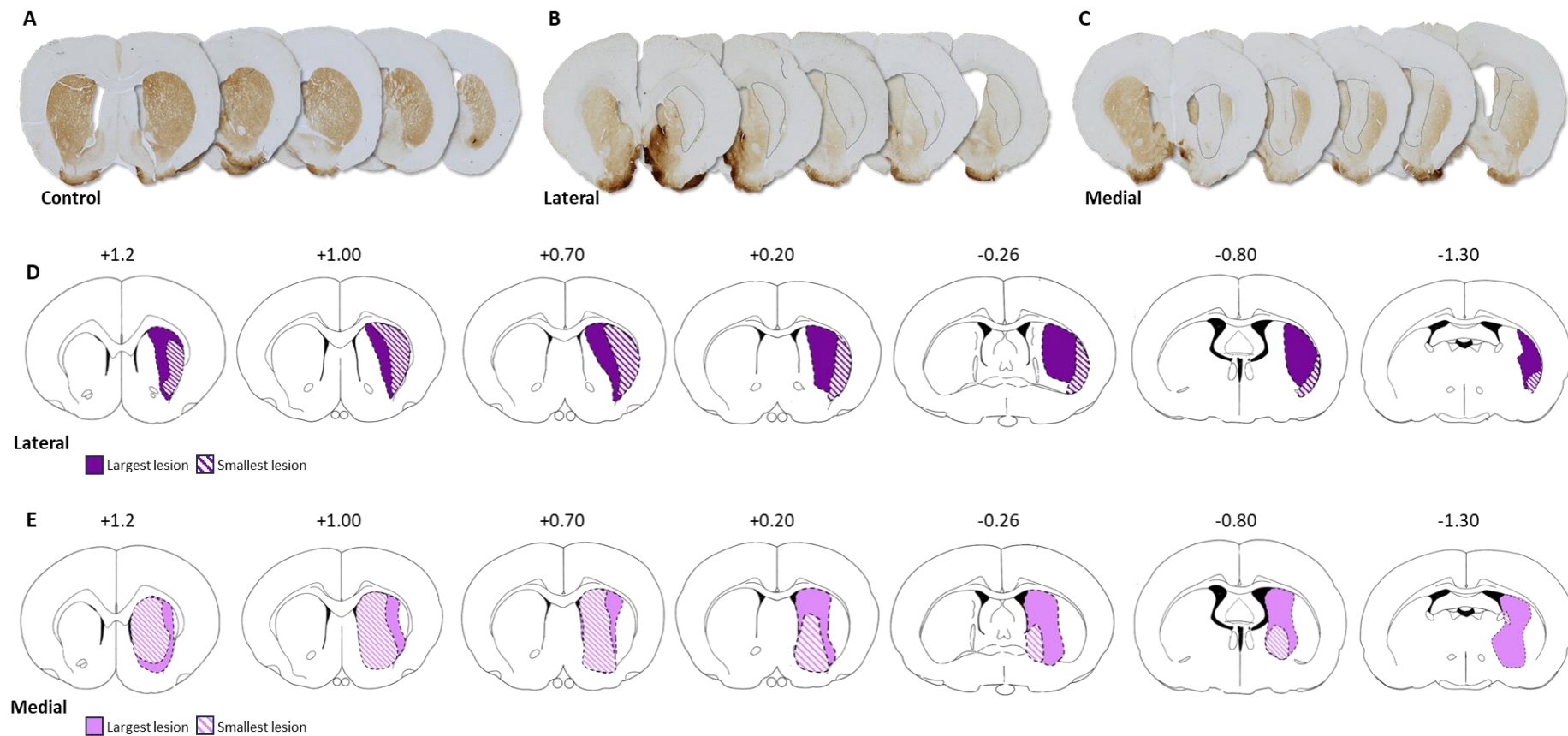
*Figure 5.4. Histological characterisation of striatal lesions. **A)** Control animals have a fully innervated striatum and balanced TH expression in both hemispheres. **B-C)** Both Lateral and Medial striatal 6-OHDA lesions are indicated by a loss of TH expression in their respective areas. Images taken at 125x magnification. **D)** Schematic of largest and smallest distribution of 6-OHDA in two animals from the Lateral lesion group. E) Schematic of largest and smallest distribution of 6-OHDA in two animals from the Medial lesion group.*
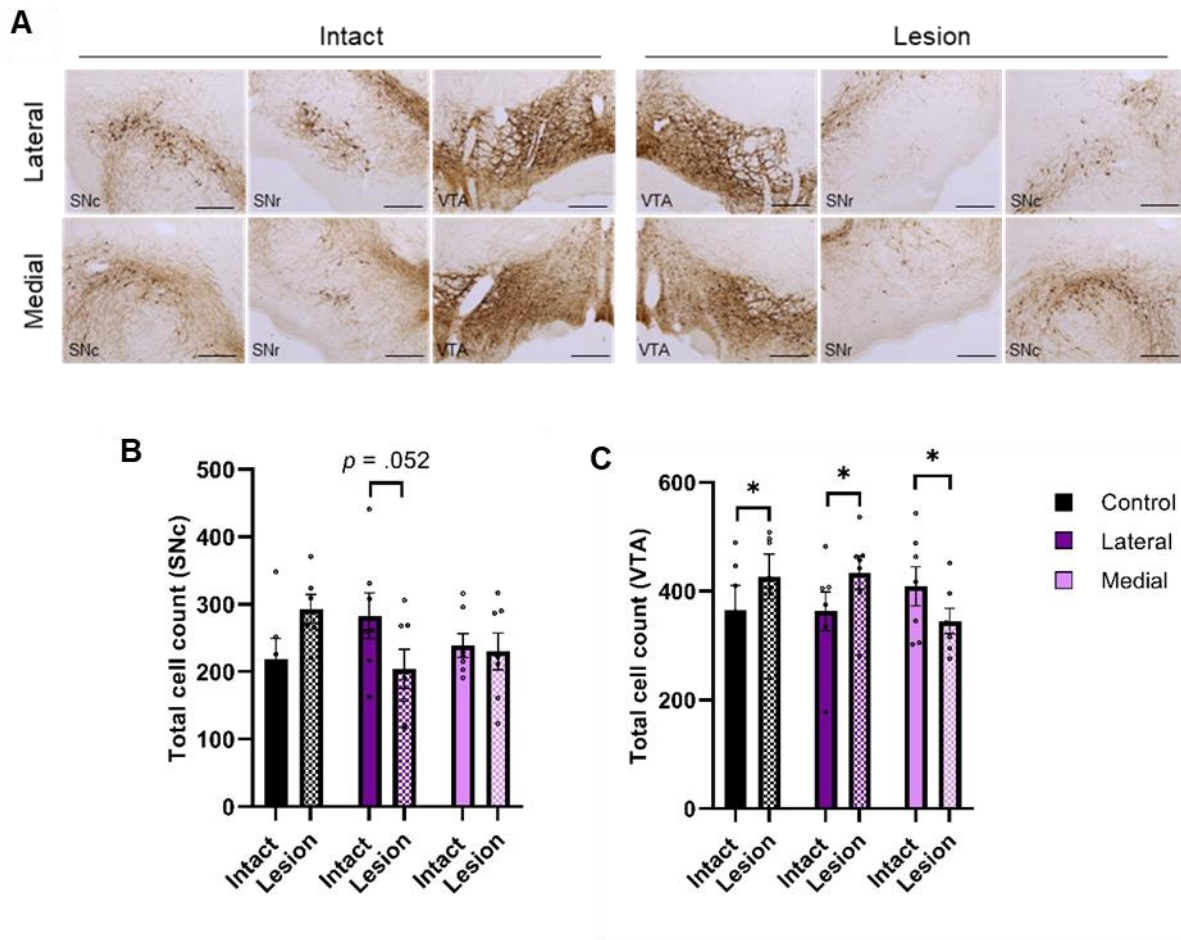
*Figure 5.5.Histological analysis of the ventral midbrain. A) Representative histological images of TH expression within the ventral midbrain. Total estimated cell counts of TH +ve cells in the B) SNc and C) VTA. Images taken at 100x magnification. Significant loss of TH +ve cells in the VTA of Medial striatal lesioned rats and a trend for loss of TH +ve cells in the SNc due to lateral striatal lesions. Significant differences are indicated as * p < .05. Error bars represent standard error of mean.*

5.4.1 Histological analysis of striatal lesions

6-OHDA induced discrete lesions in medial and lateral striatum

TH immunostaining showed the extent of the unilateral intrastriatal lesions throughout the brain (Figure 5.4). Intact controls highlighted the non-disrupted DA input to the striatum in both hemispheres, with the striatum fully expressing TH (Figure 5.4.A) Lateral striatal lesioned brains displayed a loss of TH in the striatal terminals restricted to the lateral portion of the striatum. When evaluating the animals in the lateral lesion group with the largest distribution (Figure 5.4.D), TH loss was mostly restricted to the dorsolateral region throughout the rostral-caudal axis. The smallest lesion within the group indicated TH loss mostly in the rostral part of the striatum, which was very discrete to the lateral striatum. Within medial striatal lesions, Figure 5.4.C depicts TH denervation in both the medial striatum and the NAc. The largest lesion within the medial lesioned group had extensive TH loss in the rostral part of the striatum which covered most of the striatal nuclei whilst preserving a small portion of the dorsomedial region (Figure 5.4.E). As the lesion extends along the rostral-caudal axis, the TH loss is largely restricted to the medial striatum and NAc. In the most caudal part of the brain (-0.80 to -1.30 AP), TH loss is also visible within the globus pallidus (GP). In the smallest lesioned animal within the striatal lesion, loss is largely restricted to the GP, with much of the caudal striatum still innervated by DA fibres due to limited visible TH loss.

Retrograde loss of DA neurons within the VTA due to medial striatal lesions

Terminal-end striatal lesions had a retrograde effect on DA neurons in the midbrain (Figure 5.5). Medial striatal lesions resulted in a reduction in the number of TH +ve neurons within the VTA on the lesion side compared to the intact side, however, both control and lateral lesion had more TH+ve cells on the lesioned side compared to intact side (Figure 5.5.B. Region*Group: $F(2,17) = 8.294$, $p = .003$, Medial: Intact vs Lesion ($p = .025$), Control: Intact vs Lesion ($p = .041$), Lateral: intact vs Lesion ($p = .014$). Lateral striatal lesions suggested a trend for a reduction in TH +ve neurons in the SNc on the lesioned side compared to intact (Figure 5.5.A: Region*Group: $F(2,17) = 3.771$, $p = .044$, Lateral: Intact vs Lesion $p = .052$).
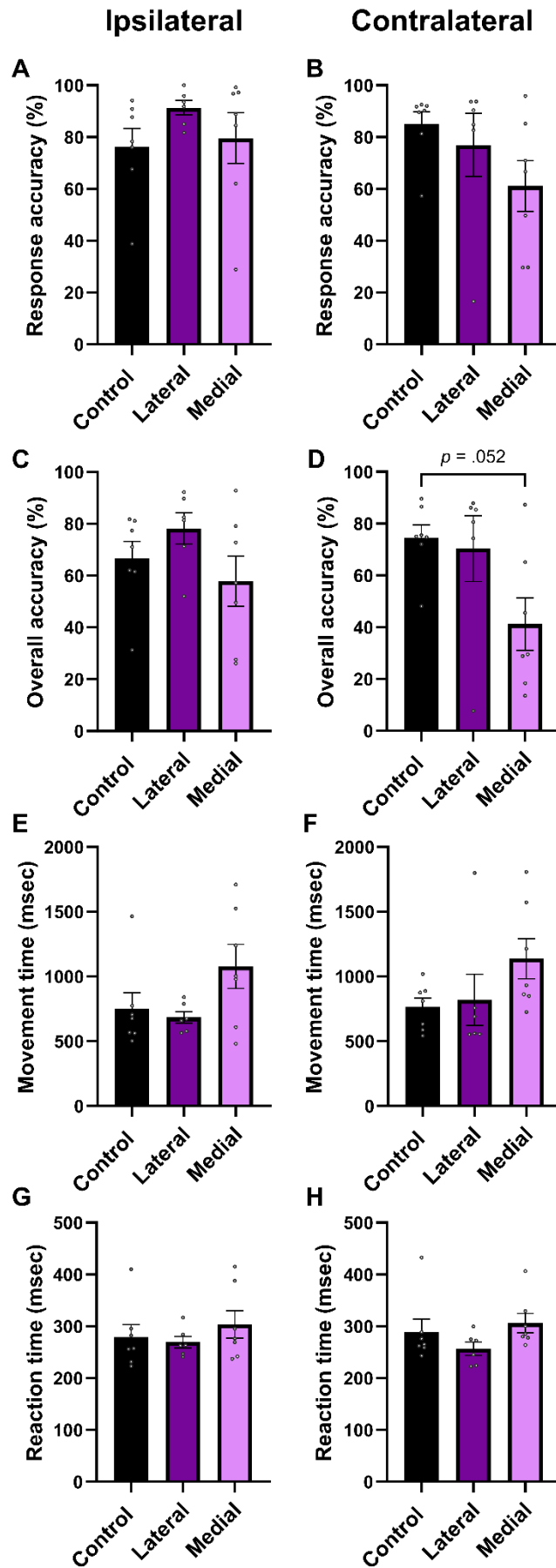
*Figure 5.6. Impact of striatal lesions on lateralised parameters of LCRT task. **A-B)** Response accuracy was not impaired at 3 weeks post-toxin on either the ipsilateral or contralateral side. **C-D)** There is a trend of impairment in overall accuracy on the contralateral side due to medial striatal lesions, with no impairment in performance on the ipsilateral side. **E-F)** Movement time and Reaction time **(G-H)** are not impaired on either the ipsilateral or contralateral side. Error bars represent standard error of the mean (SEM). Significant differences are indicated as p = .052.*

5.4.2 Impact of striatal lesions on LCRT performance

Trend for medial striatal lesion to worsen LCRT performance

All groups were tested on the LCRT task 3 weeks post-toxin to identify any deficits on the task. Behaviour on the ipsilateral side was not affected by unilateral striatal lesions compared to control (Figure 5.6.A. Response accuracy: ($F_{(2,17)}$ = 1.060, p = n.s), Overall accuracy: (Figure 5.6.C. $F_{(2,17)}$ = 1.658, p = n.s), Movement time: (Figure 5.6.E. $F_{(2,17)}$ = 2.633, p = n.s), Reaction time: (Figure 5.6.G. $F_{(2,17)}$ = .601, p = n.s). On the contralateral side however, there is an indication of unilateral striatal lesions impacting LCRT performance. Control and lateral striatal lesioned rats were just below 80% accurate in their overall accuracy, but medial striatal lesioned rats had a trend towards impaired accuracy on the task (Figure 5.6.D. $F_{(2,17)}$ = 3.787, p = .004; Control vs. medial p = .052). Apart from overall accuracy, no other contralateral parameters were significantly affected by striatal lesions 3 weeks post-toxin (Figure 5.6.B. Response accuracy: $F_{(2,17)}$ = 1.840, p = n.s, Movement time: Figure 5.6.F. $F_{(2,17)}$ = 1.987, p = n.s, Reaction time: Figure 5.6. H. $F_{(2,17)}$ = 1.555, p = n.s).
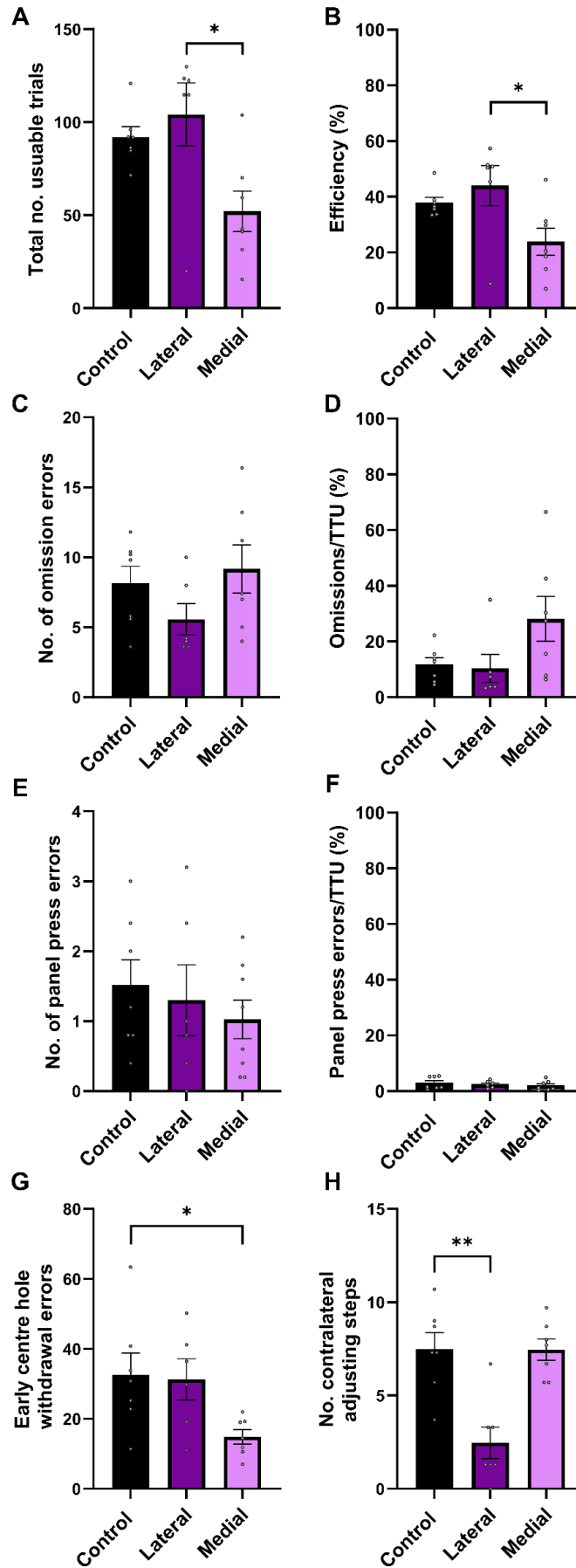
*Figure 5.7. Impact of striatal lesions on non-lateralised aspects of LCRT task, and on the Adjusting Steps test. **A)** Medial striatal lesioned rats performed fewer total usable trials, **B)** and were significantly less efficient on the task compared to lateral lesions. **C-D)** omission errors and the percentage of omission errors out of the total useable trials was not affected by striatal lesions **E-F)** panel press errors were not significantly affected by striatal lesions, nor the percentage of panel press errors. **G)** Fewer of early centre hole withdrawal errors were performed by medial lesioned rats **H)** Contralateral adjusting steps were significantly reduced in lateral striatal lesioned rats compared to controls. Error bars represent standard error of mean. Significant differences are indicated as * p < .05, ** p <.01.*

5.4.3 Impact of striatal lesions on non-lateralised aspects of LCRT

Incentive motivation impaired by unilateral medial striatal lesions

The total number of useable trials, a surrogate measure of incentive motivation to perform the task was significantly impaired due to a medial lesion, when compared to those with a lateral lesion (Figure 5.7. A. Total useable trials: $F_{(2,17)} = 5.592$, $p = .014$. Lateral vs medial, $p = .015$), as well as the efficiency at performing the task (Figure 5.7.B. $F_{(2,17)} = 4.397$, $p = .029$), Lateral vs Medial, $p = .028$). The number of omission errors (Figure 5.7.C. $F_{(2,17)} = 1.697$, $p = $ n.s) and panel press errors were not impacted by striatal lesions (Figure 5.7.E. $F_{(2,17)} = 1.480$, $p = .256$) When analysed as a percentage of the total useable trials, omission errors did not significantly differ among groups (Figure 5.7D, Group: $F_{(2,17)} = 3.019$, $p = .076$) nor did panel press errors (Figure 5.7.F, Group: $F_{(2,17)} = .475$, $p = $ n.s).The number of early withdrawals from the centre hole was reduced in medial lesioned rats, which is directly associated with the lower number of useable trials (Figure 5.7.G. $F_{(2,17)} = 4.019$, $p = .037$. Control vs Medial, $p = .05$)

Lateral intrastriatal lesion impairs motor function

Alongside cognitive function, forelimb akinesia was measured at 3 weeks post-lesion. All control animals performed a high number of contralateral adjusting steps. Interestingly, in contrast to performance on the LCRT task seen in Figure 5.6 and Figure 5.7, rats with a lateral lesion performed fewer contralateral adjusting steps (Figure 5.7.H. $F_{(2,18)} = 14.098$, $p < .001$). Rats with medial striatal lesions displayed no motor impairment in adjusting steps at 3 weeks post-toxin.

Ipsilateral   Contralateral
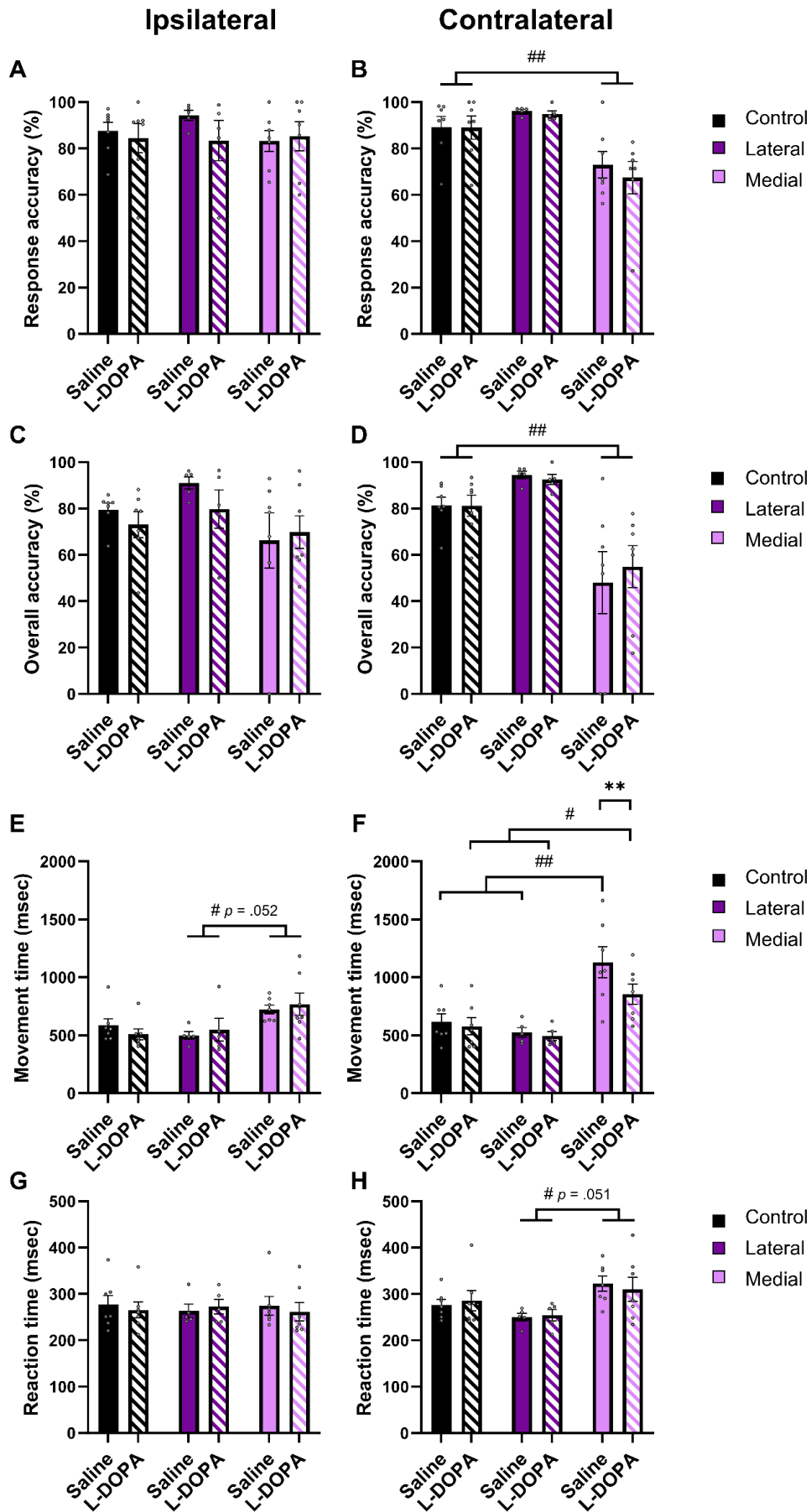
*Figure 5.8. Impact of 4.5mg/kg L-DOPA on performance during lateralised aspects of the LCRT task on striatal lesioned rats. No effect of lesion or L-DOPA was observed on the ipsilateral side for **A)** response accuracy, **C)** overall accuracy and **G)** reaction time. **E)** A trend for reduced movement time on the ipsilateral side was observed in medial lesioned rats. **B)** Response accuracy, **D)** overall accuracy and **H)** reaction time on the contralateral side was significantly impaired in medial lesioned rats compared to control, with no impact observed due to L-DOPA administration. **F)** Medial striatal lesions induced significantly slower movement time at 4 weeks post-toxin, and L-DOPA administration improved the movement time impairment in medial striatal lesioned rats. Error bars represent standard error of mean. Significant differences within groups are indicated as * p < .05, ** p <.01. Significant differences between groups are indicated as # p < .05, ## p <.01.*

5.4.4 Impact of L-DOPA on striatal lesions during LCRT task

L-DOPA does not improve accuracy deficits induced by striatal lesions

At 4 weeks post-toxin, rats were administered 4.5mg/kg L-DOPA and observed on the LCRT task. Rats with medial striatal lesions were significantly worse in their contralateral response accuracy (Figure 5.8.B. Drug: $F(1,16) = 3449$, p = n.s, Group: $F(2,16) = 7.826$, $p = .004$) compared to controls ($p = .025$) and lateral striatal lesions ($p = .006$), and also in their overall accuracy with or without the presence of L-DOPA (Figure 5.8.D. Drug: $F(1,16) = .101$, p = n.s, Group: $F(2,16) = 10.710$, $p = .001$, control vs medial $p = .010$ and lateral vs medial $p = .001$). No impairment in accuracy was seen on the ipsilateral side, nor was it altered due to L-DOPA administration (Figure 5.8. A) Response accuracy: $F(2,16) = 1.294$, p = n.s, C) Overall accuracy: Drug $(1,16) = 1.426$, p = n.s and Group: $F(2,16) = 1.585$, p = n.s).

L-DOPA improves movement time in medial lesioned rats

Lateral striatal lesions did not affect movement time on the contralateral side, nor did L-DOPA administration, however, overall medial striatal lesions induced slower movement time compared to controls (Figure 5.8.F. Group: ($F(2,16) = 9.644$, $p = .002$. Control vs Medial $p = .004$, Medial vs Lateral $p = .004$). Interestingly, medial lesioned rats were significantly affected by the presence of L-DOPA (Figure 5.8.F. Group*Drug: $F(2,16) = 7.311$, $p = .006$). When given L-DOPA, medial lesions were still slower in completing the task compared to controls ($p = .041$) and lateral lesions ($p = .014$) but were significantly quicker on the task than when given saline ($p < .001$). No impairment in performance, nor effect of L-DOPA was seen in the ipsilateral side, however, there was a trend for medial striatal lesions to increase movement time compared to lateral striatal lesions (Figure 5.8.E. Group $F(2,16) = 4.400$, $p = .030$, control vs medial $p = .059$, medial vs lateral $p = .052$).

Trend for slower reaction time due to medial striatal lesions, irrespective of L-DOPA

Reaction time of controls and lateral striatal lesioned rats did not differ on or off L-DOPA on the ipsilateral side (Figure 5.8.G. Drug: $F(1,16) = .422$, p = n.s, Group: $F(2,16) = .012$, p = n.s). There was a trend for rats with medial striatal lesions to react more slowly on the contralateral side compared to lateral striatal lesions (Figure 5.8.H. Group: $F(2,16) = 3.610$, $p = .051$, lateral vs medial, $p = .043$).
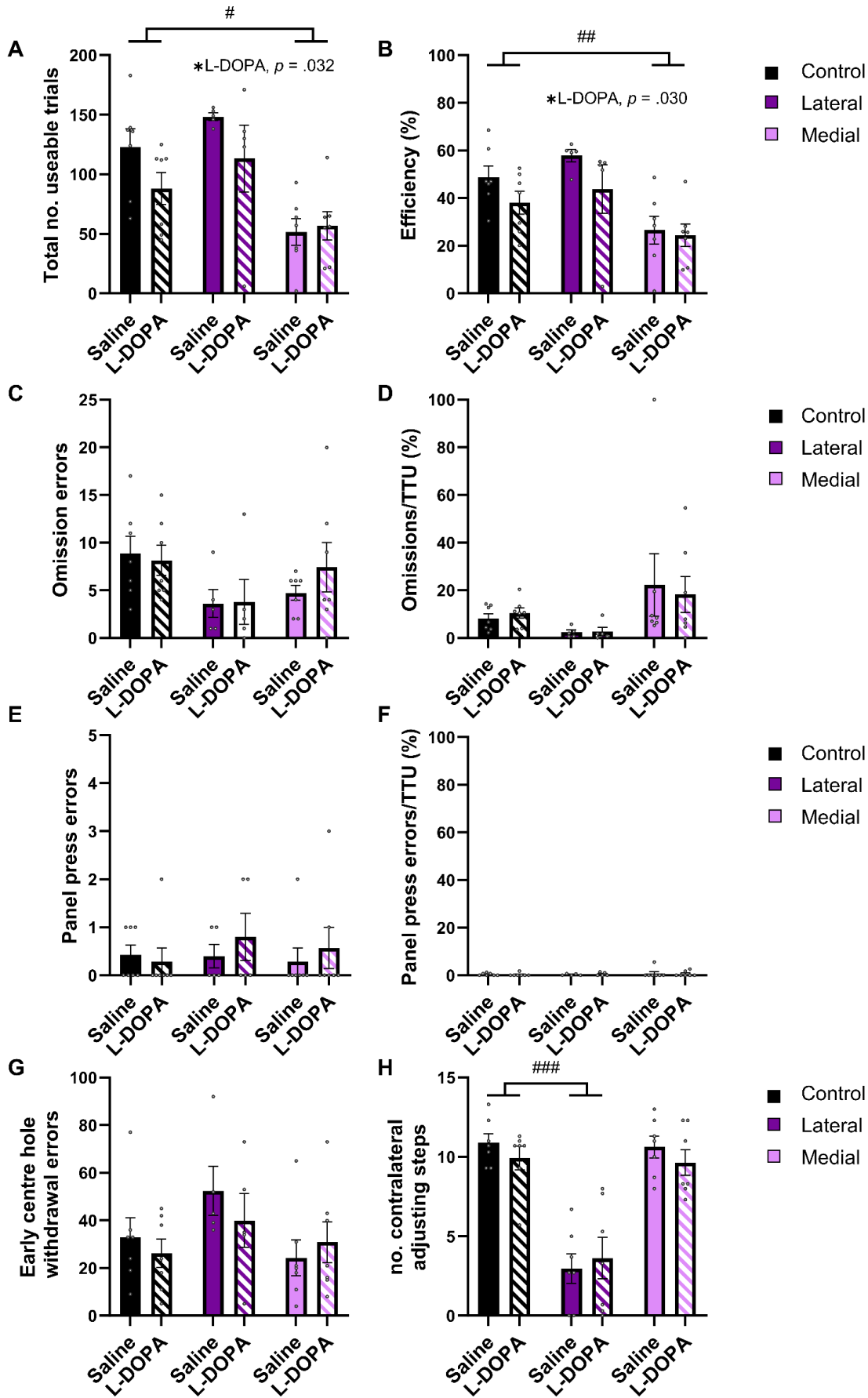
*Figure 5.9. Impact of L-DOPA on performance during non-lateralised aspects of the LCRT task on striatal lesioned rats, and on the Adjusting Steps test. **A)** Total useable trials and **B)** efficiency at the task was not affected by L-DOPA administration and was significantly reduced due to medial striatal lesions after 4 weeks post-lesion. **C)** Omissions, **E)** panel press errors **G)** and early centre hole withdrawal errors were not impacted by L-DOPA administration or significantly different amongst groups. **D,F)** There was no change in omissions or panel press errors when analysing them as a percentage of total useable trials **H)** Contralateral adjusting steps were not significantly improved in lateral striatal lesioned rats due to L-DOPA administration. Error bars represent standard error of mean. Significant group differences are indicated as # p < .05, ## p <.01, ### p <.001.*

5.4.5 Impact of L-DOPA on striatal lesions on non-lateralised aspects of LCRT performance

Impaired incentive motivation at 4 weeks post-toxin

Medial striatal lesioned rats performed the fewest usable trials overall when compared to both controls and those with lateral striatal lesions (Figure 5.9.A Group: $F_{(2,16)}$ = 9.464, p = .002 ,control vs medial p = .023, control vs lateral p = n.s., lateral vs medial p = .002). Also, L-DOPA impacted the incentive motivation to perform the LCRT task. Overall, L-DOPA led to fewer useable trials (Figure 5.9.A. Drug: $F_{(1,16)}$ = 5.489, p = .032).

Efficiency at LCRT task impaired 4 weeks post-toxin

Medial striatal lesioned rats were significantly less efficient on the task on compared to controls and lateral lesions (Figure 5.9.B. Group: $F_{(2,16)}$ = 7.757, p = .004, control vs medial (p = .028), lateral vs medial p = .005). L-DOPA worsened efficiency overall on the LCRT task (Figure 5.9.B; Drug: $F_{(1,16)}$ = 5.647, p = .030).

Common LCRT time-out errors were not impaired 4 weeks post-toxin, nor affected by L-DOPA

Omissions (Figure 5.9.C. Drug: $F_{(1,16)}$ = .407, p = n.s, Group: $F_{(2,16)}$ = 2.138, p = n.s), panel press errors (Figure 5.9.E. Drug: ($F_{(1,16)}$ = 1.388, p = n.s, Group: $F_{(2,16)}$ = 1.485, p = n.s) and early withdrawal from the centre hole errors (Figure 5.9.G. Drug: ($F_{(1,16)}$ = .452, p = n.s, Group: $F_{(2,16)}$ = .244, p = n.s) did not differ amongst groups, nor appeared to be attenuated by L-DOPA. The percentage of omissions (calculated from total useable trials) was not significantly affected by L-DOPA, nor was it different among groups (Figure 5.9.D Drug: $F_{(1,16)}$ = .007, p = n.s. Group: $F_{(2,16)}$ = 2.867, p = .086) or panel press (Figure 5.9.F Drug: $F_{(1,16)}$ = .002, p = n.s. Group: $F_{(2,16)}$ = .357, p = n.s).

Lateral striatal lesioned rats remain impaired in adjusting steps 4 weeks post-toxin

At 4 weeks post-toxin, lateral stratal lesioned rats remained impaired in their number of adjusting steps, and this impairment was not alleviated with L-DOPA administration (Figure 5.9. H. Drug: $F_{(1,18)}$ = .515, p = n.s, Group: $F_{(2,18)}$ = 33.241, p <.001, Lateral vs control and medial, p <.001). No dyskinetic like behaviours were observed during filming when

animals received 4.5mg/kg or 24mg/kg L-DOPA, so AIMS scores could not be collected (data not shown).

5.5 Discussion: Experiment 4

In Experiment 4, the aim was (1) to understand the contribution of DA innervation of medial and lateral striatal subregions to cognitive function, and (2) evaluate the impact of L-DOPA on cognitive function during the LCRT task. The findings show that DA denervation of the lateral striatum resulted in impaired adjusting steps, without impairing performance on the LCRT task. The inverse was true for medial striatal lesions, causing visuospatial deficits and decreases in incentive motivation, without inducing forelimb akinesia. Overall, L-DOPA administered at 4.5mg/kg did not improve motor function or induce abnormal dyskinetic movement allowing dissociation of the effects of L-DOPA without interference of abnormal movements. In relation to cognitive behaviour, L-DOPA overall impacted incentive motivation to perform the task performance and impairing their efficiency on the task, while also improving contralateral movement time in medial lesioned rats.

5.5.1 Medial striatal lesions impair LCRT performance whilst Lateral lesions do not

Lateral striatal lesions did not impair visuospatial function or incentive motivation on the LCRT task (Figure 5.8.B & Figure 5.9.A). As previously introduced in this chapter, published work by Faure et al. (2005) and Yin et al. (2004) found denervation in the dorsolateral striatum to impair habit formation, reverting all action in an instrumental learning task to goal-directed behaviour driven by the intact dorsomedial region. Here, the lateral lesioned rats showed unimpaired stimulus-response to the lateralised holes. In order to maintain this high accuracy and receive the reward, it seems reasonable to hypothesise that performance in lateral lesioned rats may have been governed by goal-directed behaviour. In order to support this hypothesis however, a reward devaluation parameter of pre-feeding or lithium chloride administration for example, prior to performing the LCRT task would be required, as there was no explicit testing of goal-directed driven responses vs habit formation during this task.

In contrast, at 4 weeks post-toxin, medial striatal lesions led to a reduction in response and overall accuracy on the LCRT task (Figure 5.8.B). The trend for impaired contralateral accuracy was seen at 3 weeks post-toxin (Figure 5.6.D), but the deficits were only prominent after 4 weeks. As stated above, it may be reasonable in the case of medial striatal lesions to suggest that LCRT performance is governed by goal directed behaviour. However, the impairment seen was around a 20-30% reduction at 4 weeks post-toxin. Although accuracy is reduced, these animals are still able to make lateralised stimulus responses to receive a reward. This may suggest that medial lesioned rats have formed a habit during training and responding is now driven by such processes. However, without reward devaluation this cannot be confirmed.

Another hypothesis for the reduction in accuracy during the LCRT task, is that it may be driven primarily by an impairment in visuospatial processing. This is due to impairment in response accuracy (Figure 5.8.D), which measures incorrect/correct responses only without confounding factors of omissions and panel press errors. Previous work within the field has found dorsomedial excitotoxic lesions and NMDA receptor blocking in mice to disrupt spatial learning (Lee et al. 2014; Radke et al. 2019).

5.5.2 Is there a role for the nucleus accumbens in the LCRT task?

Medial striatal lesions led to impaired incentive motivation on the LCRT task (Figure 5.7.A). Histological analysis detailed in Figure 5.4 indicated medial lesions also induced DA denervation in the NAc. The NAc has been implicated in reward seeking behaviour and motivation in rodent studies (Cardinal and Howes 2005; Peters and Büchel 2010). Atrophy of the NAc is also present in PD patients, known as Mavridis' atrophy (MA) and has important implications for prodromal cognitive impairments in PD such as apathy (Mavridis et al. 2011; Mavridis and Pyrgelis 2022).

One hypothesis is that the NAc may govern incentive motivation, whilst the medial striatum governs visuospatial function during the LCRT task. Balleine and Killcross (1994) found ibotenic lesions of the NAc to affect motivation to participate but not goal-directed response. Furthermore, Lelos et al. (2012) detail a study on intact animals who were pre-fed prior to testing. Unimpaired rats had a significant reduction in their incentive motivation to perform the task, with no disruption to their accuracy. However studies such as Annett et al. (1989)

found NAc lesions do impair visuospatial processing during the Morris water maze task, yet it is important to note that animals were only delayed and not inhibited from learning the task. As the dorsomedial striatum was still intact in Annett et al. (1989), it would appear visuospatial processing in this case is still driven by the medial striatum. It has to be considered, however, that there was no specific NAc lesion in this chapter without loss of the dorsomedial striatum also, so we cannot definitively rule out the role of the NAc in visuospatial processing or the role of the medial striatum in incentive motivation.

5.5.3 Role of the medial striatum in reaction time during the LCRT task?

Medial striatal lesions also induced a delay in reaction time on the contralateral side, whereas lateral lesions did not (Figure 5.8.H). This result may be indicative of a delay in attention during the task. The VTA projections to the caudate and NAc have been implicated in reward-based attentional bias and spatial attention during an additional singleton task and through optogenetic stimulation (Arcizet and Krauzlis 2018; Meffert et al. 2018; Flores-Dourojeanni et al. 2021). 6-OHDA NAc lesions in rats were found to impair attention during the 5-choice serial reaction time task without impairing accuracy (Cole and Robbins 1989). The results here may suggest a role for the NAc in attentional processing during the LCRT task, however there is further work required to confirm this, such as the selective activation/inactivation of the NAc and VTA during the LCRT task and perhaps specific attentional tasks such as the 5-choice serial reaction time task. It is important to note medial lesioned rats had reduced movement time during the task (Figure 5.8.F), so a delay in reaction time may be driven by movement initiation deficits.

5.5.4 Lateral striatal lesions induce forelimb akinesia, but medial striatal lesions do not

Impairment in contralateral adjusting steps was present in lateral striatal lesioned rats from 3 weeks and continued to be impaired at 4 weeks post-toxin (Figure 5.7.H & Figure 5.9.H). This supports the evidence within the literature of PD patients and pre-clinical studies that the lateral striatum mediates motor coordination (Heuer et al. 2012; Nagai et al. 2012; Schröter et al. 2022). Boix et al. (2015)'s detailed work on partial 6-OHDA MFB lesions in

mice, found TH terminal loss began in the dorsolateral striatum, extending medially as the amount of toxin injected was increased. At 0.7 µg to 1.0 µg of 6-OHDA, they report a reduction in adjusting steps by 80% and a more profound impairment at 3.4 ug. In this study, 4 µg was used and targeted to two sites within the dorsolateral striatum, and there was approximately 70% reduction in adjusting steps compared to controls at 3- and 4-weeks post-toxin. The findings in this chapter support the importance of DA innervation to the lateral striatum for mediating forelimb use, as medial lesions did not lead to the onset of forelimb akinesia.

Understanding the lesion

When evaluating the extent of TH+ve neuronal loss within the ventral midbrain (Figure 5.5), a central location along the rostral-caudal plane was chosen to carry out manual counting of the SNc and VTA as a 'snapshot' for retrograde loss. The magnitude of VTA loss in the medial group was approximately 30%, whilst loss in the SNc was only 15% and did not reach statistical significance compared to the intact side. Kirik et al. (1998) when exploring partial lesioning of the lateral striatum, found that the development of forelimb akinesia would only appear once a 'threshold' was crossed of TH +ve SNc neurons and DA striatal loss, and that the deficits got more severe the further along the rostro-caudal plane that the lesion spread. Despite this, in Experiment 4, there was distinct denervation of TH+ projections in both the lateral and medial region of the striatum respective to the targeted lesion site (Figure 5.4) which resulted in a motor impairment in the case of lateral lesions. The lateral lesions extended throughout the majority of the rostral-caudal axis but most of the DA loss was in the rostral part of the striatum, whereas the medial lesions extended as far as the globus pallidus. To improve this histological analysis, it would be important to analyse the full extent of DAergic neuronal loss within the midbrain along the rostral-caudal axis to identify any topology to DA neuronal loss and DA innervation depletion in the striatum.

5.5.5 L-DOPA does not alleviate DA-dependant deficits in the LCRT task

Overall, L-DOPA had little impact on ipsilateral and contralateral LCRT performance in terms of response and overall accuracy, as well as reaction time (Figure 5.8.A-D & G-H) and had

no impact on impaired contralateral forelimb use in medial lesioned rats (Figure 5.9.H). It was hypothesised that L-DOPA would improve motor function due to previous findings by Schneider et al. (2013) and others who showed a dose response manner to motor improvement in a PD non-human primate model (Kurlan et al. 1991). However, Schneider et al. (2013) also found a connection between doses of L-DOPA that support motor recovery and the onset of cognitive deficits in spatial working memory tasks.

L-DOPA improves movement time

Movement time in medial lesioned rats was improved due to L-DOPA administration (Figure 5.8.F). As movement time during the LCRT task is a measure of the animal to move and poke in the lateralised holes, then it could be argued that acute L-DOPA treatment has indeed improved some aspect of motor function in this experiment. However, it is important to note, contralateral movement time on the LCRT task was made slower due to medial lesions, whereas rats with lateral lesions did not show an impairment, prior to administration of L-DOPA (Figure 5.6.F). Furthermore, medial lesioned rats are not impaired on a simple motor task. These results suggest that movement time on the LCRT task is not solely governed by a motor impairment but possibly due to a delay in action selection or motor readiness. Movement time in the LCRT task has been implicated as a measure of motor readiness and execution of response (Döbrössy and Dunnett 1997). However, only adjusting steps were carried out to evaluate motor coordination, so movement time deficits being governed by motor slowing cannot be ruled out without further motor coordination tasks such as the rotarod or staircase task.

L-DOPA disrupts incentive motivation during the LCRT task

L-DOPA administration, overall, led to a reduction in TTU, which suggests an impact on incentive motivation (Figure 5.9). This drop in incentive motivation however appears to be driven by control and lateral lesioned rats, as medial lesions, although they had the greatest reduction in incentive motivation, displayed no difference in total usable trials between saline and L-DOPA administration. L-DOPA, when given to healthy individuals, provided no benefit during cognitive tasks such as a working memory training program to probe spatial

reasoning, but participants were slower to learn on L-DOPA (Lebedev et al. 2020). The findings here that L-DOPA may impair incentive motivation in intact animals and those with an intact medial striatal/NAc DA innervation, indicates a 'flooding effect' that may lead to disruption in normal DA transmission (Cools et al. 2007; Kwak et al. 2012).

5.5.6 Conclusion and future directions

Experiment 4 aimed to evaluate the contribution of two major DA circuits to aspects of cognitive and motor function. Using unilateral 6-OHDA striatal lesions, loss of DA terminals in the medial striatum impaired visuospatial function and incentive motivation, and in contrast, loss of DA terminals in the lateral striatum impaired contralateral forelimb use. The knowledge gained from this experiment provides rationale to target those same striatal subregions with viral-mediated DA synthesis and evaluate motor and cognitive performance. Specifically, given these findings, it would be anticipated that DA replacement in the medial vs lateral subregion of the striatum may differentially affect cognitive or motor function in these behavioural tasks.

5.6 Introduction: Experiment 5

5.6.1 Lessons from previous chapters

The overarching aim of this thesis is to evaluate dopamine replacement on cognitive function, and what factors in cell, viral-mediated and pharmacological DA replacement may support cognitive recovery. As detailed in Chapter 3, correlational analysis of cell therapy products on behaviour revealed that greater innervation into the lateral striatum improved recovery on amphetamine rotations, while greater innervation into the medial striatum correlated with better accuracy in the LCRT task. Lessons from chapter 4 indicate that placement of the viral vector can greatly affect behavioural output, so building upon the findings in Experiment 4, it is important to further understand the relationship between DA loss in the medial and lateral striatum and DA replacement in those areas on cognitive and motor recovery.

5.6.2 Functional benefit of DA replacement in the ventromedial vs dorsolateral striatum

In mice that were dopamine-deficit due to lack of the TH gene, viral-mediated expression of TH has been shown to allow synthesis of striatal DA and, subsequently, to correct impairments in goal-directed behaviour, incentive motivation and motor deficits (Robinson et al. 2006; Robinson et al. 2007; Palmiter 2008). Specifically probing two striatal subregions with viral-mediated DA synthesis to induce cognitive recovery has also been supported in the literature by those such as Darvas and Palmiter (2010). DA-depleted mice were targeted with a CAV2-Cre virus in the ventromedial striatum and researchers found retrograde transport to the VTA and restored DA signalling to the medial striatum. This recovery of DA signalling led to restored visuospatial functioning in an object recognition task despite poor object exploration but did however improve motivation in an instrumental conditioning task. The same technique was applied to targeting the dorsolateral striatum (Darvas and Palmiter 2009). Interestingly, restored DA signalling in the dorsolateral striatum led to retrograde

transport to the majority of the ventral midbrain, and previously DA depleted rats also had restored visuospatial function and object exploration, with reduced motivation. In Experiment 4, loss of DA in the medial and lateral striatum had distinct impacts on the behavioural indices that were tested. However, it should be noted that in Darvas and Palmiter (2009) and Darvas and Palmiter (2010), DA signalling was not quite as concentrated to the dorsolateral and dorsomedial as would be needed to segregate those two areas by function based on these experiments and this may explain the overlap in visuospatial recovery. These studies highlight the importance of evaluating targeted DA replacement within the striatum.

5.6.3 Caudate and putamen targeting in PD clinical trials

Gene therapy in PD has been assessed in clinical trials for safety and tolerability (Eberling et al. 2008; Björklund et al. 2010; Cederfjäll et al. 2015; Palfi et al. 2018). Infusions of DAergic viral vectors in non-human primates and PD patients have targeted the putamen due to its role in motor coordination, but studies have reported bleed-through of the AAV into the caudate (Badin et al. 2019). It is unknown what role direct targeting of the medial striatum with viral vectors would have on cognitive function.

5.6.4 Experiment aim

Experiment 4 identified that DA denervation in the medial vs lateral striatum can differentially impact motor and cognitive function. As detailed above, the literature supports specific targeting of striatal subregions to improve cognitive and motor deficits. Therefore, it can be hypothesised that using DA viral vectors as a probe in Experiment 5 to target the medial and lateral striatum, would differentially improve cognitive and motor function.

The aim of this chapter is as follows:

1. ***To assess the impact of selectively infusing a biscistronic TH and GCH1 expressing AAV into either the medial or lateral striatum on performance in the***

LCRT. Using the 6-OHDA MFB PD rat model, AAV-htTH-hGCH1 was infused into either the medial or lateral striatum and behaviour was observed on simple motor tasks and the LCRT task at 4, 6, and 8 weeks post-AAV. It was hypothesised that infusing the AAV into the medial striatum would improve visuospatial deficits, whilst lateral infusion would improve behaviour on simple motor tasks.

2. *To further evaluate L-DOPA administration on cognitive behaviour during the LCRT task and identify any interaction between lateral and medial AAV infusions and L-DOPA.* Rats were subcutaneously administered 4.5mg/kg L-DOPA or saline and observed on adjusting steps and during the LCRT task. It was hypothesised that L-DOPA would improve performance on the LCRT task and AAV-treated rats would mitigate the onset of L-DOPA induced dyskinesias.

5.7 Methods: Experiment 5

5.7.1 Experimental design

Female lister-hooded rats ($n = 31$) were trained on the LCRT task for 7 weeks before receiving a unilateral 6-OHDA MFB lesion as previously described. At 3-weeks post-lesion, rats underwent amphetamine-induced rotations, adjusting step, vibrissae-evoked task and LCRT testing to determine the extent of lesion-induced deficits. Two rats were excluded post-lesion due to 1 rat with an incomplete lesion as indicated by minimal rotational bias (fewer than 5 net rotations per minute) and 1 rat with poor ipsilateral accuracy on LCRT task. At 4 weeks post-lesion, ($n = 29$) rats received an infusion of AAV-htTH-hGCH1 into the medial (n = 12) or lateral striatum (n = 10) (called throughout this chapter as AAV-Medial and AAV-Lateral). Another group (n = 7) experienced a sham surgery. One sham was culled during experimentation due to ill health. A total of 3 animals from AAV-Medial and 2 animals from AAV-Lateral died due to complications during and after AAV surgery. All groups were tested on the same motor and cognitive tasks as previously stated at 4, 6 and 8 weeks post-AAV to identify any behavioural recovery induced by the medial or lateral infusion. At 5-weeks post-virus, rats received a L-DOPA challenge as described previously in Experiment 4 to review any L-DOPA induced dyskinesias, behavioural improvement due to L-DOPA or any interaction between DA precursor administration and viral-mediated DA production. Animals were transcardially perfused at 9 weeks post-AAV and brain tissue taken for histological analysis. The final n for each group analysed throughout this chapter is Sham n = 6, AAV-Lateral n = 5 and AAV-Medial n = 6. Timeline of the experiment is detailed below (Figure 5.10). To support the NC3R's recommendations for reduction in the number of animals in research when appropriate, Experiment 3 and Experiment 5 were experimentally run at the same time and share the sham group as a non-AAV treatment control.

Group	n = 31												n = 29	Sham n = 6								
														6-OHDA + AAV Lateral n = 5								
														6-OHDA + AAV Medial n = 7								
Weeks	-13	-12	-11	-10	-9	-8	-7	-6	-5	-4	-3	-2	-1	0	+1	+2	+3	+4	+5	+6	+7	+8	+9
Task			LCRT training					MFB lesion			LCRT Hand-testing	Amphet-induced rotations		AAV infusions				LCRT Hand-testing	L-DOPA Challenge	LCRT Hand-testing		LCRT Hand-testing	Perfuse

Figure 5.10. Experimental design of Experiment 5. 34 lister-hooded rats were trained on the Lateralised choice reaction time task (LCRT) for 7 weeks prior to receiving a unilateral 6-OHDA medial forebrain bundle lesion. 3 weeks post-lesion rats underwent LCRT testing and amphetamine-induced rotations task to confirm success of the lesion. Rats subsequently received a unilateral infusion of AAV-htTH-hGCH1 into either the lateral or medial striatum. Rats were tested on the LCRT task, adjusting steps and vibrissae-evoked task at 4, 6, and 8 weeks post-AAV infusion and underwent a 4.5mg/kg L-DOPA challenge at 5 weeks. Rats underwent a final round of amphetamine-induced rotations task at 9 weeks prior to perfusion.

5.7.2 AAV-htTH-hGCH1

The AAV viral vector used throughout this chapter is detailed previously in Experiment 3 and the construct is depicted in Figure 4.20. In brief, AAV-hTH-hGCH1 is a biscistronic AAV2/1 expressing the human tTH and GCH1 genes, driven by a CMV promoter and linked with the IRES sequence, EMCV. The AAV is infused at a titre of 1.45×10^{13}.

5.7.3 AAV Surgical procedure

Infusion coordinates for animals receiving either a medial or lateral infusion of AAV-htTH-hGCH1 were previously identified in Experiment 4 of this chapter (Figure 5.3). For AAV-Lateral; Site 1 and Site 2 both received 1.25 µl at DV1 and 1 µl at DV2. For AAV-Medial; Site 1 received 1 µl at an infusion rate of 0.4 µl per minute. At Site 2, DV1 received 1.25 µl, DV2 received 1 µl and DV3 received 0.25 µl. The viral vector was infused at a rate of 0.4 µl per minute. The diffusion time between each DV was 1-minute and 3-minutes at the final DV before removing the cannula.

5.7.4 LCRT program

Animals were trained on the LCRT task for 7 weeks on the protocol detailed in Table 6. Post-lesion, animals were tested on 200ms stimulus duration and 100,200,300 and 400 ms random limited hold. Rats were not tested on the modified version presented in chapter 4 due to a reasonable number of useable trials and accuracy post-lesion. Post-lesion data and week 6 average was calculated over 3 days. Average performance for week 4 and week 8 was calculated over 5 days. During the L-DOPA challenge, the majority of rats in the sham group did not initiate a contralateral response, so could not apply missing values to due being unconfident if statistical differences would be driven by the missing values or not. Therefore, only data that did not require missing values is presented. Due to some LCRT measures having mis-matched groups at baseline, baseline change modification was applied as described previously in Experiment 3.

5.7.5 AIMS scoring

AIMS scoring was carried out as previously mentioned in chapter 4 (see 4.7.5). Two animals from AAV-Lateral presented with L-DOPA induced dyskinesias and one animal in the sham group. Data is presented at as the breakdown of scores across the 7 subtypes and the final AIMS score.

5.7.6 Statistics

Analysis was undertaken using one-way ANOVA with repeated measures with Week (+0wk, +4wk, +6wk, +8wk, or 9wk for amphetamine rotations) as a within-subjects factor, and Group (Sham, AAV-Lateral and AAV-Medial) as a between-subjects factor. Tukey's post-hoc test was used for multiple comparisons with Group. During L-DOPA testing, one-way ANOVA with repeated measures was used with Drug (Saline, L-DOPA) as a factor.

5.8 Results: Experiment 5
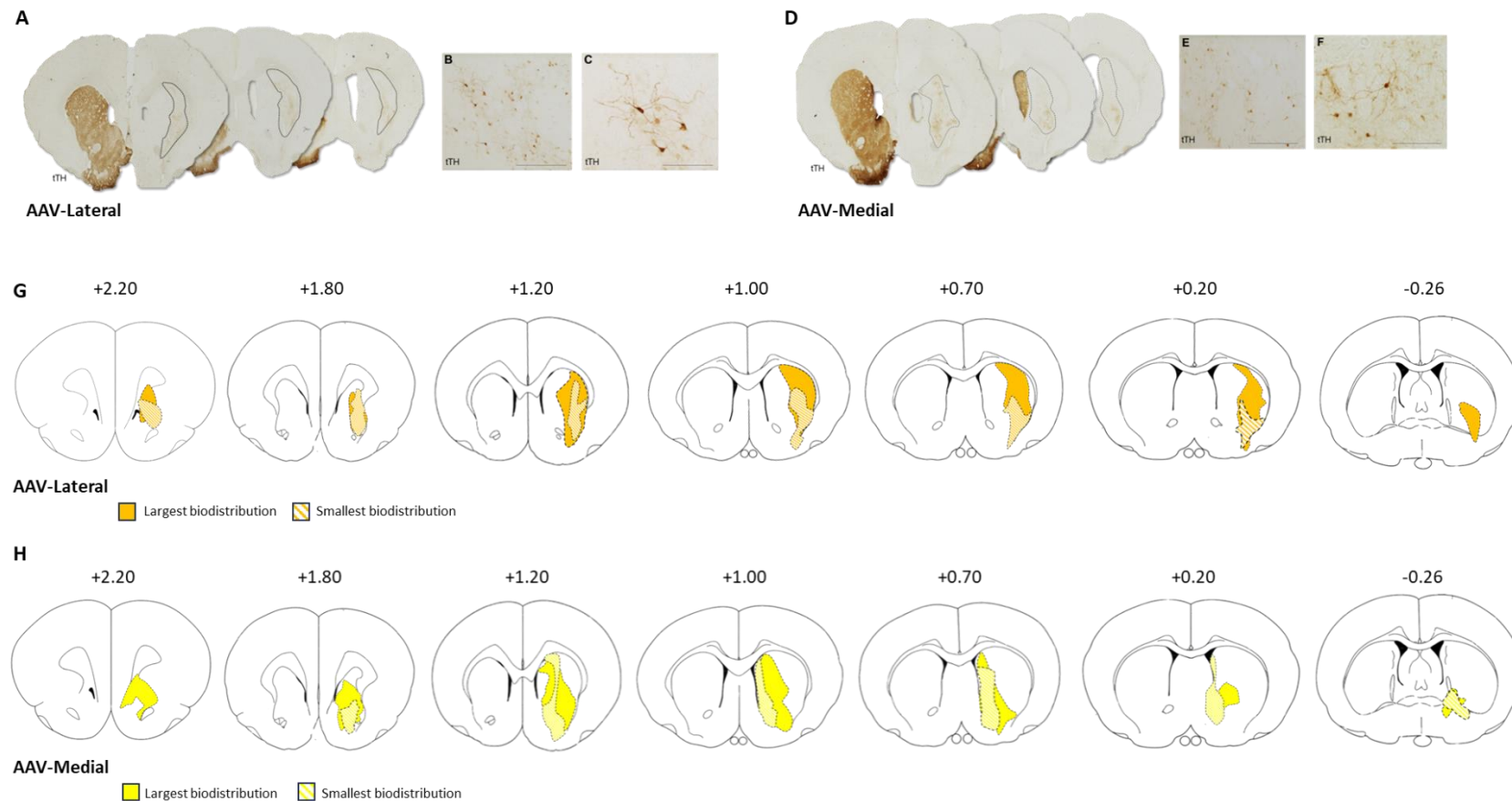
Figure 5.11. Histological analysis of viral expression of AAV-Lateral and AAV-Medial using tTH. **A-F)** Expression of AAV-htTH-hGCH1 was localised to the striatum and generally conserved to the medial and lateral striatal regions respectively. High magnification images indicated high specificity of the AAV to striatal neurons, with expression all along the axonal projections and boutons. **G-H)** Representative schematics of the AAV-htTH-hGCH1 expression detected through tTH expression at the most caudal point of expression and most rostral point of expression in with the smallest and largest biodistribution per group.

5.8.1 Histological analysis of AAV-hTH-hGCH1 in medial and lateral striatum

Localisation of AAV-htTH-hGCH1 to the medial and lateral striatum

Expression of AAV-htTH-hGCH1 was evaluated by tTH expression throughout the striatum (Figure 5.11). The biodistribution of the viral vector was conserved generally to the lateral and medial striatum respectively, with some minimal off-target expression in the corpus collosum and piriform cortex in AAV-Lateral treated brain sections. Off-target expression in AAV-Medial was concentrated to the ventral pallidum. Expression of tTH was higher in the rostral parts of the striatum, with little expression in the caudal striatal regions greater than bregma -0.3 AP). AAV-Lateral is within the same range of +2.1 AP from bregma and caudally ending around -0.3 AP. This caudal expression in AAV-Lateral tended to follow the corpus callosum. In AAV-Medial, the average positive tTH expression observed within the striatum is approximately +2.3 from bregma and the most caudal expression ends around -0.3 AP. In order to determine the range of tTH expression throughout the striatum in each group, the largest and smallest tTH expression for each animal per group was collated in Figure 5.11.G&H. The smallest expression level of tTH in AAV-Lateral was generally restricted to the lateral striatum, as was AAV-medial to the respective medial striatum, however, expression of AAV-Lateral was more uniform between groups, whereas AAV-medial tTH expression was focused around the NAc predominantly the more caudal it extended throughout the striatum.
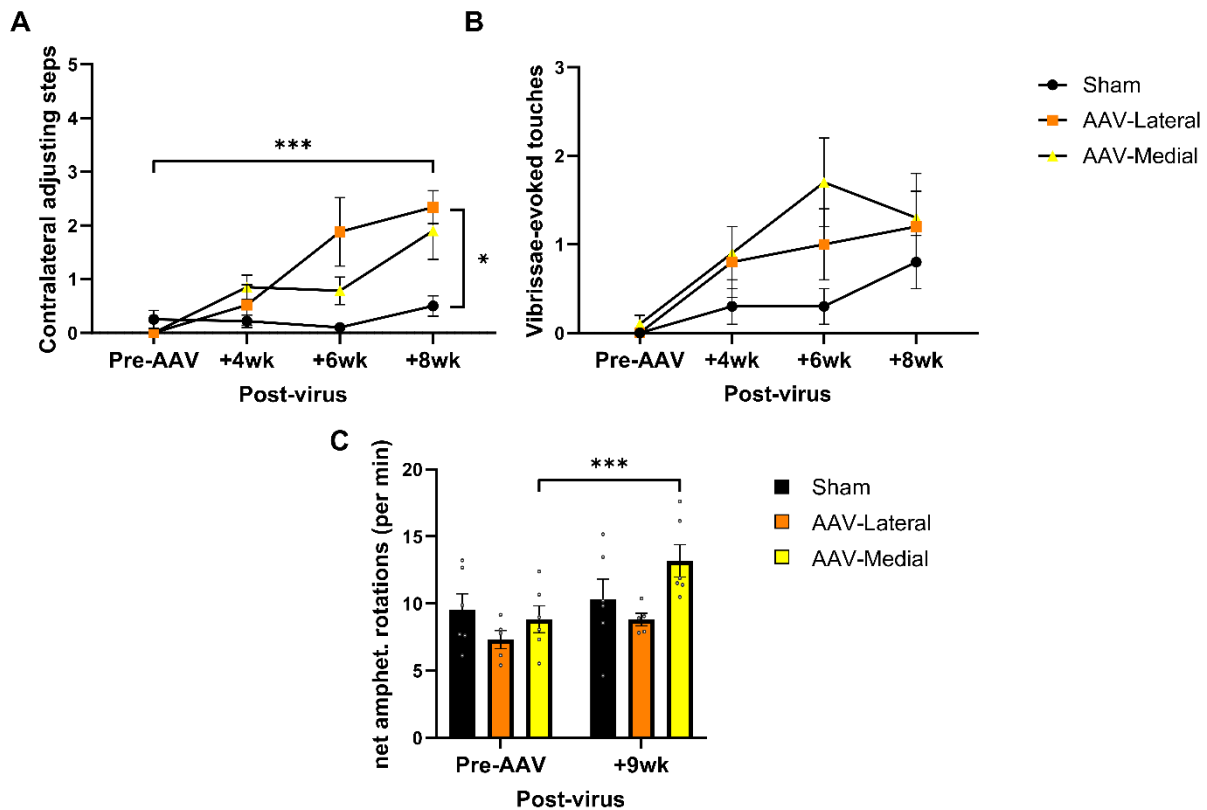
Figure 5.12. Simple motor function improved by regional-specific AAV infusion. Lateral AAV infusion improves some motor behaviour. **A)** *Contralateral adjusting steps were significantly improved due to AAV-Lateral infusion, as compared to the sham group and both AAV-Lateral and AAV-Medial from their own baseline.* **B)** *Vibrissae-evoked paw touches did not improve in either group 8 weeks post-viral infusion.* **C)** *Sham and AAV-Lateral rotational bias remained the same 9 weeks post-viral infusion, whereas AAV-Medial rotational bias increased. Scale bar for E and H represent 200μm; F and I represent 100μm. Significant differences between groups are indicated as *p <.05, and changes within groups are indicated as *** p <.001. Error bars represent standard error of the mean.*

5.8.2 Assessment of medial and lateral AAV infusions in motor recovery

AAV-htTH-hGCH1 improves contralateral adjusting steps

The impact of targeting AAV-htTH-hGCH1 expression to the medial and lateral striatal subregions was assessed using the adjusting steps test and vibrissae-evoked touch test, from 4-8 weeks post-AAV (Figure 5.12.A-C). Sham-treated rats made few contralateral adjusting steps throughout testing weeks, whereas both AAV-Lateral and AAV-Medial improved in adjusting steps, relative to their own baseline performance (Figure 5.12.A. Week*Group; $F(6,42) = 3.820$, $p = .004$); AAV-Lateral showed improvement from week 6 (Lateral; 0wk vs 6wk $p = .002$, 0wk vs 8wk, $p < .001$, 4wk vs 8wk, $p = .024$) and AAV-Medial from week 4 (0wk vs 4wk $p = .021$, 0wk vs 8wk, $p = .001$). AAV-Lateral rats performed more contralateral steps compared to Sham rats after 6 weeks post-virus (Group; $F(2,14) = 9.181$, $p = .003$, Lesion vs sham at 6wk $p = .012$ and 8wk, $p = .014$).

AAV-Lateral or AAV-Medial did not improve sensorimotor deficits or drug induced rotational bias

Vibrissae-evoked touches increased in all groups across 8 weeks resulting in lateral or medial AAV infusion not improving sensorimotor deficits (Figure 5.12.B. Week; $F(3,42) = 7.126$, $p = <.001$. Group; $F(2,14) = 2.004$, $p =$ n.s). Amphetamine-induced rotational bias did not differ compared to sham in AAV-Lateral treated rats 9 weeks post-AAV. Interestingly there was a significant increase in the number of ipsilateral rotations per minute performed by AAV-Medial treated rats (Figure 5.12.C. Week*Group; $F(2, 14) = 5.016$, $p = .023$, AAV-Medial +0wk vs +9wk, $p < .001$).
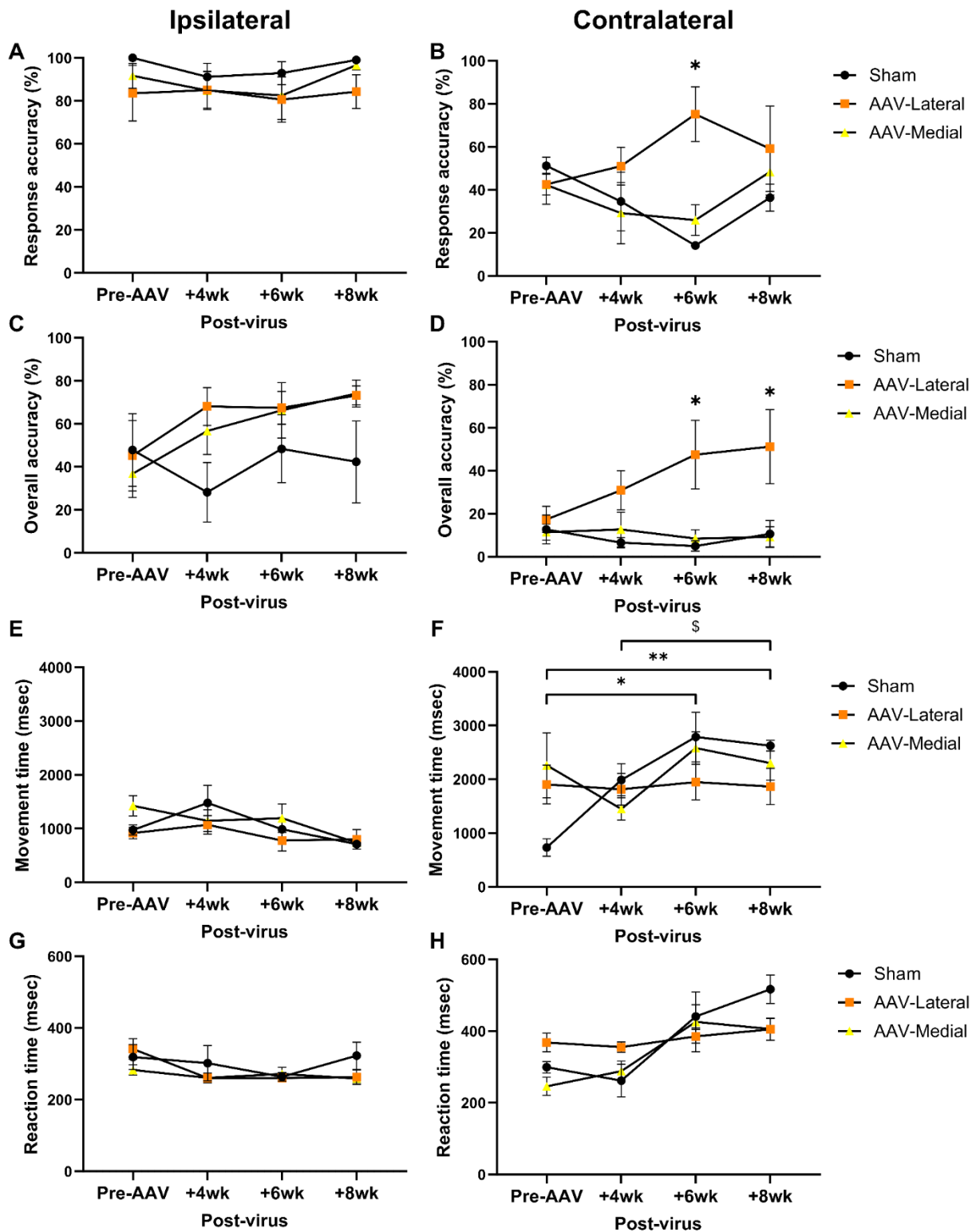
Figure 5.13. Impact of lateral and medial AAV-htTH-hGCH1 infusions on LCRT performance across 8 weeks. A) Response accuracy C) overall accuracy E) movement time and G) reaction time on the ipsilateral side did not differ among groups across the testing weeks. B) At 6 weeks post-virus, AAV-Lateral rats had a greater response accuracy than both AAV-Medial and shams. C) At both 6- and 8-weeks post-virus, AAV-Lateral infusion led to greater overall accuracy than AAV-Medial and sham. Significant differences between AAV-Lateral and Sham are indicated as *p <.05. F) Viral treated

groups showed no change in reaction time over 8 weeks post-AAV, but shams became slower at completing the task as well as AAV-Medial after 4 weeks. Significant differences within sham animals across the testing weeks for Movement time are indicated as *p <.05, **p <.01, *** p <.001. Significant differences within AAV-Medial across weeks is indicated at $ p <.05. **H)** Reaction time on contralateral side was not statistically different among groups. Error bars represent standard error of the mean.

5.8.3 Impact of localised AAV-htTH-hGCH1 on LCRT performance

AAV-Lateral improves response accuracy on LCRT task

Performance on the ipsilateral side did not differ among groups across the 8 weeks (Figure 5.13. (A) Response accuracy; $F_{(2,14)}$ = 1.165, p = n.s, (C) Overall accuracy; $F_{(2,14)}$ = 2.053, p = n.s, (E) Movement time; $F_{(2,14)}$ = .791, p = n.s, (G) Reaction time; $F_{(2,14)}$ = 1.440, p = n.s). On the contralateral side (Figure 5.13.B,D,F,H), AAV-Lateral infusions significantly improved their response accuracy after 6-weeks post-virus, whereas AAV-Medial showed no improvement (Week*Group; $F_{(6,42)}$ = 2.587, p = .032, +6wk: Lateral vs lesion p = <.001, Lateral vs medial, p = .002, Lateral; +0wk vs +6wk, p = .025, Lesion: +0wk vs +6wk, p = .005). By normalising the data, the effect of AAV-lateral improving response accuracy over time is diminished, however, overall AAV-Lateral were significantly more accurate than sham (Figure 5.15.A Group: $F_{(2,14)}$ = 3.966, p = .043. AAV-Lateral vs Sham, p = .035).

AAV-Lateral infusion improves overall accuracy on LCRT task

In relation to overall accuracy on the LCRT task (Figure 5.13.D), performance of both sham and AAV-Medial treated rats remained poor across the 8 weeks post-virus, whereas AAV-Lateral rats had significantly better overall accuracy on the task at week 6 and 8 post-virus (Week*Group; $F_{(6,42)}$ = 2.576, p = .032, +6wk: Lateral vs lesion, p = .012, Lateral vs Medial, p = .020, +8wk: Lateral vs Lesion, p = .039).

Movement time remained stable for AAV treated rats

Shams became slower across the 8 weeks post-virus (Figure 5.13.F) whereas AAV-Lateral rats remained stable in the time they took to complete the task (Group*week; $F_{(6,42)}$ = 2.895 , p = .019, Lesion: +0wk vs +6wk p = .011, +0wk vs +8wk p = .005, Medial: +4wk vs +6wk p = .058, +4wk vs +8wk p = .019). Contralateral movement time when normalised to its own baseline shows the same pattern as previously identified. Sham animals got progressively slower over time, whilst AAV-treated rats had no alteration in their movement time after 8-weeks post-AAV (Figure 5.15.B. Week*Group $F_{(6,42)}$ = 5.818, p <.001, Lesion from

baseline to wk4, 6 and 8 p = <.001. Sham vs AAV-treated groups at 4wks, p <.05, at wk6, p <.05 and at wk8, p <.01). Reaction time on the contralateral side was not significantly altered across weeks (Figure 5.13.G. Group; $F(2,14)$ = 1.053, p = n.s).
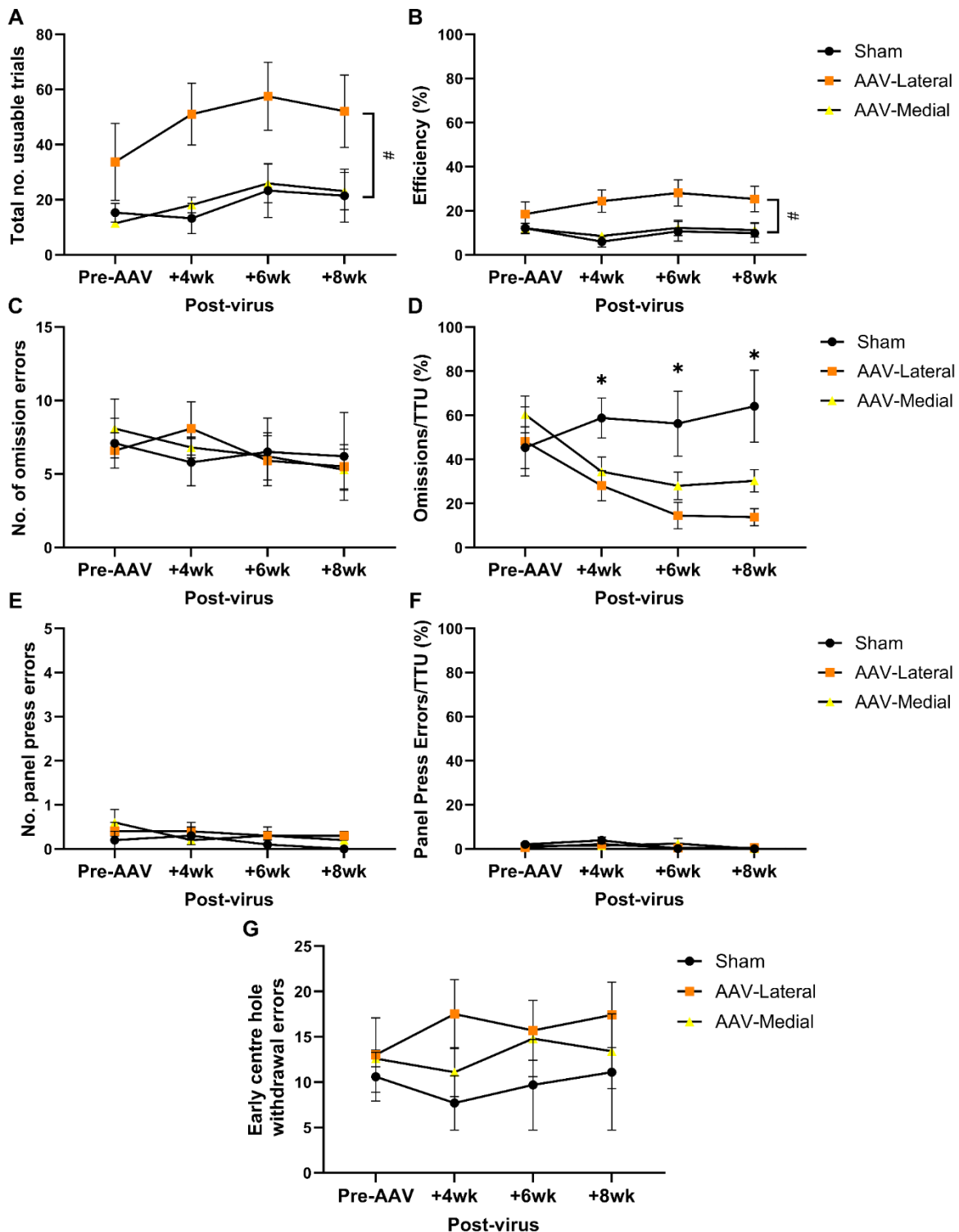
*Figure 5.14. AAV-Lateral and medial performance on non-side bias LCRT performance. **A-B)** AAV-Lateral performed more usable trials and were more efficient at the task compared to AAV-Medial and sham. **C-D)** Omission errors did not change between weeks of between groups, however when Omissions are analysed as a percentage of the total useable trials, Sham performed significantly more omissions than AAV-Lateral at 4, 6 and 8 weeks post-AAV. **E-G)** Panel press errors or early centre withdrawals did not differ among the groups across the testing period. Error bars represent standard error of the mean. Differences between groups are indicated at #p < .05. Differences between Sham and AAV-Lateral are indicated as *p = < .05.*

5.8.4 Impact of medial and lateral AAV infusion on non-lateralised aspects of LCRT

AAV infusion did not improve incentive motivation or efficiency

AAV-Medial did not differ to shams in the number of total useable trials performed across 8 weeks post-AAV whereas AAV-Lateral rats remained high in their motivation to perform the task (Figure 5.14.A. Group; $F(2,14) = 5.509$, $p = .017$, Lesion vs Lateral, $p = .025$, Lateral vs medial, $p = .032$). AAV-Lateral rats were also more efficient at performing the task (Figure 5.14.B. Group; $F(2,14) = 6.658$, $p = .009$, Sham vs AAV-Lateral $p = .012$, AAV-Lateral vs AAV-Medial $p = .023$). Improvements due to Lateral AAV infusion, seen in Figure 5.14.A-B were not robust enough to meet significance to due large variation among the groups. When normalised, AAV-Lateral treated rats were not more efficient on the LCRT task overall or across the 8-weeks post-AAV compared to Sham (Figure 5.15.C. Week: $F(3,42) = 2.423$, $p = .079$. Week*Group: 6,42 = 1.470, $p = .212$). AAV-Lateral did also not improve from their own baseline in the number of total useable trials performed across the weeks (Figure 5.15.D. Group: $F(2,14) = 1.170$, $p = $ n.s.).

AAV-htTH-hGCH1 infusion reduced omission errors

Errors performed during LCRT testing did not differ significantly between groups or alter across testing weeks (Figure 5.14. C. Group: Omission errors; $F(2,14) = .015$, $p = $ n.s, E. Panel press errors; $F(2,14) = 1.251$, $p = $ n.s. G. Early centre withdrawal errors; $F(2,14) = .793$, $p = $ n.s.). However, when the number of omissions were considered as a percentage performed out of the number of useable trials, significantly more useable trials ended up being omissions when performed by shams compared to AAV-Lateral treated rats (Figure 5.14.D. Week*Group: $F(6,42) = 3.728$, $p = .005$. Sham vs AAV-Lateral at +4wk $p = .045$, +6wk $p = .040$, +8wk $p = .017$). These findings are supported when groups are normalised to their own baseline (Figure 5.15.E. Week*Group: $F(6,42) = 2.954$, $p = .017$. Sham vs AAV-Lateral at +6wk, $p = .009$, and Medial $p = .020$. Group: $F(2,14) = 5.220$, Sham vs AAV-Lateral, $p = .039$, Sham vs Medial, $p = .050$). The percentage of panel press errors out of the total useable trials did not differ between groups or across the 8 weeks post-AAV (Figure 5.14.F. Group: 2,14 = .267, $p = $ n.s).
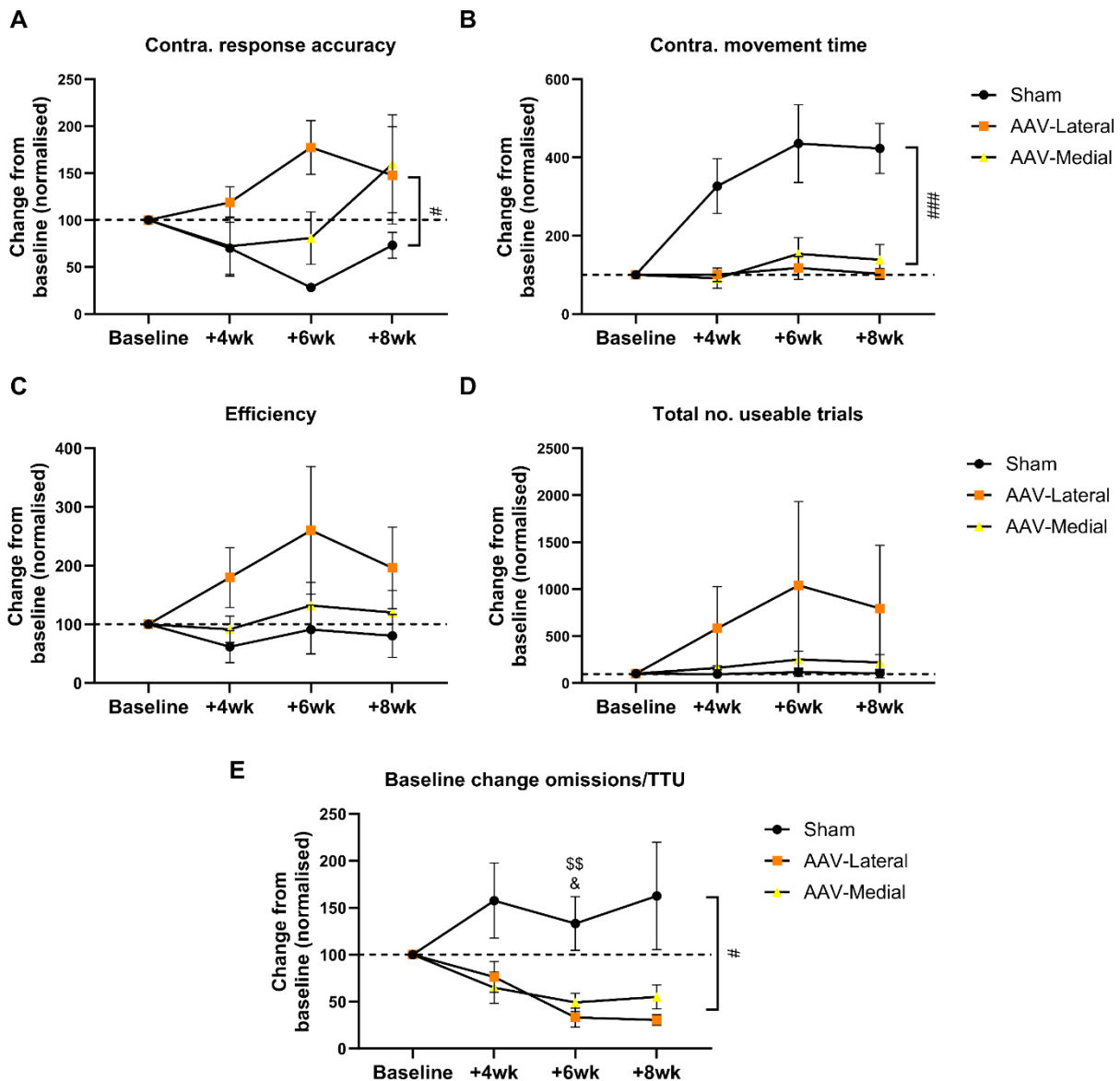
Figure 5.15. Normalisation of mis-matched baseline during LCRT performance. **A)** *Contralateral response accuracy was improved by AAV-Lateral infusion.* **B)** *Movement time is significantly slower due in sham animals compared to AAV treated rats.* **C-D)** *Efficiency and total useable trials did not change compared to sham post-AAV.* **E)** *Omissions as a percentage of the total useable trials increased in sham animals and significantly reduced over time in AAV treated rats. Error bars represent standard error of the mean (SEM). The dash line at '100' indicates baseline. Differences between groups are indicated as #p < .05, ##p <.01. Significant differences between Sham and AAV-Lateral at 6-weeks post-AAV in Omissions/TTU is indicated as $$p <.01, whereas differences between AAV-Lateral and AAV-Medial at the same timepoint is indicated a &p = <.05.*
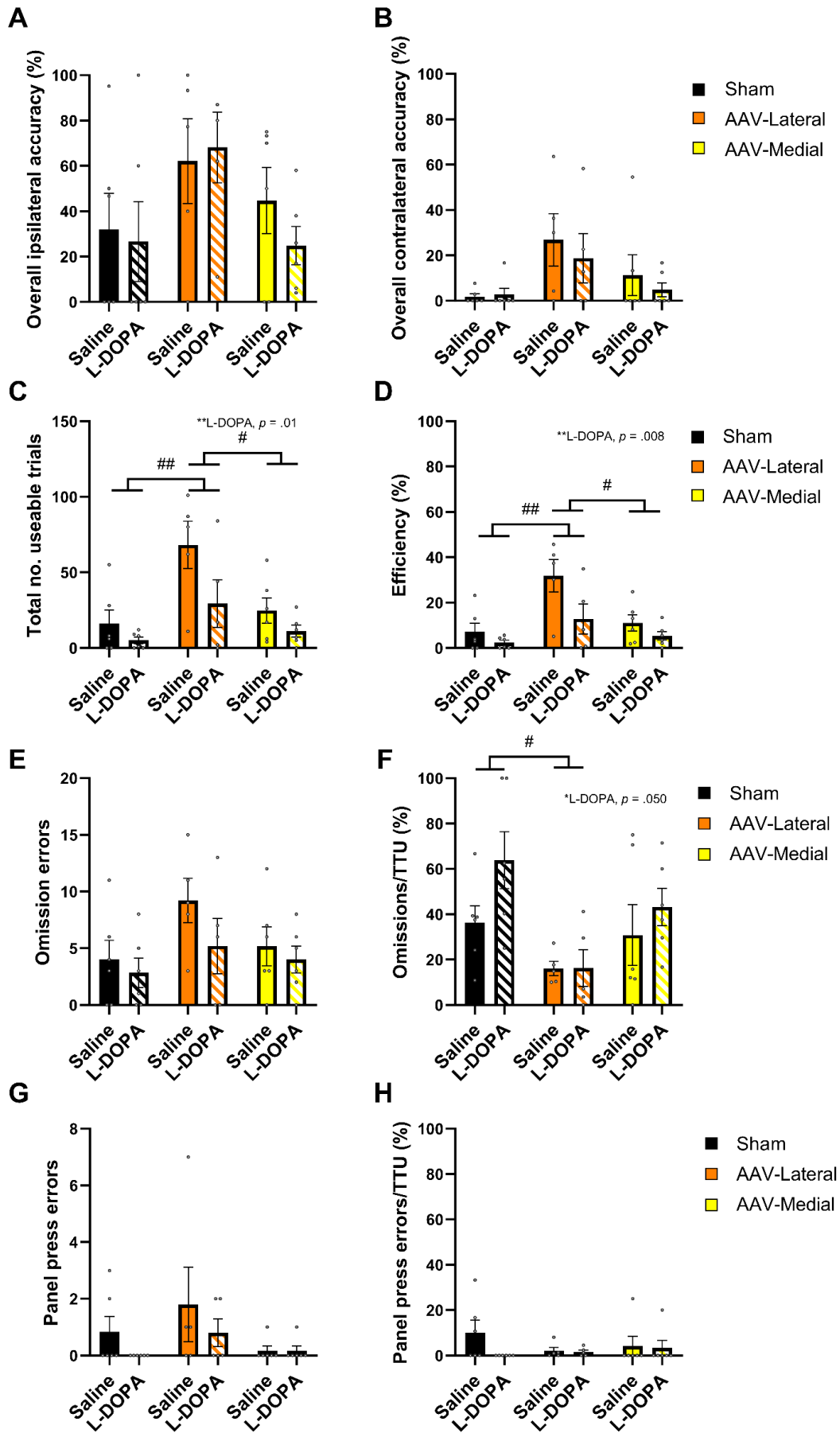
*Figure 5.16. Impact of 4.5mg/kg L-DOPA administration on localised AAV-htTH-hGCH1 infusions. **A)** Overall accuracy on the ipsilateral side was not affected by L-DOPA administration and overall accuracy was not different amongst groups. **B)** overall accuracy on the contralateral side was not impacted by L-DOPA administration. **C-D)** total useable trials an efficiency in performing the task was greater for AAV-treated rats and was not otherwise impacted by L-DOPA administration. **E&G)** The number of omissions and panel press errors were not significantly different or affected by L-DOPA. **F)** When omissions were analysed as a percentage of TTU, L-DOPA overall increased the percentage of omissions, and Shams performed significantly more than AAV-Lateral. **H)** No differences or impact of L-DOPA were found in panel press errors/TTU. Differences between groups are represented as #p <.05, ##p <.01. Error bars represent standard error of the mean.*

5.8.5 Impact of L-DOPA on LCRT performance in Sham and AAV-htTH-hGCH1 treated rats

L-DOPA does not impact overall accuracy in localised AAV-htTH-hGCH1 treated rats

On both the ipsilateral and contralateral side in relation to overall accuracy on the LCRT task (Figure 5.16.A-B), all groups were not significantly different from each other and were not otherwise impacted by the administration of 4.5mg/kg L-DOPA (Ipsilateral: Drug; $F(1,14) =$ 1.940, $p =$ n.s, Group; (2,14) = 3.390, $p =$ n.s, Contralateral: Drug; $F(1,14) = 2.592$, $p =$ n.s, Group; $F(2,14) = 2.387$, $p =$ n.s).

L-DOPA does not improve incentive motivation and worsens efficiency

Similar to Figure 5.14.A, both sham and AAV-Medial treated rats had low numbers of total useable trials (Figure 5.16.C), and performed a significantly lower number of those trials compared to AAV-Lateral when given either saline or L-DOPA (Group; $F(2,14) = 6.930$, $p =$ .008, Sham vs AAV-Lateral $p =$ .008, AAV-Lateral vs AAV-Medial $p =$ .031) however there was an overall effect of L-DOPA reducing the number of usable trials (Drug; $F(1,14) = 8.74$, $p =$ .010). AAV-Lateral infusions resulted in the greatest efficiency on the task compared to sham and AAV-Medial (Figure 5.16.D. Group; (2,14) = 7.889, $p =$ .005, AAV-Lateral vs sham $p =$ .005, AAV-Lateral vs AAV-Medial $p =$ .022). Overall, efficiency on the LCRT task appeared to be impacted by L-DOPA administration causing a reduction in efficiency (Drug; $F(1,14) = 9.410$, $p =$ .008).

No change to omissions or panel press errors due to L-DOPA

Omissions or panel press errors conducted were not affected by L-DOPA administration and did not differ among groups (Figure 5.16.E. Omissions: Drug; $F(1,14) = 2.744$, $p =$ n.s, Group; $F(2,14) = 2.090$, $p =$ n.s. G) Panel press errors: Drug; $F(1,14) = 2.395$, $p =$ n.s, Group; (2,14) = 1.669, $p =$ n.s. H) Panel press Errors/TTU: Group; $F(2,14) = .483$, $p =$ n.s). However, when omissions are calculated as a percentage of total useable trials, Sham animals perform a significantly greater number omissions compared to AAV-Lateral (Figure 5.16.F. Group: $F(2,14) = 4.102$, $p =$ .040. Sham vs AAV-Lateral, $p =$ .032). L-DOPA administration indicated a trend in increasing the number of omission errors (Drug: $F(1,14) = 4.580$, $p =$ .050).

A

B

	Rat A (Sham)		Rat B (AAV-Lateral)		Rat C (AAV-Lateral)	
	Amplitude	**Duration**	**Amplitude**	**Duration**	**Amplitude**	**Duration**
Neck dystonia	2	2	1	2	1.5	2
Trunk torsion	3	2	1	3	2	2
Forelimb dyskinesia	3	3	1	1	1	2
Hind limb dystonia	2	1	0	0	1	1
Orolingual	2	2	0	0	1	1
Head bobbing	0	0	1	1	2	2
Forelimb-facial stereotypy	1	1	1	2	1	3
Final AIMS score	26		9		18	
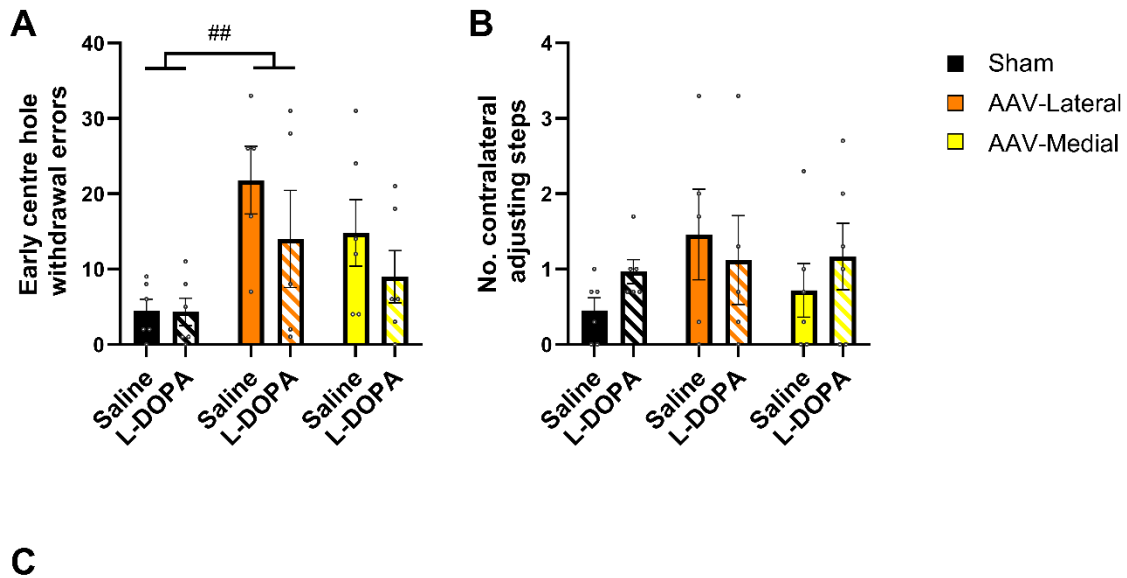
*Figure 5.17. Impact of L-DOPA on early centre hole withdrawal errors, contralateral adjusting steps, and the onset of dyskinesias evaluated by AIMS score. **A)** AAV-lateral rats had a greater number of centre hole withdrawal errors compared to Sham, and this was not affected by L-DOPA administration. **B)** Contralateral steps were not improved at 5 weeks post-AAV, nor where they improved by L-DOPA. **C)** Three animals out of all tested during the L-DOPA challenge displayed dyskinetic behaviour that could be scored with AIMS scoring. Two AAV-Lateral animals displayed dyskinetic movements, and one Sham that received the most severe score.*

5.8.6 Impact L-DOPA on medial and lateral AAV infusions in regard to early withdrawal errors and motor function

AAV-Lateral rats perform greater early centre withdrawal errors

Early centre hole withdrawal errors remained low for shams during this L-DOPA treatment task and AAV-Lateral had the greatest number of these errors compared to shams, and no difference compared to AAV-Medial rats (Figure 5.17.A). L-DOPA did not impact the number of early centre withdrawal errors (Drug; $F(1,14) = 2.725$, p = n.s, Group; $F(2,14) = 4.908$, p = .024, AAV-Lateral vs sham, p = .020, AAV-Medial vs sham or AAV-Lateral p = n.s).

L-DOPA did not improve motor function in AAV-htTH-hGCH1 treated rats

At 5 weeks post-virus (Figure 5.17.B), contralateral adjusting steps in MX1-treated groups did not differ significantly to shams and did not improve due to the administration of L-DOPA (Drug; ($F(1,14) = .645$, p = n.s, Group; $F(2,14) = .749$, p = n.s).

Evaluation of LIDs

During the 4.5mg/kg L-DOPA challenge, 3 rats displayed dyskinetic behaviour such that it was appropriate to apply the AIMS score (Figure 5.17.C). Rat A from the sham group was the most severe in AIMS scores compared to Rat B and C. Both Rat B and C displayed strong trunk torsion and forelimb dyskinesia. Rat B was less severe in AIMS score due to the ability to correct posture and return to a normal position for a brief period of time, whereas Rat A appeared locked into dystonic movements with some chewing of the forearm and hind limb dystonia.

During observation of the onset of dyskinesias among the groups, abnormal behaviour began with contralateral rotations that eventually led to chronic trunk torsion and forelimb dyskinesias in 3 rats 30 minutes post-injection. Mild contralateral rotations when given L-DOPA administration were observed in a further 2 rats but did not meet the criteria for dyskinesias (1 sham rat and 1 from the AAV-Lateral group). A few contralateral rotations were observed in 4 rats (3 from the AAV-Medial group and 1 in the sham group, however this was not during L-DOPA administration so cannot infer a relationship between rotation onset and L-DOPA. However, it is important to note that observed spontaneous contralateral rotations in those 4 animals were only observed the day after L-DOPA administration.

5.9 Discussion: Experiment 5

5.9.1 Medial AAV infusions did not improve visuospatial function

The aim of Experiment 5 was to (1) utilise viral-mediated DA biosynthesis to probe the lateral and medial striatum for motor and cognitive recovery and (2) further evaluate the impact of L-DOPA on cognitive function. As detailed in experiment 4, denervation of DA in the medial striatum impaired visuospatial function (Figure 5.8.B), so it was reasonable to expect that DA replacement in the medial striatum would support recovery in visuospatial function. Both AAV-Lateral and AAV-Medial infusions led to improvement in adjusting steps (Figure 5.12.A), however only AAV-Lateral infusions were able to alleviate visuospatial dysfunction 6 weeks post-AAV (Figure 5.13.B). L-DOPA administration of 4.5mg/kg overall led to impaired efficiency and incentive motivation on the LCRT task and resulted in LIDs in a small population of AAV-Lateral rats (Figure 5.16.C). It is important to note however that AAV-Medial and AAV-Lateral infusions led to improvements in the percentage of omissions made (Figure 5.15.E). The results in this experiment were contrary to the hypothesis that medial AAV infusions would alleviate cognitive function, outlining the complexity of cognitive recovery with DA replacement. It is important to consider what factors might contribute to this dichotomy in results from Experiment 4 to Experiment 5.

AAV-Lateral infusion might support habitual responding

In the unilateral 6-OHDA MFB lesion model there is complete denervation in both the lateral and medial striatum, therefore animals may be impaired in both goal-directed and habitual responding (Shen et al. 2008; Heuer and Dunnett 2012; Lindgren et al. 2014b). When DA is replaced in the lateral striatum in Experiment 5, one hypothesis is that the supply of DA is supporting habitual responding. Darvas and Palmiter (2009) as previously stated, showed that restoration of DA signalling in the DA depleted mice just within the dorsolateral striatum could facilitate cognitive recovery in object recognition and visuospatial learning, as could DA restoration restricted to the dorsomedial striatum, however they saw impairments in motivation due to medial restoration (Darvas and Palmiter 2010). Due to groups being mis-matched at baseline, analysing baseline change indicates that recovery in response accuracy by AAV-Lateral is robust enough to still meet significance (Figure 5.15.A), however

one major limitation to these results is that it is very underpowered with only *n* = 5 in AAV-lateral. Therefore, recovery due to AAV-lateral infusion must be caveated by the small sample size.

Does training on the LCRT task promote habitual responding?

Although the studies mentioned throughout Experiment 4 have identified different behaviours supported by the lateral and medial striatum, the striatum must be flexible and respond by shifting between habitual and goal-directed behaviour depending on the requirements, and these behaviours are considered to compete in situations of stress (Lehéricy et al. 2005; Hikosaka and Isoda 2010; Gremel and Costa 2013). One hypothesis for not seeing improvement in visuospatial function with AAV-Medial infusions is that responding on the LCRT task has shifted to require habitual responding, and due to the infusion being restricted to the medial striatum, impairments in stimulus-response habit formation could not be alleviated. Pharmacological DA replacement in PD patients has been shown to support goal-directed learning (de Wit et al. 2012; Sharp et al. 2016), leading to the original hypothesis that medial striatal DA restoration would support recovery on this task. However, medial AAV infusions did not alleviate visuospatial function, suggesting that either response on the task is governed by habitual stimulus-response, or the DA replacement in the medial AAV infusion was not optimised correctly to support goal-directed behaviours. Going forward, it would be an imperative to determine whether animals who are trained on the LCRT task after 7 weeks are responding due to goal-directed or habitual responding by running devaluation trials at different time points during training, as in this study we cannot explicitly rule in or out animals' performing due to habitual or goal-directed responding.

AAV-Medial infusions potentially disrupting cognitive function

Another hypothesis for the results in Experiment 5 is that direct targeting of the medial striatum with a viral vector is affecting MSN function and as a consequence, disrupting visuospatial function. As shown in Chapter 4 there was greater [18^F]Fallypride binding within the AAV core compared to the rest of lesioned hemisphere (Figure 4.18), therefore direct targeting of the viral vector could be upregulating D2/3 receptors within the medial striatum and disrupting local circuitry. Krabbe et al. (2015) observed that increased D2 receptor activity changed the firing pattern of the VTA neurons but did not disrupt the SNc, suggesting

that the two ventral midbrain areas mediate DA differently. However, [18^F]Fallypride imaging was not carried out within this study, or with AAV-htTH-GCH1, so cannot explicitly state that receptor changes are the cause of AAV-medial infusions not alleviating visuospatial deficits. Further PET imaging with D1 and D2 ligands could provide beneficial information relating to striatal function when targeted for TH and GCH1 gene transfer.

Optimisation of dosage

The titre of the viral vector may be a critical factor determining the impact of the gene therapy. Here only a single titre was investigated, moreover, the coverage may be variable between rats Figure 5.11.G-H indicates the largest and smallest biodistribution of the viral vector, visualised by tTH expression. Both AAV-Lateral and AAV-Medial have expression restricted to their respective areas, however the smallest AAV-Medial spread was focused to the NAc instead of the entire length of the Medial striatal region. Therefore, there could instead be an effect of the dose not being high enough to promote cognitive recovery.

In a dosing study with an AAV expressing AADC infused into a NHP PD model, researchers found the relationship between dose and behavioural improvements to be linear once a threshold had been reached where the supply of AADC was no longer rate-limiting (Forsayeth et al. 2006). However, a high titre of AAV-hTH-2AhGCH1 in Chapter 4 was found to negatively impact visuospatial function, thus highlighting the complexity of recovery of cognitive function with DA replacement. In order to determine what role dose of viral vector has on medial vs lateral governed cognitive and motor function, another experiment using a high and low dose in the same medial and lateral striatal subregions, evaluating performance on the LCRT could answer the question on whether targeted medial AAV infusions is disrupting visuospatial processing.

As visualised by histological analysis, tTH expression was located throughout the entire striatal neuron Figure 5.11.B-C & E-F), with enough detail to make out dendritic spines. It is important to note however, that tTH expression was markedly lower compared to those in Figure 4.6. Due to the level of detail available with the tTH stain, spine analysis to determine any morphological changes to MSNs due to virus uptake might provide a greater picture of the effect of transducing MSNs with the ability to release L-DOPA has on MSNs and whether they are negatively impacted by this.

5.9.2 The impact of L-DOPA treatment

The overall impact of L-DOPA in Experiment 5 was to worsen performance on the LCRT task. 4.5 mg/kg L-DOPA led to fewer total useable trials (Figure 5.16. C), worse efficiency at the task (Figure 5.16.D) and a greater number of omissions/TTU, meaning the trials that animals did initiate, a higher percentage of them are incorrect due to not poking in any lateralised hole (Figure 5.16.F). However, L-DOPA had no effect on overall accuracy (Figure 5.16.A-B). As previously stated in Darvas and Palmiter (2009), DA restoration in the lateral striatum should be enough to support recovery in visuospatial function and other cognitive measures, therefore when L-DOPA is administered to the AAV-medial rats, L-DOPA should be able to act on the denervated striatum and support visuospatial function, but this does not support the findings in this chapter.

As stated in the Chapter 4 introduction, there is evidence within the literature indicating that L-DOPA can improve cognitive function, so it is reasonable to expect L-DOPA would improve performance on the LCRT (Calabresi et al. 2007; Ketzef et al. 2017; Lebedev et al. 2020). The impact of these findings and other experiments within this thesis using L-DOPA has implications on the application of pharmacological DA replacement. The difficulty with concluding the effect of L-DOPA throughout this thesis is that is appears to improve, have no effect, or worsen different parameters of the LCRT that are all considered DA-mediated. In Experiment 2, L-DOPA impaired almost all contralateral measures in a dose response manner in the Sham group yet improved contralateral response accuracy in AAV-high treated rats. When there was greater biodistribution of viral-mediated DA throughout the striatal nuclei in Experiment 3, L-DOPA at 4.5mg/kg had no effect on the LCRT task (Figure 4.27). When DA is depleted in the medial striatum in Experiment 4, L-DOPA was able to reduce movement time deficits, yet the same pattern was found in experiment 5 with L-DOPA reducing incentive motivation (Figure 5.9.A) and efficiency at the task (Figure 5.9.B).

Impact of dose of L-DOPA on cognitive function

It is important to consider what factors may be affecting the results found with L-DOPA. One factor could be the dose. L-DOPA administration in PD patients is continuously monitored (Miller and Abercrombie 1999; Oiwa et al. 2003) and modified in alignment with their clinical symptoms (Brooks 2008). L-DOPA was administered at 4.5mg/kg throughout at a relatively low dose in order to reduce the likelihood of LIDs manifesting (Tronci and Francardo 2018).

Thus, a different dose may have different effects on behaviour, and these effects may also be different in the partial vs full lesion models. A systematic dose-response study would address this.

Due to the way that L-DOPA is administered, flooding effects in other brain regions cannot be ruled out. Measures have been taken to try and reduce the L-DOPA conversion in peripheral tissues, such as having benserazide in the solution (Rinne et al. 1972), but the drug will undoutedly affect the function of the cortex and other regions with DA receptors, which may have an effect on behaviour. Lesions in the SNc in mice have shown to induce memory deficits that could not be recovered by L-DOPA which they theorise may be due to flooding in the prefrontal cortex and hippocampus (Da Cunha et al. 2002).

5.9.3 Medial and Lateral striatal AAV infusion can support simple motor behaviour recovery

Infusions into either the medial or lateral striatum improved adjusting steps from its own baseline at 8 weeks post-AAV (Figure 5.12.A). It was theorised that due to lateral striatal lesions inducing forelimb akinesia in experiment 4, that treating the lateral striatum with AAV-htTH-hGCH1 in the 6-OHDA MFB rat model, would improve motor performance and no improvement would be seen with AAV-medial. This experiment indicates that alleviation of simple motor deficits may not depend on specific targeting. However, as indicated in the tTH expression in both AAV-medial and AAV lateral A-F), in the most rostral part of the striatum there was overlap of biodistribution into both the medial and lateral striatum, which may be responsible for the marked reduction in forelimb akinesia. It is important to note that the scale of improvement in adjusting steps was not to the level of complete reversal, as there was only about a 20% improvement in adjusting steps. Furthermore, there was no improvement in vibrissae-evoked paw touches compared to sham, nor in amphetamine-induced rotations (Figure 5.12.B-C). One theory is that the dose is too low to see considerable improvement in motor deficits, as with previous biscistronic viral vectors have shown motor recovery to be dose dependant (Cederfjäll et al. 2013; Cederfjäll et al. 2015). However, as previously stated in (chapter 4), due to the passive release of DA from due to viral vector transfection, recovery in rotational bias is not favoured. It would also be important

to evaluate a low and high viral vector titre in the medial and lateral striatum in order to corroborate findings on the dose-dependency of motor recovery.

5.9.4 Conclusion

To conclude Experiment 5, the aim was to probe the unilaterally DA depleted medial and lateral striatum with viral-mediated DA biosynthesis and evaluate cognitive function on the LCRT task. AAV-htTH-hGCH1 infusions into the lateral striatum improved visuospatial function, whilst medial infusions showed no improvement. The knowledge gained from this experiment reveal that replacement of DA to alleviate cognitive function is not as straightforward as Experiment 4 would have predicted, and further investigation is required to determine the parameters are important for optimal cognitive recovery.

5.10 Chapter Discussion

Chapter 5 provided a detailed evaluation of the contribution of striatal subregions to cognitive function in the LCRT task under DA depletion and restoration modifications. This chapter discussion aims to overview common themes that may impact cognitive recovery and what key take home messages have arisen from this chapter.

5.10.1 Replacing DA is not straightforward

There appears to be an established relationship between DA loss and loss of function, evident in Experiment 4 and throughout the literature in relation to motor function (Grealish et al. 2008; Torres and Dunnett 2012; Lindgren et al. 2014b) and inducing cognitive impairments in the LCRT task (Reading et al. 1991; Dowd and Dunnett 2004; Heuer et al. 2013c). However, the relationship between DA loss and DA replacement appears not to be as straightforward. In relation to motor improvement, the relationship between DA loss and DA replacement seems more linear. This is shown with L-DOPA in patients (Uitti et al. 1993; Sy and Fernandez 2020), fetal-derived DA grafts (Kordower et al. 1995; Olanow et al. 2003), viral vectors utilised in gene therapy (Eberling et al. 2008; Palfi et al. 2018; Christine et al. 2022) and Experiment 5 having marked adjusting steps improvement due to DA replacement (Figure 5.12.A).

This linear relationship between DA loss and DA replacement however has not been the case for cognitive recovery. There have been instances in which DA replacement has improved DA-dependant cognitive impairments such as visuospatial function as seen by AAV-Lateral infusions in Experiment 5 (Figure 5.15.A) and Lelos et al. (2016), as well as others (Dowd and Dunnett 2004). So, it is possible to alleviate DA-dependant cognitive impairments with DA, but the application of DA to alleviate cognitive impairments requires far more optimisation to prevent adverse effects.

A potential factor that could prevent DA from alleviating cognitive impairments in the LCRT task could be placement of the viral vector preventing DA synthesis of important target areas. A suggested advantage of cell and gene therapies is the ability to target select brain regions and to reduce off-target expression. Experiment 2 highlighted the importance of

minimizing off-target piriform cortex and amygdala expression of the viral-vector as this may have detrimental effects of mesocortical circuitry (Cools and D'Esposito 2011). However, an alternative argument may be that DA denervation occurs in other cortical and subcortical regions in both people with Parkinson's and in the MFB model. One example of an extra-striatal A10 target regions that is DA depleted in the 6-OHDA lesion model is the anterior cingulate cortex, which has long been associated with cognitive impairment in PD (Leech and Sharp 2014; Vogt 2019). Thus, some level of replacement in these extra-striatal regions may be necessary to support function.

AAV-Medial rats in Experiment 5 had minimal off-target cortical expression and no alleviation of visuospatial dysfunction was evident, which might suggest that more optimised targeting may be a better approach. Yet, as stated previously, cortical DA functions largely on an 'inverted U', so it could be hypothesised that certain DA replacements are enough for motor recovery yet is too much for cognitive recovery.

In addition to this, Experiment 4 aided our understanding that the medial and lateral striatum may govern different aspects of cognitive function, i.e goal-directed behaviour, habit formation and incentive motivation, and that these can be impaired when DA is depleted. This data has contributed to the understanding of DA transmission in the medial striatum, by identifying a role in incentive motivation due to impaired efficiency and overall, few usable trials, demonstrating that DA transmission in the lateral striatum is not required for this neural process.

5.10.2 The use of viral vectors to probe DA replacement

Viral vectors used in this experiment and Experiment 2, 3 and 5 were an effective tool for the biosynthesis of DA. However, the drawback of employing viral vectors to evaluate the role of DA replacement is that the results can be confounded by several technical factors (efficiency of DA production, off-target expression or poor biodistribution. Nevertheless, viral vector mediated DA biosynthesis is a vital tool to selectively induce DA transduction into a specific target region that is not offered by other forms of DA replacement such as L-DOPA administration.

To conclude, the experiments detailed in Chapter 5 have helped develop the understanding of the role of DA in a range of motor and cognitive behaviours, as well as identifying factors that may be important for DA-mediated cognitive recovery that are beneficial for both pre-clinical application of studying DA, and viral-mediated DA biosynthesis for clinical application.

Chapter 6 : General Discussion

6.1 Key findings

Experiment 1

- Both hfVM and hESC-derived DA grafts can alleviate motor impairments 21 weeks post graft

- hESC-derived DA grafts did not alleviate visuospatial dysfunction 20 weeks post-graft

---

Experiment 2

- AAV-htTH-2A-hGCH1 at a high titre (1.69×10^{13}) impairs visuospatial function

- Acute L-DOPA administration in the 6-OHDA lesioned rat model induces dyskinetic-like behaviours

---

Experiment 3

- Greater biodistribution of AAV-htTH-hGCH1 throughout the striatum leads to more accurate visuospatial processing at 6 weeks post-AAV, whilst having a subtle improvement in adjusting steps

---

Experiment 4

- Medial striatal lesions impair visuospatial function and incentive motivation, whilst Lateral striatal lesions do not

- Lateral striatal lesions induce forelimb akinesia, whilst medial striatal lesion do not

- L-DOPA improved movement time in medial lesioned rats, but overall impacted incentive motivation

---

Experiment 5

- Lateral infusion of AAV-htTH-hGCH1 into the striatum of the 6-OHDA lesioned rat improves visuospatial deficits at 6 weeks post-AAV

- Medial infusion of AAV-htTH-hGCH1 does not improve visuospatial function

---

The aim of this thesis was to understand the (1) role of DA in cognitive impairments when DA is depleted in the two major striatal-midbrain circuits, and (2) the role of DA in cognitive recovery when the dose, biodistribution, placement and source of DA is manipulated in the unilateral 6-OHDA MFB lesioned rat model. This thesis revealed that the role of DA in cognitive recovery is complex, and different factors may contribute to its success in alleviating visuospatial function in the LCRT task. This discussion aims to cover the key findings of the thesis, as well as the limitations provided by the model and the implications of these findings for the clinic.

6.2 Challenges of modelling cognitive impairments in preclinical models of PD

In order to model cognitive impairments, this project relied on the unilateral 6-OHDA lesion model and the LCRT task, with the placement of 6-OHDA changed to target the terminal ends in Experiment 4. There are clear benefits to using 6-OHDA within the field of PD research, especially when evaluating the efficacy of DA replacement, such as cell replacement therapy, however there are setbacks to using this model when evaluating both motor and cognitive impairments.

6.2.1 Assessing motor and cognitive impairments

The model has a rapid onset of nigrostriatal loss depending on the injection site which means it can be utilised within a minimum of 3 weeks to observe robust motor deficits (Torres and Dunnett 2012). Although this model was useful in evaluating the role of DA, this model lacks some pathological characteristics of PD such as alpha-synuclein aggregation, Lewy body formation and the gradual degeneration over time. This prevents evaluating the interaction between DA replacement strategies and PD pathology, such as the potential accumulation of alpha-synuclein in the graft over time (Li et al. 2008) or the ability to model degeneration and evaluate the appropriate time to administer different DA replacement strategies.

This thesis relied heavily on the lateralised choice reaction time task to be informative about cognitive deficits within the PD rat model. The benefits of the LCRT are the ability to probe for multiple cognitive behaviours and the ability to modify the task measurements (Carli et al. 1985; Heuer et al. 2013a). It is important to consider how comparable findings are on the LCRT task for PD patients. Patients do present with visuospatial dysfunction, and deficits in attention, action selection and incentive motivation. These are predominately early-stage non-motor symptoms (Magnard et al. 2016). Thus, a benefit of the LCRT task is that the cognitive changes being measured are relevant to PD and dopamine dependent.

As mentioned, one of limitations of this model is the inability to evaluate the impact of degeneration. It would be beneficial to evaluate behaviour over the course of the disease. Willard et al. (2015) gradually dosed 6-OHDA into the striatum to mimic DA terminal degeneration and found a time-dependant increase in motor deficits, so this could be a feasible option to implement in relation to cognitive behaviour. It would be informative to assess performance of the alpha-synuclein viral vector model in this task, to better characterise the manifestation of deficits as the pathology progresses.

One of the main problems with the unilateral 6-OHDA MFB lesion model is that the operant task has to work within the parameters of a unilateral motor deficit, meaning that the most common cognitive tasks cannot be applied as they are bilateral in nature. There are tests that have shown to be sensitive to unilateral cognitive deficits, such as the elevated T-maze with unilateral medial frontal cortex lesions (Croxson et al. 2014). However, the elevated T-maze is also probing for decision making which the LCRT task can also apply to, highlighting the lack of options related to cognitive tasks with a unilateral model. It is important to consider that patients experience many different non-motor symptoms that have a significant impact on quality of life such as REM sleep disorder, depression and anxiety (Pellicano et al. 2007). As such, it is important that a number of cognitive impairments are evaluated in their response to DA replacement. To address this, optimisation of the bilateral alpha-synuclein model may be a reasonable approach. However, it has been shown that there is compensation in this model long-term (Kirik et al. 2002a) and the use of immunosuppressants can significantly reduce pathology (Tamburrino et al. 2015) creating challenges for assessing human cell replacement therapies.

6.2.2 Implications for pre-clinical research

Another challenge of this model is the inability to fully distinguish the caudate from the putamen in rodents. Medial striatal lesions in Experiment 4 were found to impair visuospatial function and incentive motivation on the LCRT task. However, others have reported the opposite effect in which bilateral SNc lesions induced motivation deficits and VTA lesions did not (Decamp and Schneider 2004; Drui et al. 2014). It must be noted that 6-OHDA as a tool to selectively lesion is difficult due to the tendency of 6-OHDA to diffuse through the VTA and SNc. Therefore, it is important that NHP experiments are looked upon for the impact of the caudate and putamen in DA replacement paradigms (Choudhury and Daadi 2018).

6.3 Implications for the clinic

6.3.1 Implications of cell therapy for the clinic: too much of a good thing?

An impactful finding from this thesis is that hESC-DA grafts were not able to alleviate cognitive impairments, and this result was found in two different hESC derived cell therapy products made from different labs. The significance of this is that hESC-derived grafts are currently entering early phase clinical trials, so it is important to recognise that although many pre-clinical optimisations have been made, there are still discrepancies between hPSC-derived and hfVM transplants in their ability to alleviate cognitive impairments. This therefore highlights that it is imperative to consider carrying out cognitive tests in pre-clinical efficacy studies for PD, alongside motor tasks.

Understanding additional parameters of the graft such as the neurite outgrowth could be informative. Here, there was an increase in medial innervation observed in hfVM grafts that correlated with better accuracy on the LCRT task. As shown in US clinical trials reported in Freed et al. (2001), improvements were identified in the Schwab and England sub sections of the UPDRS score, as well as improvement on the global subjective scoring. Post-mortem

tissue from this study showed innervation out from the putamen injection site and also in the anterior caudate. This provides clinical evidence that may support the fact that medial innervation is important for cognitive improvements. However, they also reported innervation into the surrounding putamen in an older patient who did not report any clinical benefit to the transplant.

In general clinical studies have targeted transplants to the putamen (Kordower et al. 1998), however there are studies that have employed caudate transplants of hfVM tissue into PD patients (Spencer et al. 1992). Patients with caudate transplants were able to reduce their DAergic medication and researchers found normalisation of [18^F]Fallypride binding compared to before the surgery but reported that the putamen continued to decline. As outlined by Barker et al. (2015), the shift away from transplanting into the separation between the putamen and caudate was due to minimal motor recovery, therefore putamenal transplants were favoured due to their complete alleviation of rotational bias in pre-clinical studies, and better UPDRS motor scores in clinical studies.

This focus on motor recovery has directly impacted pre-clinical efficacy studies for hESC-derived DA progenitors (Grealish et al. 2014), and as a consequence, cognitive recovery appears to be overlooked. I think what can be learned from Chapter 3 is that the approach for cell replacement therapy shouldn't be to favour motor recovery without considering the cognitive implications. It might prove beneficial to reinnervate both caudate and putamen circuits in order to restore function, so perhaps smaller deposits targeting both regions might be overall beneficial to patients.

6.3.2 Implications of gene therapy for the clinic

As described throughout, viral vectors have been utilised for gene therapy and have passed safety and efficacy studies and have shown encouraging results in relation to motor improvements. This thesis used two biscistronic viral vectors to effectively transfer genes encoding TH and GCH1 to striatal MSNs to produce L-DOPA and convert that into DA. This work found important complications that may impact the application of gene therapy. Some of these complications are related to the placement, off-target expression, biodistribution.

Pre-clinical studies utilising gene therapy have shown off-target expression at titres greater and smaller than $1x10^{11}$ as used in Cederfjäll et al. (2013) and all have shown some level of motor improvement. However, pre-clinical studies utilising gene therapy have not investigated this off-target effect of cognitive impairments of PD, considering Experiment 2 highlighted a potential side-effect of off-target expression could be to disrupt cortical circuitry, further work within the field is required to optimise delivery of viral vectors.

Experiment 3 and 5 highlighted that either lateral infusion or improved biodistribution of viral-mediated DA biosynthesis was able to support visuospatial function. So, in theory, considering most of the current trials and NHP studies using biscistronic viral vectors for PD have focused on a putamenal infusion, that should be sufficient DA replacement to support cognitive recovery, however this has not been substantiated clinically (Palfi et al. 2018; Christine et al. 2022). As shown in Experiment 2, dose can be a contributing factor to worsening visuospatial function, supported by the inverted 'U' theory of cortical circuitry mediating (Cools and D'Esposito 2011). Due to the ability to titrate the amount of virus to an area, it seems reasonable to employ a caudate infusion at a lower dose than what is supplied to the putamen and evaluate the response. NHP models of PD have also been shown to have cognitive deficits in executive function and attention so would be able to isolate the two striatal regions and evaluate the impact of dose to those specific areas.

6.3.3 Implications of L-DOPA for the clinic

The consensus throughout this thesis, when evaluating the results of Experiments 3 to 5 is that acute administration of L-DOPA does not directly impact visuospatial function. Although Sham animals decreased in their visuospatial performance in a dose response manner in Experiment 2, this was confounded by the onset of abnormal dyskinetic movements in shams. This lack of effect was seen in patients observed on a visual processing tasks (Anderson and Stegemöller 2020). However, we should be tentative in making the leap that DA doesn't have a role in visuospatial function due to the inability to isolate L-DOPA just to areas of DA depletion (Vaillancourt et al. 2013). What can possibly be inferred is that continuous supplies of DA within this thesis (cell and gene therapy) showed evidence of improving visuospatial function, furthering the general consensus that pulsatile

administration of L-DOPA should not be considered for treatment of cognitive impairments in PD.

6.4 Future directions

Although this thesis has provided further understanding about the role of DA in cognitive impairments in the LCRT task, future work could build upon this knowledge with alternative techniques.

6.4.1 Spatial transcriptomics

As mentioned throughout Chapter 4 and Chapter 5, DA has been quantified through histological analysis of tTH expression within the striatum as a surrogate marker of AAV mediated gene delivery to striatal MSNs. This however does not provide any detailed information about the quantity of this gene transfer to striatal MSNs and the wider context of this to the striatum. One technique that could be beneficial to employ is spatial transcriptomics. Jang et al. (2023) detailed the use of this technique to further quantify the tropism of viral vector gene delivery. Applying this to the work described in this thesis could provide quantifiable information about the level of tTH expression within those cells, and perhaps any disruption of normal striatal MSN gene expression because of this. Spatial transcriptomics have also been employed for hESC-derived DA grafts, suggesting that this technique could also be applied to understand further about discrepancies between those and hfVM grafts (Rájová et al. 2023).

6.4.2 Optogentics

With regards to the striatal lesion experiment, the aim was to distinguish between the two distinct midbrain and striatal circuitry, and although we were able to identify a difference between the medial and lateral striatum, we are inferring upon the role of the VTA and SNc in that behaviour without directly targeting and also there was some overlapping of areas in places. One technique that would be useful is the selective switching on and off of the VTA/SNc to probe for these regions, through optogenetics. It has been previously shown

that selective stimulation of the VTA, promotes positive reinforcement during reward seeking (Adamantidis et al. 2011). Further studies using optogenetics found VTA and SNc stimulation to both have a role in promoting reward seeking. Using optogentics with the LCRT, along with devaluation parameters, would provide the ability to isolate each circuitry and probe for function during the task. Optogenetics have very recently been applied to hESC-derived DA transplants and found stimulation of the grafts improved their alleviation of motor deficits (Anderson et al. 2023).

6.5 Closing remarks

The overarching aim of this thesis was to understand more about the role of DA in cognitive impairments in a PD rat model, and what implications the findings may have for current and novel DA replacement strategies. Utilising two different cell therapy products, this thesis has outlined discrepancies between the current gold standard, hfVM, and hESC-derived grafts. In addition, this thesis used DA-ergic viral vectors and pharmacological DA replacement to isolate different factors that could be important for cognitive recovery. It was found that placement, dose, and biodistribution could all have an impact. The main finding of this thesis is that DA-mediated cognitive recovery is complex and requires considerable optimisation in order to be most beneficial. It should also be considered within the field to adopt more cognitive testing in pre-clinical studies to evaluate the impact of DA on cognitive recovery.

References

Aarsland, D., Andersen, K., Larsen, J. P., Lolk, A., Nielsen, H. and Kragh-Sørensen, P. 2001. Risk of dementia in Parkinson's disease: a community-based, prospective study. *Neurology* 56(6), pp. 730-736. doi: 10.1212/wnl.56.6.730

Abeliovich, A. et al. 2000. Mice Lacking α-Synuclein Display Functional Deficits in the Nigrostriatal Dopamine System. *Neuron* 25(1), pp. 239-252. doi: https://doi.org/10.1016/S0896-6273(00)80886-7

Abercrombie, E. D., Bonatz, A. E. and Zigmond, M. J. 1990. Effects of L-dopa on extracellular dopamine in striatum of normal and 6-hydroxydopamine-treated rats. *Brain Res* 525(1), pp. 36-44. doi: 10.1016/0006-8993(90)91318-b

Adamantidis, A. R. et al. 2011. Optogenetic interrogation of dopaminergic modulation of the multiple phases of reward-seeking behavior. *J Neurosci* 31(30), pp. 10829-10835. doi: 10.1523/jneurosci.2246-11.2011

Adams, C. D. and Dickinson, A. 1981. Instrumental Responding following Reinforcer Devaluation. *The Quarterly Journal of Experimental Psychology Section B* 33(2b), pp. 109-121. doi: 10.1080/14640748108400816

Adeosun, S. O., Hou, X., Zheng, B., Melrose, H. L., Mosley, T. and Wang, J. M. 2017. Human LRRK2 G2019S mutation represses post-synaptic protein PSD95 and causes cognitive impairment in transgenic mice. *Neurobiol Learn Mem* 142(Pt B), pp. 182-189. doi: 10.1016/j.nlm.2017.05.001

Adler, A. F. et al. 2019. hESC-Derived Dopaminergic Transplants Integrate into Basal Ganglia Circuitry in a Preclinical Model of Parkinson's Disease. *Cell Rep* 28(13), pp. 3462-3473.e3465. doi: 10.1016/j.celrep.2019.08.058

Albin, R. L., Young, A. B. and Penney, J. B. 1989. The functional anatomy of basal ganglia disorders. *Trends Neurosci* 12(10), pp. 366-375. doi: 10.1016/0166-2236(89)90074-x

Alexander, G. E. and Crutcher, M. D. 1990. Functional architecture of basal ganglia circuits: neural substrates of parallel processing. *Trends in Neurosciences* 13(7), pp. 266-271.

Alexander, G. E., DeLong, M. R. and Strick, P. L. 1986. Parallel organization of functionally segregated circuits linking basal ganglia and cortex. *Annu Rev Neurosci* 9, pp. 357-381. doi: 10.1146/annurev.ne.09.030186.002041

Alvarez-Fischer, D. et al. 2008. Modelling Parkinson-like neurodegeneration via osmotic minipump delivery of MPTP and probenecid. *J Neurochem* 107(3), pp. 701-711. doi: 10.1111/j.1471-4159.2008.05651.x

Amit, M. et al. 2000. Clonally derived human embryonic stem cell lines maintain pluripotency and proliferative potential for prolonged periods of culture. *Dev Biol* 227(2), pp. 271-278. doi: 10.1006/dbio.2000.9912

Amita, H., Kim, H. F., Smith, M. K., Gopal, A. and Hikosaka, O. 2019. Neuronal connections of direct and indirect pathways for stable value memory in caudal basal ganglia. *Eur J Neurosci* 49(5), pp. 712-725. doi: 10.1111/ejn.13936

Anderberg, R. H., Anefors, C., Bergquist, F., Nissbrandt, H. and Skibicka, K. P. 2014. Dopamine signaling in the amygdala, increased by food ingestion and GLP-1, regulates feeding behavior. *Physiology & Behavior* 136, pp. 135-144. doi: https://doi.org/10.1016/j.physbeh.2014.02.026

Anderson, K. A., Whitehead, B. J., Petersen, E. D., Kemme, M. R., Wedster, A., Hochgeschwender, U. and Sandstrom, M. I. 2023. Behavioral context improves optogenetic stimulation of transplanted dopaminergic cells in unilateral 6-OHDA rats. *Behavioural Brain Research* 441, p. 114279. doi: https://doi.org/10.1016/j.bbr.2022.114279

Anderson, S. and Stegemöller, E. L. 2020. Effects of Levodopa on Impairments to High-Level Vision in Parkinson's Disease. *Front Neurol* 11, p. 708. doi: 10.3389/fneur.2020.00708

Andersson, E. et al. 2006. Identification of intrinsic determinants of midbrain dopamine neurons. *Cell* 124(2), pp. 393-405. doi: 10.1016/j.cell.2005.10.037

Andres-Mateos, E. et al. 2009. Unexpected lack of hypersensitivity in LRRK2 knock-out mice to MPTP (1-methyl-4-phenyl-1,2,3,6-tetrahydropyridine). *J Neurosci* 29(50), pp. 15846-15850. doi: 10.1523/jneurosci.4357-09.2009

Annett, L. E., McGregor, A. and Robbins, T. W. 1989. The effects of ibotenic acid lesions of the nucleus accumbens on spatial learning and extinction in the rat. *Behavioural Brain Research* 31(3), pp. 231-242. doi: https://doi.org/10.1016/0166-4328(89)90005-3

Antonini, A., Yegin, A., Preda, C., Bergmann, L. and Poewe, W. 2015. Global long-term study on motor and non-motor symptoms and safety of levodopa-carbidopa intestinal gel in routine care of advanced Parkinson's disease patients; 12-month interim outcomes. *Parkinsonism & Related Disorders* 21(3), pp. 231-235. doi: https://doi.org/10.1016/j.parkreldis.2014.12.012

Aransay, A., Rodríguez-López, C., García-Amado, M., Clascá, F. and Prensa, L. 2015. Long-range projection neurons of the mouse ventral tegmental area: a single-cell axon tracing analysis. *Front Neuroanat* 9, p. 59. doi: 10.3389/fnana.2015.00059

Arcizet, F. and Krauzlis, R. J. 2018. Covert spatial selection in primate basal ganglia. *PLOS Biology* 16(10), p. e2005930. doi: 10.1371/journal.pbio.2005930

Arlotta, P., Molyneaux, B. J., Jabaudon, D., Yoshida, Y. and Macklis, J. D. 2008. Ctip2 controls the differentiation of medium spiny neurons and the establishment of the cellular architecture of the striatum. *J Neurosci* 28(3), pp. 622-632. doi: 10.1523/jneurosci.2986-07.2008

Ascherio, A. and Schwarzschild, M. A. 2016. The epidemiology of Parkinson's disease: risk factors and prevention. *The Lancet Neurology* 15(12), pp. 1257-1272. doi: https://doi.org/10.1016/S1474-4422(16)30230-7

Athanassi, A., Dorado Doncel, R., Bath, K. G. and Mandairon, N. 2021. Relationship between depression and olfactory sensory function: a review. *Chem Senses* 46, doi: 10.1093/chemse/bjab044

Aurich, M. F., Rodrigues, L. S., Targa, A. D., Noseda, A. C. D., Cunha, F. D. and Lima, M. M. 2017. Olfactory impairment is related to REM sleep deprivation in rotenone model of Parkinson's disease. *Sleep Science* 10(1), p. 47.

Axelsen, T. M. and Woldbye, D. P. D. 2018. Gene Therapy for Parkinson's Disease, An Update. *J Parkinsons Dis* 8(2), pp. 195-215. doi: 10.3233/jpd-181331

Azzouz, M. et al. 2002. Multicistronic lentiviral vector-mediated striatal gene transfer of aromatic L-amino acid decarboxylase, tyrosine hydroxylase, and GTP cyclohydrolase I induces sustained transgene expression, dopamine production, and functional improvement in a rat model of Parkinson's disease. *J Neurosci* 22(23), pp. 10302-10312. doi: 10.1523/jneurosci.22-23-10302.2002

Backlund, E. O. et al. 1985. Transplantation of adrenal medullary tissue to striatum in parkinsonism. First clinical trials. *J Neurosurg* 62(2), pp. 169-173. doi: 10.3171/jns.1985.62.2.0169

Badin, R. A. et al. 2019. Gene Therapy for Parkinson's Disease: Preclinical Evaluation of Optimally Configured TH:CH1 Fusion for Maximal Dopamine Synthesis. *Mol Ther Methods Clin Dev* 14, pp. 206-216. doi: 10.1016/j.omtm.2019.07.002

Balleine, B. and Killcross, S. 1994. Effects of ibotenic acid lesions of the Nucleus Accumbens on instrumental action. *Behavioural Brain Research* 65(2), pp. 181-193. doi: https://doi.org/10.1016/0166-4328(94)90104-X

Balleine, B. W. and O'Doherty, J. P. 2010. Human and Rodent Homologies in Action Control: Corticostriatal Determinants of Goal-Directed and Habitual Action. *Neuropsychopharmacology* 35(1), pp. 48-69. doi: 10.1038/npp.2009.131

Bankiewicz, K. S. et al. 2000. Convection-enhanced delivery of AAV vector in parkinsonian monkeys; in vivo detection of gene expression and restoration of dopaminergic function using pro-drug approach. *Exp Neurol* 164(1), pp. 2-14. doi: 10.1006/exnr.2000.7408

Bankiewicz, K. S. et al. 2006. Long-term clinical improvement in MPTP-lesioned primates after gene therapy with AAV-hAADC. *Mol Ther* 14(4), pp. 564-570. doi: 10.1016/j.ymthe.2006.05.005

Barbagallo, G. et al. 2017. Structural connectivity differences in motor network between tremor-dominant and nontremor Parkinson's disease. *Hum Brain Mapp* 38(9), pp. 4716-4729. doi: 10.1002/hbm.23697

Barbeau, A. 1971. Long-term side-effects of levodopa. *Lancet* 1(7695), p. 395. doi: 10.1016/s0140-6736(71)92226-4

Barker, R., Drouin-Ouellet, J. and Parmar, M. 2015. Cell-based therapies for Parkinson disease-past insights and future potential. *Nature Reviews Neurology* 11(9), pp. 492-503. doi: 10.1038/nrneurol.2015.123

Barone, P. et al. 2009. The PRIAMO study: A multicenter assessment of nonmotor symptoms and their impact on quality of life in Parkinson's disease. *Mov Disord* 24(11), pp. 1641-1649. doi: 10.1002/mds.22643

Bartus, R. T. et al. 2013. Safety/feasibility of targeting the substantia nigra with AAV2-neurturin in Parkinson patients. *Neurology* 80(18), pp. 1698-1701. doi: 10.1212/WNL.0b013e3182904faa

Basile, G. A., Bertino, S., Bramanti, A., Ciurleo, R., Anastasi, G. P., Milardi, D. and Cacciola, A. 2021. Striatal topographical organization: Bridging the gap between molecules, connectivity and behavior. *Eur J Histochem* 65(s1), doi: 10.4081/ejh.2021.3284

Bayram, E. et al. 2023. Clinical trials for cognition in Parkinson's disease: Where are we and how can we do better? *Parkinsonism Relat Disord* 112, p. 105385. doi: 10.1016/j.parkreldis.2023.105385

Beato, R. et al. 2008. Working memory in Parkinson's disease patients: clinical features and response to levodopa. *Arq Neuropsiquiatr* 66(2a), pp. 147-151. doi: 10.1590/s0004-282x2008000200001

Beccano-Kelly, D. A. et al. 2015. LRRK2 overexpression alters glutamatergic presynaptic plasticity, striatal dopamine tone, postsynaptic signal transduction, motor activity and memory. *Hum Mol Genet* 24(5), pp. 1336-1349. doi: 10.1093/hmg/ddu543

Beigi, M., Wilkinson, L., Gobet, F., Parton, A. and Jahanshahi, M. 2016. Levodopa medication improves incidental sequence learning in Parkinson's disease. *Neuropsychologia* 93(Pt A), pp. 53-60. doi: 10.1016/j.neuropsychologia.2016.09.019

Ben-Hur, T., Idelson, M., Khaner, H., Pera, M., Reinhartz, E., Itzik, A. and Reubinoff, B. E. 2004. Transplantation of human embryonic stem cell-derived neural progenitors improves behavioral deficit in Parkinsonian rats. *Stem Cells* 22(7), pp. 1246-1255. doi: 10.1634/stemcells.2004-0094

Best, J. A., Nijhout, H. F. and Reed, M. C. 2009. Homeostatic mechanisms in dopamine synthesis and release: a mathematical model. *Theor Biol Med Model* 6, p. 21. doi: 10.1186/1742-4682-6-21

Betarbet, R., Sherer, T. B., MacKenzie, G., Garcia-Osuna, M., Panov, A. V. and Greenamyre, J. T. 2000. Chronic systemic pesticide exposure reproduces features of Parkinson's disease. *Nat Neurosci* 3(12), pp. 1301-1306. doi: 10.1038/81834

Bethlem, J. and Den Hartog Jager, W. A. 1960. The incidence and characteristics of Lewy bodies in idiopathic paralysis agitans (Parkinson's disease). *J Neurol Neurosurg Psychiatry* 23(1), pp. 74-80. doi: 10.1136/jnnp.23.1.74

Bhatia, K. P. and Marsden, C. D. 1994. The behavioural and motor consequences of focal lesions of the basal ganglia in man. *Brain* 117(4), pp. 859-876. doi: 10.1093/brain/117.4.859

Bhattarai, Y. et al. 2021. Role of gut microbiota in regulating gastrointestinal dysfunction and motor symptoms in a mouse model of Parkinson's disease. *Gut Microbes* 13(1), p. 1866974. doi: 10.1080/19490976.2020.1866974

Björklund, A. and Dunnett, S. B. 2019. The Amphetamine Induced Rotation Test: A Re-Assessment of Its Use as a Tool to Monitor Motor Impairment and Functional Recovery in Rodent Models of Parkinson's Disease. *Journal of Parkinson's disease* 9, pp. 17-29. doi: 10.3233/JPD-181525

Björklund, A., Kirik, D., Rosenblad, C., Georgievska, B., Lundberg, C. and Mandel, R. J. 2000. Towards a neuroprotective gene therapy for Parkinson's disease: use of adenovirus, AAV and lentivirus vectors for gene transfer of GDNF to the nigrostriatal system in the rat Parkinson model. *Brain Res* 886(1-2), pp. 82-98. doi: 10.1016/s0006-8993(00)02915-2

Björklund, A. and Lindvall, O. 2017. Replacing Dopamine Neurons in Parkinson's Disease: How did it happen? *J Parkinsons Dis* 7(s1), pp. S21-s31. doi: 10.3233/jpd-179002

Björklund, A. and Stenevi, U. 1979. Reconstruction of the nigrostriatal dopamine pathway by intracerebral nigral transplants. *Brain Res* 177(3), pp. 555-560. doi: 10.1016/0006-8993(79)90472-4

Bjorklund, L. M. et al. 2002. Embryonic stem cells develop into functional dopaminergic neurons after transplantation in a Parkinson rat model. *Proc Natl Acad Sci U S A* 99(4), pp. 2344-2349. doi: 10.1073/pnas.022438099

Björklund, T., Carlsson, T., Cederfjäll, E. A., Carta, M. and Kirik, D. 2010. Optimized adeno-associated viral vector-mediated striatal DOPA delivery restores sensorimotor function and prevents dyskinesias in a model of advanced Parkinson's disease. *Brain* 133(Pt 2), pp. 496-511. doi: 10.1093/brain/awp314

Björklund, T. and Kirik, D. 2009. Scientific rationale for the development of gene therapy strategies for Parkinson's disease. *Biochim Biophys Acta* 1792(7), pp. 703-713. doi: 10.1016/j.bbadis.2009.02.009

Blanchet, P. J. et al. 2004. Relevance of the MPTP primate model in the study of dyskinesia priming mechanisms. *Parkinsonism Relat Disord* 10(5), pp. 297-304. doi: 10.1016/j.parkreldis.2004.02.011

Blandini, F. et al. 2009. Functional and neurochemical changes of the gastrointestinal tract in a rodent model of Parkinson's disease. *Neurosci Lett* 467(3), pp. 203-207. doi: 10.1016/j.neulet.2009.10.035

Blaschko, H. 1939. The specific action of L-dopa decarboxylase. *J Physiol* 96(50), pp. 50-51.

Blume, S. R., Cass, D. K. and Tseng, K. Y. 2009. Stepping test in mice: A reliable approach in determining forelimb akinesia in MPTP-induced Parkinsonism. *Experimental Neurology* 219(1), pp. 208-211. doi: https://doi.org/10.1016/j.expneurol.2009.05.017

Bodis-Wollner, I., Yahr, M. D., Mylin, L. and Thornton, J. 1982. Dopaminergic deficiency and delayed visual evoked potentials in humans. *Ann Neurol* 11(5), pp. 478-483. doi: 10.1002/ana.410110507

Boi, L., Johansson, Y., Tonini, R., Moratalla, R., Fisone, G. and Silberberg, G. 2023. Serotonergic and dopaminergic neurons in the dorsal raphe are differentially altered in a mouse model for Parkinson's disease. eLife Sciences Publications, Ltd.

Boix, J., Padel, T. and Paul, G. 2015. A partial lesion model of Parkinson's disease in mice – Characterization of a 6-OHDA-induced medial forebrain bundle lesion. *Behavioural Brain Research* 284, pp. 196-206. doi: https://doi.org/10.1016/j.bbr.2015.01.053

Bolam, J. P., Hanley, J. J., Booth, P. A. and Bevan, M. D. 2000. Synaptic organisation of the basal ganglia. *J Anat* 196 (Pt 4)(Pt 4), pp. 527-542. doi: 10.1046/j.1469-7580.2000.19640527.x

Booij, J. and Knol, R. J. J. 2007. SPECT imaging of the dopaminergic system in (premotor) Parkinson's disease. *Parkinsonism & Related Disorders* 13, pp. S425-S428. doi: https://doi.org/10.1016/S1353-8020(08)70042-7

Borghammer, P. 2023. The brain-first vs. body-first model of Parkinson's disease with comparison to alternative models. *J Neural Transm (Vienna)* 130(6), pp. 737-753. doi: 10.1007/s00702-023-02633-6

Brady, M. V. and Vaccarino, F. M. 2021. Role of SHH in Patterning Human Pluripotent Cells towards Ventral Forebrain Fates. *Cells* 10(4), doi: 10.3390/cells10040914

Braver, T. S. and Cohen, J. D. 2000. On the control of control: The role of dopamine in regulating prefrontal function and working memory. *Control of cognitive processes: Attention and performance XVIII* (2000),

Breger, L. S., Dunnett, S. B. and Lane, E. L. 2013. Comparison of rating scales used to evaluate l-DOPA-induced dyskinesia in the 6-OHDA lesioned rat. *Neurobiology of Disease* 50, pp. 142-150. doi: https://doi.org/10.1016/j.nbd.2012.10.013

Brooks, A. I., Chadwick, C. A., Gelbard, H. A., Cory-Slechta, D. A. and Federoff, H. J. 1999. Paraquat elicited neurobehavioral syndrome caused by dopaminergic neuron loss. *Brain Res* 823(1-2), pp. 1-10. doi: 10.1016/s0006-8993(98)01192-5

Brooks, D. J. 2008. Optimizing levodopa therapy for Parkinson's disease with levodopa/carbidopa/entacapone: implications from a clinical and patient perspective. *Neuropsychiatr Dis Treat* 4(1), pp. 39-47. doi: 10.2147/ndt.s1660

Brown, V. J. and Robbins, T. W. 1989. Deficits in response space following unilateral striatal dopamine depletion in the rat. *J Neurosci* 9(3), pp. 983-989. doi: 10.1523/jneurosci.09-03-00983.1989

Brozoski, T. J., Brown, R. M., Rosvold, H. E. and Goldman, P. S. 1979. Cognitive deficit caused by regional depletion of dopamine in prefrontal cortex of rhesus monkey. *Science* 205(4409), pp. 929-932. doi: 10.1126/science.112679

Buck, P. O., Trautman, H. and Clark, J. 2010. Scales for assessing nonmotor symptom severity changes in Parkinson's disease patients with symptom fluctuations. *Int J Neurosci* 120(8), pp. 523-530. doi: 10.3109/00207454.2010.489725

Burger, C. et al. 2004. Recombinant AAV Viral Vectors Pseudotyped with Viral Capsids from Serotypes 1, 2, and 5 Display Differential Efficiency and Cell Tropism after Delivery to Different Regions of the Central Nervous System. *Molecular Therapy* 10(2), pp. 302-317. doi: https://doi.org/10.1016/j.ymthe.2004.05.024

Burn, D. J., Rowan, E. N., Allan, L. M., Molloy, S., O'Brien, J. T. and McKeith, I. G. 2006. Motor subtype and cognitive decline in Parkinson's disease, Parkinson's disease with dementia, and dementia with Lewy bodies. *J Neurol Neurosurg Psychiatry* 77(5), pp. 585-589. doi: 10.1136/jnnp.2005.081711

Burns, R. S., Chiueh, C. C., Markey, S. P., Ebert, M. H., Jacobowitz, D. M. and Kopin, I. J. 1983. A primate model of parkinsonism: selective destruction of dopaminergic neurons in the pars compacta of the substantia nigra by N-methyl-4-phenyl-1,2,3,6-tetrahydropyridine. *Proceedings of the National Academy of Sciences* 80(14), pp. 4546-4550. doi: doi:10.1073/pnas.80.14.4546

Buttery, P. C. and Barker, R. A. 2020. Gene and Cell-Based Therapies for Parkinson's Disease: Where Are We? *Neurotherapeutics* 17(4), pp. 1539-1562. doi: 10.1007/s13311-020-00940-4

Bye, C. R., Penna, V., de Luzy, I. R., Gantner, C. W., Hunt, C. P. J., Thompson, L. H. and Parish, C. L. 2019. Transcriptional Profiling of Xenogeneic Transplants: Examining Human Pluripotent Stem Cell-Derived Grafts in the Rodent Brain. *Stem Cell Reports* 13(5), pp. 877-890. doi: 10.1016/j.stemcr.2019.10.001

Cai, J. X. and Arnsten, A. F. 1997. Dose-dependent effects of the dopamine D1 receptor agonists A77636 or SKF81297 on spatial working memory in aged monkeys. *J Pharmacol Exp Ther* 283(1), pp. 183-189.

Cai, W. et al. 2022. Dopaminergic medication normalizes aberrant cognitive control circuit signalling in Parkinson's disease. *Brain* 145(11), pp. 4042-4055. doi: 10.1093/brain/awac007

Calabresi, P., Mercuri, N. B., Sancesario, G. and Bernardi, G. 1993. Electrophysiology of dopamine-denervated striatal neurons. Implications for Parkinson's disease. *Brain* 116 (Pt 2), pp. 433-452.

Calabresi, P., Picconi, B., Tozzi, A. and Di Filippo, M. 2007. Dopamine-mediated regulation of corticostriatal synaptic plasticity. *Trends in Neurosciences* 30(5), pp. 211-219.

Caminiti, S. P. et al. 2017. Axonal damage and loss of connectivity in nigrostriatal and mesolimbic dopamine pathways in early Parkinson's disease. *NeuroImage: Clinical* 14, pp. 734-740. doi: https://doi.org/10.1016/j.nicl.2017.03.011

Cardinal, R. N. and Howes, N. J. 2005. Effects of lesions of the nucleus accumbens core on choice between small certain rewards and large uncertain rewards in rats. *BMC Neuroscience* 6(1), p. 37. doi: 10.1186/1471-2202-6-37

Carli, M., Evenden, J. L. and Robbins, T. W. 1985. Depletion of unilateral striatal dopamine impairs initiation of contralateral actions and not sensory attention. *Nature* 313(6004), pp. 679-682. doi: 10.1038/313679a0

Caroline, H. W.-G., Sarah, L. M., Jonathan, R. E., Thomas, F., Carol, B., Trevor, W. R. and Roger, A. B. 2013. The CamPaIGN study of Parkinson's disease: 10-year outlook in an incident population-based cohort. *Journal of Neurology, Neurosurgery & Psychiatry* 84(11), p. 1258. doi: 10.1136/jnnp-2013-305277

Castelli, V. et al. 2020. Effects of the probiotic formulation SLAB51 in in vitro and in vivo Parkinson's disease models. *Aging (Albany NY)* 12(5), pp. 4641-4659. doi: 10.18632/aging.102927

Caudal, D., Alvarsson, A., Björklund, A. and Svenningsson, P. 2015. Depressive-like phenotype induced by AAV-mediated overexpression of human α-synuclein in midbrain dopaminergic neurons. *Exp Neurol* 273, pp. 243-252. doi: 10.1016/j.expneurol.2015.09.002

Cederfjäll, E., Broom, L. and Kirik, D. 2015. Controlled Striatal DOPA Production From a Gene Delivery System in a Rodent Model of Parkinson's Disease. *Molecular Therapy* 23(5), pp. 896-906. doi: 10.1038/mt.2015.8

Cederfjäll, E. et al. 2013. Continuous DOPA synthesis from a single AAV: dosing and efficacy in models of Parkinson's disease. *Sci Rep* 3, p. 2157. doi: 10.1038/srep02157

Cederfjäll, E., Sahin, G., Kirik, D. and Björklund, T. 2012. Design of a single AAV vector for coexpression of TH and GCH1 to establish continuous DOPA synthesis in a rat model of Parkinson's disease. *Mol Ther* 20(7), pp. 1315-1326. doi: 10.1038/mt.2012.1

Chambers, S. M., Fasano, C. A., Papapetrou, E. P., Tomishima, M., Sadelain, M. and Studer, L. 2009a. Highly efficient neural conversion of human ES and iPS cells by dual inhibition of SMAD signaling. *Nat Biotechnol* 27(3), pp. 275-280. doi: 10.1038/nbt.1529

Chambers, S. M., Fasano, C. A., Papapetrou, E. P., Tomishima, M., Sadelain, M. and Studer, L. 2009b. Highly efficient neural conversion of human ES and iPS cells by dual inhibition of SMAD signaling. *Nature biotechnology* 27(3), p. 275. doi: 10.1038/nbt.1529

Chao, O. Y., Pum, M. E., Li, J. S. and Huston, J. P. 2012. The grid-walking test: assessment of sensorimotor deficits after moderate or severe dopamine depletion by 6-hydroxydopamine lesions in the dorsal striatum and medial forebrain bundle. *Neuroscience* 202, pp. 318-325. doi: 10.1016/j.neuroscience.2011.11.016

Charcot, J. M. 1886. *Lecons sur, les maladies du système nerveux*. Lecrosnier et Babé.

Chaudhuri, K. R., Healy, D. G. and Schapira, A. H. 2006. Non-motor symptoms of Parkinson's disease: diagnosis and management. *Lancet Neurol* 5(3), pp. 235-245. doi: 10.1016/s1474-4422(06)70373-8

Chaudhuri, K. R. and Schapira, A. H. V. 2009. Non-motor symptoms of Parkinson's disease: dopaminergic pathophysiology and treatment. *The Lancet Neurology* 8(5), pp. 464-474. doi: https://doi.org/10.1016/S1474-4422(09)70068-7

Chen, W., Hu, Y. and Ju, D. 2020. Gene therapy for neurodegenerative disorders: advances, insights and prospects. *Acta Pharm Sin B* 10(8), pp. 1347-1359. doi: 10.1016/j.apsb.2020.01.015

Choi, J. Y. et al. 2012. Evaluation of dopamine transporters and D2 receptors in hemiparkinsonian rat brains in vivo using consecutive PET scans of [18F]FPCIT and [18F]fallypride. *Applied Radiation and Isotopes* 70(12), pp. 2689-2694. doi: https://doi.org/10.1016/j.apradiso.2012.08.005

Choi, V. W., McCarty, D. M. and Samulski, R. J. 2006. Host cell DNA repair pathways in adeno-associated viral genome processing. *J Virol* 80(21), pp. 10346-10356. doi: 10.1128/jvi.00841-06

Choudhury, G. R. and Daadi, M. M. 2018. Charting the onset of Parkinson-like motor and non-motor symptoms in nonhuman primate model of Parkinson's disease. *PLoS One* 13(8), p. e0202770. doi: 10.1371/journal.pone.0202770

Christine, C. W. et al. 2022. Safety of AADC Gene Therapy for Moderately Advanced Parkinson Disease: Three-Year Outcomes From the PD-1101 Trial. *Neurology* 98(1), pp. e40-e50. doi: 10.1212/wnl.0000000000012952

Christine, C. W. et al. 2009. Safety and tolerability of putaminal AADC gene therapy for Parkinson disease. *Neurology* 73(20), pp. 1662-1669. doi: 10.1212/WNL.0b013e3181c29356

Ciesielska, A., Sharma, N., Beyer, J., Forsayeth, J. and Bankiewicz, K. 2015. Carbidopa-based modulation of the functional effect of the AAV2-hAADC gene therapy in 6-OHDA lesioned rats. *PLoS One* 10(4), p. e0122708. doi: 10.1371/journal.pone.0122708

Cohen, J. Y., Haesler, S., Vong, L., Lowell, B. B. and Uchida, N. 2012. Neuron-type-specific signals for reward and punishment in the ventral tegmental area. *Nature* 482(7383), pp. 85-88. doi: 10.1038/nature10754

Cole, B. J. and Robbins, T. W. 1989. Effects of 6-hydroxydopamine lesions of the nucleus accumbens septi on performance of a 5-choice serial reaction time task in rats: implications for theories of selective attention and arousal. *Behav Brain Res* 33(2), pp. 165-179. doi: 10.1016/s0166-4328(89)80048-8

Cole, D. G., Kobierski, L. A., Konradi, C. and Hyman, S. E. 1994. 6-Hydroxydopamine lesions of rat substantia nigra up-regulate dopamine-induced phosphorylation of the cAMP-response element-binding protein in striatal neurons. *Proc Natl Acad Sci U S A* 91(20), pp. 9631-9635. doi: 10.1073/pnas.91.20.9631

Colucci, M. et al. 2012. Intestinal dysmotility and enteric neurochemical changes in a Parkinson's disease rat model. *Auton Neurosci* 169(2), pp. 77-86. doi: 10.1016/j.autneu.2012.04.005

Cools, R. 2006. Dopaminergic modulation of cognitive function-implications for L-DOPA treatment in Parkinson's disease. *Neurosci Biobehav Rev* 30(1), pp. 1-23. doi: 10.1016/j.neubiorev.2005.03.024

Cools, R., Barker, R. A., Sahakian, B. J. and Robbins, T. W. 2001. Enhanced or impaired cognitive function in Parkinson's disease as a function of dopaminergic medication and task demands. *Cereb Cortex* 11(12), pp. 1136-1143. doi: 10.1093/cercor/11.12.1136

Cools, R. and D'Esposito, M. 2011. Inverted-U-shaped dopamine actions on human working memory and cognitive control. *Biol Psychiatry* 69(12), pp. e113-125. doi: 10.1016/j.biopsych.2011.03.028

Cools, R., Froböse, M., Aarts, E. and Hofmans, L. 2019. Dopamine and the motivation of cognitive control. *Handb Clin Neurol* 163, pp. 123-143. doi: 10.1016/b978-0-12-804281-6.00007-0

Cools, R., Lewis, S. J., Clark, L., Barker, R. A. and Robbins, T. W. 2007. L-DOPA disrupts activity in the nucleus accumbens during reversal learning in Parkinson's disease. *Neuropsychopharmacology* 32(1), pp. 180-189. doi: 10.1038/sj.npp.1301153

Cooper, J. A., Sagar, H. J., Tidswell, P. and Jordan, N. 1994. Slowed central processing in simple and go/no-go reaction time tasks in Parkinson's disease. *Brain* 117 (Pt 3), pp. 517-529. doi: 10.1093/brain/117.3.517

Corbit, L. H., Leung, B. K. and Balleine, B. W. 2013. The role of the amygdala-striatal pathway in the acquisition and performance of goal-directed instrumental actions. *J Neurosci* 33(45), pp. 17682-17690. doi: 10.1523/jneurosci.3271-13.2013

Cory-Slechta, D. A., Thiruchelvam, M., Barlow, B. K. and Richfield, E. K. 2005. Developmental pesticide models of the Parkinson disease phenotype. *Environ Health Perspect* 113(9), pp. 1263-1270. doi: 10.1289/ehp.7570

Cotzias, G. C., Papavasiliou, P. S. and Gellene, R. 1969. Modification of Parkinsonism--chronic treatment with L-dopa. *N Engl J Med* 280(7), pp. 337-345. doi: 10.1056/nejm196902132800701

Coune, P. G., Schneider, B. L. and Aebischer, P. 2012. Parkinson's disease: gene therapies. *Cold Spring Harb Perspect Med* 2(4), p. a009431. doi: 10.1101/cshperspect.a009431

Cousins, M. and Salamone, J. 1996. Involvement of ventrolateral striatal dopamine in movement initiation and execution: a microdialysis and behavioral investigation. *Neuroscience* 70(4), pp. 849-859.

Croxson, P. L., Walton, M. E., Boorman, E. D., Rushworth, M. F. and Bannerman, D. M. 2014. Unilateral medial frontal cortex lesions cause a cognitive decision-making deficit in rats. *Eur J Neurosci* 40(12), pp. 3757-3765. doi: 10.1111/ejn.12751

Cui, H. et al. 2023. Nigrostriatal 6-hydroxydopamine lesions increase alpha-synuclein levels and permeability in rat colon. *Neurobiology of Aging* 129, pp. 62-71. doi: https://doi.org/10.1016/j.neurobiolaging.2023.05.007

Cunningham, M. G., Connor, C. M., Zhang, K. and Benes, F. M. 2005. Diminished serotonergic innervation of adult medial prefrontal cortex after 6-OHDA lesions in the newborn rat. *Developmental Brain Research* 157(2), pp. 124-131. doi: https://doi.org/10.1016/j.devbrainres.2005.02.020

Da Cunha, C., Angelucci, M. E. M., Canteras, N. S., Wonnacott, S. and Takahashi, R. N. 2002. The Lesion of the Rat Substantia Nigra pars compacta Dopaminergic Neurons as a Model for Parkinson's Disease Memory Disabilities. *Cellular and Molecular Neurobiology* 22(3), pp. 227-237. doi: 10.1023/A:1020736131907

Da Cunha, C. et al. 2001. Memory disruption in rats with nigral lesions induced by MPTP: a model for early Parkinson's disease amnesia. *Behavioural Brain Research* 124(1), pp. 9-18. doi: https://doi.org/10.1016/S0166-4328(01)00211-X

Darvas, M. and Palmiter, R. D. 2009. Restriction of dopamine signaling to the dorsolateral striatum is sufficient for many cognitive behaviors. *Proc Natl Acad Sci U S A* 106(34), pp. 14664-14669. doi: 10.1073/pnas.0907299106

Darvas, M. and Palmiter, R. D. 2010. Restricting dopaminergic signaling to either dorsolateral or medial striatum facilitates cognition. *J Neurosci* 30(3), pp. 1158-1165. doi: 10.1523/jneurosci.4576-09.2010

de Luzy, I. R. et al. 2021. Human stem cells harboring a suicide gene improve the safety and standardisation of neural transplants in Parkinsonian rats. *Nature Communications* 12(1), p. 3275. doi: 10.1038/s41467-021-23125-9

de Luzy, I. R. et al. 2022. Identifying the optimal developmental age of human pluripotent stem cell-derived midbrain dopaminergic progenitors for transplantation in a rodent model of Parkinson's disease. *Exp Neurol* 358, p. 114219. doi: 10.1016/j.expneurol.2022.114219

de Wit, S., Barker, R. A., Dickinson, A. D. and Cools, R. 2011. Habitual versus goal-directed action control in Parkinson disease. *J Cogn Neurosci* 23(5), pp. 1218-1229. doi: 10.1162/jocn.2010.21514

de Wit, S., Standing, H. R., Devito, E. E., Robinson, O. J., Ridderinkhof, K. R., Robbins, T. W. and Sahakian, B. J. 2012. Reliance on habits at the expense of goal-directed control following dopamine precursor depletion. *Psychopharmacology (Berl)* 219(2), pp. 621-631. doi: 10.1007/s00213-011-2563-2

Decamp, E. and Schneider, J. S. 2004. Attention and executive function deficits in chronic low-dose MPTP-treated non-human primates. *Eur J Neurosci* 20(5), pp. 1371-1378. doi: 10.1111/j.1460-9568.2004.03586.x

Decressac, M., Mattsson, B., Lundblad, M., Weikop, P. and Björklund, A. 2012. Progressive neurodegenerative and behavioural changes induced by AAV-mediated overexpression of α-synuclein in midbrain dopamine neurons. *Neurobiol Dis* 45(3), pp. 939-953. doi: 10.1016/j.nbd.2011.12.013

Desban, M., Kemel, M. L., Glowinski, J. and Gauchy, C. 1993. Spatial organization of patch and matrix compartments in the rat striatum. *Neuroscience* 57(3), pp. 661-671. doi: 10.1016/0306-4522(93)90013-6

Descarries, L., Soghomonian, J.-J., Garcia, S., Doucet, G. and Bruno, J. P. 1992. Ultrastructural analysis of the serotonin hyperinnervation in adult rat neostriatum following neonatal dopamine denervation with 6-hydroxydopamine. *Brain Research* 569(1), pp. 1-13. doi: https://doi.org/10.1016/0006-8993(92)90363-E

Di Chiara, G., Morelli, M., Barone, P. and Pontieri, F. 1992. Priming as a model of behavioural sensitization. *Dev Pharmacol Ther* 18(3-4), pp. 223-227.

Dick, F. D. et al. 2007. Environmental risk factors for Parkinson's disease and parkinsonism: the Geoparkinson study. *Occup Environ Med* 64(10), pp. 666-672. doi: 10.1136/oem.2006.027003

Dickinson, A., Balleine, B., Watt, A., Gonzales, F. and Boakes, R. 1995. Overtraining and the motivational control of instrumental action. *Anim Learn Behav* 22, pp. 197-206.

Döbrössy, M. D. and Dunnett, S. B. 1997. Unilateral striatal lesions impair response execution on a lateralised choice reaction time task. *Behav Brain Res* 87(2), pp. 159-171. doi: 10.1016/s0166-4328(97)02283-3

Doi, D. et al. 2020. Pre-clinical study of induced pluripotent stem cell-derived dopaminergic progenitor cells for Parkinson's disease. *Nat Commun* 11(1), p. 3369. doi: 10.1038/s41467-020-17165-w

Dowd, E. and Dunnett, S. B. 2004. Deficits in a lateralized associative learning task in dopamine-depleted rats with functional recovery by dopamine-rich transplants. *European Journal of Neuroscience* 20(7), pp. 1953-1959. doi: 10.1111/j.1460-9568.2004.03637.x

Dowd, E., Monville, C., Torres, E. M. and Dunnett, S. B. 2005. The Corridor Task: a simple test of lateralised response selection sensitive to unilateral dopamine deafferentation and graft-derived dopamine replacement in the striatum. *Brain Res Bull* 68(1-2), pp. 24-30. doi: 10.1016/j.brainresbull.2005.08.009

Drevin, J., Nyholm, D., Widner, H., Van Vliet, T., Viberg Johansson, J., Jiltsova, E. and Hansson, M. 2022. Patients' views on using human embryonic stem cells to treat Parkinson's disease: an interview study. *BMC Medical Ethics* 23(1), p. 102. doi: 10.1186/s12910-022-00840-6

Driver-Dunckley, E., Samanta, J. and Stacy, M. 2003. Pathological gambling associated with dopamine agonist therapy in Parkinson's disease. *Neurology* 61(3), pp. 422-423. doi: 10.1212/01.wnl.0000076478.45005.ec

Drouin, L. M. and Agbandje-McKenna, M. 2013. Adeno-associated virus structural biology as a tool in vector development. *Future Virol* 8(12), pp. 1183-1199. doi: 10.2217/fvl.13.112

Drucker-Colín, R. et al. 1999. Transplant of cultured neuron-like differentiated chromaffin cells in a Parkinson's disease patient. A preliminary report. *Arch Med Res* 30(1), pp. 33-39. doi: 10.1016/s0188-0128(98)00007-4

Drui, G., Carnicella, S., Carcenac, C., Favier, M., Bertrand, A., Boulet, S. and Savasta, M. 2014. Loss of dopaminergic nigrostriatal neurons accounts for the motivational and affective deficits in Parkinson's disease. *Mol Psychiatry* 19(3), pp. 358-367. doi: 10.1038/mp.2013.3

Dunnett, S. B., Björklund, A., Stenevi, U. and Iversen, S. D. 1981. Behavioural recovery following transplantation of substantia nigra in rats subjected to 6-OHDA lesions of the nigrostriatal pathway. I. Unilateral lesions. *Brain Res* 215(1-2), pp. 147-161. doi: 10.1016/0006-8993(81)90498-4

Durieux, P. F., Schiffmann, S. N. and de Kerchove d'Exaerde, A. 2012. Differential regulation of motor control and response to dopaminergic drugs by D1R and D2R neurons in distinct dorsal striatum subregions. *Embo j* 31(3), pp. 640-653. doi: 10.1038/emboj.2011.400

Dusonchet, J. et al. 2011. A rat model of progressive nigral neurodegeneration induced by the Parkinson's disease-associated G2019S mutation in LRRK2. *J Neurosci* 31(3), pp. 907-912. doi: 10.1523/jneurosci.5092-10.2011

Eberling, J. L., Jagust, W. J., Christine, C. W., Starr, P., Larson, P., Bankiewicz, K. S. and Aminoff, M. J. 2008. Results from a phase I safety trial of hAADC gene therapy for Parkinson disease. *Neurology* 70(21), pp. 1980-1983. doi: 10.1212/01.wnl.0000312381.29287.ff

Eisenhofer, G. et al. 1997. Substantial production of dopamine in the human gastrointestinal tract. *J Clin Endocrinol Metab* 82(11), pp. 3864-3871. doi: 10.1210/jcem.82.11.4339

Ellett, L. J. et al. 2016. Restoration of intestinal function in an MPTP model of Parkinson's Disease. *Scientific Reports* 6(1), p. 30269. doi: 10.1038/srep30269

Elsworth, J. D., Taylor, J. R., Sladek, J. R., Collier, T. J., Redmond, D. E. and Roth, R. H. 1999. Striatal dopaminergic correlates of stable parkinsonism and degree of recovery in old-world primates one year after MPTP treatment. *Neuroscience* 95(2), pp. 399-408. doi: https://doi.org/10.1016/S0306-4522(99)00437-6

Engelhardt, E. and Gomes, M. D. M. 2017. Lewy and his inclusion bodies: Discovery and rejection. *Dement Neuropsychol* 11(2), pp. 198-201. doi: 10.1590/1980-57642016dn11-020012

Erro, R. et al. 2014. Do subjective memory complaints herald the onset of mild cognitive impairment in Parkinson disease? *J Geriatr Psychiatry Neurol* 27(4), pp. 276-281. doi: 10.1177/0891988714532015

Fabbri, M. et al. 2017. Response of non-motor symptoms to levodopa in late-stage Parkinson's disease: Results of a levodopa challenge test. *Parkinsonism & Related Disorders* 39, pp. 37-43. doi: https://doi.org/10.1016/j.parkreldis.2017.02.007

Fan, H. C. et al. 2020. The Association Between Parkinson's Disease and Attention-Deficit Hyperactivity Disorder. *Cell Transplant* 29, p. 963689720947416. doi: 10.1177/0963689720947416

Farassat, N. et al. 2019. In vivo functional diversity of midbrain dopamine neurons within identified axonal projections. *Elife* 8, p. e48408. doi: 10.7554/eLife.48408

Farrell, K., Lak, A. and Saleem, A. B. 2022. Midbrain dopamine neurons signal phasic and ramping reward prediction error during goal-directed navigation. *Cell Rep* 41(2), p. 111470. doi: 10.1016/j.celrep.2022.111470

Faure, A., Haberland, U., Condé, F. and El Massioui, N. 2005. Lesion to the nigrostriatal dopamine system disrupts stimulus-response habit formation. *J Neurosci* 25(11), pp. 2771-2780. doi: 10.1523/jneurosci.3894-04.2005

Fearnley, J. M. and Lees, A. J. 1991. Ageing and Parkinson's disease: substantia nigra regional selectivity. *Brain* 114 (Pt 5), pp. 2283-2301. doi: 10.1093/brain/114.5.2283

Fiorenzato, E., Antonini, A., Bisiacchi, P., Weis, L. and Biundo, R. 2021. Asymmetric Dopamine Transporter Loss Affects Cognitive and Motor Progression in Parkinson's Disease. *Mov Disord* 36(10), pp. 2303-2313. doi: 10.1002/mds.28682

Fischer, D. L., Gombash, S. E., Kemp, C. J., Manfredsson, F. P., Polinski, N. K., Duffy, M. F. and Sortwell, C. E. 2016. Viral Vector-Based Modeling of Neurodegenerative Disorders: Parkinson's Disease. *Methods Mol Biol* 1382, pp. 367-382. doi: 10.1007/978-1-4939-3271-9_26

Flores-Dourojeanni, J. P., van Rijt, C., van den Munkhof, M. H., Boekhoudt, L., Luijendijk, M. C. M., Vanderschuren, L. and Adan, R. A. H. 2021. Temporally Specific Roles of Ventral Tegmental Area Projections to the Nucleus Accumbens and Prefrontal Cortex in Attention and Impulse Control. *J Neurosci* 41(19), pp. 4293-4304. doi: 10.1523/jneurosci.0477-20.2020

Ford, C. P. 2014. The role of D2-autoreceptors in regulating dopamine neuron activity and transmission. *Neuroscience* 282, pp. 13-22. doi: 10.1016/j.neuroscience.2014.01.025

Forsayeth, J. R. et al. 2006. A dose-ranging study of AAV-hAADC therapy in Parkinsonian monkeys. *Mol Ther* 14(4), pp. 571-577. doi: 10.1016/j.ymthe.2006.04.008

Fox, M. E., Mikhailova, M. A., Bass, C. E., Takmakov, P., Gainetdinov, R. R., Budygin, E. A. and Wightman, R. M. 2016. Cross-hemispheric dopamine projections have functional significance. *Proc Natl Acad Sci U S A* 113(25), pp. 6985-6990. doi: 10.1073/pnas.1603629113

Fox, S. H. and Brotchie, J. M. 2010. The MPTP-lesioned non-human primate models of Parkinson's disease. Past, present, and future. *Prog Brain Res* 184, pp. 133-157. doi: 10.1016/s0079-6123(10)84007-5

Frank, M. J. 2005. Dynamic dopamine modulation in the basal ganglia: a neurocomputational account of cognitive deficits in medicated and nonmedicated Parkinsonism. *J Cogn Neurosci* 17(1), pp. 51-72. doi: 10.1162/0898929052880093

Freed, C. R. et al. 2001. Transplantation of Embryonic Dopamine Neurons for Severe Parkinson's Disease. *New England Journal of Medicine* 344(10), pp. 710-719. doi: 10.1056/nejm200103083441002

Freed, W. J., Perlow, M. J., Karoum, F., Seiger, A., Olson, L., Hoffer, B. J. and Wyatt, R. J. 1980. Restoration of dopaminergic function by grafting of fetal rat substantia nigra to the caudate nucleus: long-term behavioral, biochemical, and histochemical studies. *Ann Neurol* 8(5), pp. 510-519. doi: 10.1002/ana.410080508

Freeman, W. D., Tan, K. M., Glass, G. A., Linos, K., Foot, C. and Ziegenfuss, M. 2007. ICU management of patients with Parkinson's disease or Parkinsonism. *Current Anaesthesia & Critical Care* 18(5), pp. 227-236. doi: https://doi.org/10.1016/j.cacc.2007.09.007

Freichel, C. et al. 2007. Age-dependent cognitive decline and amygdala pathology in alpha-synuclein transgenic mice. *Neurobiol Aging* 28(9), pp. 1421-1435. doi: 10.1016/j.neurobiolaging.2006.06.013

Frick, A., Björkstrand, J., Lubberink, M., Eriksson, A., Fredrikson, M. and Åhs, F. 2022. Dopamine and fear memory formation in the human amygdala. *Molecular Psychiatry* 27(3), pp. 1704-1711. doi: 10.1038/s41380-021-01400-x

Fu, Y., Paxinos, G., Watson, C. and Halliday, G. M. 2016. The substantia nigra and ventral tegmental dopaminergic neurons from development to degeneration. *Journal of Chemical Neuroanatomy* 76(Pt B), pp. 98-107. doi: 10.1016/j.jchemneu.2016.02.001

Fullard, M. E., Morley, J. F. and Duda, J. E. 2017. Olfactory Dysfunction as an Early Biomarker in Parkinson's Disease. *Neurosci Bull* 33(5), pp. 515-525. doi: 10.1007/s12264-017-0170-x

Gauthier, J., Parent, M., Lévesque, M. and Parent, A. 1999. The axonal arborization of single nigrostriatal neurons in rats. *Brain Research* 834(1), pp. 228-232. doi: https://doi.org/10.1016/S0006-8993(99)01573-5

Gerfen, C. R., Engber, T. M., Mahan, L. C., Susel, Z., Chase, T. N., Monsma, F. J., Jr. and Sibley, D. R. 1990. D1 and D2 dopamine receptor-regulated gene expression of striatonigral and striatopallidal neurons. *Science* 250(4986), pp. 1429-1432. doi: 10.1126/science.2147780

Gerfen, C. R. and Surmeier, D. J. 2011. Modulation of striatal projection systems by dopamine. *Annu Rev Neurosci* 34, pp. 441-466. doi: 10.1146/annurev-neuro-061010-113641

Giguère, N., Burke Nanni, S. and Trudeau, L. E. 2018. On Cell Loss and Selective Vulnerability of Neuronal Populations in Parkinson's Disease. *Front Neurol* 9, p. 455. doi: 10.3389/fneur.2018.00455

Giladi, N., McDermott, M. P., Fahn, S., Przedborski, S., Jankovic, J., Stern, M. and Tanner, C. 2001. Freezing of gait in PD: prospective assessment in the DATATOP cohort. *Neurology* 56(12), pp. 1712-1721. doi: 10.1212/wnl.56.12.1712

Gill, S. S. et al. 2003. Direct brain infusion of glial cell line-derived neurotrophic factor in Parkinson disease. *Nat Med* 9(5), pp. 589-595. doi: 10.1038/nm850

Gittis, A. H., Nelson, A. B., Thwin, M. T., Palop, J. J. and Kreitzer, A. C. 2010. Distinct roles of GABAergic interneurons in the regulation of striatal output pathways. *J Neurosci* 30(6), pp. 2223-2234. doi: 10.1523/jneurosci.4870-09.2010

Glajch, K. E., Fleming, S. M., Surmeier, D. J. and Osten, P. 2012. Sensorimotor assessment of the unilateral 6-hydroxydopamine mouse model of Parkinson's disease. *Behav Brain Res* 230(2), pp. 309-316. doi: 10.1016/j.bbr.2011.12.007

Glinka, Y. Y. and Youdim, M. B. H. 1995. Inhibition of mitochondrial complexes I and IV by 6-hydroxydopamine. *European Journal of Pharmacology: Environmental Toxicology and Pharmacology* 292(3), pp. 329-332. doi: https://doi.org/10.1016/0926-6917(95)90040-3

Golbe, L. I. 1991. Young-onset Parkinson's disease: a clinical review. *Neurology* 41(2 (Pt 1)), pp. 168-173. doi: 10.1212/wnl.41.2_part_1.168

Goldberg, M. S. et al. 2003. Parkin-deficient Mice Exhibit Nigrostriatal Deficits but Not Loss of Dopaminergic Neurons*. *Journal of Biological Chemistry* 278(44), pp. 43628-43635. doi: https://doi.org/10.1074/jbc.M308947200

Goldman, J. G. et al. 2018. Cognitive impairment in Parkinson's disease: a report from a multidisciplinary symposium on unmet needs and future directions to maintain cognitive health. *NPJ Parkinsons Dis* 4, p. 19. doi: 10.1038/s41531-018-0055-3

Goldstein, M. and Lieberman, A. 1992. The role of the regulatory enzymes of catecholamine synthesis in Parkinson's disease. *Neurology* 42(4 Suppl 4), pp. 8-12; discussion 41-18.

Goodwin, F. K. 1971. Psychiatric Side Effects of Levodopa in Man. *JAMA* 218(13), pp. 1915-1920. doi: 10.1001/jama.1971.03190260031009

Gotham, A. M., Brown, R. G. and Marsden, C. D. 1988. 'Frontal' cognitive function in patients with Parkinson's disease 'on' and 'off' levodopa. *Brain* 111 (Pt 2), pp. 299-321. doi: 10.1093/brain/111.2.299

Grathwohl, S. A., Steiner, J. A., Britschgi, M. and Brundin, P. 2013. Mind the gut: secretion of α-synuclein by enteric neurons. *J Neurochem* 125(4), pp. 487-490. doi: 10.1111/jnc.12191

Grealish, S. et al. 2014. Human ESC-derived dopamine neurons show similar preclinical efficacy and potency to fetal neurons when grafted in a rat model of Parkinson's disease. *Cell Stem Cell* 15(5), pp. 653-665. doi: 10.1016/j.stem.2014.09.017

Grealish, S., Mattsson, B., Draxler, P. and Björklund, A. 2010. Characterisation of behavioural and neurodegenerative changes induced by intranigral 6-hydroxydopamine lesions in a mouse model of Parkinson's disease. *Eur J Neurosci* 31(12), pp. 2266-2278. doi: 10.1111/j.1460-9568.2010.07265.x

Grealish, S., Xie, L., Kelly, M. and Dowd, E. 2008. Unilateral axonal or terminal injection of 6-hydroxydopamine causes rapid-onset nigrostriatal degeneration and contralateral motor impairments in the rat. *Brain Research Bulletin* 77(5), pp. 312-319. doi: https://doi.org/10.1016/j.brainresbull.2008.08.018

Greenamyre, J. T., Cannon, J. R., Drolet, R. and Mastroberardino, P. G. 2010. Lessons from the rotenone model of Parkinson's disease. *Trends Pharmacol Sci* 31(4), pp. 141-142; author reply 142-143. doi: 10.1016/j.tips.2009.12.006

Greffard, S. et al. 2006. Motor score of the Unified Parkinson Disease Rating Scale as a good predictor of Lewy body-associated neuronal loss in the substantia nigra. *Arch Neurol* 63(4), pp. 584-588. doi: 10.1001/archneur.63.4.584

Gremel, C. M. and Costa, R. M. 2013. Orbitofrontal and striatal circuits dynamically encode the shift between goal-directed and habitual actions. *Nat Commun* 4, p. 2264. doi: 10.1038/ncomms3264

Grieger, J. C. and Samulski, R. J. 2005. Adeno-associated virus as a gene therapy vector: vector development, production and clinical applications. *Adv Biochem Eng Biotechnol* 99, pp. 119-145.

Grospe, G. M., Baker, P. M. and Ragozzino, M. E. 2018. Cognitive Flexibility Deficits Following 6-OHDA Lesions of the Rat Dorsomedial Striatum. *Neuroscience* 374, pp. 80-90. doi: 10.1016/j.neuroscience.2018.01.032

Growdon, J. H., Kieburtz, K., McDermott, M. P., Panisset, M. and Friedman, J. H. 1998. Levodopa improves motor function without impairing cognition in mild non-demented Parkinson's disease patients. Parkinson Study Group. *Neurology* 50(5), pp. 1327-1331. doi: 10.1212/wnl.50.5.1327

Gubinelli, F. et al. 2022. Lateralized deficits after unilateral AAV-vector based overexpression of alpha-synuclein in the midbrain of rats on drug-free behavioral tests. *Behav Brain Res* 429, p. 113887. doi: 10.1016/j.bbr.2022.113887

Haber, S. N. 2014. The place of dopamine in the cortico-basal ganglia circuit. *Neuroscience* 282, pp. 248-257. doi: 10.1016/j.neuroscience.2014.10.008

Hagell, P. and Nilsson, M. H. 2009. The 39-Item Parkinson's Disease Questionnaire (PDQ-39): Is it a Unidimensional Construct? *Ther Adv Neurol Disord* 2(4), pp. 205-214. doi: 10.1177/1756285609103726

Hall, H., Jewett, M., Landeck, N., Nilsson, N., Schagerlöf, U., Leanza, G. and Kirik, D. 2013. Characterization of Cognitive Deficits in Rats Overexpressing Human Alpha-Synuclein in the Ventral Tegmental Area and Medial Septum Using Recombinant Adeno-Associated Viral Vectors. *PLoS One* 8(5), p. e64844. doi: 10.1371/journal.pone.0064844

Hallett, P. J., Cooper, O., Sadi, D., Robertson, H., Mendez, I. and Isacson, O. 2014. Long-term health of dopaminergic neuron transplants in Parkinson's disease patients. *Cell Rep* 7(6), pp. 1755-1761. doi: 10.1016/j.celrep.2014.05.027

Halliday, G. M., Blumbergs, P. C., Cotton, R. G., Blessing, W. W. and Geffen, L. B. 1990. Loss of brainstem serotonin- and substance P-containing neurons in Parkinson's disease. *Brain Res* 510(1), pp. 104-107. doi: 10.1016/0006-8993(90)90733-r

Hammond, L. J. 1980. The effect of contingency upon the appetitive conditioning of free-operant behavior. *J Exp Anal Behav* 34(3), pp. 297-304. doi: 10.1901/jeab.1980.34-297

Hanna-Pladdy, B., Pahwa, R. and Lyons, K. E. 2015. Paradoxical effect of dopamine medication on cognition in Parkinson's disease: relationship to side of motor onset. *J Int Neuropsychol Soc* 21(4), pp. 259-270. doi: 10.1017/s1355617715000181

Hartmann, C. J., Fliegen, S., Groiss, S. J., Wojtecki, L. and Schnitzler, A. 2019. An update on best practice of deep brain stimulation in Parkinson's disease. *Ther Adv Neurol Disord* 12, p. 1756286419838096. doi: 10.1177/1756286419838096

Harvey, B. K., Wang, Y. and Hoffer, B. J. 2008. Transgenic rodent models of Parkinson's disease. *Acta Neurochir Suppl* 101, pp. 89-92. doi: 10.1007/978-3-211-78205-7_15

Hauser, R. A., Freeman, T. B., Snow, B. J., Nauert, M., Gauger, L., Kordower, J. H. and Olanow, C. W. 1999. Long-term evaluation of bilateral fetal nigral transplantation in Parkinson disease. *Arch Neurol* 56(2), pp. 179-187. doi: 10.1001/archneur.56.2.179

Hawkes, C. H., Del Tredici, K. and Braak, H. 2007. Parkinson's disease: a dual-hit hypothesis. *Neuropathol Appl Neurobiol* 33(6), pp. 599-614. doi: 10.1111/j.1365-2990.2007.00874.x

Heimrich, K. G., Schönenberg, A., Santos-García, D., Mir, P., Coppadis Study, G. and Prell, T. 2023. The Impact of Nonmotor Symptoms on Health-Related Quality of Life in Parkinson's Disease: A Network Analysis Approach. *J Clin Med* 12(7), doi: 10.3390/jcm12072573

Hely, M. A., Morris, J. G., Reid, W. G. and Trafficante, R. 2005. Sydney Multicenter Study of Parkinson's disease: non-L-dopa-responsive problems dominate at 15 years. *Mov Disord* 20(2), pp. 190-199. doi: 10.1002/mds.20324

Heuer, A. and Dunnett, S. B. 2012. Unilateral 6-OHDA lesions induce lateralised deficits in a 'skinner box' operant choice reaction time task in rats. *J Parkinsons Dis* 2(4), pp. 309-320. doi: 10.3233/jpd-2012-012133

Heuer, A., Lelos, M. J., Kelly, C., Torres, E. M. and Dunnett, S. B. 2013a. Dopamine-rich grafts alleviate deficits in contralateral response space induced by extensive dopamine depletion in rats.

Heuer, A., Lelos, M. J., Kelly, C. M., Torres, E. M. and Dunnett, S. B. 2013b. Dopamine-rich grafts alleviate deficits in contralateral response space induced by extensive dopamine depletion in rats. *Exp Neurol* 247, pp. 485-495. doi: 10.1016/j.expneurol.2013.01.020

Heuer, A., Smith, G. A. and Dunnett, S. B. 2013c. Comparison of 6-hydroxydopamine lesions of the substantia nigra and the medial forebrain bundle on a lateralised choice reaction time task in mice. *Eur J Neurosci* 37(2), pp. 294-302. doi: 10.1111/ejn.12036

Heuer, A., Smith, G. A., Lelos, M. J., Lane, E. L. and Dunnett, S. B. 2012. Unilateral nigrostriatal 6-hydroxydopamine lesions in mice I: motor impairments identify extent of dopamine depletion at three different lesion sites. *Behav Brain Res* 228(1), pp. 30-43. doi: 10.1016/j.bbr.2011.11.027

Hikosaka, O. and Isoda, M. 2010. Switching from automatic to controlled behavior: cortico-basal ganglia mechanisms. *Trends Cogn Sci* 14(4), pp. 154-161. doi: 10.1016/j.tics.2010.01.006

Hills, R. et al. 2023. Neurite Outgrowth and Gene Expression Profile Correlate with Efficacy of Human Induced Pluripotent Stem Cell-Derived Dopamine Neuron Grafts. *Stem Cells Dev* 32(13-14), pp. 387-397. doi: 10.1089/scd.2023.0043

Honkanen, E. A., Saari, L., Orte, K., Gardberg, M., Noponen, T., Joutsa, J. and Kaasinen, V. 2019. No link between striatal dopaminergic axons and dopamine transporter imaging in Parkinson's disease. *Mov Disord* 34(10), pp. 1562-1566. doi: 10.1002/mds.27777

Huang, K. W., Ochandarena, N. E., Philson, A. C., Hyun, M., Birnbaum, J. E., Cicconet, M. and Sabatini, B. L. 2019. Molecular and anatomical organization of the dorsal raphe nucleus. *Elife* 8, doi: 10.7554/eLife.46464

Hussein, A., Tielemans, A., Baxter, M. G., Benson, D. L. and Huntley, G. W. 2022. Cognitive deficits and altered cholinergic innervation in young adult male mice carrying a Parkinson's disease Lrrk2(G2019S) knockin mutation. *Exp Neurol* 355, p. 114145. doi: 10.1016/j.expneurol.2022.114145

Hynes, M. and Rosenthal, A. 1999. Specification of dopaminergic and serotonergic neurons in the vertebrate CNS. *Curr Opin Neurobiol* 9(1), pp. 26-36. doi: 10.1016/s0959-4388(99)80004-x

Iancu, R., Mohapel, P., Brundin, P. and Paul, G. 2005. Behavioral characterization of a unilateral 6-OHDA-lesion model of Parkinson's disease in mice. *Behav Brain Res* 162(1), pp. 1-10. doi: 10.1016/j.bbr.2005.02.023

Ikeda, M., Kataoka, H. and Ueno, S. 2017. Can levodopa prevent cognitive decline in patients with Parkinson's disease? *Am J Neurodegener Dis* 6(2), pp. 9-14.

Ikemoto, S. 2007. Dopamine reward circuitry: two projection systems from the ventral midbrain to the nucleus accumbens-olfactory tubercle complex. *Brain Res Rev* 56(1), pp. 27-78. doi: 10.1016/j.brainresrev.2007.05.004

Itier, J. M. et al. 2003. Parkin gene inactivation alters behaviour and dopamine neurotransmission in the mouse. *Hum Mol Genet* 12(18), pp. 2277-2291. doi: 10.1093/hmg/ddg239

Iwaki, H. et al. 2019. Genetic risk of Parkinson disease and progression:: An analysis of 13 longitudinal cohorts. *Neurology. Genetics* 5(4), pp. e348-e348. doi: 10.1212/NXG.0000000000000348

Jaeger, I. et al. 2011. Temporally controlled modulation of FGF/ERK signaling directs midbrain dopaminergic neural progenitor fate in mouse and human pluripotent stem cells. *Development (Cambridge, England)* 138(20), p. 4363. doi: 10.1242/dev.066746

Jang, M. J. et al. 2023. Spatial transcriptomics for profiling the tropism of viral vectors in tissues. *Nature biotechnology* 41(9), pp. 1272-1286. doi: 10.1038/s41587-022-01648-w

Jankovic, J. 2008. Parkinson's disease: clinical features and diagnosis. *Journal of Neurology, Neurosurgery &amp; Psychiatry* 79(4), p. 368. doi: 10.1136/jnnp.2007.131045

Jarraya, B. et al. 2009. Dopamine gene therapy for Parkinson's disease in a nonhuman primate without associated dyskinesia. *Sci Transl Med* 1(2), p. 2ra4. doi: 10.1126/scitranslmed.3000130

Javitch, J. A., D'Amato, R. J., Strittmatter, S. M. and Snyder, S. H. 1985. Parkinsonism-inducing neurotoxin, N-methyl-4-phenyl-1,2,3,6 -tetrahydropyridine: uptake of the metabolite N-methyl-4-phenylpyridine by dopamine neurons explains selective toxicity. *Proceedings of the National Academy of Sciences* 82(7), pp. 2173-2177. doi: doi:10.1073/pnas.82.7.2173

Jellinger, K. A. 1999. Post mortem studies in Parkinson's disease--is it possible to detect brain areas for specific symptoms? *J Neural Transm Suppl* 56, pp. 1-29. doi: 10.1007/978-3-7091-6360-3_1

Jenner, P. and Marsden, C. D. 1986. The actions of 1-methyl-4-phenyl-1,2,3,6-tetrahydropyridine in animals as a model of Parkinson's disease. *J Neural Transm Suppl* 20, pp. 11-39.

Jeon, B. S., Jackson-Lewis, V. and Burke, R. E. 1995. 6-Hydroxydopamine lesion of the rat substantia nigra: time course and morphology of cell death. *Neurodegeneration* 4(2), pp. 131-137. doi: 10.1006/neur.1995.0016

Jerussi, T. P. and Glick, S. D. 1975. Apomorphine-induced rotation in normal rats and interaction with unilateral caudate lesions. *Psychopharmacologia* 40(4), pp. 329-334. doi: 10.1007/bf00421471

Jiang, Z. H., Liu, Z. G., Chen, S. D., Zhou, W. B., Cai, J., Ni, Z. M. and Zhou, C. F. 1995. [Fate of human fetal dopamine neurons transplanted into rhesus monkey model of Parkinson's disease: a tyrosine hydroxylase immunocytochemical study]. *Sheng Li Xue Bao* 47(1), pp. 31-37.

Jørgensen, J. R. et al. 2006. Identification of novel genes regulated in the developing human ventral mesencephalon. *Exp Neurol* 198(2), pp. 427-437. doi: 10.1016/j.expneurol.2005.12.023

Juárez Olguín, H., Calderón Guzmán, D., Hernández García, E. and Barragán Mejía, G. 2016. The Role of Dopamine and Its Dysfunction as a Consequence of Oxidative Stress. *Oxid Med Cell Longev* 2016, p. 9730467. doi: 10.1155/2016/9730467

Kaakkola, S. 2000. Clinical pharmacology, therapeutic use and potential of COMT inhibitors in Parkinson's disease. *Drugs* 59(6), pp. 1233-1250. doi: 10.2165/00003495-200059060-00004

Kalia, L. V. and Lang, A. E. 2015. Parkinson's disease. *The Lancet* 386(9996), pp. 896-912. doi: https://doi.org/10.1016/S0140-6736(14)61393-3

Kallik, C., Finau, M., Sparks, A. and Ghosh, P. 2021. Association of Medication Mismanagement with Hospital-Related Complications in Patients with Parkinson's Disease at The George Washington University Hospital (GWUH) (1432). *Neurology* 96(15 Supplement), p. 1432.

Kamalkhani, N. and Zarei, M. 2022. Distinct atrophy of septal nuclei in Parkinson's disease. *Clin Park Relat Disord* 7, p. 100171. doi: 10.1016/j.prdoa.2022.100171

Kamińska, K., Lenda, T., Konieczny, J., Czarnecka, A. and Lorenc-Koci, E. 2017. Depressive-like neurochemical and behavioral markers of Parkinson's disease after 6-OHDA administered unilaterally to the rat medial forebrain bundle. *Pharmacol Rep* 69(5), pp. 985-994. doi: 10.1016/j.pharep.2017.05.016

Kaplitt, M. G. et al. 2007. Safety and tolerability of gene therapy with an adeno-associated virus (AAV) borne GAD gene for Parkinson's disease: an open label, phase I trial. *Lancet* 369(9579), pp. 2097-2105. doi: 10.1016/s0140-6736(07)60982-9

Kefalopoulou, Z. et al. 2014. Long-term clinical outcome of fetal cell transplantation for Parkinson disease: two case reports. *JAMA Neurol* 71(1), pp. 83-87. doi: 10.1001/jamaneurol.2013.4749

Ketzef, M., Spigolon, G., Johansson, Y., Bonito-Oliva, A., Fisone, G. and Silberberg, G. 2017. Dopamine Depletion Impairs Bilateral Sensory Processing in the Striatum in a Pathway-Dependent Manner. *Neuron* 94(4), pp. 855-865.e855. doi: https://doi.org/10.1016/j.neuron.2017.05.004

Kim, H. J. et al. 2009. Nonmotor symptoms in de novo Parkinson disease before and after dopaminergic treatment. *J Neurol Sci* 287(1-2), pp. 200-204. doi: 10.1016/j.jns.2009.07.026

Kirik, D., Annett, L. E., Burger, C., Muzyczka, N., Mandel, R. J. and Björklund, A. 2003. Nigrostriatal alpha-synucleinopathy induced by viral vector-mediated overexpression of human alpha-synuclein: a new primate model of Parkinson's disease. *Proc Natl Acad Sci U S A* 100(5), pp. 2884-2889. doi: 10.1073/pnas.0536383100

Kirik, D., Georgievska, B., Burger, C., Winkler, C., Muzyczka, N., Mandel, R. J. and Bjorklund, A. 2002a. Reversal of motor impairments in parkinsonian rats by continuous intrastriatal delivery of L-dopa using rAAV-mediated gene transfer. *Proc Natl Acad Sci U S A* 99(7), pp. 4708-4713. doi: 10.1073/pnas.062047599

Kirik, D., Rosenblad, C. and Björklund, A. 1998. Characterization of Behavioral and Neurodegenerative Changes Following Partial Lesions of the Nigrostriatal Dopamine System Induced by Intrastriatal 6-Hydroxydopamine in the Rat. *Experimental Neurology* 152(2), pp. 259-277. doi: https://doi.org/10.1006/exnr.1998.6848

Kirik, D. et al. 2002b. Parkinson-like neurodegeneration induced by targeted overexpression of alpha-synuclein in the nigrostriatal system. *J Neurosci* 22(7), pp. 2780-2791. doi: 10.1523/jneurosci.22-07-02780.2002

Kirkeby, A. et al. 2012. Generation of Regionally Specified Neural Progenitors and Functional Neurons from Human Embryonic Stem Cells under Defined Conditions. *Cell Reports* 1(6), pp. 703-714. doi: 10.1016/j.celrep.2012.04.009

Kirkeby, A. et al. 2017. Predictive markers guide differentiation to improve graft outcome in clinical translation of hESC-based therapy for Parkinson's Disease.

Kish, S. J., Tong, J., Hornykiewicz, O., Rajput, A., Chang, L. J., Guttman, M. and Furukawa, Y. 2008. Preferential loss of serotonin markers in caudate versus putamen in Parkinson's disease. *Brain* 131(Pt 1), pp. 120-131. doi: 10.1093/brain/awm239

Klann, E. M. et al. 2021. The Gut-Brain Axis and Its Relation to Parkinson's Disease: A Review. *Front Aging Neurosci* 13, p. 782082. doi: 10.3389/fnagi.2021.782082

Kordower, J. H. et al. 1998. Fetal nigral grafts survive and mediate clinical benefit in a patient with Parkinson's disease. *Mov Disord* 13(3), pp. 383-393. doi: 10.1002/mds.870130303

Kordower, J. H. et al. 1995. Neuropathological evidence of graft survival and striatal reinnervation after the transplantation of fetal mesencephalic tissue in a patient with Parkinson's disease. *N Engl J Med* 332(17), pp. 1118-1124. doi: 10.1056/nejm199504273321702

Kordower, J. H. et al. 2013. Disease duration and the integrity of the nigrostriatal system in Parkinson's disease. *Brain* 136(8), pp. 2419-2431. doi: 10.1093/brain/awt192

Kosaka, K. 2014. Latest concept of Lewy body disease. *Psychiatry Clin Neurosci* 68(6), pp. 391-394. doi: 10.1111/pcn.12179

Koschel, J., Ray Chaudhuri, K., Tönges, L., Thiel, M., Raeder, V. and Jost, W. H. 2022. Implications of dopaminergic medication withdrawal in Parkinson's disease. *J Neural Transm (Vienna)* 129(9), pp. 1169-1178. doi: 10.1007/s00702-021-02389-x

Krabbe, S. et al. 2015. Increased dopamine D2 receptor activity in the striatum alters the firing pattern of dopamine neurons in the ventral tegmental area. *Proc Natl Acad Sci U S A* 112(12), pp. E1498-1506. doi: 10.1073/pnas.1500450112

Kraemmer, J., Kovacs, G. G., Perju-Dumbrava, L., Pirker, S., Traub-Weidinger, T. and Pirker, W. 2014. Correlation of striatal dopamine transporter imaging with post mortem substantia nigra cell counts. *Mov Disord* 29(14), pp. 1767-1773. doi: 10.1002/mds.25975

Kriks, S. et al. 2011. Dopamine neurons derived from human ES cells efficiently engraft in animal models of Parkinson's disease. *Nature* 480(7378), pp. 547-551. doi: 10.1038/nature10648

Kulisevsky, J. 2000. Role of dopamine in learning and memory: implications for the treatment of cognitive dysfunction in patients with Parkinson's disease. *Drugs Aging* 16(5), pp. 365-379. doi: 10.2165/00002512-200016050-00006

Kulisevsky, J., Avila, A., Barbanoj, M., Antonijoan, R., Berthier, M. L. and Gironell, A. 1996. Acute effects of levodopa on neuropsychological performance in stable and fluctuating Parkinson's disease patients at different levodopa plasma levels. *Brain* 119 (Pt 6), pp. 2121-2132. doi: 10.1093/brain/119.6.2121

Kumer, S. C. and Vrana, K. E. 1996. Intricate regulation of tyrosine hydroxylase activity and gene expression. *J Neurochem* 67(2), pp. 443-462. doi: 10.1046/j.1471-4159.1996.67020443.x

Kurlan, R., Kim, M. H. and Gash, D. M. 1991. Oral levodopa dose-response study in MPTP-induced hemiparkinsonian monkeys: assessment with a new rating scale for monkey parkinsonism. *Mov Disord* 6(2), pp. 111-118. doi: 10.1002/mds.870060205

Kurtis, M. M., Rajah, T., Delgado, L. F. and Dafsari, H. S. 2017. The effect of deep brain stimulation on the non-motor symptoms of Parkinson's disease: a critical review of the current evidence. *NPJ Parkinsons Dis* 3, p. 16024. doi: 10.1038/npjparkd.2016.24

Kwak, Y., Müller, M. L., Bohnen, N. I., Dayalu, P. and Seidler, R. D. 2012. l-DOPA changes ventral striatum recruitment during motor sequence learning in Parkinson's disease. *Behav Brain Res* 230(1), pp. 116-124. doi: 10.1016/j.bbr.2012.02.006

Lama, J., Buhidma, Y., Fletcher, Edward J. R. and Duty, S. 2021. Animal models of Parkinson's disease: a guide to selecting the optimal model for your research. *Neuronal Signaling* 5(4), doi: 10.1042/ns20210026

Lang, A. E. et al. 2006. Randomized controlled trial of intraputamenal glial cell line-derived neurotrophic factor infusion in Parkinson disease. *Ann Neurol* 59(3), pp. 459-466. doi: 10.1002/ana.20737

Langston, J. W., Irwin, I., Langston, E. B. and Forno, L. S. 1984a. 1-Methyl-4-phenylpyridinium ion (MPP+): identification of a metabolite of MPTP, a toxin selective to the substantia nigra. *Neurosci Lett* 48(1), pp. 87-92. doi: 10.1016/0304-3940(84)90293-3

Langston, J. W., Langston, E. B. and Irwin, I. 1984b. MPTP-induced parkinsonism in human and non-human primates--clinical and experimental aspects. *Acta Neurol Scand Suppl* 100, pp. 49-54.

Lapointe, N., St-Hilaire, M., Martinoli, M. G., Blanchet, J., Gould, P., Rouillard, C. and Cicchetti, F. 2004. Rotenone induces non-specific central nervous system and systemic toxicity. *Faseb j* 18(6), pp. 717-719. doi: 10.1096/fj.03-0677fje

Lebedev, A. V. et al. 2020. Effects of daily L-dopa administration on learning and brain structure in older adults undergoing cognitive training: a randomised clinical trial. *Sci Rep* 10(1), p. 5227. doi: 10.1038/s41598-020-62172-y

Lee, A., André, J. and Pittenger, C. 2014. Lesions of the dorsomedial striatum delay spatial learning and render cue-based navigation inflexible in a water maze task in mice. *Frontiers in Behavioral Neuroscience* 8, doi: 10.3389/fnbeh.2014.00042

Lee, M. K. et al. 2002. Human α-synuclein-harboring familial Parkinson's disease-linked Ala-53→ Thr mutation causes neurodegenerative disease with α-synuclein aggregation in transgenic mice. *Proceedings of the National Academy of Sciences* 99(13), pp. 8968-8973.

Lee, S. B., Kim, W., Lee, S. and Chung, J. 2007. Loss of LRRK2/PARK8 induces degeneration of dopaminergic neurons in Drosophila. *Biochem Biophys Res Commun* 358(2), pp. 534-539. doi: 10.1016/j.bbrc.2007.04.156

Leech, R. and Sharp, D. J. 2014. The role of the posterior cingulate cortex in cognition and disease. *Brain* 137(Pt 1), pp. 12-32. doi: 10.1093/brain/awt162

Lees, A. J. 1989. The on-off phenomenon. *J Neurol Neurosurg Psychiatry* Suppl(Suppl), pp. 29-37. doi: 10.1136/jnnp.52.suppl.29

Lehéricy, S., Benali, H., Van de Moortele, P. F., Pélégrini-Issac, M., Waechter, T., Ugurbil, K. and Doyon, J. 2005. Distinct basal ganglia territories are engaged in early and advanced motor sequence learning. *Proc Natl Acad Sci U S A* 102(35), pp. 12566-12571. doi: 10.1073/pnas.0502762102

Lelos, M. J., Dowd, E. and Dunnett, S. B. 2012a. Chapter 7 - Nigral grafts in animal models of Parkinson's disease. Is recovery beyond motor function possible? In: Dunnett, S.B. and Björklund, A. eds. *Progress in Brain Research*. Vol. 200. Elsevier, pp. 113-142.

Lelos, M. J., Harrison, D. J. and Dunnett, S. B. 2012b. Intrastriatal excitotoxic lesion or dopamine depletion of the neostriatum differentially impairs response execution in extrapersonal space. *Eur J Neurosci* 36(10), pp. 3420-3428. doi: 10.1111/j.1460-9568.2012.08256.x

Lelos, M. J., Morgan, R. J., Kelly, C. M., Torres, E. M., Rosser, A. E. and Dunnett, S. B. 2016. Amelioration of non-motor dysfunctions after transplantation of human dopamine neurons in a model of Parkinson's disease. *Experimental Neurology* 278, pp. 54-61. doi: 10.1016/j.expneurol.2016.02.003

Leriche, L. et al. 2009. Positron emission tomography imaging demonstrates correlation between behavioral recovery and correction of dopamine neurotransmission after gene therapy. *J Neurosci* 29(5), pp. 1544-1553. doi: 10.1523/jneurosci.4491-08.2009

Leroi, I., McDonald, K., Pantula, H. and Harbishettar, V. 2012. Cognitive impairment in Parkinson disease: impact on quality of life, disability, and caregiver burden. *J Geriatr Psychiatry Neurol* 25(4), pp. 208-214. doi: 10.1177/0891988712464823

Levin, J., Kurz, A., Arzberger, T., Giese, A. and Höglinger, G. U. 2016. The Differential Diagnosis and Treatment of Atypical Parkinsonism. *Dtsch Arztebl Int* 113(5), pp. 61-69. doi: 10.3238/arztebl.2016.0061

Levy, G. et al. 2002. Memory and executive function impairment predict dementia in Parkinson's disease. *Mov Disord* 17(6), pp. 1221-1226. doi: 10.1002/mds.10280

Lewis, S. J., Slabosz, A., Robbins, T. W., Barker, R. A. and Owen, A. M. 2005. Dopaminergic basis for deficits in working memory but not attentional set-shifting in Parkinson's disease. *Neuropsychologia* 43(6), pp. 823-832. doi: 10.1016/j.neuropsychologia.2004.10.001

LeWitt, P. A. et al. 2011. AAV2-GAD gene therapy for advanced Parkinson's disease: a double-blind, sham-surgery controlled, randomised trial. *Lancet Neurol* 10(4), pp. 309-319. doi: 10.1016/s1474-4422(11)70039-4

Li, C. and Samulski, R. J. 2020. Engineering adeno-associated virus vectors for gene therapy. *Nature Reviews Genetics* 21(4), pp. 255-272. doi: 10.1038/s41576-019-0205-4

Li, J. Y. et al. 2008. Lewy bodies in grafted neurons in subjects with Parkinson's disease suggest host-to-graft disease propagation. *Nat Med* 14(5), pp. 501-503. doi: 10.1038/nm1746

Li, W. et al. 2016. Extensive graft-derived dopaminergic innervation is maintained 24 years after transplantation in the degenerating parkinsonian brain. *Proceedings of the National Academy of Sciences* 113(23), pp. 6544-6549. doi: doi:10.1073/pnas.1605245113

Lindgren, H. S., Demirbugen, M., Bergqvist, F., Lane, E. L. and Dunnett, S. B. 2014a. The effect of additional noradrenergic and serotonergic depletion on a lateralised choice reaction time task in rats with nigral 6-OHDA lesions. *Exp Neurol* 253, pp. 52-62. doi: 10.1016/j.expneurol.2013.11.015

Lindgren, H. S., Klein, A. and Dunnett, S. B. 2014b. Nigral 6-hydroxydopamine lesion impairs performance in a lateralised choice reaction time task--impact of training and task parameters. *Behav Brain Res* 266, pp. 207-215. doi: 10.1016/j.bbr.2014.02.043

Lindgren, H. S., Wickens, R., Tait, D. S., Brown, V. J. and Dunnett, S. B. 2013. Lesions of the dorsomedial striatum impair formation of attentional set in rats. *Neuropharmacology* 71, pp. 148-153. doi: 10.1016/j.neuropharm.2013.03.034

Lindvall, O. et al. 1987. Transplantation in Parkinson's disease: two cases of adrenal medullary grafts to the putamen. *Ann Neurol* 22(4), pp. 457-468. doi: 10.1002/ana.410220403

Lindvall, O. et al. 1990. Grafts of Fetal Dopamine Neurons Survive and Improve Motor Function in Parkinson's Disease. *Science* 247(4942), pp. 574-577. doi: doi:10.1126/science.2105529

Magistrelli, L., Amoruso, A., Mogna, L., Graziano, T., Cantello, R., Pane, M. and Comi, C. 2019. Probiotics May Have Beneficial Effects in Parkinson's Disease: In vitro Evidence. *Front Immunol* 10, p. 969. doi: 10.3389/fimmu.2019.00969

Magnard, R. et al. 2016. What can rodent models tell us about apathy and associated neuropsychiatric symptoms in Parkinson's disease? *Transl Psychiatry* 6(3), p. e753. doi: 10.1038/tp.2016.17

Mahul-Mellier, A. L. et al. 2020. The process of Lewy body formation, rather than simply α-synuclein fibrillization, is one of the major drivers of neurodegeneration. *Proc Natl Acad Sci U S A* 117(9), pp. 4971-4982. doi: 10.1073/pnas.1913904117

Maini Rekdal, V., Bess, E. N., Bisanz, J. E., Turnbaugh, P. J. and Balskus, E. P. 2019. Discovery and inhibition of an interspecies gut bacterial pathway for Levodopa metabolism. *Science* 364(6445), doi: 10.1126/science.aau6323

Mark, D. H., Robert, D. S. and Kevin, N. G. 2006. A Physiologically Plausible Model of Action Selection and Oscillatory Activity in the Basal Ganglia. *The Journal of Neuroscience* 26(50), p. 12921. doi: 10.1523/JNEUROSCI.3486-06.2006

Martini, S., Marino, F., Magistrelli, L., Contaldi, E., Cosentino, M. and Comi, C. 2023. The PROB-PD trial: a pilot, randomised, placebo-controlled study protocol to evaluate the feasibility and potential efficacy of probiotics in modulating peripheral immunity in subjects with Parkinson's disease. *Pilot Feasibility Stud* 9(1), p. 77. doi: 10.1186/s40814-023-01306-1

Masliah, E. et al. 2000. Dopaminergic loss and inclusion body formation in α-synuclein mice: implications for neurodegenerative disorders. *Science* 287(5456), pp. 1265-1269.

Matsuda, W., Furuta, T., Nakamura, K. C., Hioki, H., Fujiyama, F., Arai, R. and Kaneko, T. 2009. Single nigrostriatal dopaminergic neurons form widely spread and highly dense axonal arborizations in the neostriatum. *J Neurosci* 29(2), pp. 444-453. doi: 10.1523/jneurosci.4029-08.2009

Matsumoto, N., Hanakawa, T., Maki, S., Graybiel, A. M. and Kimura, M. 1999. Role of [corrected] nigrostriatal dopamine system in learning to perform sequential motor tasks in a predictive manner. *J Neurophysiol* 82(2), pp. 978-998. doi: 10.1152/jn.1999.82.2.978

Mattay, V. S. et al. 2002. Dopaminergic modulation of cortical function in patients with Parkinson's disease. *Annals of Neurology* 51(2), pp. 156-164. doi: 10.1002/ana.10078

Mavridis, I., Boviatsis, E. and Anagnostopoulou, S. 2011. The human nucleus accumbens suffers parkinsonism-related shrinkage: a novel finding. *Surg Radiol Anat* 33(7), pp. 595-599. doi: 10.1007/s00276-011-0802-1

Mavridis, I. N. and Pyrgelis, E. S. 2022. Nucleus accumbens atrophy in Parkinson's disease (Mavridis' atrophy): 10 years later. *Am J Neurodegener Dis* 11(2), pp. 17-21.

McGregor, M. M. and Nelson, A. B. 2019. Circuit Mechanisms of Parkinson's Disease. *Neuron* 101(6), pp. 1042-1056. doi: https://doi.org/10.1016/j.neuron.2019.03.004

McNamee, D., Liljeholm, M., Zika, O. and O'Doherty, J. P. 2015. Characterizing the associative content of brain structures involved in habitual and goal-directed actions in humans: a multivariate FMRI study. *J Neurosci* 35(9), pp. 3764-3771. doi: 10.1523/jneurosci.4677-14.2015

McRitchie, D. A., Cartwright, H. R. and Halliday, G. M. 1997. Specific A10 Dopaminergic Nuclei in the Midbrain Degenerate in Parkinson's Disease. *Experimental Neurology* 144(1), pp. 202-213. doi: 10.1006/exnr.1997.6418

Meffert, H., Penner, E., VanTieghem, M. R., Sypher, I., Leshin, J. and Blair, R. J. R. 2018. The role of ventral striatum in reward-based attentional bias. *Brain Res* 1689, pp. 89-97. doi: 10.1016/j.brainres.2018.03.036

Mejías-Aponte, C. A., Drouin, C. and Aston-Jones, G. 2009. Adrenergic and noradrenergic innervation of the midbrain ventral tegmental area and retrorubral field: prominent inputs from medullary homeostatic centers. *J Neurosci* 29(11), pp. 3613-3626. doi: 10.1523/jneurosci.4632-08.2009

Mela, F., Millan, M. J., Brocco, M. and Morari, M. 2010. The selective D(3) receptor antagonist, S33084, improves parkinsonian-like motor dysfunction but does not affect L-DOPA-induced dyskinesia in 6-hydroxydopamine hemi-lesioned rats. *Neuropharmacology* 58(2), pp. 528-536. doi: 10.1016/j.neuropharm.2009.08.017

Mendes-Pinheiro, B. et al. 2021. Unilateral Intrastriatal 6-Hydroxydopamine Lesion in Mice: A Closer Look into Non-Motor Phenotype and Glial Response. *Int J Mol Sci* 22(21), doi: 10.3390/ijms222111530

Mendez, I. et al. 2005. Cell type analysis of functional fetal dopamine cell suspension transplants in the striatum and substantia nigra of patients with Parkinson's disease. *Brain* 128(Pt 7), pp. 1498-1510. doi: 10.1093/brain/awh510

Menegas, W. et al. 2015. Dopamine neurons projecting to the posterior striatum form an anatomically distinct subclass. *Elife* 4, p. e10032. doi: 10.7554/eLife.10032

Meredith, G. E. and Rademacher, D. J. 2011. MPTP mouse models of Parkinson's disease: an update. *J Parkinsons Dis* 1(1), pp. 19-33. doi: 10.3233/jpd-2011-11023

Miller, D. W. and Abercrombie, E. D. 1999. Role of high-affinity dopamine uptake and impulse activity in the appearance of extracellular dopamine in striatum after administration of exogenous L-DOPA: studies in intact and 6-hydroxydopamine-treated rats. *J Neurochem* 72(4), pp. 1516-1522. doi: 10.1046/j.1471-4159.1999.721516.x

Miller, G. W. 2007. Paraquat: The Red Herring of Parkinson's Disease Research. *Toxicological Sciences* 100(1), pp. 1-2. doi: 10.1093/toxsci/kfm223

Miyachi, S., Hikosaka, O., Miyashita, K., Kárádi, Z. and Rand, M. K. 1997. Differential roles of monkey striatum in learning of sequential hand movement. *Exp Brain Res* 115(1), pp. 1-5. doi: 10.1007/pl00005669

Miyamoto, Y., Nagayoshi, I., Nishi, A. and Fukuda, T. 2019. Three divisions of the mouse caudal striatum differ in the proportions of dopamine D1 and D2 receptor-expressing cells, distribution of dopaminergic axons, and composition of cholinergic and GABAergic interneurons. *Brain Struct Funct* 224(8), pp. 2703-2716. doi: 10.1007/s00429-019-01928-3

Moffat, M., Harmon, S., Haycock, J. and O'Malley, K. L. 1997. L-Dopa and dopamine-producing gene cassettes for gene therapy approaches to Parkinson's disease. *Exp Neurol* 144(1), pp. 69-73. doi: 10.1006/exnr.1996.6390

Moore, R. and Bloom, F. 1978. Central catecholamine neuron systems: anatomy and physiology of the dopamine systems. *Annual review of neuroscience* 1(1), pp. 129-169.

Morais, L. H. et al. 2012. Characterization of motor, depressive-like and neurochemical alterations induced by a short-term rotenone administration. *Pharmacological Reports* 64(5), pp. 1081-1090.

Moratalla, R., Quinn, B., DeLanney, L. E., Irwin, I., Langston, J. W. and Graybiel, A. M. 1992. Differential vulnerability of primate caudate-putamen and striosome-matrix dopamine systems to the neurotoxic effects of 1-methyl-4-phenyl-1,2,3,6-tetrahydropyridine. *Proc Natl Acad Sci U S A* 89(9), pp. 3859-3863. doi: 10.1073/pnas.89.9.3859

Moreno, M., Azocar, V., Vergés, A. and Fuentealba, J. A. 2021. High impulsive choice is accompanied by an increase in dopamine release in rat dorsolateral striatum. *Behav Brain Res* 405, p. 113199. doi: 10.1016/j.bbr.2021.113199

Morizane, A. 2023. Cell therapy for Parkinson's disease with induced pluripotent stem cells. *Inflammation and Regeneration* 43(1), p. 16. doi: 10.1186/s41232-023-00269-3

Morris, R. W., Dezfouli, A., Griffiths, K. R., Le Pelley, M. E. and Balleine, B. W. 2022. The Neural Bases of Action-Outcome Learning in Humans. *J Neurosci* 42(17), pp. 3636-3647. doi: 10.1523/jneurosci.1079-21.2022

Morrish, P. K., Rakshi, J. S., Bailey, D. L., Sawle, G. V. and Brooks, D. J. 1998. Measuring the rate of progression and estimating the preclinical period of Parkinson's disease with [18F]dopa PET. *J Neurol Neurosurg Psychiatry* 64(3), pp. 314-319. doi: 10.1136/jnnp.64.3.314

Morrison, C. E., Borod, J. C., Brin, M. F., Hälbig, T. D. and Olanow, C. W. 2004. Effects of levodopa on cognitive functioning in moderate-to-severe Parkinson's disease (MSPD). *J Neural Transm (Vienna)* 111(10-11), pp. 1333-1341. doi: 10.1007/s00702-004-0145-8

Moustafa, A. A., Sherman, S. J. and Frank, M. J. 2008. A dopaminergic basis for working memory, learning and attentional shifting in Parkinsonism. *Neuropsychologia* 46(13), pp. 3144-3156. doi: 10.1016/j.neuropsychologia.2008.07.011

Mukherjee, J., Christian, B. T., Dunigan, K. A., Shi, B., Narayanan, T. K., Satter, M. and Mantil, J. 2002. Brain imaging of 18F-fallypride in normal volunteers: blood analysis, distribution, test-retest studies, and preliminary assessment of sensitivity to aging effects on dopamine D-2/D-3 receptors. *Synapse* 46(3), pp. 170-188. doi: 10.1002/syn.10128

Murphy, B. L., Arnsten, A. F., Goldman-Rakic, P. S. and Roth, R. H. 1996. Increased dopamine turnover in the prefrontal cortex impairs spatial working memory performance in rats and monkeys. *Proc Natl Acad Sci U S A* 93(3), pp. 1325-1329. doi: 10.1073/pnas.93.3.1325

Muslimovic, D., Post, B., Speelman, J. D. and Schmand, B. 2005. Cognitive profile of patients with newly diagnosed Parkinson disease. *Neurology* 65(8), pp. 1239-1245. doi: 10.1212/01.wnl.0000180516.69442.95

Nagai, Y., Minamimoto, T., Ando, K., Obayashi, S., Ito, H., Ito, N. and Suhara, T. 2012. Correlation between decreased motor activity and dopaminergic degeneration in the ventrolateral putamen in monkeys receiving repeated MPTP administrations: A positron emission tomography study. *Neuroscience Research* 73(1), pp. 61-67. doi: https://doi.org/10.1016/j.neures.2012.02.007

Nakamura, K., Santos, G. S., Matsuzaki, R. and Nakahara, H. 2012. Differential reward coding in the subdivisions of the primate caudate during an oculomotor task. *J Neurosci* 32(45), pp. 15963-15982. doi: 10.1523/jneurosci.1518-12.2012

Naso, M. F., Tomkowicz, B., Perry, W. L., 3rd and Strohl, W. R. 2017. Adeno-Associated Virus (AAV) as a Vector for Gene Therapy. *BioDrugs* 31(4), pp. 317-334. doi: 10.1007/s40259-017-0234-5

Naughton, C., O'Toole, D., Kirik, D. and Dowd, E. 2017. Interaction between subclinical doses of the Parkinson's disease associated gene, α-synuclein, and the pesticide, rotenone, precipitates motor dysfunction and nigrostriatal neurodegeneration in rats. *Behav Brain Res* 316, pp. 160-168. doi: 10.1016/j.bbr.2016.08.056

Naz, F. et al. 2022. Bromocriptine therapy: Review of mechanism of action, safety and tolerability. *Clin Exp Pharmacol Physiol* 49(8), pp. 903-922. doi: 10.1111/1440-1681.13678

Niemann, N. and Jankovic, J. 2019. Juvenile parkinsonism: Differential diagnosis, genetics, and treatment. *Parkinsonism Relat Disord* 67, pp. 74-89. doi: 10.1016/j.parkreldis.2019.06.025

Nolbrant, S., Andreas, H., Malin, P. and Agnete, K. 2017. Generation of high-purity human ventral midbrain dopaminergic progenitors for in vitro maturation and intracerebral transplantation. *Nature Protocols* 12(9), p. 1962. doi: 10.1038/nprot.2017.078

Norris, S. A., Tian, L., Williams, E. L. and Perlmutter, J. S. 2023. Transient dystonia correlates with parkinsonism after 1-methyl-4-phenyl-1,2,3,6- tetrahydropyridine in non- human primates. *Dystonia* 2, doi: 10.3389/dyst.2023.11019

Nutt, J. G., Obeso, J. A. and Stocchi, F. 2000. Continuous dopamine-receptor stimulation in advanced Parkinson's disease. *Trends in Neurosciences* 23, pp. S109-S115. doi: https://doi.org/10.1016/S1471-1931(00)00029-X

Nuzum, N. D., Loughman, A., Szymlek-Gay, E. A., Teo, W. P., Hendy, A. M. and Macpherson, H. 2022. To the Gut Microbiome and Beyond: The Brain-First or Body-First Hypothesis in Parkinson's Disease. *Front Microbiol* 13, p. 791213. doi: 10.3389/fmicb.2022.791213

O'Neill, M. and Brown, V. J. 2007. The effect of striatal dopamine depletion and the adenosine A2A antagonist KW-6002 on reversal learning in rats. *Neurobiol Learn Mem* 88(1), pp. 75-81. doi: 10.1016/j.nlm.2007.03.003

O'Sullivan, S. S., Williams, D. R., Gallagher, D. A., Massey, L. A., Silveira-Moriyama, L. and Lees, A. J. 2008. Nonmotor symptoms as presenting complaints in Parkinson's disease: a clinicopathological study. *Movement Disorders* 23(1), pp. 101-106.

Ogura, T. et al. 2005. Impaired acquisition of skilled behavior in rotarod task by moderate depletion of striatal dopamine in a pre-symptomatic stage model of Parkinson's disease. *Neurosci Res* 51(3), pp. 299-308. doi: 10.1016/j.neures.2004.12.006

Oiwa, Y., Eberling, J. L., Nagy, D., Pivirotto, P., Emborg, M. E. and Bankiewicz, K. S. 2003. Overlesioned hemiparkinsonian non human primate model: correlation between clinical, neurochemical and histochemical changes. *Front Biosci* 8, pp. a155-166. doi: 10.2741/1104

Olanow, C. W. et al. 2021. Continuous Subcutaneous Levodopa Delivery for Parkinson's Disease: A Randomized Study. *J Parkinsons Dis* 11(1), pp. 177-186. doi: 10.3233/jpd-202285

Olanow, C. W. et al. 2003. A double-blind controlled trial of bilateral fetal nigral transplantation in Parkinson's disease. *Ann Neurol* 54(3), pp. 403-414. doi: 10.1002/ana.10720

Olney, J. J., Warlow, S. M., Naffziger, E. E. and Berridge, K. C. 2018. Current perspectives on incentive salience and applications to clinical disorders. *Curr Opin Behav Sci* 22, pp. 59-69. doi: 10.1016/j.cobeha.2018.01.007

Olsson, M., Nikkhah, G., Bentlage, C. and Bjorklund, A. 1995. Forelimb akinesia in the rat Parkinson model: differential effects of dopamine agonists and nigral transplants as assessed by a new stepping test. *The Journal of Neuroscience* 15(5), p. 3863. doi: 10.1523/JNEUROSCI.15-05-03863.1995

Pagano, G., Ferrara, N., Brooks, D. J. and Pavese, N. 2016. Age at onset and Parkinson disease phenotype. *Neurology* 86(15), pp. 1400-1407. doi: 10.1212/wnl.0000000000002461

Palencia, C. A. and Ragozzino, M. E. 2004. The influence of NMDA receptors in the dorsomedial striatum on response reversal learning. *Neurobiol Learn Mem* 82(2), pp. 81-89. doi: 10.1016/j.nlm.2004.04.004

Palencia, C. A. and Ragozzino, M. E. 2005. The contribution of NMDA receptors in the dorsolateral striatum to egocentric response learning. *Behav Neurosci* 119(4), pp. 953-960. doi: 10.1037/0735-7044.119.4.953

Palfi, S. et al. 2018. Long-Term Follow-Up of a Phase I/II Study of ProSavin, a Lentiviral Vector Gene Therapy for Parkinson's Disease. *Hum Gene Ther Clin Dev* 29(3), pp. 148-155. doi: 10.1089/humc.2018.081

Palmiter, R. D. 2008. Dopamine signaling in the dorsal striatum is essential for motivated behaviors: lessons from dopamine-deficient mice. *Ann N Y Acad Sci* 1129, pp. 35-46. doi: 10.1196/annals.1417.003

Panman, L. et al. 2014. Sox6 and Otx2 Control the Specification of Substantia Nigra and Ventral Tegmental Area Dopamine Neurons. *Cell Reports* 8(4), pp. 1018-1025. doi: 10.1016/j.celrep.2014.07.016

Paredes-Rodriguez, E., Vegas-Suarez, S., Morera-Herreras, T., De Deurwaerdere, P. and Miguelez, C. 2020. The Noradrenergic System in Parkinson's Disease. *Front Pharmacol* 11, p. 435. doi: 10.3389/fphar.2020.00435

Park, A. and Stacy, M. 2011. Dopamine-induced nonmotor symptoms of Parkinson's disease. *Parkinsons Dis* 2011, p. 485063. doi: 10.4061/2011/485063

Parkinson, J. 1817. *An essay on the shaking palsy*. Sherwood: Needley and Jones.

Pascual-Sedano, B. et al. 2008. Levodopa and executive performance in Parkinson's disease: a randomized study. *J Int Neuropsychol Soc* 14(5), pp. 832-841. doi: 10.1017/s1355617708081010

Paumier, K. L. et al. 2013. Behavioral characterization of A53T mice reveals early and late stage deficits related to Parkinson's disease. *PLoS One* 8(8), p. e70274. doi: 10.1371/journal.pone.0070274

Pavese, N., Metta, V., Bose, S. K., Chaudhuri, K. R. and Brooks, D. J. 2010. Fatigue in Parkinson's disease is linked to striatal and limbic serotonergic dysfunction. *Brain* 133(11), pp. 3434-3443. doi: 10.1093/brain/awq268

Paxinos, G. and Watson, C. 2006. *The rat brain in stereotaxic coordinates: hard cover edition*. Elsevier.

Pearson, T. S. et al. 2021. Gene therapy for aromatic L-amino acid decarboxylase deficiency by MR-guided direct delivery of AAV2-AADC to midbrain dopaminergic neurons. *Nature Communications* 12(1), p. 4251. doi: 10.1038/s41467-021-24524-8

Pelicioni, P. H. S., Menant, J. C., Latt, M. D. and Lord, S. R. 2019. Falls in Parkinson's Disease Subtypes: Risk Factors, Locations and Circumstances. *Int J Environ Res Public Health* 16(12), doi: 10.3390/ijerph16122216

Pellicano, C., Benincasa, D., Pisani, V., Buttarelli, F. R., Giovannelli, M. and Pontieri, F. E. 2007. Prodromal non-motor symptoms of Parkinson's disease. *Neuropsychiatr Dis Treat* 3(1), pp. 145-152. doi: 10.2147/nedt.2007.3.1.145

Pena, M. C. S., Sobreira, E. S. T., Souza, C. P., Oliveira, G. N., Tumas, V. and do Vale, F. A. C. 2008. Visuospatial cognitive tests for the evaluation of patients with Parkinson's disease. *Dement Neuropsychol* 2(3), pp. 201-205. doi: 10.1590/s1980-57642009dn20300007

Perlow, M. J., Freed, W. J., Hoffer, B. J., Seiger, A., Olson, L. and Wyatt, R. J. 1979. Brain grafts reduce motor abnormalities produced by destruction of nigrostriatal dopamine system. *Science (New York, N.Y.)* 204(4393), p. 643. doi: 10.1126/science.571147

Peters, J. and Büchel, C. 2010. Neural representations of subjective reward value. *Behavioural Brain Research* 213(2), pp. 135-141. doi: https://doi.org/10.1016/j.bbr.2010.04.031

Peto, V., Jenkinson, C., Fitzpatrick, R. and Greenhall, R. 1995. The development and validation of a short measure of functioning and well being for individuals with Parkinson's disease. *Qual Life Res* 4(3), pp. 241-248. doi: 10.1007/bf02260863

Pfeiffer, R. F. 2018. Gastrointestinal Dysfunction in Parkinson's Disease. *Curr Treat Options Neurol* 20(12), p. 54. doi: 10.1007/s11940-018-0539-9

Piao, J. et al. 2021. Preclinical Efficacy and Safety of a Human Embryonic Stem Cell-Derived Midbrain Dopamine Progenitor Product, MSK-DA01. *Cell Stem Cell* 28(2), pp. 217-229.e217. doi: 10.1016/j.stem.2021.01.004

Pihlstrøm, L. et al. 2018. A comprehensive analysis of SNCA-related genetic risk in sporadic parkinson disease. *Annals of Neurology* 84(1), pp. 117-129. doi: 10.1002/ana.25274

Pileblad, E., Fornstedt, B., Clark, D. and Carlsson, A. 1985. Acute effects of 1-methyl-4-phenyl-1,2,3,6-tetrahydropyridine on dopamine metabolism in mouse and rat striatum. *J Pharm Pharmacol* 37(10), pp. 707-711. doi: 10.1111/j.2042-7158.1985.tb04947.x

Pine, A., Shiner, T., Seymour, B. and Dolan, R. J. 2010. Dopamine, time, and impulsivity in humans. *J Neurosci* 30(26), pp. 8888-8896. doi: 10.1523/jneurosci.6028-09.2010

Pinsker, M., Amtage, F., Berger, M., Nikkhah, G. and van Elst, L. T. 2013. Psychiatric side-effects of bilateral deep brain stimulation for movement disorders. *Acta Neurochir Suppl* 117, pp. 47-51. doi: 10.1007/978-3-7091-1482-7_8

Poewe, W., Antonini, A., Zijlmans, J. C., Burkhard, P. R. and Vingerhoets, F. 2010. Levodopa in the treatment of Parkinson's disease: an old drug still going strong. *Clin Interv Aging* 5, pp. 229-238. doi: 10.2147/cia.s6456

Poletti, M. and Bonuccelli, U. 2013. Acute and chronic cognitive effects of levodopa and dopamine agonists on patients with Parkinson's disease: a review. *Therapeutic Advances in Psychopharmacology* 3(2), pp. 101-113. doi: 10.1177/2045125312470130

Politis, M. and Loane, C. 2011. Serotonergic dysfunction in Parkinson's disease and its relevance to disability. *ScientificWorldJournal* 11, pp. 1726-1734. doi: 10.1100/2011/172893

Porenta, G. and Riederer, P. 1982. A mathematical model of the dopaminergic synapse: stability and sensitivity analyses, and simulation of Parkinson's disease and aging processes. *Cybernetics and System* 13(3), pp. 257-274.

Postuma, R. B., Gagnon, J. F., Bertrand, J. A., Génier Marchand, D. and Montplaisir, J. Y. 2015. Parkinson risk in idiopathic REM sleep behavior disorder: preparing for neuroprotective trials. *Neurology* 84(11), pp. 1104-1113. doi: 10.1212/wnl.0000000000001364

Potts, Y. and Bekkers, J. M. 2022. Dopamine Increases the Intrinsic Excitability of Parvalbumin-Expressing Fast-Spiking Cells in the Piriform Cortex. *Front Cell Neurosci* 16, p. 919092. doi: 10.3389/fncel.2022.919092

Prashanth, L. K., Fox, S. and Meissner, W. G. 2011. l-Dopa-induced dyskinesia-clinical presentation, genetics, and treatment. *Int Rev Neurobiol* 98, pp. 31-54. doi: 10.1016/b978-0-12-381328-2.00002-x

Precious, S. V. et al. 2016. FoxP1 marks medium spiny neurons from precursors to maturity and is required for their differentiation. *Exp Neurol* 282, pp. 9-18. doi: 10.1016/j.expneurol.2016.05.002

Prensa, L. and Parent, A. 2001. The nigrostriatal pathway in the rat: A single-axon study of the relationship between dorsal and ventral tier nigral neurons and the striosome/matrix striatal compartments. *J Neurosci* 21(18), pp. 7247-7260. doi: 10.1523/jneurosci.21-18-07247.2001

Prodoehl, J., Planetta, P. J., Kurani, A. S., Comella, C. L., Corcos, D. M. and Vaillancourt, D. E. 2013. Differences in brain activation between tremor- and nontremor-dominant Parkinson disease. *JAMA Neurol* 70(1), pp. 100-106. doi: 10.1001/jamaneurol.2013.582

Przedborski, S., Levivier, M., Jiang, H., Ferreira, M., Jackson-Lewis, V., Donaldson, D. and Togasaki, D. M. 1995. Dose-dependent lesions of the dopaminergic nigrostriatal pathway induced by intrastriatal injection of 6-hydroxydopamine. *Neuroscience* 67(3), pp. 631-647. doi: 10.1016/0306-4522(95)00066-r

Przuntek, H. et al. 1996. Early institution of bromocriptine in Parkinson's disease inhibits the emergence of levodopa-associated motor side effects. Long-term results of the PRADO study. *J Neural Transm (Vienna)* 103(6), pp. 699-715. doi: 10.1007/bf01271230

Quinn, N., Critchley, P. and Marsden, C. D. 1987. Young onset Parkinson's disease. *Mov Disord* 2(2), pp. 73-91. doi: 10.1002/mds.870020201

Quintino, L. et al. 2019. GDNF-mediated rescue of the nigrostriatal system depends on the degree of degeneration. *Gene Therapy* 26(1), pp. 57-64. doi: 10.1038/s41434-018-0049-0

Radad, K., Al-Shraim, M., Al-Emam, A., Wang, F., Kranner, B., Rausch, W. D. and Moldzio, R. 2019. Rotenone: from modelling to implication in Parkinson's disease. *Folia Neuropathol* 57(4), pp. 317-326. doi: 10.5114/fn.2019.89857

Radke, A. K., Zweifel, L. S. and Holmes, A. 2019. NMDA receptor deletion on dopamine neurons disrupts visual discrimination and reversal learning. *Neurosci Lett* 699, pp. 109-114. doi: 10.1016/j.neulet.2019.02.001

Rahman, M. M., Uddin, M. J., Chowdhury, J. H. and Chowdhury, T. I. 2014. Effect of levodopa and carbidopa on non-motor symptoms and signs of Parkinson's disease. *Mymensingh Med J* 23(1), pp. 18-23.

Rájová, J. et al. 2023. Deconvolution of spatial sequencing provides accurate characterization of hESC-derived DA transplants in vivo. *Mol Ther Methods Clin Dev* 29, pp. 381-394. doi: 10.1016/j.omtm.2023.04.008

Rath, A. et al. 2013. Survival and Functional Restoration of Human Fetal Ventral Mesencephalon following Transplantation in a Rat Model of Parkinson's Disease. *Cell Transplantation* 22(7), pp. 1281-1293. doi: 10.3727/096368912x654984

Reading, P. J., Dunnett, S. B. and Robbins, T. W. 1991. Dissociable roles of the ventral, medial and lateral striatum on the acquisition and performance of a complex visual stimulus-response habit. *Behavioural Brain Research* 45(2), pp. 147-161. doi: 10.1016/S0166-4328(05)80080-4

Reed, X., Bandrés-Ciga, S., Blauwendraat, C. and Cookson, M. R. 2019. The role of monogenic genes in idiopathic Parkinson's disease. *Neurobiology of Disease* 124, pp. 230-239. doi: https://doi.org/10.1016/j.nbd.2018.11.012

Reimsnider, S., Manfredsson, F. P., Muzyczka, N. and Mandel, R. J. 2007. Time course of transgene expression after intrastriatal pseudotyped rAAV2/1, rAAV2/2, rAAV2/5, and rAAV2/8 transduction in the rat. *Mol Ther* 15(8), pp. 1504-1511. doi: 10.1038/sj.mt.6300227

Reiner, A., Hart, N., Lei, W. and Deng, Y. 2010. Corticostriatal Projection Neurons – Dichotomous Types and Dichotomous Functions. *Frontiers in Neuroanatomy* 4, doi: 10.3389/fnana.2010.00142

Richard, I. H. et al. 2012. A randomized, double-blind, placebo-controlled trial of antidepressants in Parkinson disease. *Neurology* 78(16), p. 1229. doi: 10.1212/WNL.0b013e3182516244

Rietdijk, C. D., Perez-Pardo, P., Garssen, J., van Wezel, R. J. A. and Kraneveld, A. D. 2017. Exploring Braak's Hypothesis of Parkinson's Disease. *Frontiers in Neurology* 8, doi: 10.3389/fneur.2017.00037

Rinne, J. O., Rummukainen, J., Paljärvi, L. and Rinne, U. K. 1989. Dementia in Parkinson's disease is related to neuronal loss in the medial substantia nigra. *Ann Neurol* 26(1), pp. 47-50. doi: 10.1002/ana.410260107

Rinne, U. K., Sonninen, V. and Sirtola, T. 1972. Treatment of Parkinson's disease with L-DOPA and decarboxylase inhibitor. *Z Neurol* 202(1), pp. 1-20. doi: 10.1007/bf00316422

Robinson, S., Rainwater, A. J., Hnasko, T. S. and Palmiter, R. D. 2007. Viral restoration of dopamine signaling to the dorsal striatum restores instrumental conditioning to dopamine-deficient mice. *Psychopharmacology (Berl)* 191(3), pp. 567-578. doi: 10.1007/s00213-006-0579-9

Robinson, S., Sotak, B. N., During, M. J. and Palmiter, R. D. 2006. Local dopamine production in the dorsal striatum restores goal-directed behavior in dopamine-deficient mice. *Behav Neurosci* 120(1), pp. 196-200. doi: 10.1037/0735-7044.120.1.000

Rosa, M. et al. 2017. Adaptive deep brain stimulation controls levodopa-induced side effects in Parkinsonian patients. *Mov Disord* 32(4), pp. 628-629. doi: 10.1002/mds.26953

Rosenberg-Katz, K., Herman, T., Jacob, Y., Giladi, N., Hendler, T. and Hausdorff, J. M. 2013. Gray matter atrophy distinguishes between Parkinson disease motor subtypes. *Neurology* 80(16), pp. 1476-1484. doi: 10.1212/WNL.0b013e31828cfaa4

Rosenblad, C. et al. 2019a. Vector-mediated l-3,4-dihydroxyphenylalanine delivery reverses motor impairments in a primate model of Parkinson's disease. *Brain* 142(8), pp. 2402-2416. doi: 10.1093/brain/awz176

Rosenblad, C. et al. 2019b. Vector-mediated l-3,4-dihydroxyphenylalanine delivery reverses motor impairments in a primate model of Parkinson's disease. *Brain* 142(8), pp. 2402-2416. doi: 10.1093/brain/awz176

Royall, D. R., Cordes, J. A. and Polk, M. 1998. CLOX: an executive clock drawing task. *J Neurol Neurosurg Psychiatry* 64(5), pp. 588-594. doi: 10.1136/jnnp.64.5.588

Sakuma, T., Barry, M. A. and Ikeda, Y. 2012. Lentiviral vectors: basic to translational. *Biochem J* 443(3), pp. 603-618. doi: 10.1042/bj20120146

Sancandi, M., Schul, E. V., Economides, G., Constanti, A. and Mercer, A. 2018. Structural Changes Observed in the Piriform Cortex in a Rat Model of Pre-motor Parkinson's Disease. *Front Cell Neurosci* 12, p. 479. doi: 10.3389/fncel.2018.00479

Sánchez-Pernaute, R., Harvey-White, J., Cunningham, J. and Bankiewicz, K. S. 2001. Functional effect of adeno-associated virus mediated gene transfer of aromatic L-amino acid decarboxylase into the striatum of 6-OHDA-lesioned rats. *Mol Ther* 4(4), pp. 324-330. doi: 10.1006/mthe.2001.0466

Santoro, M., Fadda, P., Klephan, K. J., Hull, C., Teismann, P., Platt, B. and Riedel, G. 2023. Neurochemical, histological, and behavioral profiling of the acute, sub-acute, and chronic MPTP mouse model of Parkinson's disease. *J Neurochem* 164(2), pp. 121-142. doi: 10.1111/jnc.15699

Schallert, T., Fleming, S. M., Leasure, J. L., Tillerson, J. L. and Bland, S. T. 2000. CNS plasticity and assessment of forelimb sensorimotor outcome in unilateral rat models of stroke, cortical ablation, parkinsonism and spinal cord injury. *Neuropharmacology* 39(5), pp. 777-787. doi: 10.1016/S0028-3908(00)00005-8

Schmidt, N. and Ferger, B. 2001. Neurochemical findings in the MPTP model of Parkinson's disease. *J Neural Transm (Vienna)* 108(11), pp. 1263-1282. doi: 10.1007/s007020100004

Schmidt, R. H., Björklund, A., Stenevi, U., Dunnett, S. B. and Gage, F. H. 1983. Intracerebral grafting of neuronal cell suspensions. III. Activity of intrastriatal nigral suspension implants as assessed by measurements of dopamine synthesis and metabolism. *Acta Physiol Scand Suppl* 522, pp. 19-28.

Schneider, J. S., Pioli, E. Y., Jianzhong, Y., Li, Q. and Bezard, E. 2013. Levodopa improves motor deficits but can further disrupt cognition in a macaque Parkinson model. *Mov Disord* 28(5), pp. 663-667. doi: 10.1002/mds.25258

Schrag, A., Jahanshahi, M. and Quinn, N. 2000. What contributes to quality of life in patients with Parkinson's disease? *J Neurol Neurosurg Psychiatry* 69(3), pp. 308-312. doi: 10.1136/jnnp.69.3.308

Schrag, A., Spottke, A., Quinn, N. P. and Dodel, R. 2009. Comparative responsiveness of Parkinson's disease scales to change over time. *Mov Disord* 24(6), pp. 813-818. doi: 10.1002/mds.22438

Schröter, N. et al. 2022. Disentangling nigral and putaminal contribution to motor impairment and levodopa response in Parkinson's disease. *NPJ Parkinsons Dis* 8(1), p. 132. doi: 10.1038/s41531-022-00401-z

Schultz, W., Studer, A., Romo, R., Sundström, E., Jonsson, G. and Scarnati, E. 1989. Deficits in reaction times and movement times as correlates of hypokinesia in monkeys with MPTP-induced striatal dopamine depletion. *J Neurophysiol* 61(3), pp. 651-668. doi: 10.1152/jn.1989.61.3.651

Schüpbach, W. M., Corvol, J. C., Czernecki, V., Djebara, M. B., Golmard, J. L., Agid, Y. and Hartmann, A. 2010. Segmental progression of early untreated Parkinson's disease: a novel approach to clinical rating. *J Neurol Neurosurg Psychiatry* 81(1), pp. 20-25. doi: 10.1136/jnnp.2008.159699

Seamans, J. K. and Yang, C. R. 2004. The principal features and mechanisms of dopamine modulation in the prefrontal cortex. *Progress in Neurobiology* 74(1), pp. 1-58. doi: https://doi.org/10.1016/j.pneurobio.2004.05.006

Shan, Q., Ge, M., Christie, M. J. and Balleine, B. W. 2014. The acquisition of goal-directed actions generates opposing plasticity in direct and indirect pathways in dorsomedial striatum. *J Neurosci* 34(28), pp. 9196-9201. doi: 10.1523/jneurosci.0313-14.2014

Sharp, M. E., Duncan, K., Foerde, K. and Shohamy, D. 2020. Dopamine is associated with prioritization of reward-associated memories in Parkinson's disease. *Brain* 143(8), pp. 2519-2531. doi: 10.1093/brain/awaa182

Sharp, M. E., Foerde, K., Daw, N. D. and Shohamy, D. 2016. Dopamine selectively remediates 'model-based' reward learning: a computational approach. *Brain* 139(Pt 2), pp. 355-364. doi: 10.1093/brain/awv347

Shen, W., Flajolet, M., Greengard, P. and Surmeier, D. J. 2008. Dichotomous dopaminergic control of striatal synaptic plasticity. *Science* 321(5890), pp. 848-851.

Shink, E., Bevan, M. D., Bolam, J. P. and Smith, Y. 1996. The subthalamic nucleus and the external pallidum: two tightly interconnected structures that control the output of the basal ganglia in the monkey. *Neuroscience* 73(2), pp. 335-357. doi: 10.1016/0306-4522(96)00022-x

Shulman, L. M., Taback, R. L., Bean, J. and Weiner, W. J. 2001. Comorbidity of the nonmotor symptoms of Parkinson's disease. *Mov Disord* 16(3), pp. 507-510. doi: 10.1002/mds.1099

Shulman, L. M., Taback, R. L., Rabinstein, A. A. and Weiner, W. J. 2002. Non-recognition of depression and other non-motor symptoms in Parkinson's disease. *Parkinsonism Relat Disord* 8(3), pp. 193-197. doi: 10.1016/s1353-8020(01)00015-3

Silvestri, S. et al. 2000. Increased dopamine D2 receptor binding after long-term treatment with antipsychotics in humans: a clinical PET study. *Psychopharmacology (Berl)* 152(2), pp. 174-180. doi: 10.1007/s002130000532

Simón-Sánchez, J. et al. 2009. Genome-wide association study reveals genetic risk underlying Parkinson's disease. *Nature Genetics* 41(12), pp. 1308-1312. doi: 10.1038/ng.487

Simon, H., Scatton, B. and Moal, M. L. 1980. Dopaminergic A10 neurones are involved in cognitive functions. *Nature* 286(5769), pp. 150-151. doi: 10.1038/286150a0

Sixel-Döring, F., Zimmermann, J., Wegener, A., Mollenhauer, B. and Trenkwalder, C. 2016. The Evolution of REM Sleep Behavior Disorder in Early Parkinson Disease. *Sleep* 39(9), pp. 1737-1742. doi: 10.5665/sleep.6102

Smith, Y., Bevan, M. D., Shink, E. and Bolam, J. P. 1998. Microcircuitry of the direct and indirect pathways of the basal ganglia. *Neuroscience* 86(2), pp. 353-387. doi: 10.1016/s0306-4522(98)00004-9

Soh, S. E., Morris, M. E. and McGinley, J. L. 2011. Determinants of health-related quality of life in Parkinson's disease: a systematic review. *Parkinsonism Relat Disord* 17(1), pp. 1-9. doi: 10.1016/j.parkreldis.2010.08.012

Sonja, K. et al. 2011. Dopamine neurons derived from human ES cells efficiently engraft in animal models of Parkinson's disease. *Nature* 480(7378), p. 547. doi: 10.1038/nature10648

Spencer, D. D. et al. 1992. Unilateral transplantation of human fetal mesencephalic tissue into the caudate nucleus of patients with Parkinson's disease. *N Engl J Med* 327(22), pp. 1541-1548. doi: 10.1056/nejm199211263272201

Spillantini, M. G., Schmidt, M. L., Lee, V. M., Trojanowski, J. Q., Jakes, R. and Goedert, M. 1997. Alpha-synuclein in Lewy bodies. *Nature* 388(6645), pp. 839-840. doi: 10.1038/42166

Srivastava, A. 2016. In vivo tissue-tropism of adeno-associated viral vectors. *Curr Opin Virol* 21, pp. 75-80. doi: 10.1016/j.coviro.2016.08.003

Stacy, M. A., Murck, H. and Kroenke, K. 2010. Responsiveness of motor and nonmotor symptoms of Parkinson disease to dopaminergic therapy. *Prog Neuropsychopharmacol Biol Psychiatry* 34(1), pp. 57-61. doi: 10.1016/j.pnpbp.2009.09.023

Standaert, D. G. et al. 2017. Effect of Levodopa-carbidopa Intestinal Gel on Non-motor Symptoms in Patients with Advanced Parkinson's Disease. *Mov Disord Clin Pract* 4(6), pp. 829-837. doi: 10.1002/mdc3.12526

Stefanis, L. 2012. α-Synuclein in Parkinson's disease. *Cold Spring Harb Perspect Med* 2(2), p. a009399. doi: 10.1101/cshperspect.a009399

Stephenson-Jones, M., Samuelsson, E., Ericsson, J., Robertson, B. and Grillner, S. 2011. Evolutionary conservation of the basal ganglia as a common vertebrate mechanism for action selection. *Curr Biol* 21(13), pp. 1081-1091. doi: 10.1016/j.cub.2011.05.001

Studer, L. 2012. Derivation of dopaminergic neurons from pluripotent stem cells. *Prog Brain Res* 200, pp. 243-263. doi: 10.1016/b978-0-444-59575-1.00011-9

Sun, J. et al. 2023. Disruption of locus coeruleus-related functional networks in Parkinson's disease. *NPJ Parkinsons Dis* 9(1), p. 81. doi: 10.1038/s41531-023-00532-x

Swoboda, K. J., Saul, J. P., McKenna, C. E., Speller, N. B. and Hyland, K. 2003. Aromatic L-amino acid decarboxylase deficiency: overview of clinical features and outcomes. *Ann Neurol* 54 Suppl 6, pp. S49-55. doi: 10.1002/ana.10631

Sy, M. A. C. and Fernandez, H. H. 2020. Pharmacological Treatment of Early Motor Manifestations of Parkinson Disease (PD). *Neurotherapeutics* 17(4), pp. 1331-1338. doi: 10.1007/s13311-020-00924-4

Takahashi, J. 2020. iPS cell-based therapy for Parkinson's disease: A Kyoto trial. *Regen Ther* 13, pp. 18-22. doi: 10.1016/j.reth.2020.06.002

Takahashi, K., Tanabe, K., Ohnuki, M., Narita, M., Ichisaka, T., Tomoda, K. and Yamanaka, S. 2007. Induction of pluripotent stem cells from adult human fibroblasts by defined factors. *Cell* 131(5), pp. 861-872. doi: 10.1016/j.cell.2007.11.019

Tamburrino, A. et al. 2015. Cyclosporin promotes neurorestoration and cell replacement therapy in pre-clinical models of Parkinson's disease. *Acta Neuropathol Commun* 3, p. 84. doi: 10.1186/s40478-015-0263-6

Tanaka, S. C., Balleine, B. W. and O'Doherty, J. P. 2008. Calculating consequences: brain systems that encode the causal effects of actions. *J Neurosci* 28(26), pp. 6750-6755. doi: 10.1523/jneurosci.1808-08.2008

Tanimura, A., Pancani, T., Lim, S. A. O., Tubert, C., Melendez, A. E., Shen, W. and Surmeier, D. J. 2018. Striatal cholinergic interneurons and Parkinson's disease. *Eur J Neurosci* 47(10), pp. 1148-1158. doi: 10.1111/ejn.13638

Taylor, J. L., Bishop, C. and Walker, P. D. 2005. Dopamine D1 and D2 receptor contributions to L-DOPA-induced dyskinesia in the dopamine-depleted rat. *Pharmacol Biochem Behav* 81(4), pp. 887-893. doi: 10.1016/j.pbb.2005.06.013

Tedford, S. E., Persons, A. L. and Napier, T. C. 2015. Dopaminergic lesions of the dorsolateral striatum in rats increase delay discounting in an impulsive choice task. *PLoS One* 10(4), p. e0122063. doi: 10.1371/journal.pone.0122063

Tessitore, A. et al. 2002. Dopamine modulates the response of the human amygdala: a study in Parkinson's disease. *J Neurosci* 22(20), pp. 9099-9103. doi: 10.1523/jneurosci.22-20-09099.2002

Tetrud, J., Langston, J., Redmond, D., Roth, R., Sladek, J. and Angel, R. eds. 1986. *MPTP-INDUCED TREMOR IN HUMAN AND NONHUMAN-PRIMATES*. *Neurology.* LIPPINCOTT-RAVEN PUBL 227 EAST WASHINGTON SQ, PHILADELPHIA, PA 19106.

Tetsuhiro, K. et al. 2017. Human iPS cell-derived dopaminergic neurons function in a primate Parkinson's disease model. *Nature* 548(7669), p. 592. doi: 10.1038/nature23664

Thomson, J. A., Itskovitz-Eldor, J., Shapiro, S. S., Waknitz, M. A., Swiergiel, J. J., Marshall, V. S. and Jones, J. M. 1998. Embryonic stem cell lines derived from human blastocysts. *Science* 282(5391), pp. 1145-1147. doi: 10.1126/science.282.5391.1145

Tiklová, K. et al. 2020. Single cell transcriptomics identifies stem cell-derived graft composition in a model of Parkinson's disease. *Nat Commun* 11(1), p. 2434. doi: 10.1038/s41467-020-16225-5

Tomer, R., Aharon-Peretz, J. and Tsitrinbaum, Z. 2007. Dopamine asymmetry interacts with medication to affect cognition in Parkinson's disease. *Neuropsychologia* 45(2), pp. 357-367. doi: 10.1016/j.neuropsychologia.2006.06.014

Torres-Pasillas, G. et al. 2023. Olfactory Dysfunction in Parkinson’s Disease, Its Functional and Neuroanatomical Correlates. *NeuroSci* 4(2), pp. 134-151.

Torres, E. M. and Dunnett, S. B. 2012. 6-OHDA Lesion Models of Parkinson's Disease in the Rat. In: Lane, E.L. and Dunnett, S.B. eds. *Animal Models of Movement Disorders: Volume I*. Totowa, NJ: Humana Press, pp. 267-279.

Toti, L. and Travagli, R. A. 2014. Gastric dysregulation induced by microinjection of 6-OHDA in the substantia nigra pars compacta of rats is determined by alterations in the brain-gut axis. *Am J Physiol Gastrointest Liver Physiol* 307(10), pp. G1013-1023. doi: 10.1152/ajpgi.00258.2014

Tricomi, E., Balleine, B. W. and O'Doherty, J. P. 2009. A specific role for posterior dorsolateral striatum in human habit learning. *Eur J Neurosci* 29(11), pp. 2225-2232. doi: 10.1111/j.1460-9568.2009.06796.x

Trojanowski, J. Q. and Lee, V. M. 1998. Aggregation of neurofilament and alpha-synuclein proteins in Lewy bodies: implications for the pathogenesis of Parkinson disease and Lewy body dementia. *Arch Neurol* 55(2), pp. 151-152. doi: 10.1001/archneur.55.2.151

Tronci, E. and Francardo, V. 2018. Animal models of L-DOPA-induced dyskinesia: the 6-OHDA-lesioned rat and mouse. *J Neural Transm (Vienna)* 125(8), pp. 1137-1144. doi: 10.1007/s00702-017-1825-5

Türker, R. K. and Khairallah, P. A. 1967. Demethylimipramine (Desipramine), an α-adrenergic blocking agent. *Experientia* 23(4), pp. 252-252. doi: 10.1007/BF02135664

Uc, E. Y., Rizzo, M., Anderson, S. W., Qian, S., Rodnitzky, R. L. and Dawson, J. D. 2005. Visual dysfunction in Parkinson disease without dementia. *Neurology* 65(12), pp. 1907-1913. doi: 10.1212/01.wnl.0000191565.11065.11

Uitti, R. J., Ahlskog, J. E., Maraganore, D. M., Muenter, M. D., Atkinson, E. J., Cha, R. H. and O'Brien, P. C. 1993. Levodopa therapy and survival in idiopathic Parkinson's disease: Olmsted County project. *Neurology* 43(10), pp. 1918-1926. doi: 10.1212/wnl.43.10.1918

Ungerstedt, U. 1968. 6-Hydroxy-dopamine induced degeneration of central monoamine neurons. *Eur J Pharmacol* 5(1), pp. 107-110. doi: 10.1016/0014-2999(68)90164-7

Ungerstedt, U. 1971a. Adipsia and aphagia after 6-hydroxydopamine induced degeneration of the nigro-striatal dopamine system. *Acta Physiol Scand Suppl* 367, pp. 95-122. doi: 10.1111/j.1365-201x.1971.tb11001.x

Ungerstedt, U. 1971b. Striatal dopamine release after amphetamine or nerve degeneration revealed by rotational behaviour. *Acta Physiol Scand Suppl* 367, pp. 49-68. doi: 10.1111/j.1365-201x.1971.tb10999.x

Ungerstedt, U. and Arbuthnott, G. W. 1970. Quantitative recording of rotational behavior in rats after 6-hydroxy-dopamine lesions of the nigrostriatal dopamine system. *Brain Research* 24(3), pp. 485-493. doi: 10.1016/0006-8993(70)90187-3

Vaillancourt, D. E., Schonfeld, D., Kwak, Y., Bohnen, N. I. and Seidler, R. 2013. Dopamine overdose hypothesis: evidence and clinical implications. *Mov Disord* 28(14), pp. 1920-1929. doi: 10.1002/mds.25687

Valjent, E. and Gangarossa, G. 2021. The Tail of the Striatum: From Anatomy to Connectivity and Function. *Trends Neurosci* 44(3), pp. 203-214. doi: 10.1016/j.tins.2020.10.016

van Wamelen, D. J. et al. 2021. The Non-Motor Symptoms Scale in Parkinson's disease: Validation and use. *Acta Neurol Scand* 143(1), pp. 3-12. doi: 10.1111/ane.13336

Verbaan, D., van Rooden, S. M., Visser, M., Marinus, J. and van Hilten, J. J. 2008. Nighttime sleep problems and daytime sleepiness in Parkinson's disease. *Mov Disord* 23(1), pp. 35-41. doi: 10.1002/mds.21727

Vermeiren, Y., Hirschberg, Y., Mertens, I. and De Deyn, P. P. 2020. Biofluid Markers for Prodromal Parkinson's Disease: Evidence From a Catecholaminergic Perspective. *Frontiers in Neurology* 11, doi: 10.3389/fneur.2020.00595

Vijayraghavan, S., Wang, M., Birnbaum, S. G., Williams, G. V. and Arnsten, A. F. T. 2007. Inverted-U dopamine D1 receptor actions on prefrontal neurons engaged in working memory. *Nature Neuroscience* 10(3), pp. 376-384. doi: 10.1038/nn1846

Visanji, N. P., Fox, S. H., Johnston, T., Reyes, G., Millan, M. J. and Brotchie, J. M. 2009. Dopamine D3 receptor stimulation underlies the development of L-DOPA-induced dyskinesia in animal models of Parkinson's disease. *Neurobiol Dis* 35(2), pp. 184-192. doi: 10.1016/j.nbd.2008.11.010

Visser, M., Verbaan, D., van Rooden, S., Marinus, J., van Hilten, J. and Stiggelbout, A. 2009. A longitudinal evaluation of health-related quality of life of patients with Parkinson's disease. *Value Health* 12(2), pp. 392-396. doi: 10.1111/j.1524-4733.2008.00430.x

Vo, Q., Gilmour, T. P., Venkiteswaran, K., Fang, J. and Subramanian, T. 2014. Polysomnographic Features of Sleep Disturbances and REM Sleep Behavior Disorder in the Unilateral 6-OHDA Lesioned Hemiparkinsonian Rat. *Parkinsons Dis* 2014, p. 852965. doi: 10.1155/2014/852965

Vogelsang, D. A. and D'Esposito, M. 2018. Is There Evidence for a Rostral-Caudal Gradient in Fronto-Striatal Loops and What Role Does Dopamine Play? *Front Neurosci* 12, p. 242. doi: 10.3389/fnins.2018.00242

Vogt, B. A. 2019. Cingulate cortex in Parkinson's disease. *Handb Clin Neurol* 166, pp. 253-266. doi: 10.1016/b978-0-444-64196-0.00013-3

Volpicelli-Daley, L. A., Kirik, D., Stoyka, L. E., Standaert, D. G. and Harms, A. S. 2016. How can rAAV-α-synuclein and the fibril α-synuclein models advance our understanding of Parkinson's disease? *J Neurochem* 139 Suppl 1(Suppl 1), pp. 131-155. doi: 10.1111/jnc.13627

Voorn, P., Vanderschuren, L. J., Groenewegen, H. J., Robbins, T. W. and Pennartz, C. M. 2004. Putting a spin on the dorsal-ventral divide of the striatum. *Trends Neurosci* 27(8), pp. 468-474. doi: 10.1016/j.tins.2004.06.006

Walaas, S. I. and Greengard, P. 1984. DARPP-32, a dopamine- and adenosine 3':5'-monophosphate-regulated phosphoprotein enriched in dopamine-innervated brain regions. I. Regional and cellular distribution in the rat brain. *J Neurosci* 4(1), pp. 84-98. doi: 10.1523/jneurosci.04-01-00084.1984

Wang, J. et al. 2023. Common and distinct roles of amygdala subregional functional connectivity in non-motor symptoms of Parkinson's disease. *NPJ Parkinsons Dis* 9(1), p. 28. doi: 10.1038/s41531-023-00469-1

Wang, J., Tian, Y., Shi, X., Feng, Z., Jiang, L. and Hao, Y. 2022a. Safety and Efficacy of Cell Transplantation on Improving Motor Symptoms in Patients With Parkinson's Disease: A Meta-Analysis. *Front Hum Neurosci* 16, p. 849069. doi: 10.3389/fnhum.2022.849069

Wang, L. et al. 2022b. Dopamine depletion and subcortical dysfunction disrupt cortical synchronization and metastability affecting cognitive function in Parkinson's disease. *Hum Brain Mapp* 43(5), pp. 1598-1610. doi: 10.1002/hbm.25745

Wang, Z. et al. 2020. Cognitive flexibility deficits in rats with dorsomedial striatal 6-hydroxydopamine lesions tested using a three-choice serial reaction time task with reversal learning. *NeuroReport* 31(15), pp. 1055-1064. doi: 10.1097/wnr.0000000000001509

Warnecke, T., Schäfer, K. H., Claus, I., Del Tredici, K. and Jost, W. H. 2022. Gastrointestinal involvement in Parkinson's disease: pathophysiology, diagnosis, and management. *NPJ Parkinsons Dis* 8(1), p. 31. doi: 10.1038/s41531-022-00295-x

Warren Olanow, C. et al. 2013. Factors predictive of the development of Levodopa-induced dyskinesia and wearing-off in Parkinson's disease. *Mov Disord* 28(8), pp. 1064-1071. doi: 10.1002/mds.25364

Watson, G. S. and Leverenz, J. B. 2010. Profile of Cognitive Impairment in Parkinson's Disease. *Brain Pathology* 20(3), pp. 640-645. doi: https://doi.org/10.1111/j.1750-3639.2010.00373.x

Weil, R. S. and Reeves, S. 2020. Hallucinations in Parkinson's disease: new insights into mechanisms and treatments. *Advances in clinical neuroscience & rehabilitation : ACNR* 19(4), pp. ONNS5189-ONNS5189. doi: 10.47795/ONNS5189

Weintraub, D. et al. 2017. Cognition and the course of prodromal Parkinson's disease. *Mov Disord* 32(11), pp. 1640-1645. doi: 10.1002/mds.27189

Weintraub, D. et al. 2006. Association of dopamine agonist use with impulse control disorders in Parkinson disease. *Arch Neurol* 63(7), pp. 969-973. doi: 10.1001/archneur.63.7.969

Wenning, G. K. et al. 1997. Short- and long-term survival and function of unilateral intrastriatal dopaminergic grafts in Parkinson's disease. *Ann Neurol* 42(1), pp. 95-107. doi: 10.1002/ana.410420115

Westin, J. E., Andersson, M., Lundblad, M. and Cenci, M. A. 2001. Persistent changes in striatal gene expression induced by long-term L-DOPA treatment in a rat model of Parkinson's disease. *European Journal of Neuroscience* 14(7), pp. 1171-1176. doi: 10.1046/j.0953-816X.2001.01743.x

Whishaw, I. Q., Woodward, N. C., Miklyaeva, E. and Pellis, S. M. 1997. Analysis of limb use by control rats and unilateral DA-depleted rats in the Montoya staircase test: movements, impairments and compensatory strategies. *Behavioural Brain Research* 89(1), pp. 167-177. doi: https://doi.org/10.1016/S0166-4328(97)00057-0

Wictorin, K., Brundin, P., Sauer, H., Lindvall, O. and Björklund, A. 1992. Long distance directed axonal growth from human dopaminergic mesencephalic neuroblasts implanted along the nigrostriatal pathway in 6-hydroxydopamine lesioned adult rats. *J Comp Neurol* 323(4), pp. 475-494. doi: 10.1002/cne.903230403

Willard, A. M., Bouchard, R. S. and Gittis, A. H. 2015. Differential degradation of motor deficits during gradual dopamine depletion with 6-hydroxydopamine in mice. *Neuroscience* 301, pp. 254-267. doi: 10.1016/j.neuroscience.2015.05.068

Wilson, H., Giordano, B., Turkheimer, F. E., Chaudhuri, K. R. and Politis, M. 2018. Serotonergic dysregulation is linked to sleep problems in Parkinson's disease. *Neuroimage Clin* 18, pp. 630-637. doi: 10.1016/j.nicl.2018.03.001

Wong, K. L. L., Nair, A. and Augustine, G. J. 2021. Changing the Cortical Conductor's Tempo: Neuromodulation of the Claustrum. *Frontiers in Neural Circuits* 15, doi: 10.3389/fncir.2021.658228

Xiong, Y., Dawson, T. M. and Dawson, V. L. 2017. Models of LRRK2-Associated Parkinson's Disease. *Adv Neurobiol* 14, pp. 163-191. doi: 10.1007/978-3-319-49969-7_9

Yagi, S., Yoshikawa, E., Futatsubashi, M., Yokokura, M., Yoshihara, Y., Torizuka, T. and Ouchi, Y. 2010. Progression from unilateral to bilateral parkinsonism in early Parkinson disease: implication of mesocortical dopamine dysfunction by PET. *J Nucl Med* 51(8), pp. 1250-1257. doi: 10.2967/jnumed.110.076802

Yang, D. et al. 2019. The Role of the Gut Microbiota in the Pathogenesis of Parkinson's Disease. *Front Neurol* 10, p. 1155. doi: 10.3389/fneur.2019.01155

Yang, J., Pourzinal, D., McMahon, K. L., Byrne, G. J., Copland, D. A., O'Sullivan, J. D. and Dissanayaka, N. N. 2021. Neural correlates of attentional deficits in Parkinson's disease patients with mild cognitive impairment. *Parkinsonism Relat Disord* 85, pp. 17-22. doi: 10.1016/j.parkreldis.2021.02.009

Yarnall, A. J. et al. 2014. Characterizing mild cognitive impairment in incident Parkinson disease: the ICICLE-PD study. *Neurology* 82(4), pp. 308-316. doi: 10.1212/wnl.0000000000000066

Yates, J. R., Darna, M., Beckmann, J. S., Dwoskin, L. P. and Bardo, M. T. 2016. Individual differences in impulsive action and dopamine transporter function in rat orbitofrontal cortex. *Neuroscience* 313, pp. 122-129. doi: 10.1016/j.neuroscience.2015.11.033

Yin, H. H., Knowlton, B. J. and Balleine, B. W. 2004. Lesions of dorsolateral striatum preserve outcome expectancy but disrupt habit formation in instrumental learning. *Eur J Neurosci* 19(1), pp. 181-189. doi: 10.1111/j.1460-9568.2004.03095.x

Yin, H. H., Knowlton, B. J. and Balleine, B. W. 2005. Blockade of NMDA receptors in the dorsomedial striatum prevents action-outcome learning in instrumental conditioning. *Eur J Neurosci* 22(2), pp. 505-512. doi: 10.1111/j.1460-9568.2005.04219.x

Yu, J. et al. 2007. Induced pluripotent stem cell lines derived from human somatic cells. *Science* 318(5858), pp. 1917-1920. doi: 10.1126/science.1151526

Zach, H., Dirkx, M. F., Roth, D., Pasman, J. W., Bloem, B. R. and Helmich, R. C. 2020. Dopamine-responsive and dopamine-resistant resting tremor in Parkinson disease. *Neurology* 95(11), pp. e1461-e1470. doi: 10.1212/wnl.0000000000010316

Zahrt, J., Taylor, J. R., Mathew, R. G. and Arnsten, A. F. 1997. Supranormal stimulation of D1 dopamine receptors in the rodent prefrontal cortex impairs spatial working memory performance. *The Journal of neuroscience : the official journal of the Society for Neuroscience* 17(21), pp. 8528-8535. doi: 10.1523/JNEUROSCI.17-21-08528.1997

Zhang, D. et al. 2021a. Microglial activation contributes to cognitive impairments in rotenone-induced mouse Parkinson's disease model. *J Neuroinflammation* 18(1), p. 4. doi: 10.1186/s12974-020-02065-z

Zhang, L. et al. 2016. The Neural Basis of Postural Instability Gait Disorder Subtype of Parkinson's Disease: A PET and fMRI Study. *CNS Neurosci Ther* 22(5), pp. 360-367. doi: 10.1111/cns.12504

Zhang, L. et al. 2021b. Aberrant Changes in Cortical Complexity in Right-Onset Versus Left-Onset Parkinson's Disease in Early-Stage. *Front Aging Neurosci* 13, p. 749606. doi: 10.3389/fnagi.2021.749606

Zhang, W., Sun, C., Shao, Y., Zhou, Z., Hou, Y. and Li, A. 2019. Partial depletion of dopaminergic neurons in the substantia nigra impairs olfaction and alters neural activity in the olfactory bulb. *Sci Rep* 9(1), p. 254. doi: 10.1038/s41598-018-36538-2

Zhu, X. R., Maskri, L., Herold, C., Bader, V., Stichel, C. C., Güntürkün, O. and Lübbert, H. 2007. Non-motor behavioural impairments in parkin-deficient mice. *Eur J Neurosci* 26(7), pp. 1902-1911. doi: 10.1111/j.1460-9568.2007.05812.x

Zigmond, M. J., Abercrombie, E. D., Berger, T. W., Grace, A. A. and Stricker, E. M. 1990. Compensations after lesions of central dopaminergic neurons: some clinical and basic implications. *Trends Neurosci* 13(7), pp. 290-296. doi: 10.1016/0166-2236(90)90112-n

Zigmond, M. J. and Stricker, E. M. 1972. Deficits in feeding behavior after intraventricular injection of 6-hydroxydopamine in rats. *Science* 177(4055), pp. 1211-1214. doi: 10.1126/science.177.4055.1211

Ztaou, S. and Amalric, M. 2019. Contribution of cholinergic interneurons to striatal pathophysiology in Parkinson's disease. *Neurochem Int* 126, pp. 1-10. doi: 10.1016/j.neuint.2019.02.019

Ztaou, S., Lhost, J., Watabe, I., Torromino, G. and Amalric, M. 2018. Striatal cholinergic interneurons regulate cognitive and affective dysfunction in partially dopamine-depleted mice. *Eur J Neurosci* 48(9), pp. 2988-3004. doi: 10.1111/ejn.14153

Zuch, C. L., Nordstroem, V. K., Briedrick, L. A., Hoernig, G. R., Granholm, A. C. and Bickford, P. C. 2000. Time course of degenerative alterations in nigral dopaminergic neurons following a 6-hydroxydopamine lesion. *J Comp Neurol* 427(3), pp. 440-454. doi: 10.1002/1096-9861(20001120)427:3<440::aid-cne10>3.0.co;2-7